UNIVERSITÉ
DE LORRAINE

École doctorale SIMPPÉ

UNIVERSITÉ DE LORRAINE

lermab

LRGP LABORATOIRE RÉACTIONS ET GÉNIE DES PROCÉDÉS

Laboratoire d'Etude et de Recherche sur le Matériau Bois (EA 4370)

Laboratoire Réactions et Génie des Procédés (UMR7274)

Thèse de doctorat

Préparation et modification de composites thermoplastiques/tannins par extrusion réactive

Présentée en vue de l'obtention du titre de
Docteur de l'Université de Lorraine
Spécialité : Sciences du Bois et des Fibres
Par
Jingjing LIAO
Soutenance le 16 Juillet 2019

Membres du jury:

Rapporteurs

Mme. Véronique BOUNOR-LEGARE, Directeur de Recherche CNRS, IMP, UMR 5223, CNRS Université Claude Bernard Lyon 1, France

M. Jalel LABIDI, Professeur, Department of Chemical and Environmental Engineering Universidad del País Vasco, Espagne

Examinateurs

M. Nicolas BROSSE, Professeur, LERMAB, EA 4370, Université de Lorraine, France

Mme. Sandrine HOPPE, Chargée de recherche CNRS, LRGP, UMR7274, CNRS Université de Lorraine, France

Invités

Mme. Sara RONASI, Chercheuse, Norner Research AS, Norvège

Acknowledgement

the great moment to spend with them in France.

I am extremely grateful to my beloved parents for their love, supporting, caring and sacrifices for educating and preparing me for my future. I thank my sister to accompany much more than me with my parents. Also, I would like to thank I am my dear husband for his continuing support to complete my thesis. His positive life attitude is like the sunshine in my life, which means a lot to me.

Table of contents

Résumé

Les biopolymères issus de ressources renouvelables et leur utilisation dans la science des matériaux est aujourd'hui un sujet qui fait l'objet d'études approfondies en raison de l'épuisement des ressources pétrolières et des préoccupations environnementales. Dans la nature, les co-produits des industries forestières et agricoles peuvent fournir une vaste gamme de matériaux ou de biopolymères (fibres naturelles, cellulose, hémicellulose, lignine, tanins, amidon, huiles…). Les recherches antérieures se sont principalement concentrées sur l'utilisation des fibres naturelles et de la cellulose comme renfort dans les composites polymères en raison de leur faible coût, de leur facilité de préparation, de leur faible impact sur l'environnement. La densité relativement faible des fibres naturelles comparée à celle des renforts issus de ressources fossiles est également un avantage pour la conception de composites légers. Les caractéristiques fonctionnelles des biopolymères en tant qu'additifs fonctionnels dans les polymères suscitent également un intérêt croissant. Par exemple, la lignine est étudiée pour la conception de matériaux stables à la chaleur et aux UV et ignifuges. Cependant, relativement peu de recherches ont été menées concernant l'utilisation des tanins dans le domaine des composites polymères.

Les tanins condensés (CTs) sont des biopolymères très abondants dans le règne végétal. Les CTs sont les deuxièmes biopolymères phénoliques par odre d'abondance et peuvent être facilement extraits des résidus forestiers et agricoles tels que les écorces de bois et les peaux de raisins. Au cours des dernières décennies, les polyphénols ont joué un rôle important dans les systèmes thermodurcissables (par exemple, les adhésifs pour le collage du bois, les matériaux en mousse) en raison de leur réactivité chimique. Cependant, les CTs ont une également une gamme de propriétés insuffisamment exploitées telles que la résistance aux UV, les propriétés antioxydants, l'activité antimicrobienne et la capacité de formation de résidus de carbonisation (pour les applications comme retardateur de flamme), qui suscite un intérêt pour le développement de composites thermoplastiques innovants. Cependant afin d'être en mesure d'utiliser les tanins à des teneurs élevées dans les matériaux polymères pour différentes applications, l'amélioration de leur compatibilité dans la matrice polymère est le facteur critique à considérer.

Dans cette étude, le polypropylène (PP) et le poly(acide lactique) (PLA) ont été

1

choisis comme matrices thermoplastiques pour développer des biocomposites thermoplastiques/tanins. Le PP est l'un des plastiques les plus utilisés industriellement et pour des applications courantes. Il est néanmoins très sensible à la dégradation par les UV, à l'oxydation et il est très inflammable. Les caractéristiques fonctionnelles des tanins (comme la capacité antioxydante, anti-UV, de formation de résidus de carbonisation) suscitent actuellement un intérêt dans le cadre du développement de matériaux à base de PP de haute performance et durable à long terme. De plus, le PP présente des caractéristiques favorables, telles qu'un faible coût de production, une flexibilité de conception et une bonne recyclabilité, qui permettent de l'utiliser dans le domaine des composites par de nombreuses méthodes de transformation telles que l'extrusion. Le PLA est le polymère d'origine biologique commercial le plus populaire de par sa biodégradabilité, ses bonnes propriétés mécaniques et son prix modéré par rapport aux autres polymères d'origine biologique comme les polyhydroxyalcanoates. La bonne aptitude au traitement thermique du PLA permettrait de traiter des composites PLA-tanins par extrusion. La combinaison du PLA et des tanins permettra de développer des biocomposites « verts » à faible impact environnemental et peu onéreux. En outre, le PLA étant un polymère couramment utilisé en impression 3D, les propriétés fonctionnelles des tanins pourraient s'adapter à des matériaux d'impression 3D polyvalents sous différentes formes pour la fabrication additive. L'utilisation des tanins comme matière première pour l'impression 3D non seulement répond à la demande de durabilité, mais également pourrait minimiser certains effets négatifs associés aux polymères synthétiques dans des applications ciblées, tels que la dégradabilité, la recyclabilité, les produits de dégradation nocifs et les additifs rejetés.

Dans cette étude, nous nous sommes intéressés à la préparation de thermoplastiques/tanins par extrusion, cette technologie présentant une excellente capacité de mélange et une grande souplesse de mise en œuvre. En outre, une température d'extrusion élevée permet également d'envisager des réactions chimiques pendant le processus d'extrusion à l'aide de réactifs (par exemple des modificateurs ou des agents de couplage ou des compatibilisants). Cette approche constitue une voie prometteuse pour améliorer la compatibilité des tanins et de la matrice polymère, les tanins condensés pouvant réagir avec de nombreux groupes fonctionnels (aldéhydes, amines, isocyanates, etc.). La capacité de copolymérisation fournit une voie potentielle pour minimiser les groupes hydroxyles des tanins afin de réduire la différence de

polarité et, par conséquent, d'améliorer la compatibilité des tanins et de la matrice polymère. Dans cette thèse, le tanin a été modifié par copolymérisation avec l'hexamine, le glyoxal, les isocyanates et le 3-aminopropytriéthoxysilane. De plus, les tanins estérifiés se sont avérés très miscibles avec le PLA, conduisant à un mélange potentiel pour l'impression 3D, ce qui peut être attribué à la polyvalence des matériaux d'impression 3D. A cet égard, nos recherches peuvent être divisées en trois chapitres basés sur différentes matrices polymères et différents objectifs de recherche. Le cadre de cette thèse et les principaux objets de recherche sont présentés dans la Figure 0-1.
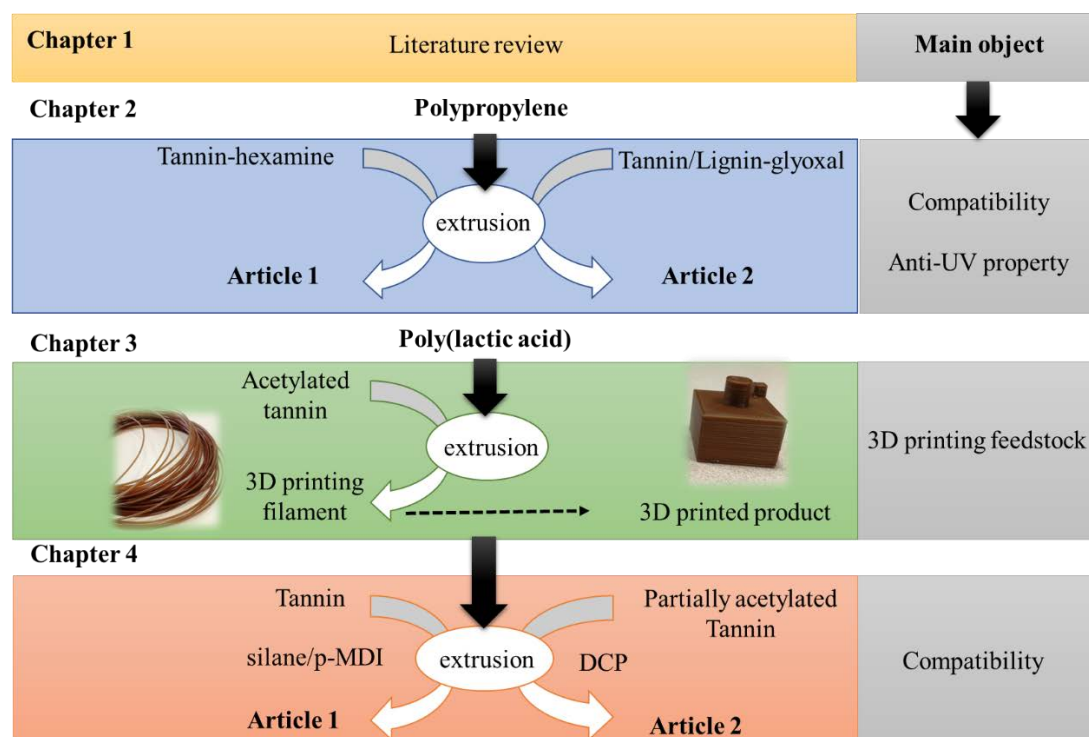
Figure 0-1. Le cadre de cette thèse et les principaux objets de recherche

Le chapitre 1 est une revue de la littérature se compose de quatre parties ont été censés présenter les tanins, typique à base d'essence à base de polymère PP et de polymère à base de bio-polymère PLA, procédé d'extrusion pour la préparation de biocomposites, et une technique 3D innovante pour la fabrication de produits en plastique. De grandes inspirations peuvent être tirées d'une vue d'ensemble de ces littératures pour transformer les tanins d'une application traditionnelle à une application plus large dans les matériaux polymères.

Le chapitre 2 décrit la préparation des composites PP/polyphénols (CTs et lignine) par vulcanisation dynamique. Deux réactifs réactifs, l'hexaméthylènetétramine (hexamine) (article 1) et le glyoxal (article 2), ont été utilisés comme agents de

réticulation pour réticuler le tanin pendant le processus d'extrusion. La capacité antioxydante des polyphénols réticulés a été étudiée.

Le premier article du chapitre 2 présente le processus de réussite du composite PP/CTs par extrusion dynamique. Au cours du processus d'extrusion, les CTs ont été réticulés avec de l'hexamine dans des proportions différentes. L'étude morphologique a montré de petites particules de tanin réticulé (TH) bien dispersées dans la matrice PP. Suite à la détermination du module de Young et des comportements rhéologiques des échantillons testés, le tanin réticulé a servi de charge pour renforcer la rigidité de la matrice PP. En outre, le tanin réticulé a eu un impact positif en termes de cristallinité du PP et de stabilité thermique. De plus, lorsque les composites ont été soumis à une altération accélérée sous UV, les composites PP/TH ont présenté une bien meilleure performance de résistance à la photodégradation caractérisée par moins de fissures de surface (Figure 0-2, a), un indice carbonyle inférieur et une diminution de la cristallinité, ralentissant ainsi les scissions des chaînes macromoléculaires du PP. Par ailleurs, l'ajout de tanin réticulé au PP peut prévenir la perte de propriétés mécaniques en limitant physiquement la mobilité des chaînes polymères (Figure 0-2, b).
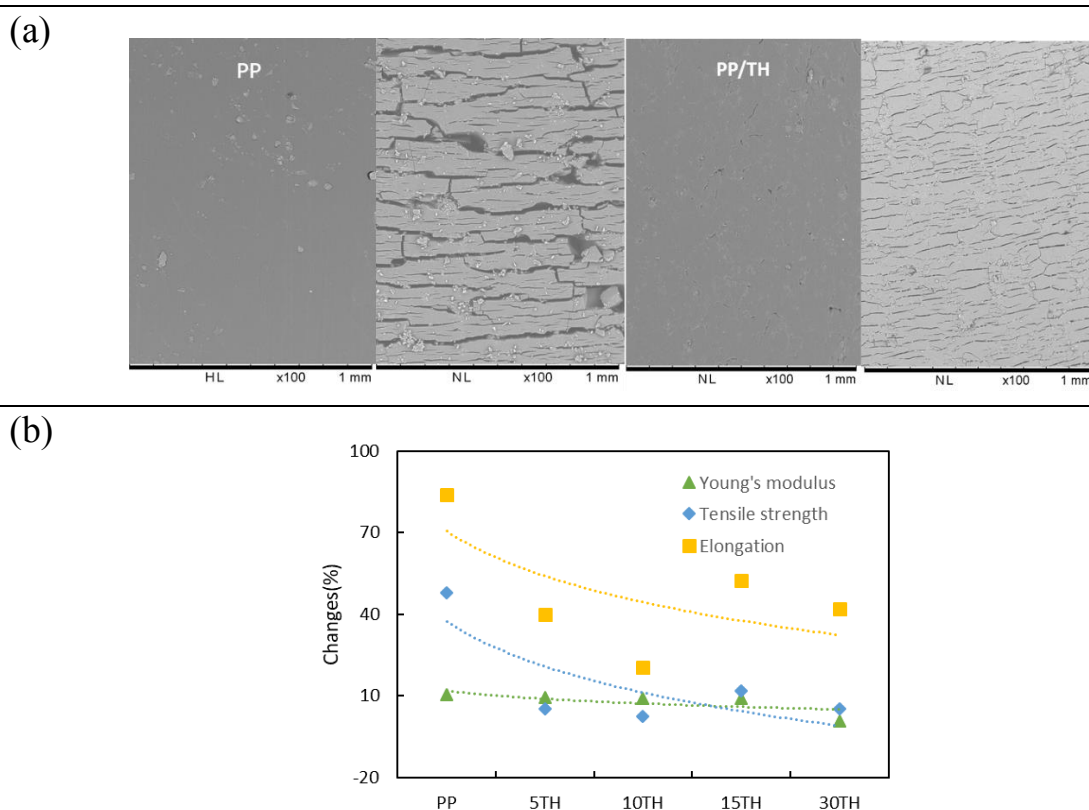
Figure 0-2. Modification de la morphologie de surface (a) et des propriétés mécaniques (b) du PP et des composites PP/TH avant et après vieillissement UV.

Même si les CTs sont bien connus pour leurs propriétés antioxydantes, l'effet du processus de réticulation sur leur capacité de protection UV n'est pas encore clair. Par ailleurs, il devrait être intéressant d'utiliser la vulcanisation dynamique avec des mélanges PP/lignine car la lignine est largement étudiée et est un polyphénol peu coûteux. A cet effet, les PP/polyphénols (CTs et lignine) ont été modifiés au glyoxal par la technique de vulcanisation dynamique comme présenté dans le deuxième article du chapitre 2. Leur influence sur les propriétés mécaniques, la cristallinité, la stabilité thermique ainsi que les propriétés de protection contre les UV de la matrice PP ont été étudiées et comparées aux polyphénols naturels. Le procédé d'extrusion conduit à la réticulation des polyphénols en particules rigides thermodurcissables, contribuant ainsi à l'amélioration des modules de Young des composites. Après extrusion vulcanisée, l'hydrophilie des polyphénols a été réduite ce qui a augmenté la compatibilité dans la matrice PP et donc la résistance à la traction. En outre, les TC et les TC vulcanisés peuvent agir comme agents de nucléation du PP en raison de la taille de leurs particules. Les polyphénols vulcanisés ont une meilleure performance sur la stabilité thermique du PP par rapport aux polyphénols naturels, en particulier pour la lignine vulcanisée au PP (*Figure 0-3*). D'après les données rhéologiques, les polyphénols vulcanisés ont montré une fonction de renforcement et confirmé leur meilleure capacité de dispersion dans la matrice PP par rapport aux polyphénols naturels. De plus, les polyphénols vulcanisés présentent une meilleure performance de protection contre les UV, démontrée par des changements moindres de la morphologie de surface, l'indice de carbonyle (Figure 0-4, a), la cristallinité (Figure 0-4, b), la viscosité et de la résistance à la traction.
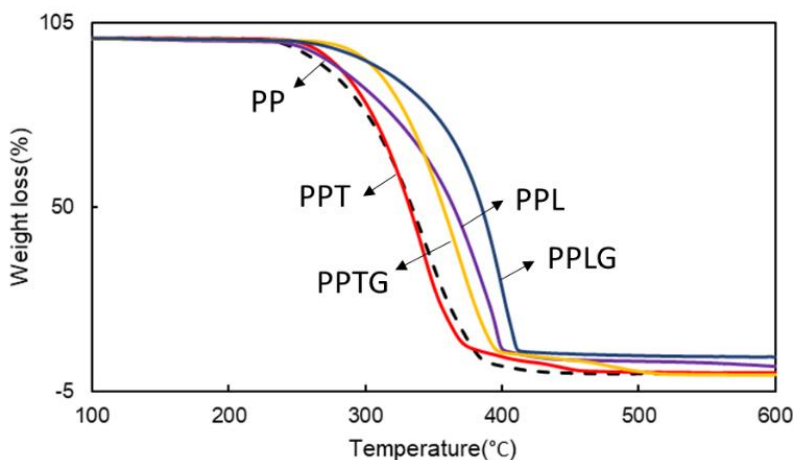
Figure 0-3. Comportements thermiques du PP, des mélanges PP/polyphenol et des mélanges PP/polyphenol réticulés: (a) TGA

(a)   (b)
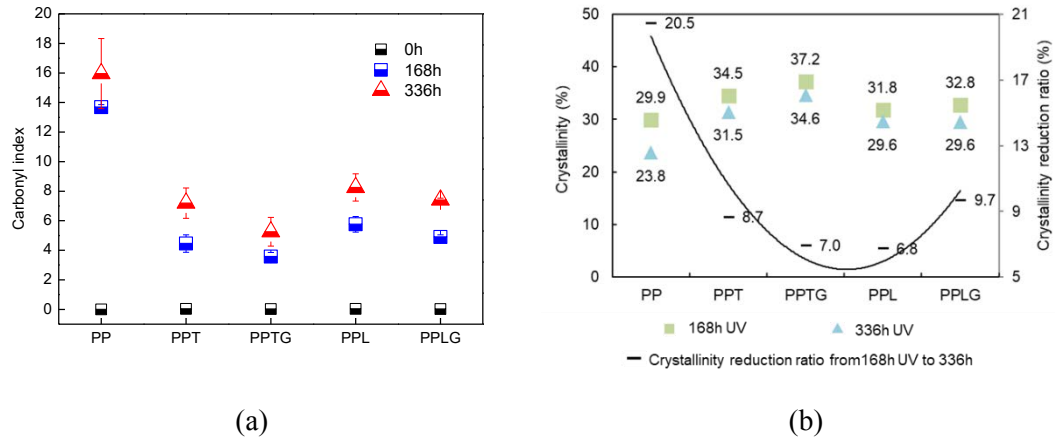
Figure 0-4. Index carbonyle du PP et des mélanges PP/polyphenol en fonction du temps d'exposition (a); cristallinité du f PP et des mélanges PP/polyphenol en fonction du temps d'exposition (b)

Dans le chapitre 3, les TC ont été utilisés comme matière première pour développer de nouveaux matériaux d'impression 3D. Les CTs modifiés avec de l'anhydride acétique présentaient une compatibilité accrue avec la matrice polymère PLA. Jusqu'à 30 % en poids de tanin acétylé (AT) peut être incorporé avec succès au PLA tandis que le PLA contenant jusqu'à 20 % en poids d'AT n'a pas détérioré les propriétés mécaniques et la morphologie de surface des composites. Le procédé de préparation des filaments et d'addition par fusion est illustré à la Figure 0-5.

Figure 0-5. Préparation de filaments PLA/AT par mélange en voie fondue par un procédé d'extrusion et procédé d'impression 3D par dépôt de fil fondu.

L'AT améliore l'absorption d'eau des filaments et favorise la dégradation par hydrolyse du PLA, en particulier en milieu alcalin. En outre, on s'attend à ce que les filaments de PLA chargés d'AT présentant des structures hautement amorphes montrent un taux de dégradation plus élevé. Ces propriétés pourraient probablement profiter à des applications à court terme comme les dispositifs implantables dans des applications biomédicales. En outre, l'incorporation de l'AT n'a montré aucun effet significatif sur la température de fusion et de transition vitreuse. Une température d'impression inférieure à 250°C convient pour de tels filaments sans provoquer de décomposition du matériau. Différents filaments à charge AT sont imprimables par FDM à différentes températures comprises entre 180 et 220 °C, mais la résistance à la traction des échantillons imprimés est inférieure à celle des méthodes de fabrications traditionnelles. Des défauts d'impression peuvent être observés dans les filaments remplis d'AT en raison de la séparation de phases et de l'agrégation d'AT, en particulier les filaments à haute teneur en charge AT.

Le chapitre 4 propose d'améliorer l'adhérence interfaciale entre le PLA et le tanin par une voie de compatibilisation réactive en utilisant un agent de couplage silane (3-aminopropytriéthoxysilane), des agents de compatibilité (diisocyanate de méthylène diphényle, p-MDI) (article 1) et du peroxyde de dicumyle (DCP) (article 2). Pour ralentir la cinétique des réactions complexes, les tanins ont été partiellement acétylés lors de l'utilisation de DCP comme promoteur d'adhésion.

Le premier article du chapitre 4 décrit l'amélioration de la compatibilité du tanin PLA par un procédé de compatibilisation en une étape avec l'ajout de diisocyanate de méthylène diphényle (p-MDI) et de 3-aminopropytriéthoxysilane (APS). Les résultats de traction ont montré que les mélanges PLA/tanin compatibilisés par p-MDI et APS présentaient des modules de Young et une résistance à la traction plus élevés, liés à une meilleure adhésion interfaciale entre le tanin et la matrice PLA. Les changements des propriétés en traction peuvent être expliqués par l'interaction du PLA, du tanin et du p-MDI/APS, formant des particules de tanin réticulé et/ou une structure de réseau local de réticulation et d'interpénétration du tanin-PLA pendant le processus de mélange à chaud, les réactions proposées entre PLA, tanin et p-MDI/APS sont présentées dans le schéma 1. La formation d'une microstructure de réticulation entre les chaînes de tanins et de polymères PLA a été confirmée par le comportement rhéologique en raison du

comportement en plateau et de l'augmentation de la viscosité complexe avec l'ajout d'APS et p-MDI. De plus, le comportement thermique a montré une augmentation de Tm et une réduction de la cristallinité, ce qui suggère une amélioration de l'interaction interfaciale entre le tanin et la matrice PLA. Les résultats de l'analyse thermogravimétrique ont révélé que l'ajout de tanin réduisait la température de décomposition initiale, tandis que le réseau réticulé entre le PLA et le tanin provoquait une augmentation des résidus à haute température. Cette approche efficace d'amélioration de la compatibilité a le potentiel d'être adaptée à d'autres systèmes composites PLA/biopolymères.

Schéma 1. Proposition de représentation de la structure de mélanges de PLA/tanin et illustration des réactions de réticulation entre PLA, tanin et p-MDI/APS
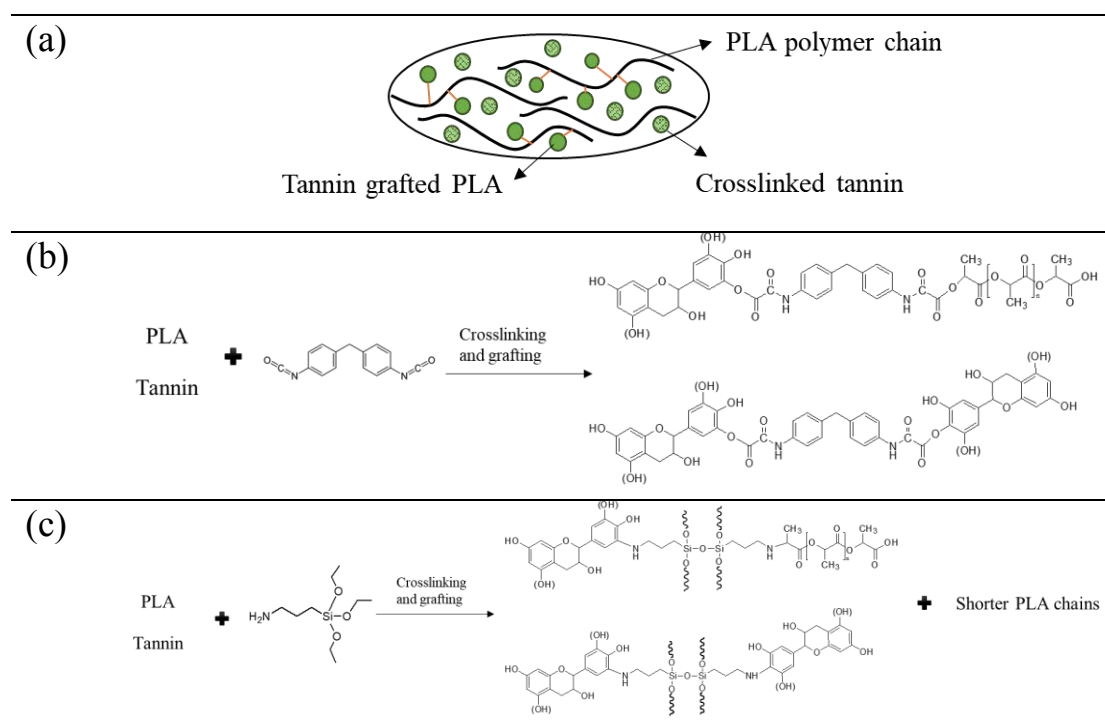
Le deuxième article du chapitre 4 est la préparation de composites verts PLA/AT par greffage radicalaire lors de l'extrusion en fusion pour améliorer l'adhésion interfaciale. Les effets du taux d'acétylation de l'AT sur l'amélioration interfaciale ont été étudiés. Dans le milieu réactionnel, le DCP se décompose d'abord par scission β en acétophénone et en radicaux méthyles qui peuvent réagir avec le PLA et l'AT, donnant des radicaux PLA· et AT·. Les radicaux s'attaquent de préférence aux groupes OH phénoliques libres de l'AT (ou aux protons du noyau phényle selon le taux d'acétylation des ATs), ce qui donne des sites de réaction différents. Dans le cas du PLA, une élimination préférentielle du proton tertiaire a été signalée, entraînant des réactions de

scission en chaîne, de ramification et de réticulation pendant le mélange à l'état fondu Les réactions et structures possibles des mélanges PLA/AT sont résumées dans le schéma 2.
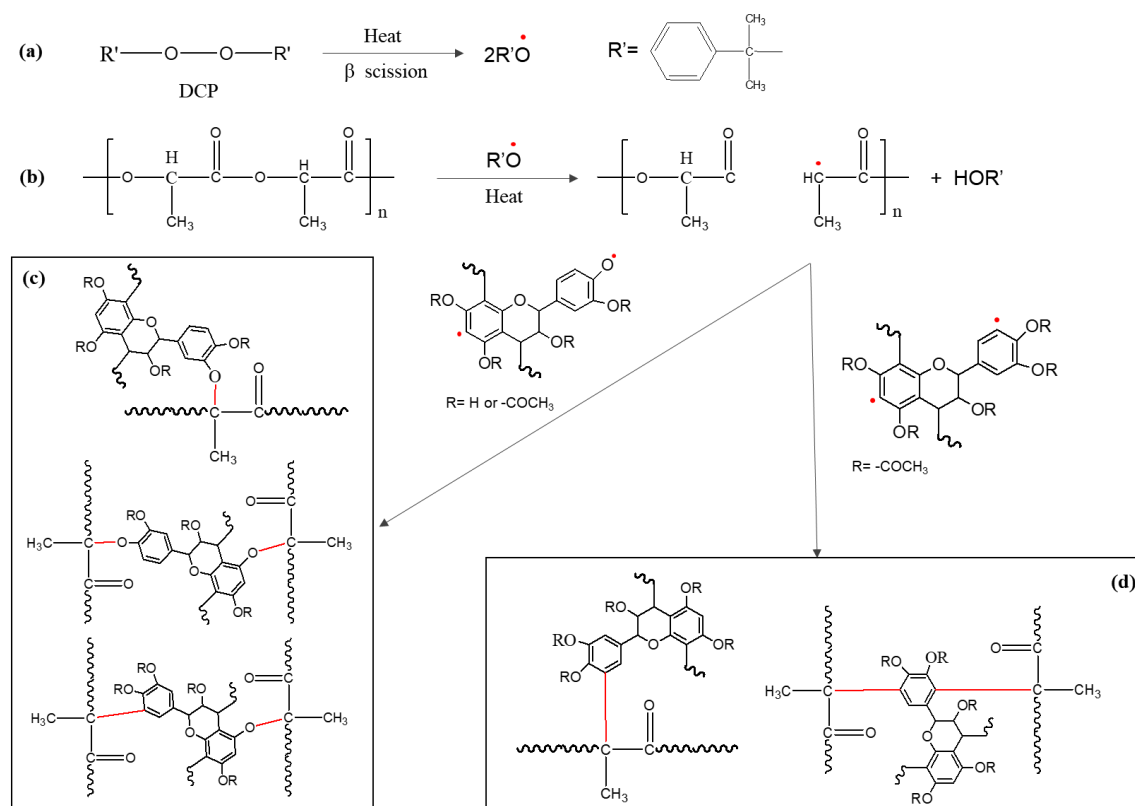
Schéma 2. Illustration schématique de la réaction de greffage de AT surPLA

Compte tenu de la complexité des phénomènes impliqués lors de la copolymérisation in situ de composants composites initiée par des radicaux peroxydes, la détermination précise des réactions impliquées et des structures produites est très difficile. Cependant, l'analyse physico-chimique des composites obtenus nous a permis de tirer quelques observations et conclusions. L'amélioration du poids moléculaire des mélanges PLA/AT a confirmé la formation d'une structure réticulée par greffage en chaîne ou réactions de ramification des PLA et AT. Cette structure réticulée dans les mélanges PLA/AT entraîne une viscosité complexe, des modules de stockage et des modules de perte plus élevés que dans les mélanges PLD. Les mélanges PLA/AT modifiés DCP présentaient une bonne résistance à la traction et des modules de Young, ce qui implique une forte résistance interfaciale charge/matrice. L'augmentation de la Tg a également confirmé la structure réticulée des mélanges PLA/AT puisque cette structure entraîne une mobilité macromoléculaire difficile des chaînes polymères. La grande similitude de la stabilité thermique des mélanges PLA/AT suggère une forte

9

adhérence interfaciale. Selon les résultats expérimentaux, un taux élevé d'acétylation des tanins a conduit à une plus grande efficacité de la greffe. Cette méthode d'extrusion réactive in situ en une seule étape constitue une stratégie pratique et simple pour développer des mélanges thermoplastiques/biopolymères aux performances améliorées. Cette modification de greffage peut être appliquée pour incorporer du tanin comme composant de polymères à valeur ajoutée pour donner des propriétés spéciales et réduire le coût de ces matériaux.

General Introduction

Biopolymers from renewable resources and their utilization in material science is nowadays an intensively investigated topic driven by the depletion of petroleum resources together with environmental concerns. In nature, forestry crops/residues and agricultural crops/residues can provide a broad range of materials or biopolymers, including natural fibers, cellulose, hemicellulose, lignin, tannin, starch, oil. Previous researches have been primarily focused on the use of natural fibers and cellulose as reinforcement in polymer composites because of their low cost, easy preparation, low environmental impact, and low specific weight compared with fossil-based reinforcements. Researchers also focus on the functional characteristics of biopolymers as functional additives in polymers. For example, lignin was dominated have heat stable, UV stable, and flame retardancy function in polymers. However, there are limited researches concerning the application of tannins on polymer composites.

Condensed tannin (CTs) are widely distributed biopolymers and highly abundant in nature. CTs are the second most abundant phenolic biopolymers and they can be easily extracted from forestry and agricultural residues such as wood barks and grape skins. In the past decades, CTs have played an important role in thermosetting systems (e.g. adhesives for wood bonding, foam material) because of their chemical reactivity. However, CTs have a range of inherent properties such as UV resistance, antioxidant, antimicrobial activity, and char forming capacity, which are attracting interests for developing thermoplastic composites. In order to transform CTs from traditional application to a broader application in polymeric materials, enhance the compatibility of CTs in a polymer matrix is the critical factor to consider. The combination of CTs in high loading content and functional versatility with thermoplastic are achievable by using of compatibilizers and/or via chemical modification.

Polypropylene (PP) and poly (lactic acid) (PLA) were chosen as matrix materials to develop tannin-based biocomposites in this study. PP is one of the most widely used plastic in industrial and daily products. It is highly susceptible to UV irradiant, oxidant, and high flammability. The functional characteristics of CTs, like antioxidant, anti-UV, char forming capacity, are attracting interests for developing high performance and long-term application PP-based material. Besides, PP has low production cost, design flexibility, and recyclability, which is preferable to process composites via many

efficient converting methods such as extrusion process. PLA is the most popular commercial bio-based polymer since its biodegradability, good mechanical property and favorable price compared with other bio-based polymers like polyhydroxyalkanoates. The good thermal processability of PLA makes it suitable to process composite with CTs through the extrusion process. The combination of PLA and CTs is possible to develop whole biocomposites with low environmental impact and cost efficiency. Besides, PLA is a preferable 3D printing material, the functional properties of tannins can tailor into versatile 3D printing materials in different forms for 3D manufacturing. Using CTs as 3D printing feedstock not only meet the demand for sustainability, but also truly reduce a possibility in the negative effects associated with some synthetic polymers in biomedical applications, such as degradability, recyclability, harmful breakdown products, and released additives.

In this thesis, the preparation of thermoplastic/CTs by using extrusion process since its high efficiency, excellent mixing capacity, and flexible extruded condition setting. In addition, high extrusion temperature enables chemical reactions during extrusion process with the help of reagents (e.g. modifiers or coupling agents or compatibilizers), which is a promising route to enhance compatibility of CTs and polymer matrix. CTs can react with many functional groups (e.g. aldehydes, amines, isocyanates, etc). The copolymerization capacity provides a potential pathway to minimize the hydroxyl groups of tannins to reduce the polar difference, therefore, to enhance compatibility of tannins and polymer matrix. In this work, CTs was modified via copolymerization with hexamine, glyoxal, isocyanates, and 3-aminopropytriethoxysilane. Additionally, esterified CTs have been proved high miscible with PLA, they are potential 3D printing feedstock which can attribute to the versatility of 3D printing materials. On this regard, our researches can be divided into three chapters based on different polymer matrix and different research purposes, the framework of this thesis and main research objects is presented in Figure 0-1.

Chapter 1 is a literature review consist of four parts were supposed to introduce tannins, typical petrol-based polymer PP and bio-based polymer PLA, extrusion process for biocomposites preparation, and an innovative 3D technique for manufacturing plastic products. Great inspirations can be drawn from an overview of this literature to transform tannins from traditional application to a broader application in polymeric materials.

Chapter 2 aim to reduce the hydrophilic property of tannin by copolymerization with hexamethylenetetramine (hexamine) and glyoxal during the extrusion process. With this approach, tannin is respected to be crosslinked and form thermoset particles, which display reinforce function for PP matrix. The anti-UV property of crosslinked tannin is also investigated. In addition, a similar modified pathway also applies to lignin.

Chapter 3 investigate the mechanical, crystal, and solvent degradable properties of a biocomposite based on PLA and acetylated tannin. The printability of this 3D printing filament is also evaluated.

Chapter 4 propose to improve the interfacial adhesion between PLA and tannin via reactive compatibilization pathway by using silane coupling agent (3-aminopropytriethoxysilane), compatibilizers (methylene diphenyl diisocyanate, p-MDI), and dicumyl peroxide (DCP). For slow down the kinetics of complex reactions, tannin was partially acetylated when using DCP as an adhesion promoter.
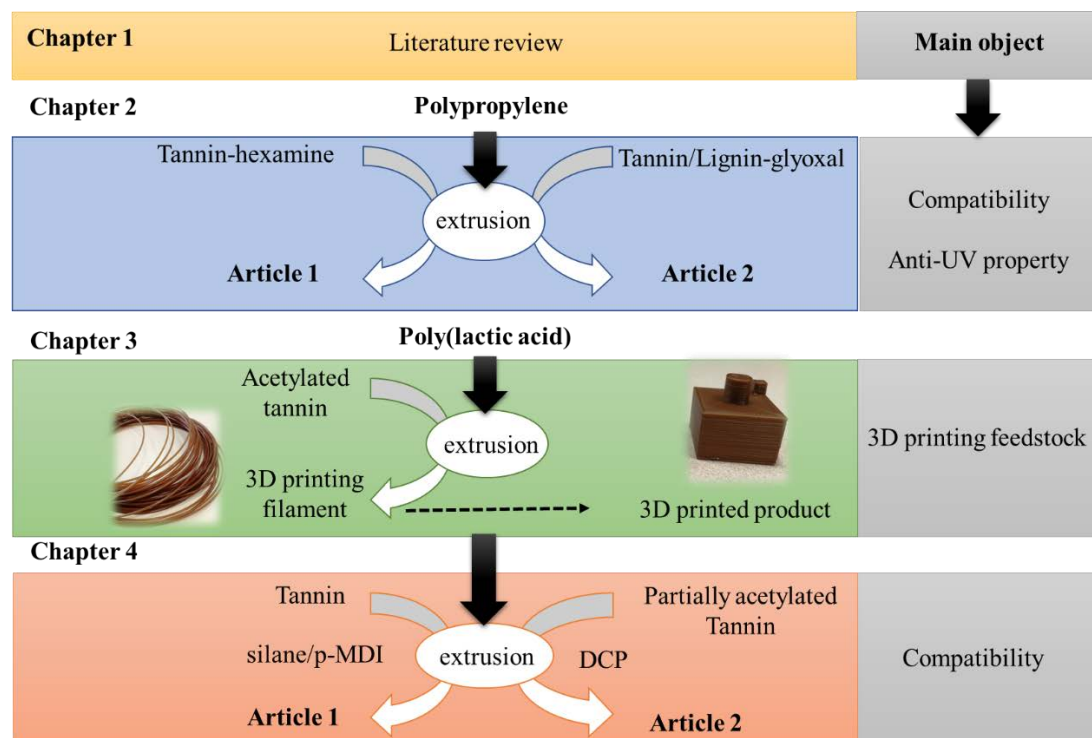
Figure 0-1. Thesis organization and main research object in each chapter

Chapter 1.   Literature review

This chapter presents a literature review covering the areas of interest in our research. The literature review will be divided into four parts:

Part I introduce the characteristic of tannin, their functional and modification pathway, and their application towards materials. The introduction of tannins will cover their structure, sources, chemistry, physicochemical property, and biological property. Additionally, useful modification and functionalization of tannins towards material science will be discussed. At last, the traditional application of tannins in thermoset material, and their innovative application in thermoplastic materials will be presented.

Part II is an introduction of the polymer matrix we used in this research. Biocomposites based on PP/biopolymers and PLA/ biopolymers will be presented. The functional property of widely used biopolymers (e.g. plant fibers, cellulose, starch, vegetable oil, hemicellulose, lignin) will be discussed.

Part III presents the extrusion process methodology that is the most widely used method to process biocomposites. Efficient reactive blending as a promising methodology for developing biocomposites and improving interfacial adhesion of biopolymer-thermoplastic matrix will be presented.

Part IV introduce the most widely used 3D printing process: fused deposition modeling and the principles for obtaining qualified products via fused deposition modeling process. Published literature regarding the application of PLA-based biocomposites as 3D printing filament can be found in this part.

Part I   Tannins and Tannin-based materials

1.   Tannins, a family of natural phenolic compounds

1.1.   Structure, classification, and source

Tannins are one of the five major classes of secondary metabolites, present in all vascular plants and in some non-vascular plants. They play an important role in regulating plant growth, protecting the plant from predation and pesticides, as well as contributing towards the color and sensory features of fruits and vegetables [1–3]. In 1957, an industrial chemist Theodore White, defined the term "tannin" as plant polyphenolic materials having molecular masses between 500 and 3000 Da and a sufficiently large number of phenolic groups to be capable of forming hydrogen-bonded cross-linked structures with collagen molecules (the act of tanning) [4]. Structurally, tannins are classified into two major groups: the hydrolyzable tannins and the condensed tannins [5,6].

Hydrolyzable tannins are phenolic compounds containing a central core of glucose esterified with gallic and digallic acids [7]. These tannins can be divided into two families: the gallotannins and the ellagitannins [8]. The former produce gallic acid and its derivatives from hydrolysis while the later produce ellagic acid after hydrolysis.

gallic acid   ellagic acid
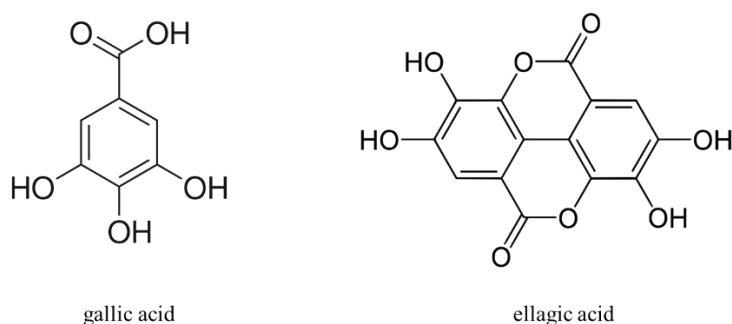
Figure 1-1. Structure of hydrolyzable tannins, gallotannins-gallic acid, ellagitannins-ellagic acid

Condensed tannins are composed of flavonoid units (Figure 1-1) in varying degrees of condensation. The flavonoid units of condensed tannins consist of three flavans rings, labeled A, B, C ring, respectively. As shown in Figure 1-2, there are two possible patterns with each ring, generating four basic nonoflavonoid building blocks of condensed tannins. These building blocks are condensed by C4→C6 or/and C4→C8 linkages [9]. The structural variation in flavonoid units resulting in the formation of different condensed tannins, which differ in reactivities. In each flavonoid unit, the A

15

ring is more reactive than the B ring since different number and position of hydroxyl groups in the two rings dictated their reactivity towards aromatic electrophilic substitution reaction. As an example, mimosa tannins mainly consist of 70% type I nonoflavonoid based on resorcinol A rings and pyrogallol B rings (Figure 1-2, I), and 25% type II based on resorcinol A rings and catechol B rings (Figure 1-2, II). The repeating units are mostly condensed by C4→C6 linkages and some C4→C8 linkages [10]. While pine tannins are dominated by type III flavonoid units based on phloroglucinol A ring and catechol B ring (Figure 1-2, III). As a consequence, pine tannins are more reactive compared with those tannins containing only resorcinol A ring [9]. Except for flavonoid compounds, condensed tannins are commonly combined with some carbohydrates, hydrocolloid gums and small amino and imino acid fractions. The hydrocolloid gums significantly affect the viscosity of tannins in spite of their low concentration. The degree of polymerization varying considerably from species to species, which account for a considerable range of structural variation. For instance, mimosa and quebracho tannins contain oligomers of 2-11flavonoid units with an average 4 to 5 times degree of polymerization, while pine tannins have about 30 units with an average 6 to 7 times degree of polymerization [9].
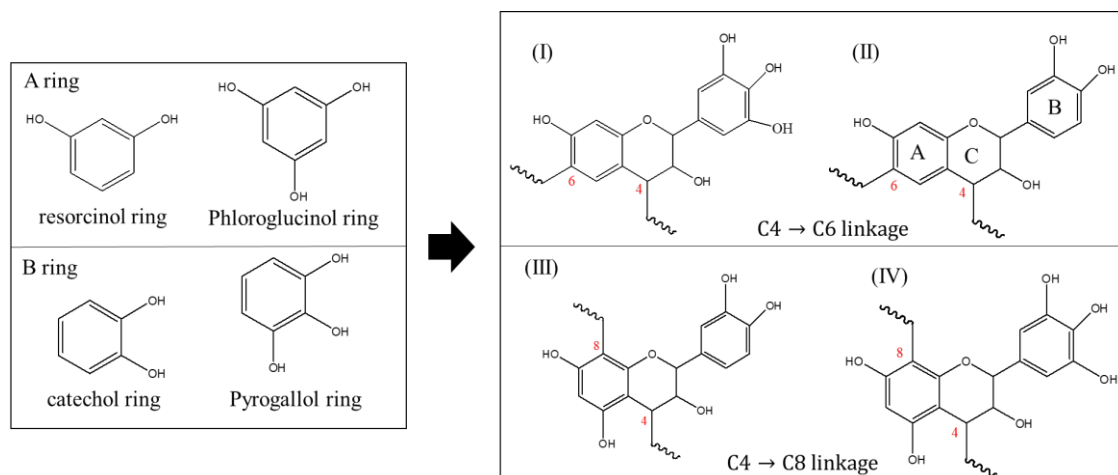
Figure 1-2. Structure of four main nonoflavonoid building blocks. Linkage between flavonoid units: C4→C6(I)(II); C4→C8(III)(IV) (modify from reference [8,11])

Tannins are widely distributed and rich in nature. They are found in vascular plants in various species (e.g. monocotyledons, dicotyledons, ferns, and conifers), and in various plant tissues (e.g. leaves, cone, seed pot, wood, blade, stipe, and bark) [12,13]. Besides, they have been also discovered in some non-vascular plants (e.g. algae).

Hydrolyzable tannins are distributed in a limited extent in some dicotyledonous

species, for instance, chestnut (Castanea sp.), myrabolans (Terminalia and Phyllantus sp.), dividivi (Caesalpinia sp.), oak (Quercus sp.), eucalyptus (Eucalyptus sp.), and extracts of Asian Myricasp [12]. Besides, they are also found in the husk and peels of some fruits and nuts, including pomegranates, strawberries, raspberries, blackberries, cloudberries, muscadine grapes, almonds, and walnuts [14]. Hydrolyzable tannins exhibit weak nucleophilicity properties thus they are less attractive in material science and the industrial worldwide production is relatively low.

Condensed tannins are distributed in various species and particularly for their considerable concentration in barks, including wattle or mimosa (Acacia mearnsii), quebracho (Schinopsis balansae or lorentzii), hemlock (Tsuga), sumach (Rhus) and various pine(Pinus) species [10,15]. They are also rich in some agricultural by-products such as grape skins and seeds [16]. Condensed tannins represent more than 90% of the total world production of commercial tannins and are more interesting as natural phenolic polymers in material science [10].

1.2. Physicochemical property

Tannins are low-density amorphous non-crystalline pale yellow-slightly brown solid oligomers/polymers. Dried tannins exhibit strong hygroscopic property. At room temperature, tannins are soluble in water, methanol, ethanol, and acetone aqueous solutions, displaying an acid pH value. However, their solubility is a function of their polymerization degree. Tannins dissolve in water usually forming colloidal solution since the appearance of strong hydrogen bridge with water molecules and their -OH groups [11].

Tannins have been implicated in diverse physicochemical properties, including protection against solar radiation, the capability to scavenge reactive oxygen species, as well as resistance against microbial pathogens, insects, symbiotic fungi, and bacteria. These properties are a result of their phenol functional groups. The physicochemical properties and reactivities of the phenol functional group have been well discussed by Quideau [4]. The phenyl rings and hydroxy substituent of phenol functions result in both hydrophobic and hydrophilic character, which can act either as a hydrogen-bond donor or as an acceptor (*Figure 1-3*). In general, tannins have absorption maxima within the UV-B light range (280-320 nm) and they are generally sensitive to oxidation processes since the relatively weak bond of the phenolic O-H bond enables the

production of phenoxy radicals by hydrogen abstraction, especially when the ortho and/or para positions are substituted with alkyl and/or alkoxy groups. Thus, catechol- and pyrogallol-type phenols can lead to the formation of reactive quinonoid species though oxidative dehydrogenation. These reactive species have been proposed as electrophiles able to react with nucleophilic biomolecules such as proteins.
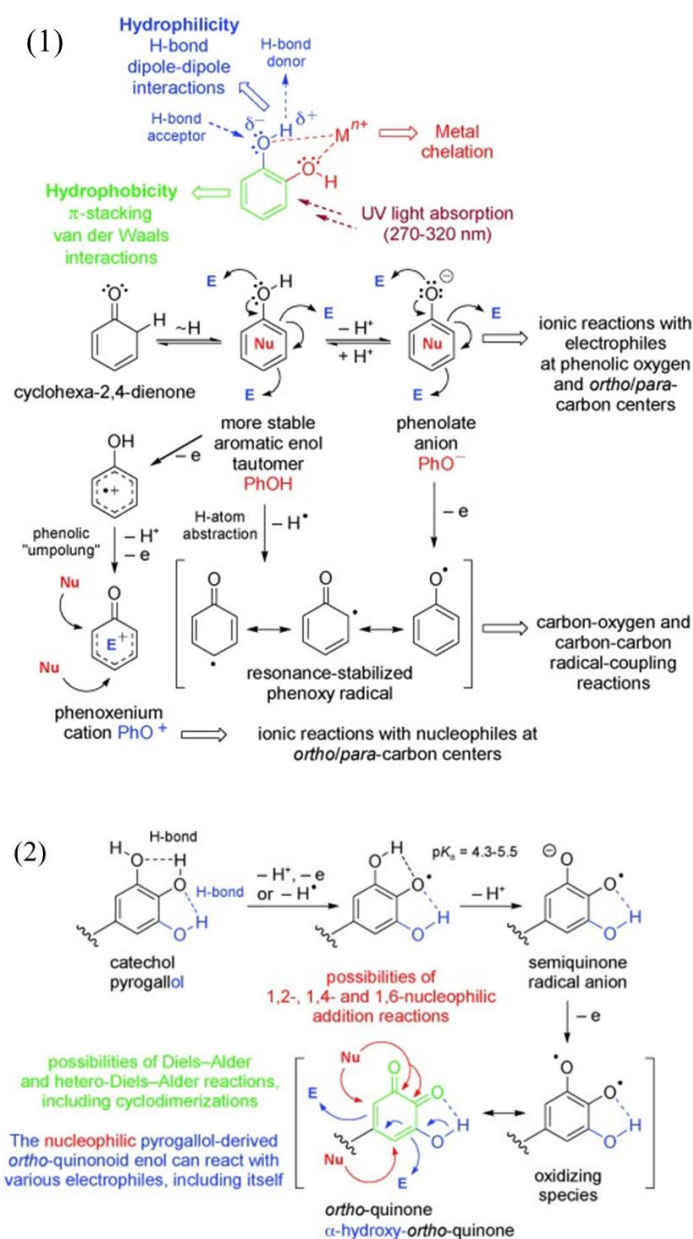
Figure 1-3. (1) Basic physicochemical properties and reactivities of the phenol functional group. E = Electrophile, Nu = Nucleophile; (2) Oxidative dehydrogenation of catechol- and pyrogallol-type phenols into reactive quinonoid species. Modified from [4].

1.3. Thermal property and glass transition

Tannins generally degrade in three main steps under air condition. The first weight loss related to the loss of adsorbed water; the second step (200-250 °C) associated with

18

the decomposition of linkage between flavonoid units; the third step at temperature 400-500 °C corresponding to the pyrolytic degradation (Figure 1-4 (a)) [17]. The diversity of thermal behavior depends strongly on purity degrade, chemical structure, and polymerization degree. The degradation onset temperature significantly increases by reducing the residual carbohydrates. The presence of sulfonate group was reported to have a negative effect on stability. Tannins functionalized with different functional agents have various decompose temperature (Table 1-1). Tannins functionalized with acetic anhydride presented lower thermal stability due to the degradation of grafted polyether chains and the higher thermal sensitivity of the ether groups [17]. However, long chain grafting tannin retarded the decomposition [18]. A higher polymerization degree of tannins usually leads to increased thermal stability and a higher degradation onset temperature because the polymerization limits their pyrolysis. Thus, in the case of thermosetting polyurethane, the cross-link density can enhance thermal stability [19]. Danny considered the mechanisms of thermal decomposition of tannins is dominate by the substitution pattern on both the B-ring and the C_{15}-C_{15} linkage type [11]. However, the thermo-protective role of tannins, as well as tannins derivatives in thermoplastics, is still unclear.

The grass transition (T_g) of condensed tannins is normally in a range of 120 to 180 ℃ [11], which is generally higher than that of lignins in similar molecular mass since the presence of C-C bonds in tannin leading to lower chain mobility [20]. Generally, the derivatization of hydroxyl groups (methylation [21], oxypropylation [22], acetylation) was generally reported to lead to a reduction in T_g (Figure 1-4(b)). This stems from the blocking of the subsequent H bonds and the increasing free volume caused by the introduction of the functional groups [20].
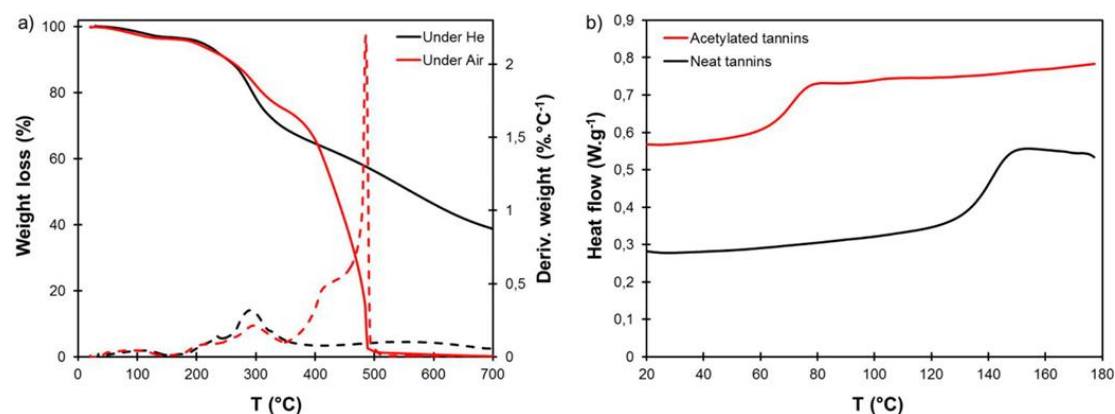
Figure 1-4. (a) TGA thermograms of A. catechu tannin under helium and air condition; (b)
The T_g of neat and acetylated catechu tannin, from ref. [20]

Table 1-1. The onset temperature of degradation of some tannins and their derivatives

Sample	Functionating agent	T_{onset}/T_{peak}(°C)	Reference
Mimosa tannin	No	146	
Quebracho tannin	No	150	[18]
	stearic acid chloride	200	
Pine tannin	No	150/241*	[17,18]
	stearic acid chloride	200	[18]
	acetic anhydride	189*	[17]
Gambier tannin	No	150/270*	[22]
	propylene oxide	200*	
Larch tannin	No	170	[23]
A. catechu tannin	No	190/294*	[20]
Sumac tannins	No	185	[24]

*Note: * Peak temperature of degradation*

1.4. Biological property

Bruyne reported the main biological and pharmacological effects of condensed tannins, including anti-oxidative effects, antibacterial and antiviral activities, enzyme inhibition, antimutagenic and antitumoral properties. The physicochemical properties of the polyphenolic structure in tannins enable the anticipated interaction with biological systems, including anti-inflammatory effects, vascular and cardiac effects, anti-diarrhoeal activity, anti-ulcer activity [25].

1.5. Modification and functionalization

Tannins with high chemical reactivity can be modified and functionalized in the various pathway. The hydrolysis or condensation of tannins often occurs through heterocycle ring under acid or base condition. Besides, tannins can copolymerize with other monomers (e.g. aldehydes, hexamine, furfuryl alcohol, isocyanates, epoxy, fatty acids) through the aromatic structure or hydroxyl groups to elaborate thermoset resin. Moreover, the phenolic and aliphatic hydroxyl groups can be functionalized to obtain several tannin derivatives through esterification, oxyalkylation, epoxidation, polymer graft, etc. These tannin derivatives exhibit improved solubility in organic solvents,

and/or OH chemical reactivity, and/or lipophilicity, which can broaden their potential applications in material science. Some modifications and functionalization pathways of tannins which might be interesting in material science will be presented in detail below.

1.5.1. polymerization

The polymerization of tannins leads to a cross-linked three-dimensional network, the published copolymers and their related reaction parameter and mechanism were summarized as follow.

1.5.1.1. Reaction with aldehydes

Tannins react with aldehydes widely used for preparing adhesives, foam material and composite matrices resin [7,26]. The polymerization of tannin and aldehydes is mainly through methylene bridge linkages (Figure 1-5) to reactive positions of the flavonoid molecules, mainly the A-rings. In condensed tannins, the linkages with aldehydes are mainly formed with the A-ring [9]. Since the presence of interflavonoid bonds, the A rings of flavonoid units retain only one highly reactive nucleophilic site. Tannins containing resorcinol type of A-rings(mimosa), the reaction site is in the C8 position while those containing phloroglucinol A-rings(pine), the reaction site is in the C6 position (Figure 1-5). In the reaction with aldehydes, C8 position is considered less sterically hindered than C6 position, thus, phloroglucinol type of tannins are more reactive in polymerization [9]. The B-rings (pyrogallol or catechol) are less reactive but it can be activated by anion formation at high pH (approximately 10) or catalyzed by zinc acetate at lower pHs [27]. The activated B-rings participate in the polymerization process and help to further cross-link the network of tannin and aldehydes. However, this type of polymerization is commonly incomplete, leading weak and brittle networks. Once the crosslink reaction starts, tannin molecules become immobile at a low level of condensation with aldehydes, methylene bridges are hardly formed since bridge distance is too large. Thus, bridging agents with longer molecules like phenolic resin has been used to solve this problem [28,29].
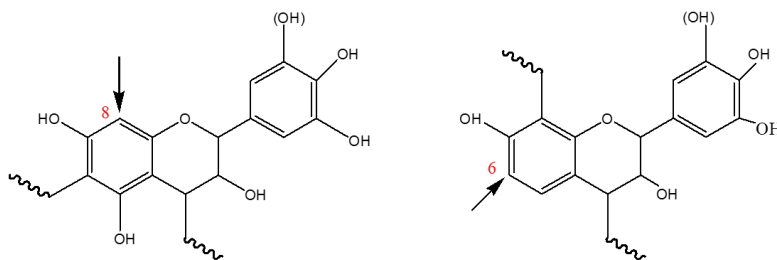
Figure 1-5. Reactive sites of condensed tannins: (left) resorcinol type of A-rings; (right)
phloroglucinol A-rings
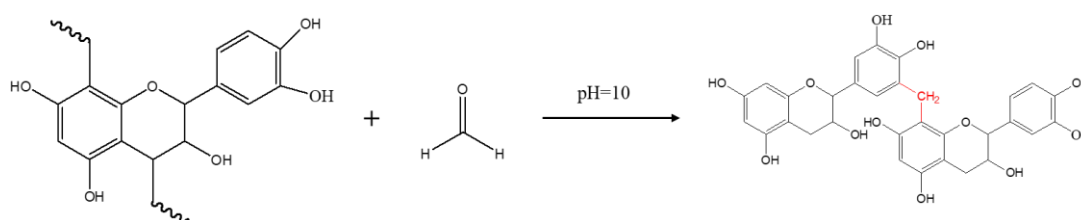
Figure 1-6. Polymerization of tannin and formaldehyde

Tannins have been described as being able to react with various aldehydes, including alkyl aldehydes, di-aldehydes, unsaturated carbonyl aldehydes. Formaldehyde, the most widely used aldehyde, exhibits the fastest reaction rate in both phloroglucinol and resorcinol type of tannins due to less steric hindrance [30]. The reaction mechanism is shown in Figure 1-6. However, the high reaction rate generally results in short pot-life and premature immobilization of the network and thus incomplete network formation. In general, the polycondensation of tannin and aldehydes can be performed in acidic (pH<3.3) or basic (pH>8) conditions [9,31]. In a study of García [30], the relationship between aldehyde/tannin reactivity and C-stage resin properties as a function of aldehyde chain length, functionality and unsaturation degree was investigated. With increasing chain lengths of alkyl aldehydes, the reactivity with tannin (pine) decreased while C-stage resins exhibited enhance of bulk density, T_g and thermal stability. However, the di-aldehydes and αβ-unsaturated aldehydes displayed an opposite trend. The polymerization condition of tannin with some aldehydes was shown in Table 1-2.

Table 1-2. *polymerization experiments of tannin(mimosa) with aldehydes, amounts, pH levels, and temperatures.*

Copolymer	Amount (%)	pH	Reaction T(°C)	Observations
Formaldehyde	4,6,8,25	Every	20 to 103	pH 2 and 9 harden at lower T
Glyoxal	12.5, 25	Every	90 to 103	Elastic solids
Glutaraldehyde	50	9	70	weak gel
p-Phthalaldehyde	12.5	9	50	two phases

Notes: T-temperature

1.5.1.2. Reaction with hexamine

The polymerization with hexamethylenetetramine (hexamine) was studied as a substitute for formaldehyde to avoid the toxic formaldehyde. The polymerization of tannins and hexamine is not at all a formaldehyde-yielding compound, yielding extremely low formaldehyde emission in bonded wood joints. The reaction condition is generally performed at high pH. Under such a base condition, hexamine tends to form very reactively but unstable intermediate fragments, mainly imines and imino amino methylene bases. These intermediate fragments rapidly react with tannin forming amino methylene bridges before yielding formaldehyde [32,33]. The decomposition of hexamine under alkaline conditions and the polymerization with tannins shown in Figure 1-7.

Figure 1-7. Schematic representation of the decomposition of hexamine to imino amino methylene bases in presence of a reactive species such as tannin to form (i) ionic polymeric complexes at ambient temperature and (ii) a stable benzylamine covalently bridged network during hardening, at a higher temperature, without producing or releasing any formaldehyde [32].

1.5.1.3. Reaction with furfuryl alcohol

Furfuryl alcohol is a green chemical commodity industrially produced by hydrogenation of furfural, which is obtained from the hydrolysis and dehydration of pentosan-rich biomass. The polymerization of mimosa tannin and furfuryl alcohol catalyzed by para-toluene-4-sulphonic acid has been reported. This reaction involves two main reactions, including the self-condensation of furfuryl alcohol and inter-polymerization of tannin-furfuryl alcohol, Figure 1-8. While, under acidic conditions, self-condensation is predominant. For the improvement of cross-linking between tannin and furfuryl alcohol, the reaction was also performed in alkaline conditions [34]. However, both in acid and alkaline conditions, aldehydes or diisocyanate are used occasionally for obtaining satisfactory performance in application [34,35].
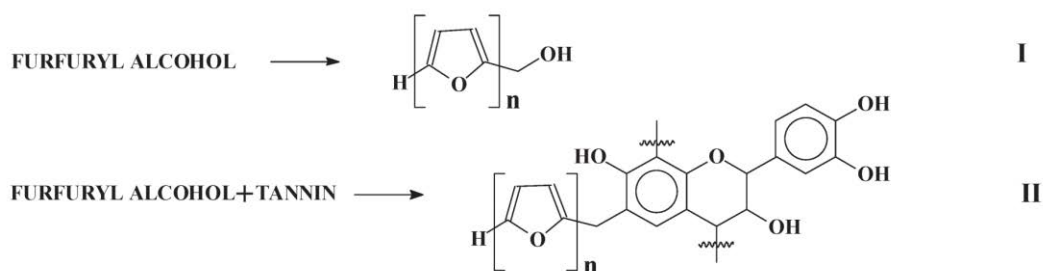
Figure 1-8. Proposed reaction scheme of a tannin and furfuryl alcohol [35]

1.5.1.4. Reaction with epoxy groups

The reactivity of epoxy resins is based on that of the epoxy group in or at the end of the aliphatic chain or on the aromatic ring. The high reactivity of the epoxy group is due to the high tension in the three-membered epoxide ring as well as to the polarity caused by the oxygen atom. This group is loosened by an electrophilic or nucleophile agent, and the curing may proceed by the effect of lewis-bases or lewis-acids or by compounds possessing active hydrogen. According to the study of the reaction mechanism of phenol and epoxy group, the phenolic hydroxyl displays high reactivity with an epoxy group [36]. Similarity reaction mechanism can be found in the reaction of pine tannins and ethylene glycol diglycidyl ether [8] (Figure 1-9).
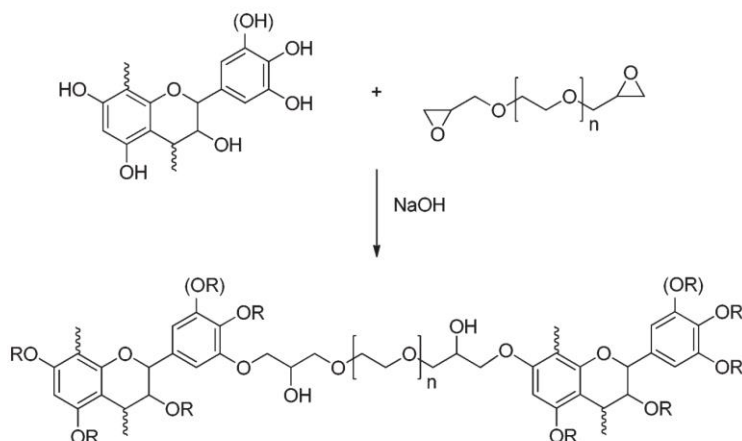
Figure 1-9. Reaction of pine tannins with ethylene glycol diglycidyl ether [8]

1.5.1.5. Reaction with isocyanates

The reactivity of diisocyanate and condensed tannin was studied by a model reaction of phenyl isocyanate and (+)-catechin [37]. The experimental results showed that the hydroxyl groups of (+)-catechin easily reacted with phenyl isocyanate to produce three major urethane derivatives. However, only the OH group in B-ring participated in this reaction with isocyanate [38] (Figure 1-10).

R=H, CONHC$_6$H$_5$
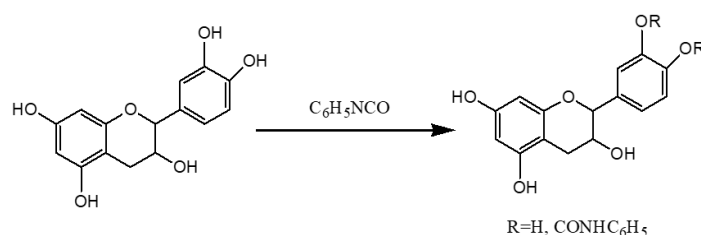
Figure 1-10. The reaction of catechin with phenyl isocyanate [38]

1.5.2. Esterification

Esterification is a routine pathway that is generally used to enhance the solubility of tannins for structural analysis. This reaction occurs in both phenolic and aliphatic groups of tannins and enhances tannin hydrophobicity. Whatever the level of esterification, tannin esters become thermoplastic with a melting point around 150 °C [8,39].

In general, tannins can be esterified by direct acylation using various reagents such as acyl chlorides and anhydrides with a catalyst (e.g. pyridine [39], 1-methylimidazole [40])(Figure 1-11). Solvent (e.g. pentanone, acetone, pyridine, and chloroform) can be used for better solubility of tannins. The reaction condition was summarized in

Table 1-3. Tannins can be esterified with anhydrides in different ester chain (acetic, propanoic, butyric and hexanoic anhydrides) [39,40]. The degree of substitution depends on the acid anhydride ratio, the catalyst level, and the anhydride chain length. Without catalyst results in a reduced degree of substitution, with this more obvious with increasing ester chain length. While preparation of tannin acetate with 1% catalyst achieved maximal substitution, synthesis of higher chain length tannin esters becomes increasingly difficult. However, esterifying tannins via acyl chlorides tend to be easier to prepare tannin ester with longer ester chains. The esterification of quebracho and radiate pine tannin was performed with stearic acid chloride catalyzed by 1-methylimidazole in acetone solvent with the protection of nitrogen [18]. With 6 molar ratio of stearic acid chloride to tannin, quebracho and pine tannin can reach the maximum degree of substitution. The degree of esterification results in greater organic solubility and higher thermal stability.

Recently, maleic anhydride was used as an esterification reagent for tannins. The reaction condition is shown in

Table 1-3. This derivation reaction can be performed in room temperature without obtaining side-chain products. The unsaturated polycarboxylic acid of maleinated tannin is desirable for polymerization pathways (e.g., radical, ionic, and coordination). Besides, they might improve the miscibility between polyphenols and selected thermoplastics [41].
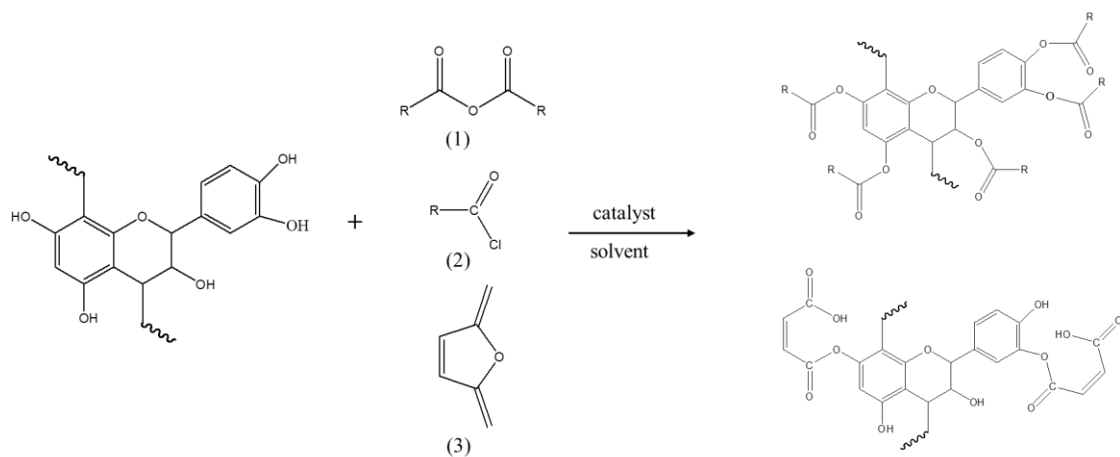
Figure 1-11. Tannins esterified with anhydrides (1), acyl chlorides (2), and maleic anhydrides (3).

Table 1-3. Reaction condition of conventional esterified tannins

Tannin	Reagent	solvent	catalyst	T(°C)	Time(h)	Ref
Pinus radiate	acetic, propanoic, butyric and hexanoic anhydrides	2-entanone acetone	1-ethylimidazole	70	4	[40]
Mimosa	acetic anhydride	No	pyridine	70	6	[39]
Pine bark/ quebracho	stearic acid chloride	acetone	1-ethylimidazole	*	3	[18]
pine bark	maleic anhydride	DMSO	No	20	24	[41]

Notes: * refers no mention in the reference.

Transesterification is also an interesting route to prepare tannin esters because it may provide different site selectivity compared to conventional acylation approaches [42]. An example of a transesterification pathway is shown as follow(Figure 1-12) and the reaction condition is summarized in Table 1-4. Each mixture was stirred for 48h. With this pathway, partially substituted tannin derivatives can be obtained with a preference for substitution at the catechol ring. These tannin laurates showed hydrophobicity and thermal stability to at least 100°C. In addition, partially substituted pine laurate retained moderate antioxidant capacity, offering promising properties for therapeutic applications or as an additive in the polymer system.
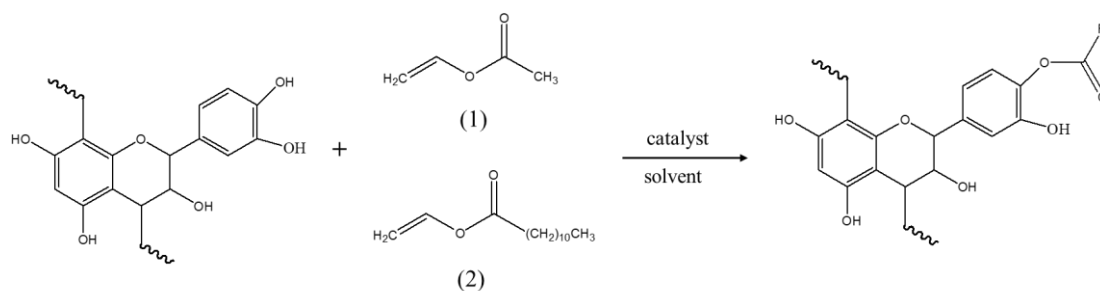
Figure 1-12. Tannins esterified with Vinyl Acetate (1) and Vinyl Laurate (2); R=CH$_3$ or (CH$_2$)$_{10}$CH$_3$

Table 1-4. Reaction Conditions and Degree of Substitution (DS) through Transesterification

Tannin	Reagent	solvent	catalyst	T(°C)	DS
Pine	Vinyl	Water/THF	KOH	20	0.2
Quebracho	Acetate				0.3
Pine	Vinyl	DMSO	TEA	70	0.9
Quebracho	Laurate				4.8

1.5.3. Oxyalkylation

The oxyalkylation is an important pathway to increase the reactivity and the accessibility of phenolic OH groups of biopolymers, such as lignin. Oxyalkylation is a ring-opening polymerization of alkylene oxides (e.g. propylene oxide(PO), and 1,2-butylene oxide (BO)) through OH groups [43]. The reactivity of -OH towards propylene oxide was A-ring $\geq$ B-ring $>$ C-ring [44]. The most common pathway to modify tannins with alkylene oxides is through base-catalyzed ring opening reaction. Potassium hydroxide (KOH) [22] and sodium hydroxide (NaOH) [45] are typical catalysts. The obtained products are usually a mixture of oxyakylated tannin and alkylene oxides homopolymer from the transfer reactions during the anionic grafting mechanism, Figure 1-13. In fact, alkoxy anions are formed from the OH groups of tannin in presence of catalyst resulting at the beginning of chain growth [46]. Main parameters of oxyalkylation are summarized in Table 1-5.

R= CH$_3$: Oxyprolylated tannin
R=CH$_2$CH$_3$: Oxybutylated tannin

R= CH$_3$: Poly(propylene oxide) homopolymer
R=CH$_2$CH$_3$: Poly(butylene oxide) homopolymer
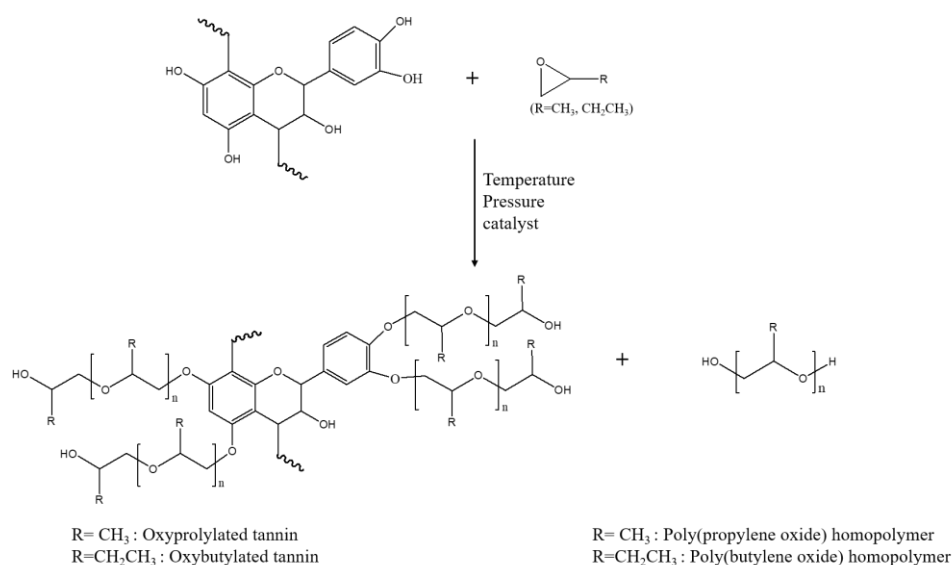
Figure 1-13. Reaction scheme for tannin oxypropylation

Table 1-5. Reaction Conditions of oxyalkylation

Tannin	Catalyst	alkylene oxides	Temperature (°C)	Time (h)	Ref.
Pine bark Mimosa Quebracho	NaOH	PO	20-22	24	[45,47,48]
Gambier	KOH	PO	150	X	[22]
Pine bark Quebracho	Triethylamine	PO	110	24	[46]
Pine bark/ Mimosa/ Quebracho/ Gambier	Potassium hydroxide	BO	150	X	[44]

Oxypropylation can be performed via mild derivatization [45,48]. Three condensed tannins (pine, mimosa, and quebracho) were modified with PO in aqueous alkali at room temperature (20~22 °C) with a reasonable yield range from 60-90%. The experimental results showed that mimosa and quebracho tannins are less reactive toward hydroxypropylation compared with pine tannin [48]. These derivatives displayed better solubility in organic solvents, thermal stability, and lower glass transition temperature (T_g) compared with unmodified tannin [46]. The obtained tannin oligomers were detected as high structural heterogeneity [44].

Another synthesize route was performed in a high-pressure batch reactor at high temperature with pressure. A fully oxypropylated tannin modified with PO catalyzed by KOH at 150 °C under stirring. This oxypropylated tannin had a final bio-based content of up to 42%. Bridson [49] presented an efficient, one-pot solvent-free synthesis using mild base catalysis (triethylamine) to prepare hydroxyalkylated tannin with a Teflon-lined stainless steel pressure reactor. The etherified products were obtained in very good isolated yield (≥80%) at 1–5 mol equivalents of PO and moderate yield (28–84%) at higher PO ratios. The BO can also be an interesting alkylene oxide for tannin oxyalkylation since it can be easily biobased and biosynthesized from biomass. For the

first time, tannins (e.g. pine, mimosa, quebracho, gambier) were oxybutylated to obtain aromatic and fully biobased polyols. This reaction was carried out using potassium hydroxide as a catalyst, in a high-pressure batch reactor, without solvent. The oxybutylation reaction mechanism is presented in Figure 1-14.
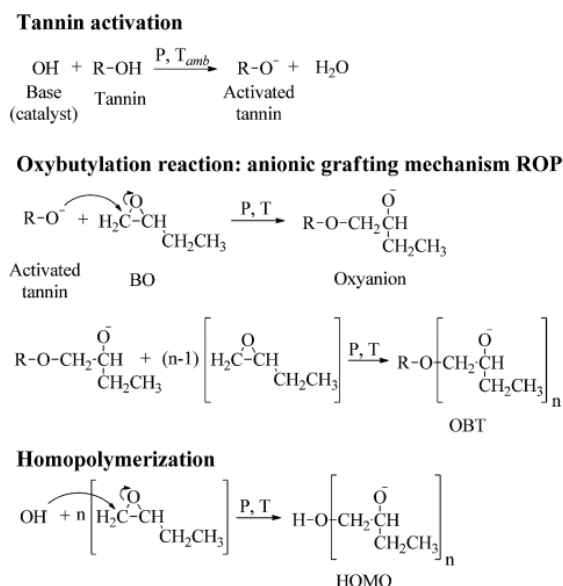
Figure 1-14. Schematic representation of the oxybutylation reaction mechanism with tannin activation, anionic grafting reaction, and homopolymerization steps [46].

1.5.4. Benzoylation

Benzoylation of tannins was carried out to reduce the number of -OH group according to the Schotten-Baumann method (Figure 1-15) [50]. This reaction can be used to prepare tannin-based polyurethane for reducing the cross-linking network of the final product to avoid brittle character. Besides, sugars can be easily separated from tannins during the precipitating process in aqueous solution. In the study of Sunija, tannin from *cashew nut* husk was benzoylated by treatment with benzoyl peroxide in the presence of 10% NaOH. This benzoylated tannin was used to prepared thermosetting polyurethane [51]. Besides, this method was also reported to modify natural fibers for improving their compatibility with thermoplastic matrix [51].
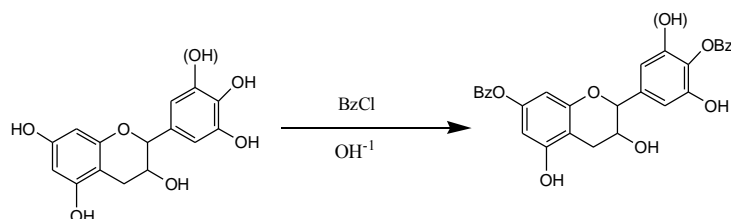
Figure 1-15. Benzoylation of tannin according to the Schotten–Baumann method

1.5.5. Epoxidation

Tannins can be functionalized by the reaction with epichlorohydrin in the presence of a catalyst. The epoxidation of catechin was initially substituted bisphenol-A diglycidyl ether because of its toxicity. Two epoxidation pathways of catechin are shown in Figure 1-16 and reported reaction conditions of tannins were summarized in Table 1-6. *Reaction conditions of epoxidation*. The widely used reaction is as following: (1) the tannin is dissolved in NaOH solution and stirred vigorously at 60 °C for 30min; (2) epichlorohydrin is added and the mixture is heated at 98 °C for 3 or 4 hours [52–54]. For mimosa tannin, this reaction is performed at 80 °C for 3 hours [55]. The other was reported by Benyahya [56], tannins, epichlorohydrin and benzyltriethylammonium chloride (BnEt$_3$NCl, 0.05 Mequiv./substrate) were firstly reacted at 100 °C for one hour. Then, the second reaction was performed at 30 °C with 20 wt% (2 Mequiv./OH) an aqueous solution of NaOH and 0.05 Mequiv. of phase transfer catalyst (BnEt$_3$NCl) were added.
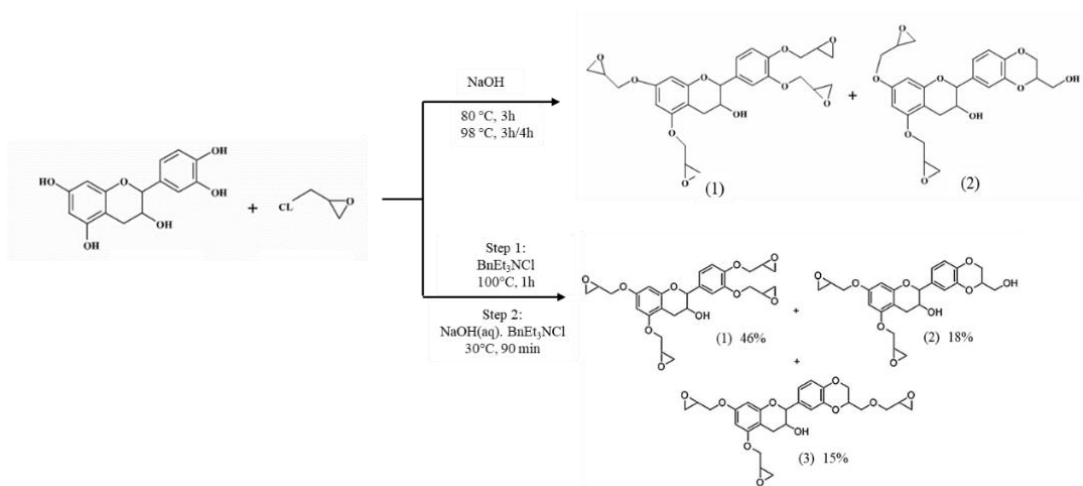
Figure 1-16. Reaction of catechin glycidylation

Table 1-6. Reaction conditions of epoxidation

Tannin	Reagent	catalyst	Temperature(°C)	Time	Ref.
green tea		BnEt$_3$NCl	100	60min	[56]
			30	90min	
eucalyptus bark	epichlorohydrin	NaOH	98	240min	[53,54]
mimosa		NaOH	80	180min	[55]

1.5.6. Grafting reaction

To improve the compatibility of tannins with biodegradable polyester. A novel

tannin grafted polycaprolactone is firstly synthesized via ring-opening polymerization reaction by Song et al [57]. This grafted tannin was described to maintain the tannic bioactivity. The grafted tannin had less experimental molecular weight than the theoretical because of the complicated stereo structure and large steric hindrance of tannin, but the polydispersity of grafted tannin is narrow. The tannin grafted polycaprolactone is changed from amorphous form to crystalline structure and it is soluble in chloroform.
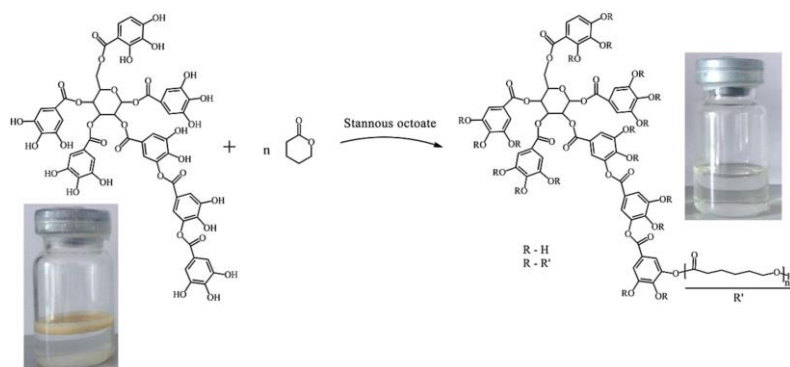
Figure 1-17. Synthetic pathway for tannin grafted polycaprolactones and their dissolubility in chloroform

2. Tannins towards material science

Tannins have been discovered a long time ago due to their ability to precipitate proteins in animal hides and they have been initially used in the leather industry. As polyphenols, condensed tannins also present a great potential for use in various fields because of their multifunctional character and high abundance. Tannins utilizations include anticorrosive and antifouling agent for varnish primers or coating of metals [58–60], flocculant agent [35,35] to remove anionic pollutants in water or wastewater, selective depressant [50,61,62] in the flotation process, fluidifying agent for drilling mud [63], plasticizing additives for cement [38], precursors for wood adhesives [7,9]. However, an increasing number of studies has been published concerning the innovative utilization of tannins in material preparation over the past decades. Among them, tannins have been exploited to prepare composites compounded with natural reinforcements, like non-woven mats of flax or hemp fibers. Tannins have also been explored to prepare rigid and flexible foams, with applications as insulating materials, adsorbents for wastewater treatment, or precursor for carbon foams. Besides, the reactivity of tannin OH groups have been utilized to prepare different kinds of polymers, such as polyols or polyurethanes. More recently, application in

thermoplastics as functional additives have been reported. In this section, the innovative application of tannins in material science will be presented in detail.

2.1. Tannin-based thermoset materials

2.1.1. Material based on tannin-aldehydes/ hexamine resin

In the early 2000s, new composites were developed by utilization of renewable filler and resins. These materials were expected to combine low cost, low environment impact, and good mechanical property. Mosiewicki [64] described tannin resin crosslinked with hexamethylenetetramine and pine wood floor as reinforcing material to prepared composites materials. The obtained product displayed good flexural and compression mechanical properties but was very sensitive to humid environments. The author [65] considered that the incomplete curing of tannin resin and the high number of inert hydroxyls and polar ammonia groups from the hexamine decomposition in the final material should be blamed for this poor moisture resistance. Thus, the addition of rubber was expected to improve the toughness and reduce water uptake because of its low polarity. However, the addition of rubber was found to improve the flexibility properties without improving the water-resistant capacity in the composites.

The composites made from non-woven mats of flax and hemp fibers as reinforcement in tannin-hexamine and tannin-lignin-hexamine based matrices have been reported. These composites were successfully prepared in high, medium and low density [66,67]. The composites based on tannin-lignin-hexamine based resin as a matrix presented thermoplastic property after a first pressing. The flat sheets can be thermoformed into the shape wanted after the first pressing. Based on these applications, Zhu developed tannin-based flax fiber reinforced composites by modifying flax fiber fabric configurations [68] for structural applications in vehicles. Sauget [69] suggested a two-step mats preparation method: full drying of the pre-impregnated mats for storage first and then rehydratation (with a moisture content of 20% on dry material) just before pressing under slow curing at low temperature (130°C for 35 min). Besides, the tannin-hexamine resin was prepared without the addition of NaOH. With these methods, the final product had a good modulus of elasticity and tensile strength in traction as well as good resistance to water swelling.

2.1.2.   Material based on tannin-furfuryl resin

Considerable interest has been generated in the utilization of tannin-furfuryl resin due to their renewable, environment-friendly raw composition together with lower cost and ease of preparation.

Based on the polymerization of tannin and furfuryl alcohol, a 100% bio-sourced thermosetting plastic material has been prepared [70]. This material was found to have a high glass transition temperature (211 °C) and good thermal property. The 95% weight loss occurred at 244 ℃ in a nitrogen and 240 °C in an air atmosphere and its char yield as high as 52%. Moreover, this new thermoset material shows excellent mechanical properties: a Brinell hardness of 23 HBS, which is higher than commercial acrylic, polyvinyl chloride, and a little lower than that of solid polystyrene. The compressive break strength was found to be as high as 194.4 MPa, thus higher than that of filled phenolic resins, and much higher than that of solid polystyrene and of acetal resins. Highly flexible films have also been prepared by reacting partially aminated tannins with furfuryl alcohol plasticized by glycerol or polyethylene imine [71].

Tannin furfuryl alcohol resin can be filled with abrasive particles of aluminum trioxide to develop cutting and grinding discs. These discs were characterized and showed excellent abrasiveness and cutting properties. Their mechanical resistance was found to be comparable to that of commercial grinding discs bonded with synthetic phenolic resins [72]. Another application is the incorporation of inorganic particles and fibers to process automotive brake pads, for which the mechanical resistance was found to be comparable to that of commercial automotive brake pads bonded with synthetic phenolic resins [73]. Tannin furfuryl alcohol resin reinforced with nonwoven flax fiber mat was reported to manufacture green composites. These composites displayed lightweight with good mechanical properties and a very short curing time with a regular hot press [73].

Tannin-furfuryl alcohol resin can apply to paper sheets impregnation cover for panels. These impregnated papers performed excellent water vapor resistance, the cross-cut test and abrasion resistance were comparable to papers impregnated with MUF resin according to relevant standards [74]. Similar performance can be found in high-pressure paper laminates based on tannin-furfuryl alcohol resin [75].

Tannin furfuryl resin was also reported as an alternative for formaldehyde free, environment-friendly adhesives from renewable materials to process panel [34]. For a

better bonding performance, such adhesive can be modified by formaldehyde [76].

The most studied application of tannin-furfuryl resin is rigid foams [7,77]. For obtaining foam materials, the blowing agent was generally used. The polymerization process generates heat, thus, low boiling point blowing agent evaporates during the curing process. By controlling the amounts and type of blowing agent and catalyst, foams generate different property and density [35,76,77]. Ingredients like aldehydes/diisocyanate, plasticizer, and filler sometimes used for guaranteeing quantity crosslinked network, improving the flexibility or mechanical property [78–80]. These rigid foams displayed excellent thermal stability, fire resistance, acoustic insulation, a wood/foam sandwich panels have been developed for sound and fire insulation. Moreover, tannin resin-based foams as adsorbents were widely reported for wastewater treatment and catalyst supports [81–84].

2.1.3. Material based on epoxy resin

Tannin can be used as a treating or coating composition for epoxy resin for imparting excellent corrosion resistance to metals and exhibits excellent substrate and intercoat adhesion [85]. In this context, the reaction of tannins with diglycidyl and polyglycidyl ether type epoxide resins is the most described [85]. Recently, tannins were studied to react with epichlorohydrin, forming glycidyl ether derivatives [56,83,86]. These tannin epoxy derivatives were cured with isophorone diamine to obtain epoxy resins. These tannin-based epoxy resins showed a high thermal resistance and interesting mechanical properties due to a high crosslinking density. Khundamri [87] also presented a flexible epoxy foam synthesized from epoxidized soybean oil and epoxidized mangosteen tannin without a catalyst. The epoxidized tannin was used as a reinforcing material to co-crosslink with epoxidized soybean oil and methyltetrahydrophthalic anhydride because of its rigid benzene ring. The foam density and compressive strength were increasing with increase epoxidized tannin content. Such foam material showed subzero T-g (-6.5 to -5.4 °C) and semi-closed cells with irregular shapes.

2.1.4. Material based on polyurethane

Tannins were investigated as a copolymer component for polyurethane material. It was found that tannin had a positive effect on the density of crosslinking, miscibility of components and the morphology of starch-based polyurethane, improving thermal

behavior and mechanical properties of films [88]. Besides, tannins incorporated with polyurethane coating displayed improvement of coating adhesion and accelerated curing rate [89]. A highly flexible/elastic partially bio-sourced polyurethane foam obtained by the simultaneous copolymerization of condensed flavonoid tannins with an alkoxylated fatty amine and polymeric diphenylmethane isocyanate. In this study, tannin also contributed to flame retardant capacity [90].

Polyurethane was also developed from isocyanates (e.g. diisocyanate, polymeric methylene diphenyl diisocyanate, methylenediphenyl diisocyanate, hexamethylenediisocyanate) with benzoylated [91] or oxypropylated tannins [19] as hydroxyl source. Benzoylated tannins-based polyurethanes were investigated as surface coatings and wood adhesives with the addition of small amounts of tannin/formaldehyde cold-setting adhesives [9]. More interesting applications could be developed as foam materials. The density of polyurethane foams was adjustable by controlling the addition of the catalyst, the isocyanate/hydroxyl group ratio, and the water content [92]. These polyurethane foams had the abilities to adsorb heavy metal ions and protein and had good performance in biodegradation and bacteriostasis [92].

Tannins were investigated as copolymer components for polyurethane materials. It was found that tannin had a positive effect on the density of crosslinking, miscibility of components and the morphology of starch-based polyurethane, improving thermal behavior and mechanical properties of films [88]. Besides, tannins incorporated with polyurethane coating were found improvement of coating adhesion and accelerated curing rate [93]. Besides, a highly flexible/elastic partially bio-sourced polyurethane foam obtained by the simultaneous copolymerization of condensed flavonoid tannins with an alkoxylated fatty amine and polymeric diphenylmethane isocyanate. In this study, tannin also contributed to flame retardant capacity [90].

2.1.5. Material based on polyesters

Bio-based polyesters have been produced from fatty acid modified tannins. Polyester thermosets have been prepared from copolymerization of condensed tannin-fatty acid esters with vegetable oils. Polymer films ranging from soft rubbers to rigid were obtained by oxidative copolymerization of tannin linoleate/acetate mixed esters with linseed oil and tung oil catalyzed by cobalt/zirconium metal driers. Here, the aromatic rings of tannin esters provided rigidity and unsaturated chains performed as

crosslinkers. A rubber-like material was prepared similarly with tannin oleate esters and vegetable oils.

2.2.   Tannin-based thermoplastics materials

Functional additives are important components of plastic material, which contribute to heat stability, UV stability, plasticization, nucleation, flame retardancy, and impact modification [89]. Driven by the environmental concerns, biopolymers as plastic additives have to gain interesting during the past decades, including cellulose, lignin, and vegetable oils, etc. However, the utilization of tannins has only been emerging for a decade. Tannins were investigated as good antioxidants for thermoplastics. However, the problem of incompatibility between the hydrophilic tannin and the matrix is to be managed. With high hydrophilic polymers content, a sharp decrease of mechanical properties of the final product was generally found. To address this problem, various modification pathway of tannins and few studies concerning the addition of compatibilizer were reported to enhance the compatibility of tannins and thermoplastic.

2.2.1.   Thermoplastics based on native tannins

Tannins as well-known natural antioxidants [94], tannins rich products or tannins without modification were exploited as stabilizers for UV sensitive petroleum-based thermoplastics, including polypropylene (PP), polyvinyl chloride (PVC), polyethylene (PE). According to these studies, tannins display radical scavenging properties, reducing the impact of thermo-oxidative and UV degradation. It should be noted that the mechanical properties of the plastics were slightly altered in the presence of low tannins concentration. In the study of Nanni [95], PP blended with tannin-rich byproducts (6%), solid wine wastes (peels, seeds, and stalks) were also displayed stable capacity without significantly affecting the mechanical property, but this capacity was not sufficient compared with commercial tannin extract. Ambrogi [96] and co-workers studied the stabilization property of tannins rich products and other phenol by-products on PP. Compared to commercial phenolic antioxidants and according to experimental results (thermogravimetric analysis and oxidative induction time measurement) tannins exhibited very good results. Samper [97] evaluated the stabilizer capacity of tannins on PP by using several natural phenolic compounds derived from the structures of flavonoids: a flavone (chrysin), a flavanol (quercetin), two flavanone glycosides (hesperidin and naringin), and flavanoligand (silibinin). The experimental results

confirmed that flavonoid compounds in the type of quercetin and silibinin provide the best results in stabilizing both against oxidation and against the action of UV radiation. Olejar [98] also evaluated the antioxidant of grape tannin on both PP and PE. Significant antioxidant activity was observed at 1% tannin inclusion in all polymer blends. The antioxidant activity was observed to increase steadily with a greater concentration of grape tannins, the highest increases being seen with polypropylene. The mechanical and thermal properties of the polymer films following antioxidant incorporation were minimally altered with up to 3% grape tannins [98]. Besides, the synergetic function of tannins used as co-stabilizer for PVC was investigated by Shnawa and have shown an improvement in thermal stabilization and thermal stability and did not cause negative impacts during production process [99]. Pine bark tannin and mimosa tannin were demonstrated as effective short-term stabilizers for low-density PE films, increasing the oxidative induction time measurement of low-density PE and improved the strength and elongation retention after accelerated weathering.

The native tannin as filler material of poly (lactic acid) (PLA) was found in the report of Answer [100]. The experimental results reveal a worse dispersion and a larger particle size of tannin in the PLA matrix compared with lignin, resulting in worse thermal and mechanical properties. Unlike lignin, tannin lack of the softening characteristic at the processing temperature, and high chemical reactivity of tannin inducing crosslinked network, which may be contributors to a greater particle dispersion capability. Therefore, in the case of tannin chemical modifications seem to be necessary for composite applications. Besides, without modification, the poor adhesion between tannin and PLA matrix resulted in poor tensile strength especially with higher filler content (15%). As a result of this incompatibility, even with low tannins content (5% of native tannins), the condensed tannin / PLA is difficult to process [101]. However, in the study of Sunthornvarabhas [102], a kind of PLA submicron fiber (500-700 nm, Figure 1-18) containing 14.3 and 22.3 wt% tara tannin with antioxidant capacity, was successfully produced by electrospinning process. This encouraging result is related to the mixing process pathway and to the chemical structure of tara tannin. PLA and tannin were mixed through the solution, which can improve the dispersion of tannins in the polymer matrix. Moreover, tara tannin is a hydrolyzable tannin mainly composed of galloylated quinic acid structure[103]. The ester linkage and low degree of polymerization make it easier to disperse in the polymer

matrix compared with condensed tannin.
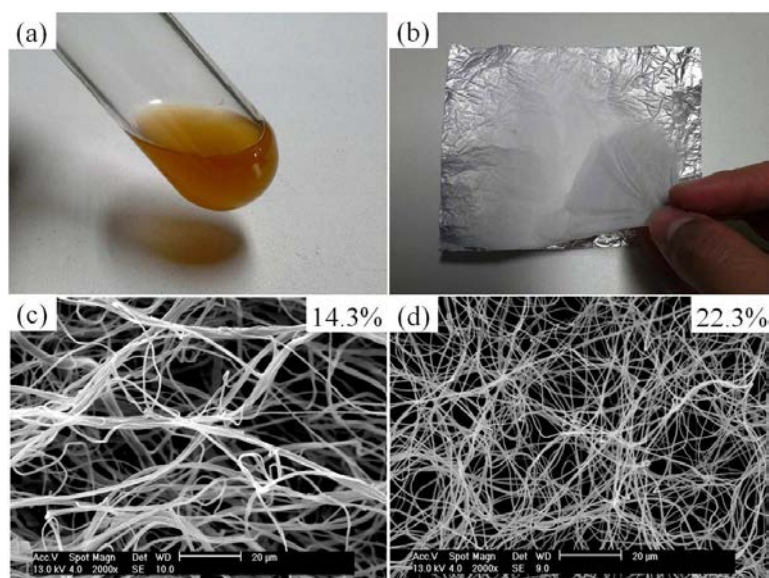
Figure 1-18. Images of mixed solution between tara tannins and polylactic acid (a) before and (b) after the electrospinning process. Images of electron micrographs of composite fiber at different loadings: (c) for 14.3% and (d) for 22.3%. From ref[102].

Good compatibility of native tannin can be found in the incorporation with polyvinyl alcohol (PVA) [104] because both larch bark tannin and PVA are rich in hydroxyl groups. This green food packaging materials for antioxidant and ultraviolet (UV)-protective. The mechanical and crystallization properties of the composite membranes did not significantly decrease with the addition of larch bark tannin.

2.2.2. Thermoplastics based on modified tannins

2.2.2.1. Esterified tannins

Tannin esters demonstrated good compatibility and dispersion capacity with various plastic. In the study of Grigsby [40], condensed tannins derived from radiata pine barks were modified by acetic anhydride as natural additives of PBS. The dispersion and compatibility of tannin acetate were characterized by IR chemical imaging. Those tannin acetate particles exhibited some heterogeneous phase in PBS matrix because of the agglomerates of tannins. However, those particle sizes ($< 100\mu m$) can be completely wetted by PBS with good compatibility. According to the study of Grigsby [105], tannins modified with longer ester chain can significantly reduce their incompatibility in the biodegradable plastic matrix (Figure 1-19), including PLA, poly(hydroxybutyrate-co-hydroxyvalerate), and poly(butylene succinate adipate).

Those tannin esters bearing long ester chain appear to be more attractive as PLA plastic additives because of lower melting temperatures, leading to better processability. However, the substitution of higher chain length on tannin flavonoid units becomes increasingly difficult due to the increasing steric hindrance. It should be noted that the esterification of tannin reduced UV absorbance capacity to some extent according to the substitution degree, negatively affecting their UV protection role on plastics. However, each tannin ester neither has a significant effect on the mechanical property of those biodegradable plastics with compounding with less than 10% tannin, nor their biodegradation capacity.
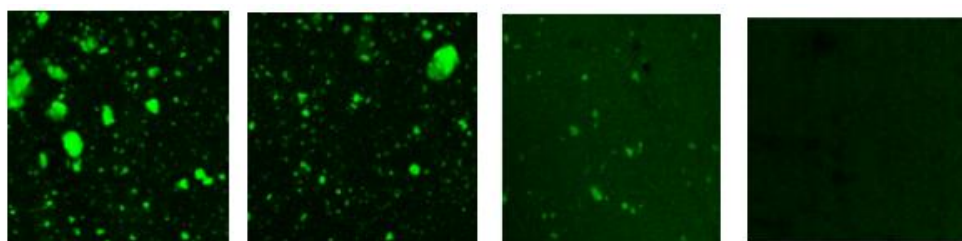
Figure 1-19. Confocal microscopy images: the distribution of tannin esters bearing different ester chain dispersed in PLA matrix

In order to better investigate the functional role of tannins in plastics, anti-UV, anti-oxidant, reinforce function were studied in the different plastic system. Reconfirmed by Grigsby[106], tannin esters, as well as native tannin up to 10% concentration, have minimal effect on plastic mechanical properties. However, the diversity of stable function occurred between native tannin, partly esterified tannin, and fully esterified tannin in polypropylene and the aliphatic polyester Bionolle. Both tannin esters contributed to the prevention of oxidative degradation on both polypropylene and Bionolle. The stabilize function depends on the esterification degree, partly esterified tannin esters having greater efficacy than a synthetic UV stabilizer at comparable loading.

Another study of Grigsby developed tannin acetate as a reinforcement of PLA fiber[101](Figure 1-20). PLA with up to 50% tannin acetate content can be readily processed by melt spinning. This promising melt spun fibers tend to be precursor fibers for processing textiles or carbon fiber. It should be noted that PLA blend with native tannin as well as partly esterified tannin, even in only 5% loading content with the presence of transesterification catalyst is unsuitable for fiber process due to the poor compatibility. PLA fiber can be easily processed with fully esterified tannins to achieve

high tannin content fiber. However, the transesterification catalyst does not de-esterify the tannin acetate nor lead to transesterification between tannin and PLA chains. PLA polymer properties and NMR relaxation parameters suggest higher tannin acetate content gives a greater change to PLA molecular mobility and reduced crystallinity and thermal stability, particularly in the presence of the transesterification catalyst.
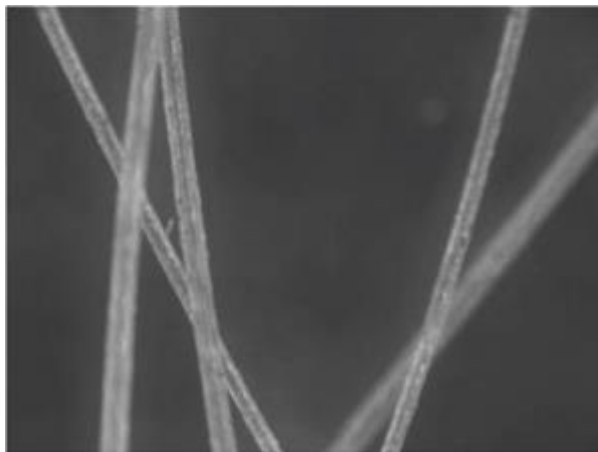
Figure 1-20. Tannin reinforced PLA fiber[101]

Tannins can be also esterified with maleic anhydride. These maleinated tannins were investigated as functional additives for PLA, PE, and polystyrene (PS), contributing to better miscibility[41]. An increase in the polyphenol amount in the blends led to a decrease in the decomposition temperature in PLA-based blends. An increase in the polyflavonoids load increased the elasticity modulus (E) of the PS- and PLA-based blends.

2.2.2.2. Hydroxypropyl tannins

Hydroxypropylated tannin as a functional building block for PLA was studied by García[47]. In this report, with the help of binary- and ternary- blends and plasticizer polyethylene glycol (PEG), relative high content (up to 40%) of hydroxypropylated tannin can be compounded with PLA. This tannin derivative performed good miscibility, processability, and nucleating agent. Bridson[49] proposed an application of the hydroxypropylated tannins by compounding with poly(lactic acid) to produce high tannin content(up to 50%) melt-spun fibers((ca. 30–50 μm diameter). Unlike compounding with tannin ester, high content of glycerol as a plasticizer is important for melt spinning. Compared with PLA/tannin ester blend with the proportion of 75/25, the use of a transesterification catalyst (DBTO) in the absence of glycerol also led to the successful formation of PLA fibers. Another potential utility of hydroxypropyl

tannin was presented by Garcia [107] through an in situ polymerization pathway(melt-blending urethanization, Figure 1-21). The polymeric methyl diisocyanate was applied to improve the compatibility between hydroxypropyl tannin and PLA matrix through the polymerization between polyflavonoids and isocyanate during the melt-blending. The urethanization during the melt-blending was evidenced by: (1) the carbamate moiety (R1–O–CO–NH–R2) identified by the FTIR analysis, (2) the atypical fluorescence pattern detected by confocal microscopy, and (3) the second T_g of the blend from the DSC-thermogram. Urethanization can be recognized as a viable strategy to enhance the compatibility between highly polar biologically active polyflavonoids, and the biodegradable PLA-polymer for plastic engineering.
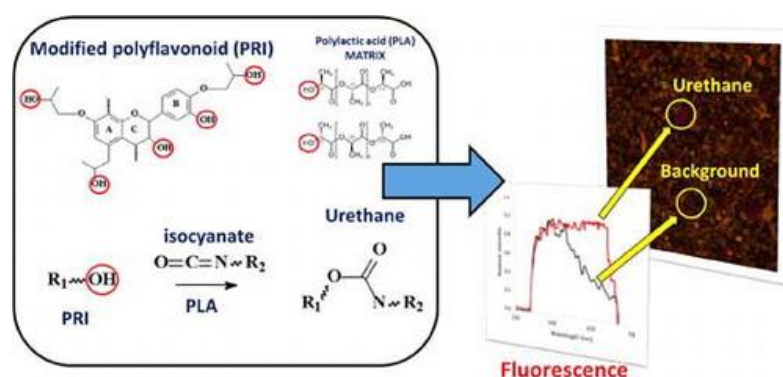
Figure 1-21. melt-blending urethanization pathway. Left: Possible reaction mechanism; right: confocal image illustrating particles[107].

2.2.2.3. Epoxied tannins

Epoxy compounds are well known as a typical nonmetallic stabilizer. Tannin-based epoxy resin has been described to have the ability to work as primary and secondary thermal stabilizers for poly (vinyl chloride) (PVC) [53,54]. The addition of tannin epoxy resin provided enhanced dynamic thermal and process stability and improved the rheological properties, which are comparable to commercial thermal stability. Besides, PVC incorporated with tannin epoxy resin exhibited smooth and homogenous surface properties compared to the Ca/Zn-based commercial thermal stabilizer.

2.2.2.4. Copolymerized tannins

The possibility of tannin copolymer with various chemicals was discussed in the previous section (1.5.1). For promoting the compatibility of tannin and linear low-density polyethylene (PE), Bridson used various copolymers, including ethylene vinyl

alcohol, maleic anhydride modified polyethylene and ethylene acrylic ester maleic anhydride [108]. The better compatibility was confirmed by smaller tannin particle size and it had positive effects on thermo- and UV- oxidative stability of PE films.

Tannin grafted polyvinyl chloride (PVC) copolymer was reported by Shnawa [109]. The concentration of antioxidants is an important factor for the effectiveness of oxidative resistant capacity. However, the concentration of antioxidants gradually decreases during long term uses. Grafted high content of antioxidants into polymer chains by chemical reactions is an effective attempt for long term protection. Besides, it tends to be a potential pathway to improve the compatibility of biopolymers and plastic matrix. This PVC derivative was investigated as a polymeric antioxidant for high-density polyethylene (HDPE). According to the differential scanning calorimetry (DSC) scans, the oxidation reactions of HDPE was retarded to a higher temperature. A tannin-grafted poly(ε-caprolactone) was used to blend with poly(L-lactic acid)(PLLA) to create novel materials of skin tissue engineering. This grafted tannin inhibited good compatibility with PLLA, smooth and thin fiber can be obtained via electrospinning. This fibrous membrane shows higher tensile strength and elongation at a break with incorporated with 15 wt% tannin-grafted poly(ε-caprolactone). This fibrous membrane is a promising candidate for skin tissue engineering due to its biocompatible and biodegradable capacity [110].

Shnawa also investigated the modification of tannin with cadmium complex [111]. The stabilizing efficiency of tannin-cadmium is superior to that of synthetic thermal stabilizer applied as a reference due to the HCl scavenging and antioxidation activities of tannin-cadmium. Besides, it had good performance in thermal oxidation resistant (Figure 1-22).
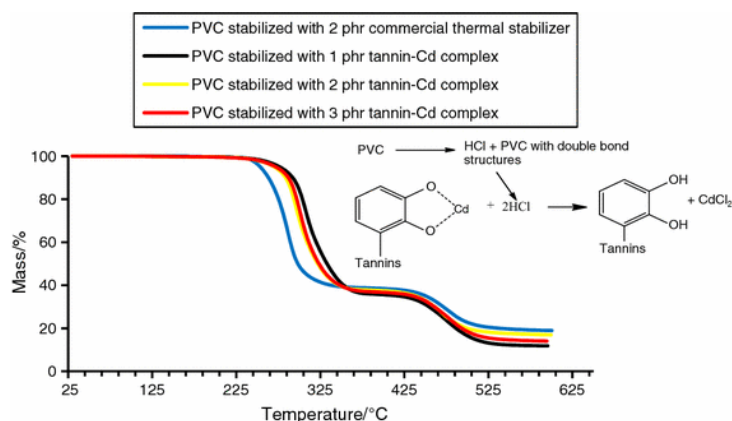
Figure 1-22. PVC stabilized with tannin-cadmium complex

2.2.2.5. Crosslinked tannins

In our recent work [112], tannin copolymerized with hexamine incorporated with polypropylene (PP) via dynamic curing extrusion. According to experimental results, tannins performed as reinforcing components for polypropylene with anti-UV properties. The copolymerization of tannin-hexamine during extrusion, thermoset particles were formed, improving Young's modulus, crystallinity, and thermal stability and reinforce the internal network of polypropylene. In this study, crosslinked tannins were investigated have good anti-UV property, polypropylene had fewer surface cracks, lower carbonyl index, fewer crystallinity decreases and less mechanical properties loss with increasing tannin content after UV accelerated weathering.

Part II   **Composites based on PP/PLA and biopolymers**

1. Introduction

A composite material is a duplex and multifunctional material composed of at least two components working together to produce a structural material with mechanical and physical properties that are enhanced compared with the properties of the components taken separately [113]. The composites generally have two phases: a continuous polymer matrix, and discontinuous fibers or particle phase (Figure 1-23). The mechanical and physicochemical properties of composites are commonly superior to those of the matrix material caused by the distinctive characteristics of fibrous or particulate component [114]. This component in the discontinuous phase is used to change and improve the physical and mechanical properties of the polymer matrix, which can be divided as reinforcements, fillers, and additives according to their functionalities. Reinforcements are stiff and strong, they can improve stiffness and strength of polymer matrix, generally, fibrous type reinforcement increases the mechanical properties of polymer composites while particular type reinforcement increase the modulus. Fillers are commonly used for the purpose of cost reduction or improve electrical and thermal conductivity. Additives (e.g. plasticizers, flame retardants, impact modifiers, heat stabilizers, antioxidants, light stabilizers, etc.) are mainly for maintaining and/or modifying polymer properties, performance and long-term use [115]. The main effects of reinforcements, fillers, and additives on polymer properties were summarized in Table 1-7 [116].
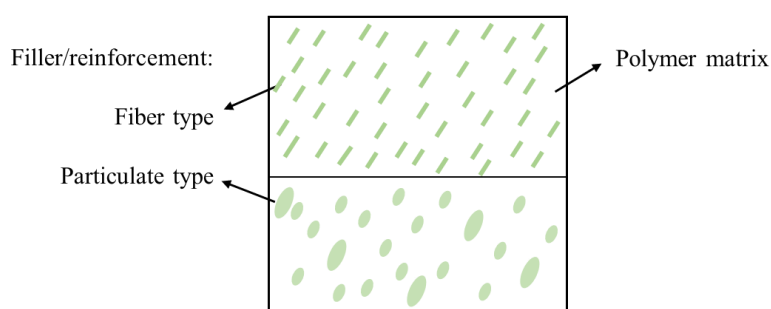
Figure 1-23 Structure of polymer composites

Table 1-7 main effects of reinforcements, fillers, and additives on polymer properties

Reinforcement/filler/additive	Examples	Effects on polymer properties
Reinforcing fibers	Carbon, fibrous minerals, glass	Increases tensile strength; Increases flexural modulus; Increases heat-deflection temperature; Resists shrinkage and warpage.
Extender Fillers	Calcium carbonate, silica, clay	Reduces material cost.
Conductive fillers	Aluminum powders Carbon fiber, graphite	Improves electrical and thermal conductivity.
Flame retardants	Chlorine, bromine, phosphorous, metallic salts	Reduces the occurrence and spread of combustion.
Coupling/ compatibilizing agents	Silane coupling agents; grafted maleic anhydride (MA)	Improves interface bonding between polymer matrix and reinforcement/filler/additives, especially at high filler contents.
Plasticizers	Monomeric liquids, low-molecular-weight materials	Improves melt flow properties Enhances flexibility.
Antioxidants and heat stabilizers	Radical Scavengers Peroxide Decomposers	Reducing oxidation and long-term discoloration from additive interactions.
Nucleating agents	Aromatic carboxylic acid salts talc or calcium carbonate(low content)	Higher crystallization and processing rate.
Antimicrobial agents	Lubricating migratory amide slip agents, polysiloxane (silicone oil) lubricants (such as polydimethylsiloxane, PDMS), grafted polymer agents, nanoclays	Infection-free medical polyolefin surfaces.
Gas barrier properties enhancement	Nanofillers Oxygen scavengers	Preventing or controlling the passage of oxygen and moisture through thin polymer layers.

Driven by the gradually diminishing of global petroleum resources, along with awareness of global environmental problems, a switch from the petroleum-based materials to renewable resources-based materials have been promoted. Remarkable attention has been paid to the eco-friendly, green and sustainable biopolymers to

develop composite for various applications in the past decades [114,115,117,118]. These biopolymers are polymeric biomolecules produced by living organisms, which contain monomeric units that are covalently bonded to form larger structures. In contrast of petroleum-based polymers will eventually deplete, they are sustainable and renewable since they derived from plant materials [119]. In nature, forestry crops/residues and agricultural crops/residues can provide a broad range of materials or biopolymers, including natural fibers, cellulose, hemicellulose, lignin, tannin, starch, oil, etc, (Figure 1-24). The advantages of using biopolymers in composites are generally their low cost, low environment impact and low specific weight compared with fossil-based polymers. In addition, each biopolymer contains individual physicochemical property; as a result, a wide range of biopolymers can substitute fossil-based reinforcement, filler, or functional additive in composites formulation[117,120,121].

Part II will discuss composites based on PP/PLA and biopolymers from two main questions:

- Why PP and PLA are important as the polymer matrixes for composite preparation?

- What kind of functional role of biopolymers for PP and PLA?
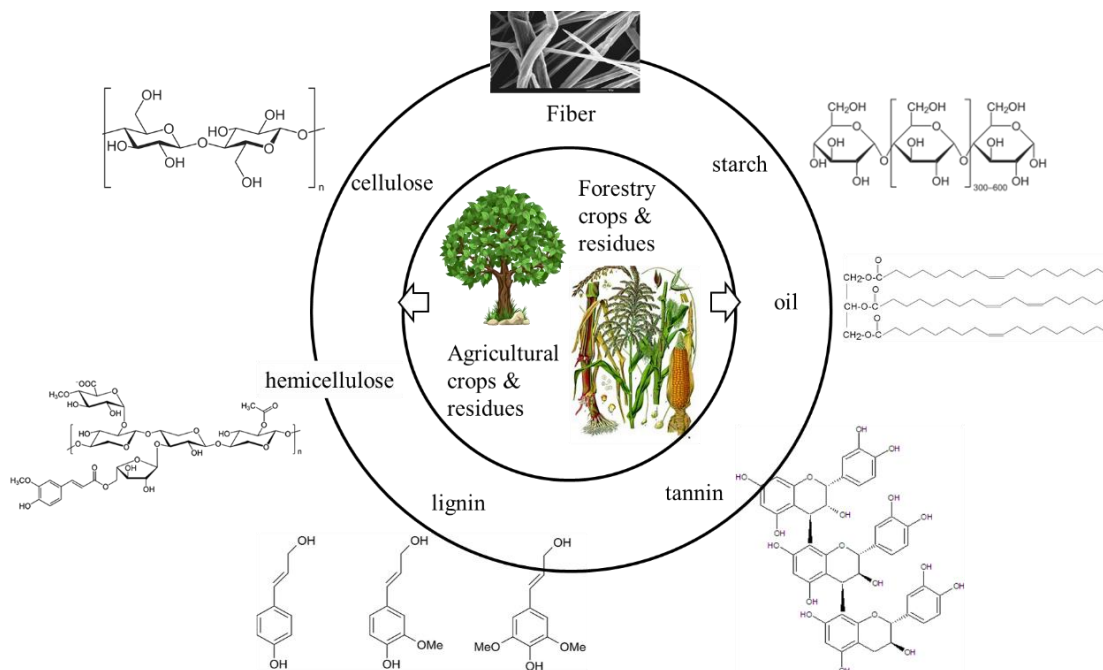
Figure 1-24. Plant fibers and main biopolymers from renewable resources

2. Polymer matrix

Many polymers can be used as a composite matrix. They can be divided into fossil-

based polymers and bio-based polymers according to their precursor resources. On this basis, fossil-based plastics are derived from petroleum or natural gas, while bio-based plastics are produced from renewable raw materials such as starch [122], vegetable oils [123], etc. It should be noted that not all bio-based plastics are biodegradable nor biodegrade more readily than commodity fossil-based plastics. Main polymers and their degradable properties are shown in Figure 1-25.
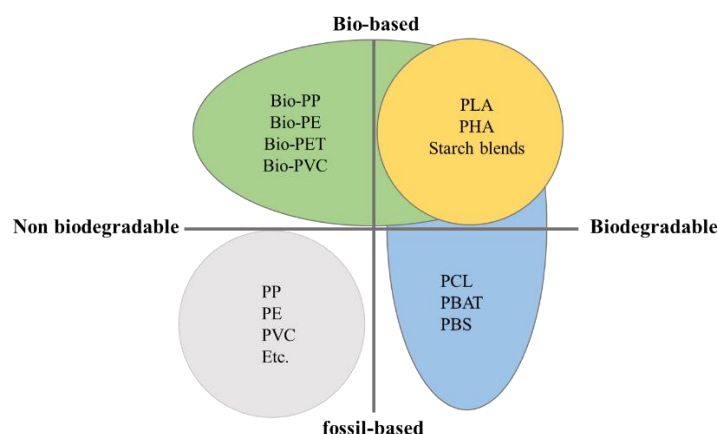
Figure 1-25. Classification of polymers. PP: polypropylene; PE: polyethylene; PET: polyethylene terephthalate; PVC: poly(vinyl chloride); PLA: poly(lactic acid); PHA: polyhydroxyalkanoates; PCL: polycaprolactone; PBAT: poly(butylene adipate-co-terephthalate); PBS: poly(butylene succinate).

The listed thermoplastics can be used as matrix materials for developing biocomposites. The fossil-based polymers are still the dominant polymers in the current industry because of their mature production processes and low production cost. For effectively balancing the price, mechanical property and environment effects, biopolymers incorporation with fossil-based polymers to process partly biocomposites is a favorable choice [124]. Such composites can reduce the dependence on fossil-based products and improve the degradability of fossil-based polymers. Among the fossil-based plastics, PP is one of the most widely used plastic in the industrial and daily products [125]. It is also a popular matrix material in composites because of its relatively high thermal stability, easy (re)processing and chemical inertness. Moreover, it can be easily processed by many efficient converting methods, like injection molding and extrusion [125]. In addition, PP has low production cost, design flexibility, and recyclability, compared with other polymers. Therefore, it can be easily filled or reinforced with biopolymers [124,126]. Besides, the functional characteristics of

biopolymers, like antioxidant, anti-UV, char forming capacity, are attracting interests for developing high performance and long-term application PP-based material since PP is highly susceptible to UV irradiant, oxidant, and high flammability. However, these attracting characteristics are still underdeveloped.

Nowadays, bio-based polymers have attracted increasing attention as composites matrix since their biodegradability and/or sustainability. Combinations of bio-based polymers with biosourced matrix to develop biocomposites are a prevailing trend by considering the environmental impact and cost efficiency [127]. PLA is produced from renewable sources and biodegrades completely into water and carbon dioxide. In addition, it is the most popular commercial bio-based polymer because of its relatively low price compared with other bio-based polymers like PHA [128]. The good thermal processability of PLA makes it suitable to process composite with various biopolymers [115] through injection molding, extrusion. Today, biopolymers are mainly developed as reinforcements or fillers for PLA to improve the mechanical property or reduce the cost. However, the other functional properties of biopolymers like antioxidant, flame retardant, plasticizing capacity for PLA are still lacking knowledge.

2.1. Polypropylene

Polypropylene (PP) is produced from propylene molecules with the presence of catalysts through an addition polymerization process. The property of PP varies according to process conditions, copolymer component, molecular weight, and molecular weight distribution. The average length of the polymer chains and the breadth of the distribution of polymer chain lengths. It can be divided into homopolymer PP and copolymer PP. The former is only propylene monomer in the PP polymer chain, while the latter contains ethylene which can improve impact property, flexibility, and clarity. However, the homopolymer PP is the most widely used PP. Such PP consist of crystalline and noncrystalline regions. The stiffness and melting temperature are affected by the proportion of crystalline region in the polymer chain.

Since discovered in 1954, PP quickly becomes one of the most popular commodity plastics due to its low density and favorable price with good mechanical properties [125]. Today, PP is still one of the most important and widely produced commodity plastic owing to its advantages (Table 1-8). Over 70 million tons of polypropylene were consumed in 2017 [129] and it is commonly used in our daily life from toys to

automotive products, carpeting, containers, laboratory equipment, etc. However, the drawbacks of PP are generally modified through copolymerization and polymer blends for different end-used purpose.

Table 1-8. Advantages and disadvantages of homopolymer PP

Advantages	Disadvantages
Cost efficient	
Thermal stability	UV degradation susceptibility
Processability	Oxidation susceptibility
Flexural strength	High flammability
Moisture resistant	Poor bonding properties
Chemical resistant	Poor chlorinated solvents and aromatics resistant
Good impact strength	
Good electricity resistance	

2.2.   Poly(lactic acid)

Poly (lactic acid) (PLA) was first synthesized by polycondensation of lactic acid in 1845. It was developed as biomedical materials in the late 1970s based on their bioabsorbable and biocompatible characteristics. However, the high cost, low availability and limited molecular weight have limited its development. The industrialization and commercialization of PLA resulted from the ring-opening polymerization of L-lactide in the mid-1990s [130,131]. Today, PLA can be produced from lactic acid using various crops like corn, sugarcane, tapioca, etc. as a raw material. The synthesis of PLA polymers can be performed through direct polycondensation of lactic acid or ring-opening polymerization of lactide, which is a cyclic diester of lactic acid (Figure 1-26). Ring-opening polymerization is the mainly used industrial production route since high-quality PLA polymers can be produced in mild reaction conditions [131]. Lactide has three stereoisomers include D, D-lactide, L, L-lactide, and D, L-lactide (meso-lactide). The stereochemical composition of lactide monomers strongly affects the melting point, crystallization characteristic, and mechanical property [131]. For example, pure poly(D-lactide) (PDLA) or poly(L-lactide) (PLLA) has a crystalline melting point of 207 °C. While, regular PLA have a melting point range from 170-180 °C caused by the imperfect crystallite, slight racemization, and impurity. A stereo-complex PLA produced by a 1:1 mixture of pure PLLA and PDLA

display better performance in mechanical property and melting temperature (up to 230 °C) compared with pure PDLA or PLLA.
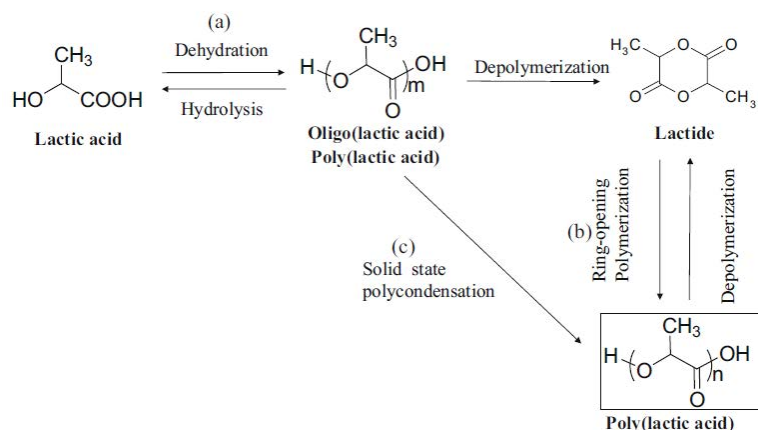
Figure 1-26. Routes for the synthesis of PLA polymers: (a) direct polycondensation of lactic acid, (b) ring-opening polymerization of lactide, and (c) melt/solid-state polycondensation [131].

PLA is one of the most consumption in the field of bio-based and biodegradable polymers in the past five years and the trend keeps increasing with the production capacity [132]. Owing to the advantages (Table 1-9) and versatile characteristics of PLA, it can be used in not only various packaging applications and short shelf-life consumer goods, but also some high-value applications such as textiles, biomedical devices, construction and automotive. The packaging is the largest field of application for PLA with almost 65 percent (1.2 million tons) of the total bioplastics market in 2018 [132]. For promoting its application diversity, numerous reports concerning the modification of PLA to overcome its limitations [133] through copolymerization or blending methodology [134].

Table 1-9. The advantages and disadvantages of PLA[128]

Advantages	Disadvantages
Eco-friendly	Poor toughness
	Slow crystallization rate
Biocompatibility	Slow degradation rate
Processability	
	Hydrophobicity
Low production costs	Lack of reactive side-chain groups

3. Biopolymers for composite preparation

PP/PLA incorporated with biopolymers have gained increasing attracts due to environment awareness. Figure 1-24 displays the mainly used biomaterials and biopolymers from forestry crops/residues and agricultural crops/residues. Among them, natural fibers, cellulose, and starch are the most widely studied for both PP and PLA polymers (Figure 1-27) to replace fossil-based reinforcement/filler. Natural fibers or cellulosic are extensively investigated as reinforcement since they are light, biodegradable, and easy to prepare when compared with synthesized fibers. Starch is mainly used as a filler to improve the biodegradability of plastics. The less investigated biopolymers are lignin, tannin, vegetable oil, and hemicellulose, which are most studied as functional additives. The properties of these biopolymers (tannin was presented in Part I) and their incorporation with PP and PLA will be discussed below.
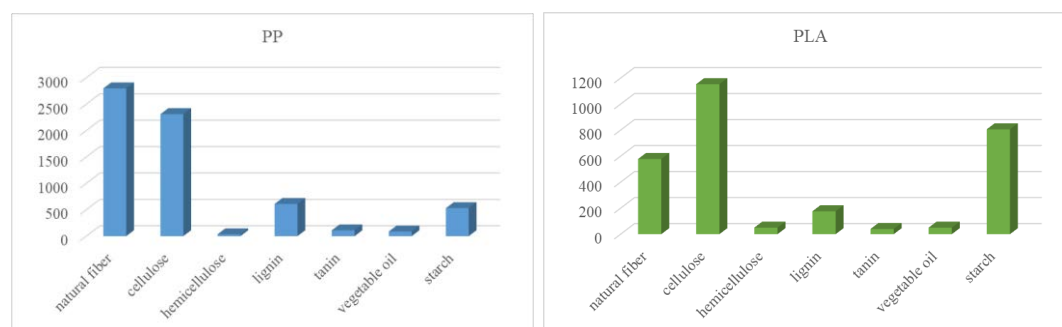
Figure 1-27. Publishes based on the topic of PP/biopolymers or PLA/biopolymers. Searched by polypropylene*/poly(lactic acid)* with natural fiber* or biofiber*; cellulose*; hemicellulose*; lignin*; tannin* or polyphenol*; vegetable oil*; starch* from 1950 to March 2019. Data from the web of science.

3.1. Reinforcement

3.1.1. Plant fibers

Natural fibers are widely distributed in woody plants and non-woody plants, providing mechanical support of cell wall. Plant fibers are mainly consisting of cellulose, hemicellulose, lignin, pectin, and ash [135]. The properties of the fiber change depending on the amount of each component. Cellulose is an important structural component of the primary cell wall of green plants and it is the main component of natural fibers. The cellulose content of cotton fiber is 90%, that of wood is 40–50%, and that of dried hemp is approximately 57% [136]. While, the hemicellulose is responsible for the moisture absorption, bio- and thermal degradation

whereas lignin ensures thermal stability but is responsible for the UV degradation [137].

Fiber materials have been extensively researched to mechanically enhance the strength and elasticity of plastics matrix. Synthetic fiber-reinforced polymer composites have been widely used in our daily life since last century. However, these synthetic fibers, such as glass fiber, carbon fibers, are mostly produced from non-renewable sources. Since 2000, there is a growing interest in replacing synthetic fibers by natural fibers to produce fiber reinforced composites because of to their lower environmental impact, lower cost, lower weight, higher electrical resistance, and better acoustic insulation[121]. According to their dimensions and the perspective of composite reinforcement, it is preferable to classify natural fibers into short fibers (1-5 mm) and long fibers (5- 30 mm)[135]. Among them, short fibers are typically used for making composites with in-plane isotropic properties, while long fibers are generally used for making composites with anisotropic properties[135]. The main source of natural fibers can be found in Figure 1-28.
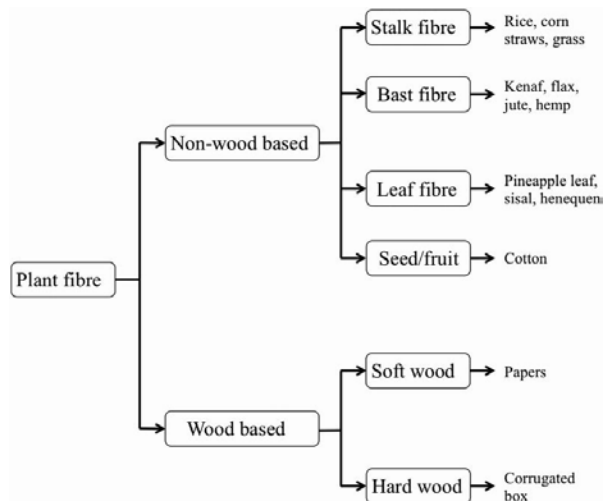
Figure 1-28. Classification of plant fibers and some exemplary (fibrous) products [138].

The limitation of natural fibers as reinforcement for PP/PLA is considered as their poor surface adhesion, mineralization. Physical treatments (e.g. corona [139,140], plasma [141], and alkali treatment [142]), biological treatments [143] (e.g. enzymes), and chemical modification [124] (e.g. acetylation) are widely used to improve the surface properties of natural fibers and promote the interfacial adhesion of polymer-fiber. Physical treatment is generally combined with coupling agents and compatibilizers that can perform bridge links through covalent bonds between fiber and polymer matrix. Silane coupling agents are one of the most widely used in polymer

composite. The silane molecule consists of a hydrolyzable group (e.g. alkoxy group) and a functional group (e.g. amino, epoxy, vinyl, etc.) that can react with hydroxyl groups of fiber [124,144]. The utilization of compatibilizer is the most effective methods for interface modification. Maleic anhydride (MA) is the most widely used functional group for improving the adhesion between fiber and matrix. For instance, MA grafted PP [145], MA grafted PLA [146]. There are some reports about the compatibilizer containing isocyanate functional groups to improve the fiber/PP [147,148] or fiber/PLA [149] interfacial adhesion since their high reactivity towards hydroxyl groups.

The main functionality of natural fibers is to improve the mechanical properties of PP/PLA, including stiffness, strength, and impact, especially with interfacial modification pathways [150,151]. In addition, higher biodegradability properties have been observed compared with neat PP/PLA [152,153]. PLA incorporated with short fibers can restrain material deformation under heat by promoting crystallinity and hindering more chain mobility [154]. For example, short basalt fibers(13–20 μm, 20-40 wt%) performed as an effective nucleating agent among the PLLA/fiber composites, significantly improving the heat resistance and thermomechanical properties of PLLA [133].

3.1.2. Cellulose

Cellulose is the main component of plant fibers and mainly obtained from wood pulp and cotton [155] and also the most abundant of natural carbohydrates polymers on earth. Cellulose is a linear chain polysaccharide, consisting of repeating β-(1,4) linked glucose units, with two glucose as the repeat unit [51]. The single glucose unit contains three hydroxy functional groups and hydrogen bonds can be easily formed between glucose units. These hydrogen bonds enable the creation of highly ordered three-dimensional crystal region [121]. The degree of polymerization of cellulose is generally high, take wood cellulose as an example [156], the polymerization degree is between 8000 and 10000, making each cellulose chain approximately 4-5 μm and the molecular weight in the order of 1.5×10^6.

Figure 1-29 presents a graphical illustration of cellulose. The cellulose microfibril is the basic structural component of cellulose, which is constituted by crystallites with interspersed amorphous regions of low degree of an order [157]. These amorphous

regions can be cut into microfibril fragments, generally named as nanocrystals, microcrystals, whiskers, microcrystalline, nanofibers, or nanofibrils [158].

Cellulose microfibrils have been extensively investigated as excellent reinforcement components for composite material because of the high stiffness of the crystal region of cellulose fiber [157]. Nanocellulose has made a great contribution to high-performance composite material in aerospace applications [115]. The widely studied cellulose nano-/micro- fibrils can be extracted through different pathways, for example, mechanical pulping, chemical pulping, steam explosion, etc [155]. Different extraction methods lead to different cellulose nano-/micro- fibrils, varying from shape and diameter; this will affect the mechanical, thermal, and barrier properties of final composite products [155,159].

The main difficult application of cellulose to process polymer composites is the incompatibility of cellulose and polymer matrix. Physical surface modification (corona/plasma discharges) [160] and chemical modification (e.g. acetylation [161]) of cellulose, grafting copolymerization [162,163], the addition of coupling agent/compatibilizers are widely reported to improve interfacial adhesion. For nanocomposite preparation, surfactants [164] are also applied to improve the dispersion of nanocellulose in the matrix.

Low nanocellulose contents in PP or PLA have been investigated to develop nanocomposites displaying dramatic improvement in mechanical properties [124,165]. Cellulose fiber in micro-size [166] and nano-size [167] were reported to slightly decreased the crystallinity of PP, while promoting the crystallinity of PLA [168,169]. Nano size cellulose can perform good gas barrier properties for packaging film materials. For example, with the addition of cellulose nanocrystal, the extrusion-blown PLA films exhibited lower water vapor permeability (∼40%) and oxygen permeability (∼75%) compared with neat PLA because of the tortuosity effect created by nanocellulose [170].
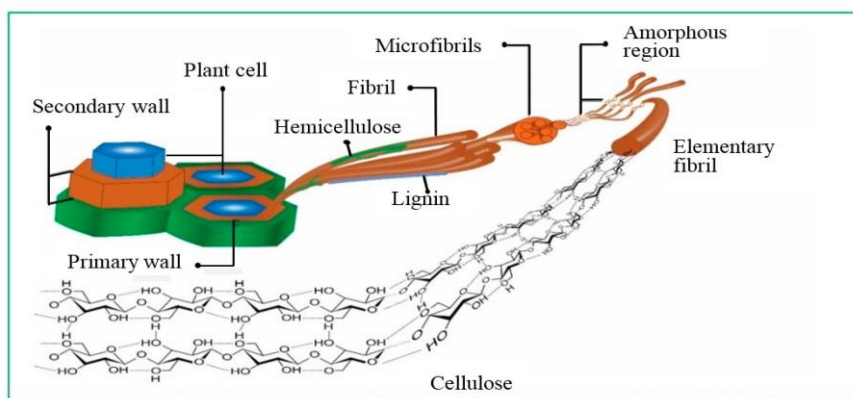
Figure 1-29. The structure of plant cell wall and the classified structure of cellulose extracted from plants [158].

3.2. Filler: starch

Starch is a main carbohydrate and abundant polysaccharide on earth. This polysaccharide is produced by most green plants as energy storage. It is the main sources of energy to sustain life for human. Highly starch contain plants are easily found and planted whatever the climate and agricultural conditions. It is widely distributed in various parts of a plant, such as the endosperm, the root, the leaf and the fruit pulp [171]. Starch can be chemically classified into two types of glucan polymer: amylose and amylopectin (Figure 1-30). Amylose is a linear macromolecule linked by (1-4) bonds of α-D-glucopyranose units and usually branched at a low level by a (1-6) linkages. While amylopectin is a highly branched glucan chains, which primarily consists of α-(1-4)-D-glucopyranose units with α-(1-6)-linkages at intervals of approximately 20 units (Figure 1-30) [172,173].

Amylose molecule   Amylopectin molecule
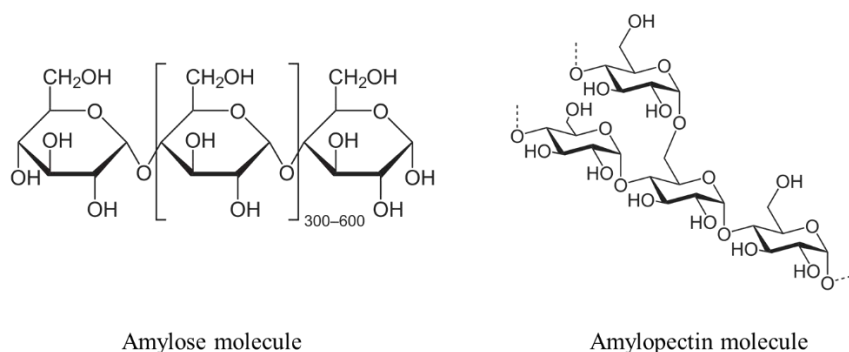
Figure 1-30. Two macromolecular components of starch

Starch is an important raw material to produce biopolymers, like lactic acid and polyhydroxyalkanoates [173]. It is also an important biopolymer for material preparation because of the biodegradability, overwhelming abundance and annual

renewal characteristic. Starch is widely used natural filler for traditional plastics (e.g. PP [154], PE [174]) or biodegradable plastics (e.g. PLA [175]) to promote the degradability and/or reduce the cost of final products. Thermoplastic starch, which produced by the mixture of plasticizer, offers a greater potential in polymer blends [176]. Thermoplastic starch displays a better processability, thus, it can be deformed and dispersed to a much finer shape than the native starch. It is a good pathway to reduce the stiffness and improve the compactivity with hydrophobic polymers. Starch with the combination with ammonium polyphosphate was reported to improve its flame retardancy of PP [177] and PLA [178,179]. Starch provide intumescent char layer on polymer surface, inhibiting heat transmission and retard inner polymer degradation.

3.3. Plasticizer: Vegetable oil

Vegetal oils are biopolymers extracted from various plants. The vegetable oils are always consisting of triglycerides formed between glycerol and various fatty acids[180] (Figure 1-31 (a)). The chain length of these fatty acids can vary from 14 to 22 carbons and contain 0-5 double bonds situated at different positions along the chain[173]. In some special oils, functional groups like hydroxyl group and epoxy group are also found in some special oils (Figure 1-31(b)). These functional groups provide reaction site for polymerization and chemical modification.

The double bonds in vegetable oils can undergo auto-oxidation with the presence of an oxygen atmosphere, free radical polymerization results in crosslinked polymeric materials[180]. These vegetable oils can be used as plasticizer to enhance the toughness of polymers[181]. Vegetable oil can be functionalized into various vegetable-oil-based monomers through different pathways. These functionalized vegetable oils are commonly blended with plastics and behavior as plasticizer [154,182] or stabilizer[183,184]. Besides, polyurethane, polyester, polyether and polyolefin have been widely prepared by vegetable-oil-based monomers [180,185]. These vegetable-oil-based polymers exhibit high flexibility due to the long fatty acids chain. Some of them also display shape memory [186] and excellent biocompatibility [187].
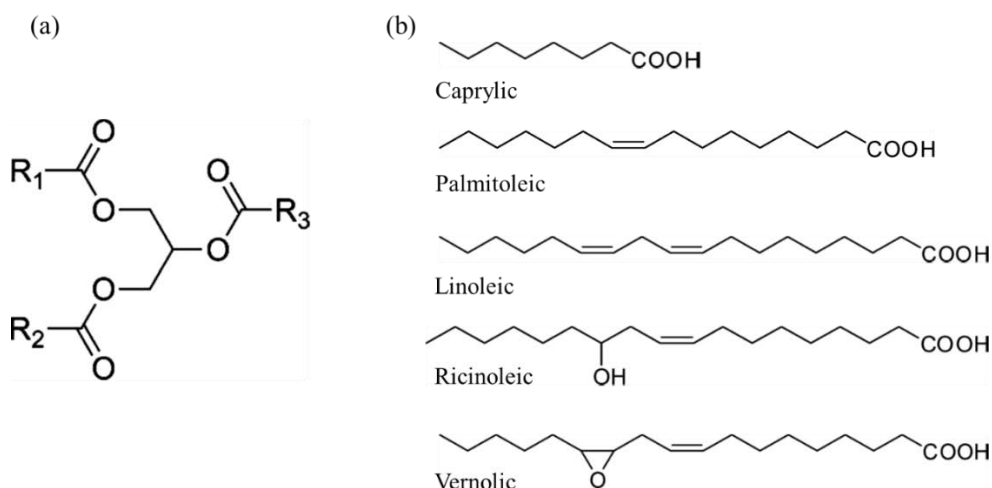
Figure 1-31. (a) Triglyceride structure of the vegetable oils (R1, R2, R3 represent fatty acid chains); (b) four examples of fatty acid [173,180].

Vegetable oils can be used as a plasticizer in thermoplastics. Chemical modification (e.g. epoxidation, melaninization, etc.) of vegetable oil have been successful used as plasticizer for plastics. The epoxied oleic acid polymer reduced processing torque of PP, the final product did not affect the crystallinity and mechanical properties [154]. Besides, the flexibility of PLA can be significantly improved by epoxied and melanized vegetable oils [182,188,189].

3.4. Functional additives

3.4.1. Hemicellulose

Hemicelluloses are the second abundant of natural carbohydrates polymers on earth. They are branched and complex polysaccharides, associated with cellulose and lignin in the plant cell wall contributing to its rigidity in lignified tissues [190] (

Figure 1-29). The main structure of hemicelluloses is consists of a sugar backbone substituted with side chains. Their physicochemical properties are determined by the nature of the monosaccharide and the linkages between structural units [121]. They can be divided into four classes of structurally different cell-wall polysaccharide types: xylans, mannans, β-glucans with mixed linkages, and xyloglucans [191]. The xylan-type polysaccharides are the main hemicellulose components of secondary cell walls of dicotyl plants (hardwoods and herbaceous plants). Such type of polysaccharide is considered as potential biopolymer since it is widely distributed in all kinds of biomass and can be extracted from the by-products of forestry, the agriculture, wood, and pulp

and paper industries [192]. The mannans-type of polysaccharides (glucomannans and galactoglucomannans) are the major hemicellulosic components of the secondary cell walls of softwoods. They also appear in the combination with xylan and fucogalactoxyloglucan in the primary cell walls of higher plants.

The isolation of hemicelluloses in polymeric form requires multi-step extraction methods to separate them from lignin or proteins and other polysaccharides since they are embedded in the cell walls. This difficulty limits the application of hemicellulose. However, with the occurrence of new extraction technique, polymeric hemicelluloses have been extracted at almost 100% yield from commercial wood chips and at a lower temperature (< 150 °C) [193]. They can also be recovered at the industrial scale from thermomechanical pulping process water by membrane technologies [194]. The utilization of hemicelluloses is gaining interest in material preparation. The most studied topic is their application in film preparation [195–197]. These films have potential applied in food packaging since their low oxygen permeability [197]. Besides, hemicellulose-based hydrogel was also found in the application as absorbent to remove heavy metal ions [198]. However, the utilization of hemicellulose in polymer composites is rare. In wood-plastic composites, hemicellulose is the most hydrophilic wood polymer component. As a result, the extraction of hemicellulose can improve the interfacial bonding of filler and matrix [199]. Hemicellulose was recently found the application in PLA. For example, xyloglucan grafted PLA copolymer was used as a compatibilizer in PLA/cellulose composites since hemicellulose presents a strong affinity for cellulose [200]. It was also reported as a feedstock material to partially replace PLA in 3D printing [201].

3.4.2. Lignin

Lignin is the second most abundant biopolymer of lignocellulosic biomass after cellulose. It is one of the three major components found in the cell walls of natural lignocellulosic materials [190] (Figure 1-32), providing strength and rigidity to cell walls. It plays an important role in water and solutes transportation through the vasculature system and pathogens invasions [202].
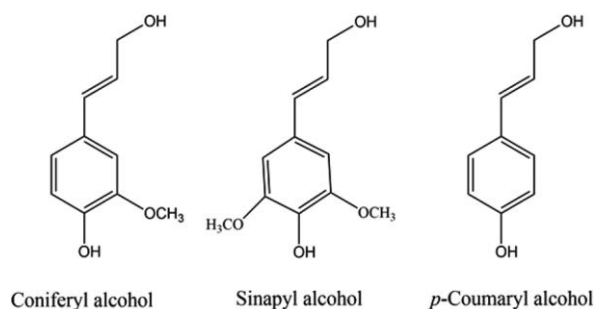
Figure 1-32. Typical phenylpropanoid precursors of lignin.

Lignin is an amorphous highly branched biopolymer. Its molecular mass is generally range from 1000 to 20,000 g/mol [203], depending on the extraction pathway. Structurally, lignin consists of three typical phenylpropane monomer units, namely sinapyl alcohol, coniferyl alcohol and paracoumaryl alcohol. The main bonds between monomers in lignin are β-O-4′ ether linkages that make up more than 50% of the linkage structures of lignin and is a crucial target for most of the degradation mechanisms. Each monomer is mainly linked through β-O-4′ ether bonds, other bonds like β-5 phenylcoumaran, β-β′ resinol, α-O-4′ ether, 4-O-5′ diphenyl ether, 5-5 biphenyl and β-1′ diphenyl methane account for small amount [204] (Figure 1-33).The molecular weight and structure of lignin vary according to the origin source and the proportion of different phenylpropane monomer units, chemical bonds.
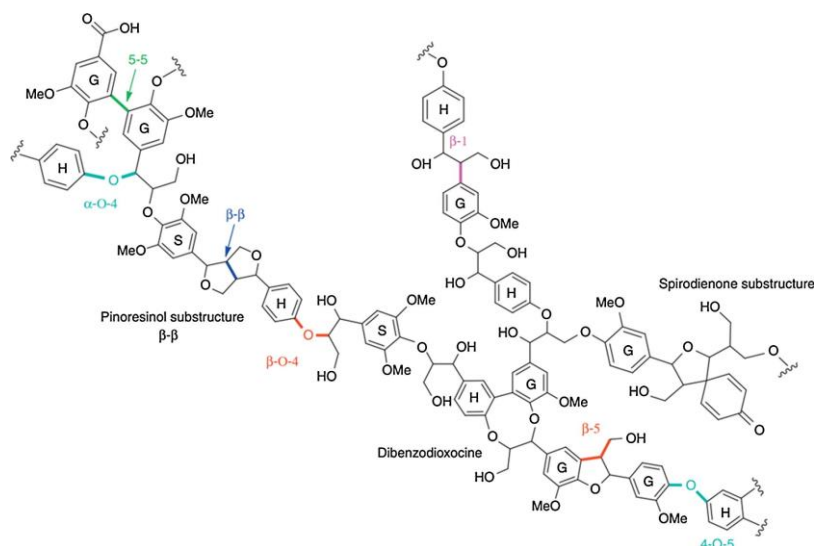
Figure 1-33. Example of the lignin structure with the main linkages: β-O-4′, β-5, β-β′, α-O-4′, 4-O-5′, 5-5 and β-1′ bonds[204].

Lignin is a waste byproduct from pulp and paper making industry and it can be extracted from sulfite, kraft, organosolv and soda processes [205]. As a phenolic

compound, lignin bearing numerous reactive functional groups and displays antioxidant, antifungal and antimicrobial capacities, UV-radiation, and fire-retardant properties. Along with its sustainable, cost-effective, and biodegradable capacity, lignin has been revealed as a potential precursor for material preparation, including polyurethanes [206], epoxy resins [207], reinforcement/functional fillers of polymer composites [205,208,209], feedstocks for carbon materials [210]. Some innovated lignin derivatives, like lignin-based nanomaterials [204], lignin-based copolymers [211] can be used in a broader range of application and allows for the design of novel materials with tailored properties.

Lignin was reported as antioxidant [154,212], stabilizer [154,154,213], flame retardant (char agent) [154], and compatibilizer [214] for PP-based composites owing to their functional groups. However, these various heterogeneous functional groups reduce compatibility and interfacial forces with PP matrix. Therefore, lignin used as a filler generally reduces the tensile strength in final products proportionally to its concentration. The interfacial adhesion between lignin and PP can nevertheless be promoted by the addition of compatibilizers, such as maleic anhydride grafted PP [215]. The main function of these compatibilizers is to form covalent or non-covalent bonding between lignin hydroxyl groups and the compatibilizer. Like natural fibers and cellulose, lignin is generally modified before its incorporation with polymer matrix. Both surface modification (e.g. plasma [216]), chemical modification (e.g. esterification, etherification, etc.) of lignin and addition of coupling agents/compatibilizers were reported [205]. Lignin was also reported to display positive effects on thermal stability [154], antioxidant [217], and flame retardancy [179] of PLA. Besides, the oxygen barrier property was slightly enhanced in PLA-lignin films [217].

Part III   Biocomposites processing: extrusion

Biocomposites based on PP/PLA and biopolymers are extensively studied. The property of such biocomposites depends on the nature of each component, interfacial adhesion, the sizes of discontinuous phase, and dispersion degree of discontinuous phase. The dispersion of filler/reinforcement/ additives has an impact on the properties of the final products, and it is generally affected by processing technique. Melt blending process is the most widely used method to develop biocomposites and it is usually performed on extruders [218]. An extruder provides an efficient mixing pathway for biocomposite preparation, because the extrusion process is continual, short cycle time, and high efficiency. Besides, solvent-free, environmentally friendly, and flexible extruded condition setting have made extrusion one of the fastest growing method of polymer processing.

Extrusion process can be simply classified into melt blending and reactive blend [115] (Figure 1-34). The melt blending is simple mixing composite components in the melt state simple without any chemical reactions during extrusion process. While reactive blend (or reactive extrusion, or reactive compatibilization) involves chemical reaction between each component during the extrusion process with the help of reagents (e.g. modifiers or coupling agents or compatibilizers). These reagents can be fed separately or ensemble with initial components. For biocomposites preparation, reactive extrusion is an efficient method to improve the interfacial interactions of filler/reinforcement/additives and polymer matrix [219].
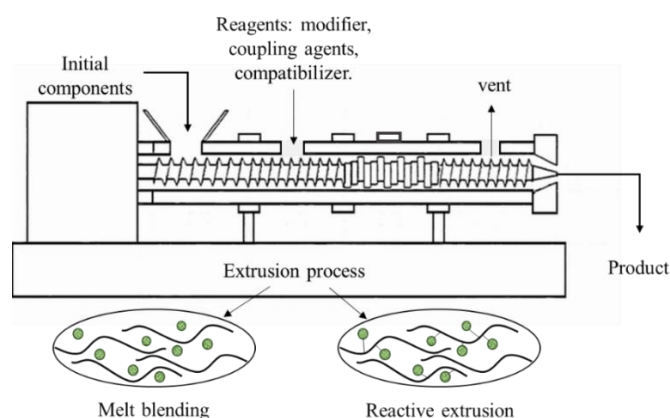
Figure 1-34. A scheme of an extruder and extrusion process include melt blending and reactive extrusion.

1. Screw extruder

Figure 1-35 shows the arrangement the different parts of a simple single screw machine. An extruder is generally consisted of hopper, screw, barrel, die, motor, gearbox, heating and cooling system. Initial components are fed to the extruder through a hopper (Figure 1-34). The screw and barrel interact together to convey and melt a solid polymer and deliver the molten polymer, and then push the melting material through the die. The screw speed is controlled by the electric motor drive unit and gearbox. A heating and cooling system is provided to control setting temperatures of the internal surface of the barrel and the external surface of the screw [220].
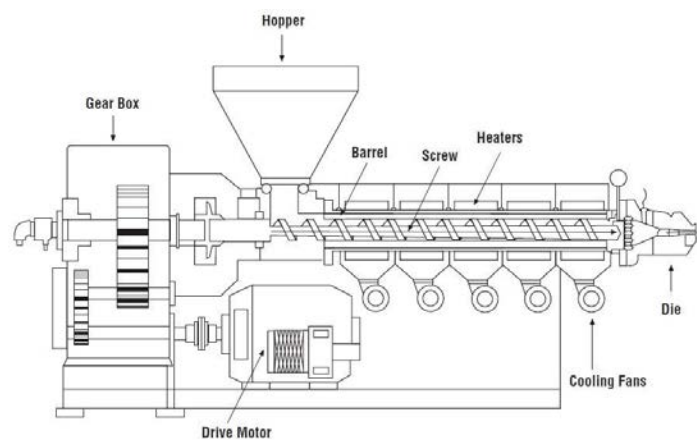
Figure 1-35. Single Screw Extruder [221]

The screw offers various experimental conditions by changing the screw profile, temperature profile, screw speed and residence time [220]. This attributes to distributive mixing, dispersive mixing, and homogenization of components in biocomposite extrusion [220]. The screws profile can be easily designed by changing screws elements. Take the configuration of twin-screws used for sugarcane bagasse pretreatment as an example [222] (Figure 1-36), the screw can be divided into a conveying zone, kneading block zones, and reaction and compression zones by using different screw elements. The initial conveying zone was built from several conveying elements that serve as drivers to convey the solid components toward the kneading block. Kneading block zone contributed to effective mixing performs. After first mixing zone, the conveying elements contribute to both reaction and convey function. The reverse conveying element is used for prolonging the mixing and reacting time.
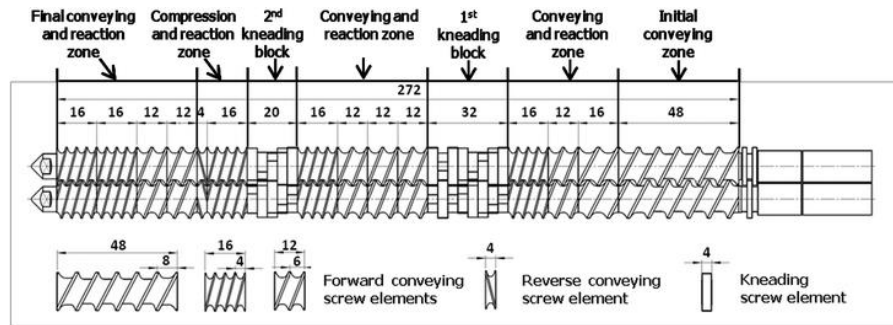
Figure 1-36. An example of a twin extruder segmented screw[222]

Extruders are generally divided into single-screw extruders(Figure 1-35), twin-screw extruders (Figure 1-36), and multi-screw extruders in terms of the number of screws. The twin-screw extruder and multi-screw extruder are preferable for composite preparation due to its good mixing capacity and they are easier to achieve good homogeneity of fibers in the composites or nanoparticles in nanocomposites. In addition, the screw can be flexibly designed to have conveying zone, mixing zone and reaction zone. This contribute to dispersion degree of fillers/reinforcements/additives, which can strongly affect the final physical, mechanical and morphological properties of final products. According to Yang's study, the tensile strength and modulus of the lignocellulosic material filled PP fabricated using the twin-screw extruding system were improved as compared with those fabricated using the single-screw extruding system, due to the improved dispersion of the fillers in the composite [223]. A superior blending and dispersing performance are provided by the triple-screw extruder due to flow and mixing properties which are different from traditional single and twin-screw extruders. But the application of triple-screw extruder in biocomposite preparation is still limited because its high costs caused by the complicated screw geometry and barrel construction [218].

2. Melt blending

For preparing good biocomposites via melt blending with an extruder, screw profile, screw speed and screw temperature are three main factors to be considered that might affect the dispersion of filled component in polymer matrix. The screw profile can be set to modulate the residence time by using various conveyors or reverse elements. The reverse screw elements increase severity of the extrusion process and the shearing with mixing or kneader elements [224]. Berzin et al. have demonstrated that the fiber length rapidly decreased after the introduction of the fibers and during the flow

through the kneading blocks. Fiber fragmentation was increased at high screw speeds and low feed rates [225]. The screw speed has strong effects on the dimensions and dispersion of fibers in polymer matrix. Mano et al. prepared PP and high-density PE based composites by using a twin-screw extruder. The length, diameter and aspect ratio of the fibers decreased with increasing screw rotation speed due to the high shear forces acting in the molten polymer and transferred to the fibers [226]. The extent of fiber breakage depends on the time, temperature, and speed of rotation [227]. The extent of fiber breakage can be reduced by using higher extruded temperature and higher screw speed to reduce the blend viscosity and the residence time, respectively. As reported by Hanawalt et al., the extrusion temperature should be set in accordance with the thermal stability of the fiber to prevent thermal degradation. Such degradations would certainly cause some flaws into the fiber bundles and decrease. According to the report of Feldmann et al. [228] , the temperatures and screw profile of the twin-screw extruder only result in different fiber length distributions but in minor differences of the morphological structure and mechanical properties of bio-based polyamide with 20 wt% cellulosic fibers. Thus, it is important to correctly define the extrusion parameters to balance a good dispersion of reinforce component and the preservation of the reinforcement properties.

3. Reactive blending

Reactive blending has been considered as the most promising methodology for short time and efficient develop of novel composite materials and to control the phase structures of multicomponent of composites. An extruder as a horizontal chemical reactor, chemical reaction such as grafting reaction, reactions between terminal groups of polymers, dynamic vulcanization, and transesterification reactions can be performed during the extrusion process.

3.1. Reactive compatibilization

Reactive compatibilization is a chemical modification process to improve the interface adhesion during melting blend. Many reagents can be used to compatibilized PLA-based biocomposites. The most common used reagents are reactive agents bearing anhydride, epoxide, isocyanate groups. Besides, free-radical initiators are commonly used to create free radical on polymer chain.

González-Lópe summarized possible strategies for reactive compatibilization,

including coupling agent incorporation, pretreatment of filled component (fiber surface treatment) , and one-step compatibilization (Figure 1-37) [229].
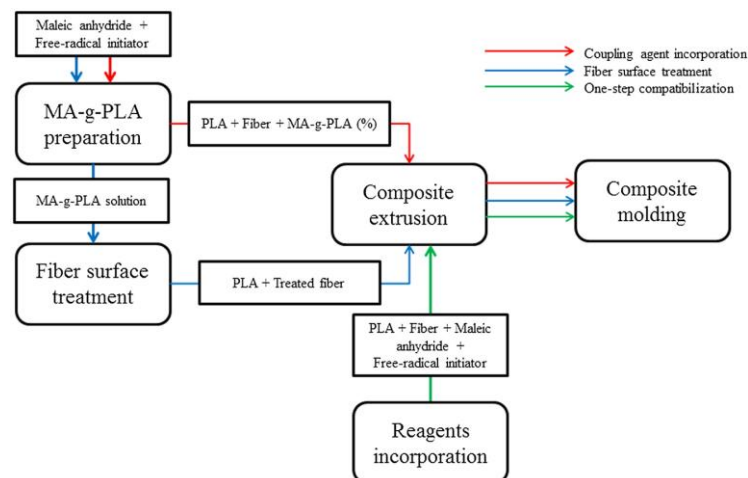
Figure 1-37. scheme of coupling agent incorporation strategies to PLA-fiber biocomposites

For PLA and cellulosic fibers blends, possible reaction mechanism between maleic anhydride (MA), PLA and cellulosic fibers is presented in Figure 1-38 [229], PLA chains form a primary free radical induced by the initiator on tertiary carbon. Then, PLA free radical reacts with the double bond of the maleic anhydride. During the extrusion process, anhydride groups in MA-g-PLA might react with hydroxide groups on fibers to form ester type bonds or interact via hydrogen bonding, acting as a bridge between fibers and matrix, improving interfacial adhesion due to crosslinking between fibers and the polymer chains. One-step compatibilization is the most effective strategy to improve compatibility in biocomposites.
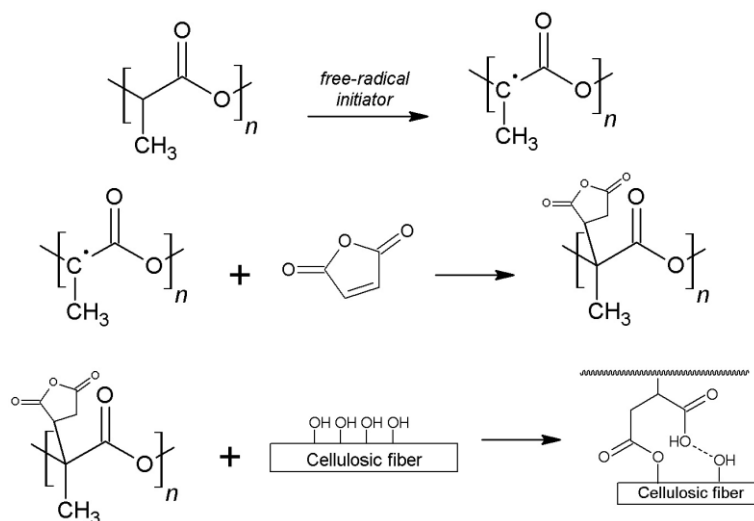
Figure 1-38. Reaction mechanism between MA, PLA and cellulosic fibers.

Nanthananon [230] prepared short-fiber reinforced PLA biocomposite via reactive blending approach to enhance the interfacial adhesion by using anhydride and epoxide groups reactive agents as compatibilizers. The compatibilized PLA biocomposite exhibited better interfacial fiber-matrix adhesion, tensile strength and storage modulus compared to non-compatibilized one. In this study, epoxide-based compatibilizer have a better performance than anhydride-based reactive agent.

3.2.   Dynamic vulcanization

Dynamic vulcanization is traditionally used to prepare thermoplastic elastomer. This is an in situ dynamic vulcanization technique, where vulcanization of an elastomer proceeds simultaneously with its mixing with a thermoplastic polymer. This process can produce unique morphology by dispersing particles of the vulcanized elastomer in a continuous thermoplastic matrix. The mechanism of dynamic vulcanization based on blend composition, the nature of vulcanizing agents, blending conditions, temperature-time superposition during the formation of network structure of the elastomer. Mixing is superimposed on the cross-linking reaction with causes changes in morphology of the elastomer phase. For example, a bio-based thermoplastic vulcanizate based on bio-based polyester elastomer and PLA processed by an in situ dynamical crosslinking and mixing method [231]. The crosslinked degree can be controlled by mixing time and crosslink agent content.
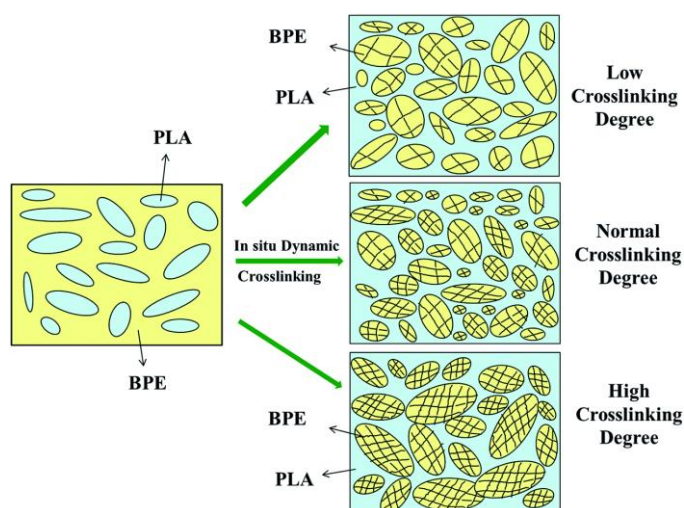
Figure 1-39. Phase inversion of bio-based TPVs with different degrees of crosslinking.

This process has been successfully applied to dynamically crosslink thermoset resin and blend with thermoplastic. With this technique, thermoset resin can be cured during

extrusion process and simultaneously dispersed in thermoplastic matrix. One example is PP/novolac composites compatibilized with maleic anhydride-grafted PP [232]. Novolac can by dynamic cured to improve the modulus, stiffness, and thermal stability of the PP. The interfacial adhesion can be further enhanced by the addition of maleic anhydride-grafted PP. Another PP/epoxy composite was dynamically cured an epoxy resin during melt mixing with compatibilized with maleic anhydride grafted PP [233]. The cured thermoset resin particles can be finely dispersed in PP matrix with the help of extruder and these cured particles could act as effective nucleating agents, accelerating the crystallization rate of PP.

Part IV   PLA-based biocomposite as 3D printing filament

1. Introduction

Plastic products are indispensable in our daily life. They are traditionally manufacturing with injection molding, extrusion molding, blow molding, and rotational molding. Today, 3D printing is an innovative technique for manufacturing plastic products. PLA is an ideal 3D printing material since its printability, stiff and good strength, good dimensional accuracy, good surface quality, user-friendly, and no toxic fumes release during printing process. The 3D printing technique allows users to quickly and easily create complex designs unattainable by traditional manufacturing processes [234]. PLA is a well-known sustainable, biodegradable, and biocompatible polymer. 3D printing enables PLA in applications of biodegradable medical devices, customized implants, drug delivery devices, 3D scaffolds for tissue engineering, etc [235].

In past decades, PLA composites with superior characteristic compared with pure PLA have been widely studied and enabled application diversity. Particularly, its incorporation with biopolymers also contribute to sustainability, biodegradability, and cost-efficient. However, the addition of functional fillers and additives in the polymer matrix changes not only the functional characteristic but also the rheological characteristic that is important for the application of 3D printing. Unfortunately, the researches regarding PLA-based biocomposites in the field of 3D printing are still limited.

2. Fused deposition modeling and their process parameters

Additive manufacturing, commonly known as 3D printing, refers to a wide variety of processes for creating 3D complex shape parts. These manufacturing technologies can be classified based on various criteria, such as nature (powder or filament) of the raw material (metal, ceramic or polymer), deposition strategy and energy source [236]. According to the standard of ASTM 52900:2015, additive manufacturing processes can be divided into seven categories, including material extrusion, vat photopolymerization, material jetting, binder jetting, powder bed fusion, direct energy deposition, and sheet lamination [237]. Among all the methods, material extrusion, well-known as fused deposition modeling (FDM) or fused filament fabrication (FFF), is one of the most widely used and economical additive manufacturing technologies. With this

70

manufacturing process, thermoplastic filament is fed through rollers pushing the thread through a heated nozzle. The molten thermoplastic ejected from the nozzle at constant speed to create a customized object by layer deposition (Figure 1-40).
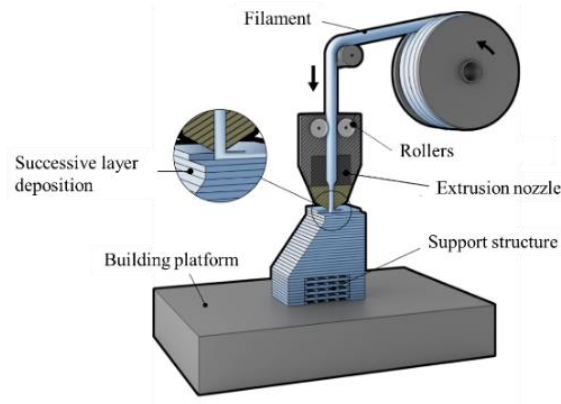
Figure 1-40. The Fused Deposition Modeling (FDM) modified from website:
https://www.manufacturingguide.com/en

Although FDM process have been widely for thermoplastic parts manufacturing, the printed products still exhibit various drawbacks, for instance, low mechanical strength, high surface roughness and low dimensional accuracy. These imperfect flaws are mainly caused by the inadequate setting printing parameters based on the properties of polymer. The quality and material properties of FDM printed parts are substantial affected by various parameters such as build orientation, layer thickness, feed rate, etc [238]. 3D printed products exhibit anisotropic behavior because of the layer-by-layer process. Thus, the deposition orientation and raster orientations are commonly considered important parameters to the mechanical properties of printed products [238–241]. The mechanical properties are also strongly affected by the adhesion among the deposited filaments since layers are formed by the bonding of deposited filaments. This physical phenomenon is described as coalescence and that is mainly controlled by the viscosity and surface tension of polymers [242]. Understanding the temperature influence on the rheological properties of polymers is important to control and improve the coalescence of deposited beads [243].

According to the work of Balani [243], the mechanical properties of printed parts is determined by interlayer adhesion and porosity (Figure 1-41). These properties are determined by the inlet velocity, shear rate and viscosity in the liquefier, however, they can be controlled by the printing parameters such as nozzle diameter, feed rate and layer height based on the physical properties of the polymer (i.e. thermal transitions and

rheological behavior). On this basis, recommended conditions for printing PLA via FDM were given:

Printing temperature is 200 °C with the consideration of completely melting filament and avoiding severe deformation and degradation of polymer. Besides, the shear rate should be bellowed 4000 s^{-1} to reduce the follow instability and surface defects. The nozzle diameter highly influences the shear rate. Increasing the nozzle diameter decreases the shear rate but reduces the precision of the printed part. Thus, a nozzle diameter of 0.4 mm or 0.5 mm is recommended. The volume flow rate based on the feed rate and the geometry of the deposited bead, such as the height of the layer and width of the deposited bead. Therefore, the height of the deposited bead must not exceed 0.4 mm, and the feed rate must be below 30 mm/s.
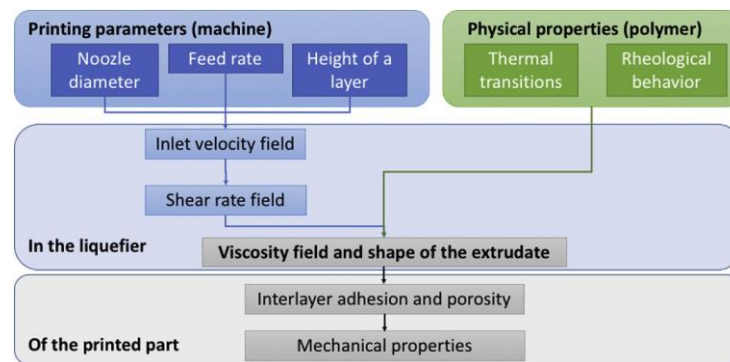
Figure 1-41. Diagram of the printing parameter effects and physical properties of the polymer on the mechanical properties of printed parts. From reference [236]

3. PLA-based biocomposite filaments

For obtaining a qualified printing product, the thermal transitions and rheological behavior of the selected polymer filament are principles for printing parameters setting. In the case of composite 3D printing materials, these factors are significantly influenced and limited by the dispersion and agglomeration of fillers [244]. Although PLA-based biocomposite have been widely studies in the past decades with different function and for various applications, their applications as 3D printing filament are still limited.

3.1. Wood powder-filled PLA filament

Wood powder is a commonly used filler for PLA for cost reduction and/or reinforce function. Brittleness and cavity could be the main limitations for wood-filled composite filaments. These drawbacks are generally caused by the filler agglomeration and

incompatibility of filler and PLA matrix. Toughening agents and lubricant/plasticizers were generally used to address these drawbacks. According to the work of Zhang, 10 wt% poplar powder combined with PLA was applied as 3D printing filament. The addition of poplar powder displayed poor fluidity and toughness of PLA due to the agglomeration. However, with the help of a toughening agent polyolefin elastomer, an improvement of the fluidity and toughness were observed. Besides, this toughening agent can fill the voids formed by poplar powder in PLA. Similar work investigated that tough agents, like polycaprolactone, poly(ethylene-co-octene), and thermoplastic polyurethane were also distributed to the toughness and the compatibility between polar flour (10 wt%) and PLA. By using polyethylene a lubricant, this wood filled PLA filament had smooth and completely infilled entity during FDM printing process [245]

Such wood-filled PLA filaments have been found commercial applications. As presented in the website SIMPLIFY3D®, this type of filaments is typically consisting of around 30% wood particles, including wood dust, cork, and other powdered wood derivatives, but the exact number may vary depending on the brand. With these particles enable 3D printed parts bearing the aesthetics of real wood. The price of these wood-filled filaments is lower or comparable with neat PLA filament might due to the wood powder treatment process. The presence of wood filler displays slightly higher stiffness, but less abrasive compared to other composite filaments such as carbon-fiber filled, and metal filled.
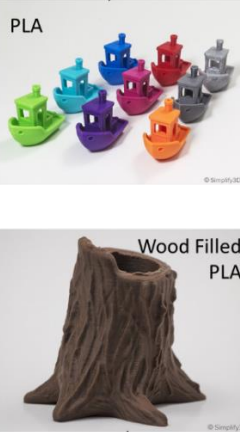
Figure 1-42. A comparation of neat PLA filament and wood-filled PLA filament.

3.2. Fiber-filled PLA filament

PLA filaments incorporated with wood fiber, bamboo fiber, and cellulose fiber are generally display superior mechanical properties and heat resistance [246,247]. The fiber orientation, fiber size, fiber dispersion, fiber distribution, fiber-matrix interfacial compatibility, and void fraction play an important role in determining the properties of final printed products. The filler and PLA molecular chains will be oriented along the printing direction during FDM process. This printing orientation has significant effect of tensile performance. For example, the fully oriented sample printed by method "parallel" has a better tensile strength with PLA/sugarcane bagasse cellulose fiber composite filament [248]. Chemical surface treatments, enzymatic-assisted modification, coupling agents, and compatibilizers were widely studied to improve the filler-matrix interfacial compatibility and fiber dispersion [246,249–252]. Micro-size or nano-size cellulose fibers are excellent reinforcement for 3D printing filament because of the superior reinforce function at low fiber loading content. The dispersion, distribution, and the interfacial interaction of cellulose particle in thermoplastic composites are also critical factors as 3D printing filaments. The printability of PLA 3D printing filaments can be greatly enhanced by using plasticizer [154]. Cellulose based nanocomposites combined with 3D printing technology are attracted in medical applications, such as wound dressing and drug delivery. For this application, 3D printing parameters should be careful controlled to minimize cellulose derivatives degradation and to improve cellulose materials dispensability within the matrix polymer [253].

3.3. Lignin-filled PLA filament

Lignin is a potential functional filler feedstock for 3D printing since its attracting characteristics such as antioxidant, antifungal and antimicrobial capacities, UV-radiation, and fire-retardant properties. However, reports of lignin-filled PLA filament for 3D printing are rare. A kind of PLA filament combined with Kraft lignin was developed by Gkartzou et al. for FFF process [254]. The addition of lignin causes a surface roughness and lignin aggregation even just 5 wt% loading content. FP Innovations and Emily Carr University of Art and Design (Vancouver) explored 3D printing of powdered lignin using powder-binding technology (Figure 1-43, a) and some printed objects are made from filaments composed of thermoplastic polymers

containing lignin filler and fiber materials based on FDM technology (Figure 1-43, b). In this report, Li et al. highlighted that lignin can be a potential filler to address the premature oxidation and flammable problems of 3D printing filament [247].
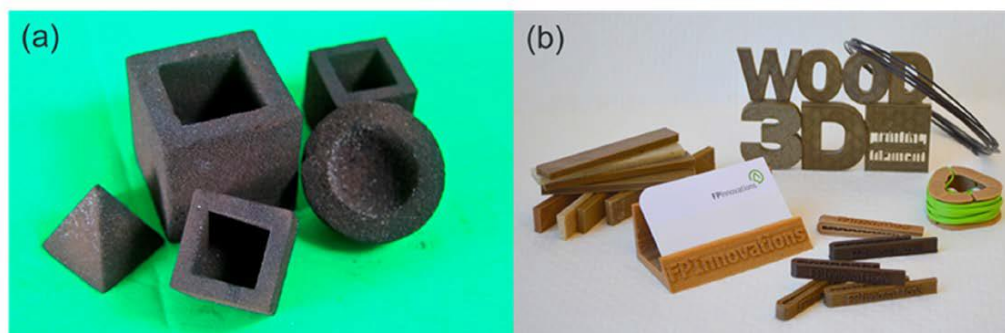
Figure 1-43. Developing lignocellulosic-based feedstock for 3D printing at FPInnovations: (a) prototypes made using the powder-binding technology; (b) prototypes made using FDM technology.

3.4.   Hemicellulose-filled PLA filament

Hemicellulose (galactoglucomannan, GGM) was reported to partially replace PLA as feedstock material in 3D printing [201] (Figure 1-44). A solvent blending approach was developed to ensure the even distribution of the formed binary biocomposites. Hemicellulose up to 25% loading content was successful incorporated with PLA and extruded into filaments by hot melt extrusion. 3D scaffold prototypes were successfully printed from the composite filaments by FDM process. The versatile active sites of hemicelluloses have the possibility to apply as carriers or molecular anchors to introduce desired functionality and features. This hemicellulose-filled PLA filament combined with 3D printing technique, would potentially boost this new composite material in various biomedical applications such as tissue engineering and drug-eluting scaffolds since the biocompatible and biodegradable feature of hemicellulose. However, the higher content of hemicellulose has rougher and more porous surface and structural morphology caused by chain entanglement and intermolecular phase separation between hemicellulose and PLA polymer chain. It should be noting that, the addition of hemicellulose increases the melting viscosity, this might result in clogging at printing nozzle and instable deposition during the printing process, resulting in a poor interlayer adhesion.
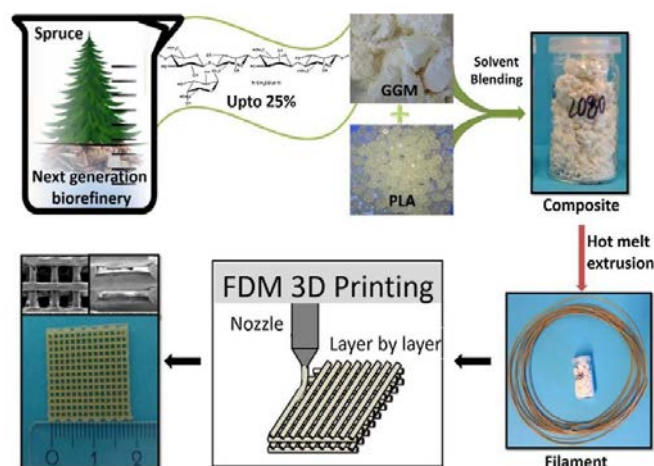
Figure 1-44. Schematic illustration of preparation of composite of GGM and PLA, filaments, and thereof scaffolds by FDM 3D printing. An example for composite ratio of 20:80 in weight of GGM and PLA is shown.

Chapter 2. Polypropylene/polyphenols composites prepared and modified via dynamic vulcanization

Introduction

The polyphenols (tannin and lignin) from renewable resources as biocomponents of PP-based composites were presented in this chapter. The composites were processed via dynamic vulcanization process. Polyphenols were expected to be cured under the pressure and temperature of the extruder. This chapter consisted of two articles. Tannin will be developed as an antioxidant component of PP via reactive blending process. The antioxidant capacity of tannins with and without dynamic curing will be investigated as well.

Organization of chapter 2:

Article 1. Dynamically Cross-Linked Tannin as a Reinforcement of Polypropylene and UV Protection Properties

Article 2. Polypropylene blend with polyphenols through dynamic vulcanization: mechanical, rheological, crystal, thermal and UV protective property

Article 1: Dynamically Cross-Linked Tannin as a Reinforcement of Polypropylene and UV Protection Properties

Abstract: Tannins were used as reinforcing components for polypropylene with anti-UV properties via dynamic curing extrusion. The influence of cross-linked tannins in different weight fraction and their anti-UV capacity on morphological, mechanical, rheological, crystallize and thermal properties were studied. The experimental results indicated that the cross-linked tannins improve Young's modulus, crystallinity, and thermal stability and reinforce the internal network of polypropylene. After UV accelerated weathering, polypropylene had fewer surface cracks, lower carbonyl index, fewer crystallinity decreases and less mechanical properties loss with increasing tannin content.

Keywords: tannin; dynamic cross-linked; polypropylene; UV weathering

1. Introduction

Over the past few decades, polymer composites have been widely studied due to their advantageous combined properties over single-component polymers. With the increasing focus on environmental awareness, considerable efforts have been made to develop composites that contain some fraction of sustainable biopolymers due to their renewable, biodegradable, chemical reactivity and physicochemical properties[124]. Among those composites, polypropylene (PP) is one of the most important and widely used composite matrix because of its low production cost, design flexibility, low density, and recyclability [255]. The combination of PP and biopolymers show many advantages, including low cost, availability of renewable natural resources, biodegradability and good mechanical properties [256–259]. For example, cellulose and cellulosic materials are widely used as a reinforcement in PP-based composites. However, PP is well known to be highly sensitive to UV light and oxygen compared with other polyolefins. The UV exposure results in photodegradation, causing color changes, surface cracking and ultimately lower mechanical properties [116].

The photodegradation mechanisms of PP is mainly initiated by UV irradiation, creating broken bonds and free radicals in the polymer (Equation (1)). Oxygen combines with free-radical species to create peroxy radicals which are reactive with polymer chain and hydroperoxides which are reactive to create hydroxyl and alkoxy radicals (Equations (2) and (3)) [260,261]. Additives with the capacity to absorb the UV energy or scavenge free-radical species or peroxides can physically or chemically prevent or interrupt the degradation processes [116]. For this reason, polymers like phenolics antioxidant are considered as effective additives of PP due to their free radical scavenging capacity.

$$RH \overset{h\nu}{\rightarrow} R \tag{1}$$

$$R \cdot + O_2 \rightarrow R$$

$$R \cdot + RH \rightarrow ROOH + R \tag{2}$$

$$ROOH \rightarrow \cdot OH + RO \tag{3}$$

Recently, natural phenolic compounds are gaining attention driven by environmental concern. Lignin is the most widely studied one for PP based composites [262]. Its reinforcing [263], antioxidant [212,264], or stable function [265] have been extensively reported. However, reports concerning the utilization of tannins in mixture

with thermoplastic resins are scarce. Tannins are the fourth most abundant sustainable biopolymers from plants (after cellulose, hemicellulose, and lignin), present in soft tissues of woody plants like leaves, needles, and bark [12]. Tannins are commonly divided into hydrolyzable tannins and condensed tannins. Condensed tannins which are mainly composed of flavonoid units (Figure 2-1) are widely distributed in nature and constitute more than 90% of the total world production of commercial tannins [8]. Because of their high chemical reactivity, tannins have played an important role in thermosetting systems for several decades, such as tannin-based adhesives for wood bonding [6,97,266], tannin-based foam material [266]. Moreover, the structure of flavonoids presents suitability for UV protection and antioxidation in plants and this has led to the application to prevent human aging [6].
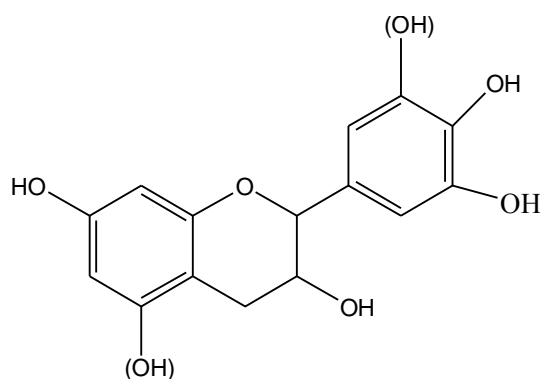
Figure 2-1. Structure of flavonoid unit of condensed tannins.

According to some recent works, the addition of flavonoid structure (chrysin, quercetin, and silibinin) on PP, yielded a good stabilization against UV radiation [97]. Ambrogi and co-workers also verified the stabilization property of tannins rich product and other phenol by-products on PP according to the experimental results of thermogravimetric analysis and oxidative induction time measurement, which is similar as a commercial phenolic antioxidant [96]. In addition, tannins used as co-stabilizer for poly (vinyl chloride) were investigated and have shown an improvement in thermal stabilization and thermal stability and did not cause negative impacts during production process [99]. Some researchers demonstrated that tannins are effective short-term stabilizers for polyethylene films, reducing the impact of thermo-oxidative and UV degradation [108]. Furthermore, tannin also is a functional component of the polyvinyl alcohol (PVA) composite membrane with antioxidant and UV-protective properties [104]. However, tannins like other biopolymers containing hydrophilic hydroxyl groups result in incompatibility with a hydrophobic polymer and therefore deteriorate

the mechanical properties of the final product when increasing their proportion. As a result, the chemical modification of biopolymers is generally considered as the most effective technique to enhance the biopolymer-matrix adhesion [208,209]. Moreover, this chemical modified biopolymer reduces not only the hydrophilicity but also develops in some cases functional property. For example, tannin-based epoxy resin (with 5, 10 or 20 phr) can provide enhanced dynamic thermal and process stability and improved the rheological properties on PVC [54]; acetylated tannin or esterified tannin exhibited improved miscibility with hydrophobic plastic matrix (e.g., poly(butylene succinate), PP, aliphatic polyester, poly(lactic acid)), and UV stability [40,106,267]. The addition of compatibilizers is also an effective pathway to improve biopolymers and plastics matrix by the formation of bonds, maleic anhydride grafted polypropylene (MAPP) being one of the most important compatibilizers for a PP matrix due to the high reactivity of maleic anhydride [125,268]. The utilization of maleic anhydride functionalized polymer has shown better compatibility for polyethylene–tannin films which further enhanced their thermal properties [108]. The goal of these interfacial modification methods is to minimize the hydroxyl groups of biopolymers to reduce their polar difference, therefore, to enhance biopolymers-matrix adhesion. On this basis, a dynamic vulcanization process might be a good technique to decrease their hydrophilicity. This process has been successfully applied to dynamically crosslink thermoplastic resin with thermoset resin system. For example, dynamically cross-linked PP/epoxy composite [233] and PP/novolac composite [232] compatibilized with MAPP were reported to exhibit higher modulus, stiffness as well as thermal stability compared to neat PP.

In the present work, tannin was dynamically cross-linked with hexamethylenetetramine (hexamine) within a twin-screw extruder to reinforce a PP matrix. Hexamine has been described as a cross-linker for tannin resins usable for wood bonding [266]. Meanwhile, 5% MAPP have been used as a compatibilizer. The influence of dynamically cross-linked tannin (TH) in different weight fraction on morphological, mechanical, rheological and thermal properties were evaluated. Moreover, the anti-UV properties has been assessed by the changes of mechanical property, surface morphology, crystallinity, rheological behavior after UV accelerated weathering test.

2. Materials and Methods

2.1. Materials

The PP was purchased from TOTAL with a melt flow index of 25 g/min according to the standard test method ISO 3146 and a melting temperature of 165 °C. The maleic anhydride grafted polypropylene, Licocene® PP MA 6252 granules wax (grafting rate 1%), were supplied by Clariant (Muttenz, Switzerland) with a viscosity (approx.) 100 mPa·s at 170 °C. Mimosa tannins were purchased from Silva Chimica, in Mondovi, Italy. The hexamethylenetetramine 99% (hexamine) and sodium hydroxide were purchased at Acros Organics (Illkirch-Graffenstaden, France) and VWR Company (Radnor, PA, USA), respectively.

2.2. Preparation of PP/TH Composites

Tannin was pre-reacted with hexamine in a stirred reactor and dried by a spray dryer (BUCHI mini spray dryer B-290, Flawil, Suisse) before blended with PP. The 100 parts of mimosa tannin extracts were dissolving in 100 parts of water and 12 parts of NaOH were mixed for adjusting its pH to 10. And tannin solutions were heated to 80 °C and then six parts of hexamine were added to the mixture for 30 min. All the compounds were added based on the weight of the dry tannin. The spray dried pre-reacted tannin-hexamine (TH) was characterized by FTIR (Figure S 2 and Table S 3).

PP blend with 5%, 10%, 15%, 30% pre-reacted tannin-hexamine (note as 5TH, 10TH, 15TH, and 30TH, respectively) were carried out in a twin-screw extruder (Thermo Scientific™ Process 11, Villebon-sur-Yvette, France) with a screw rotation speed of 200 rpm at 190 °C. The extruder had a screw diameter 11 mm and a length-to-diameter ratio L/D = 40. The screw profile is composed of three mixing zones with different configurations of kneading blocks for promoting dispersive and distributive mixing. The residence time was approximate 2 min 30 s. PP powder, pre-reacted tannin-hexamine and PPMA in different weight proportion were well blended in a baker before injecting into the extruder. Tannin-hexamine was expected to be cured under the pressure and temperature of the the extruder. Unreacted species and reaction by-products were removed by a highly efficient vacuum in zone 6.

2.3. Characterization

UV accelerated weathering test was carried out by a QUV accelerated weathering

tester (SOLAR EYE, Q-Panel Lab Products, Saarbrucken, Germany). The specimens were exposed under continuous irradiation with an irradiance intensity of approximately 0.68 W/m^2/nm at λ = 340 nm for one week (168 h) at 60 ℃ . For each batch of specimens, four replicates were used to ensure the repeatability. The anti-UV properties of TH were evaluated by the changes in surface morphology, mechanical property, rheological behavior, crystallinity and surface chemical property.

The dispersion of TH was observed by Dino-lite premier digital microscopy (AM-7013MZT, New Taipei City, Taiwan, China) with a software DinoCapture 2.0. The morphology of UV exposed surface was characterized by a scanning electron microscopy (SEM, Hitachi S4800, Los Angeles, CA, USA) with an acceleration voltage of 15 kV. All the samples were sputter coated with a thin layer of gold.

The tensile test was performed at room temperature with standard dog-bone shaped (ISO 527, type 1A) tensile test specimens, which was molded by a micro-injection molder (Xplore, Sittard, the Netherlands), on an Instron tensile testing machine (model 5569) equipped with a 50 kN load cell, operated according to EN ISO 527:1996. The cross-head speed used was of 10 mm/min. All the samples were measured four times and the the average value was calculated.

The rheological property was performed using a rheometer (TA instrument, G2 ARES, New Castle, DE, USA) with parallel-plate geometry (25 mm diameter, 1 mm gap) with the protection of nitrogen under 180 °C. Frequency sweeps between 0.05 to 100 rad/s were carried out at 10% strain in the linear viscoelastic region (LVE).

Thermogravimetric analysis (TGA) was carried out in a METTLER TOLEDO. The samples with a total weight in the 5-10 mg range were scanned in the range of 30-600 °C with a heating rate 10 °C /min in an air atmosphere (50 mL/min). The obtained data were analyzed by STARe evaluation software (version 10.0).

The Differential scanning calorimetry (DSC, METTLER TOLEDO) was employed to measure the melting temperature (T_m) and crystallinity temperature (T_c) of samples in the second heat-cool-heat circle with a scan rate of 10 °C/min within the temperature range of −50 °C to 220 °C. The measurements were using aluminum crucibles with a total sample weight 5.00 ± 1 mg under a nitrogen atmosphere (50 mL/min). Values for melting temperatures (T_m) and enthalpy of melting (H_m) were analyzed by STARe evaluation software. The percentage of crystallinity X_c was estimated by the following equation:

$$X_c(\%) = \frac{100 \times H_m}{\Delta H_m^0 \times w}$$

(4)

where X_c is the crystallinity (%), ΔH_m^0 is the enthalpy of melting 100% crystallized PP, which is equal to 207 J/g [269], H_m is the enthalpy required for melting each sample, and w is the weight fraction of PP in blends.

The Fourier Transform Infrared (FT-IR) spectra of the exposed surface of aged PP and PP/TH specimens measured by a NICOLET 6700 FT-IR spectrometer attenuated total reflection (ATR) mode for 16 scans in the range 4000–400 cm^{-1} with a resolution of 4 cm^{-1}. The curves were normalized, and peaks were analyzed without smoothing the data. The degradation of composites was characterized by c (*CI*) [269]. The calculation equation as follows:

$$CI = \frac{A_c}{A_r}$$

(5)

where A_c is the area of the carbonyl absorption band (1670–1820 cm^{-1}, C=O). A_r is the area of C-H stretch from CH$_3$ (2760–3020 cm^{-1}). The latter one was used as a reference band because it was minimally affected by UV irradiation. In addition, for a more precise evaluation, the calculated carbonyl area A_c of each sample has been minus the area before aging, considering that tannin has carbonyl groups in their structure.

4. Results and Discussion

4.1. The Effects of Dynamically Cross-Linked Tannin and Its Reinforcing Function on PP

4.1.1. Morphology

The composites have been prepared by twin extrusion of PP blend with 5% to 30% of a pre-reacted tannin-hexamine mix (TH). The morphology of PP/TH composites was observed by optical microscopy and SEM. SEM micrographs (Supplementary Materials, Figure S 1) of their fracture surface are smooth and the cross-linked tannins are difficult to observe, indicating fine cross-linked tannin particles well dispersed in the PP matrix. Similar results can be found in dynamic cured a PP/phenolic resin and PP/epoxy blends [233,270]. At the higher TH content (30%) one can observe a rough region marked with a white circle, which may be due to the agglomeration of cross-linked tannin. To further identify the morphology of PP/TH composites, film shape

materials (0.6 mm) were prepared by micro-compounder and observed by optical microscopy. The particles size distributions of PP/TH composites can be observed. Figure 2-2 (a–d) shows the micrographs of PP films with different cross-linked tannin content. Figure 2e gives the particle size distribution analyzed by software Image J. From these micrographs, the cross-linked tannin appears to be homogeneously dispersed as particles within the PP matrix. These particles are generally fine in the composites with 5% cross-linked tannin (Figure 2-2, a), while TH agglomeration starts to occur with increasing tannin content (Figure 2-2, b–d). However, the bar chart (Figure 2-2, e) confirms the good dispersion of cross-linked tannin and 90% of particles are in the average diameter range of 5–15 μm.
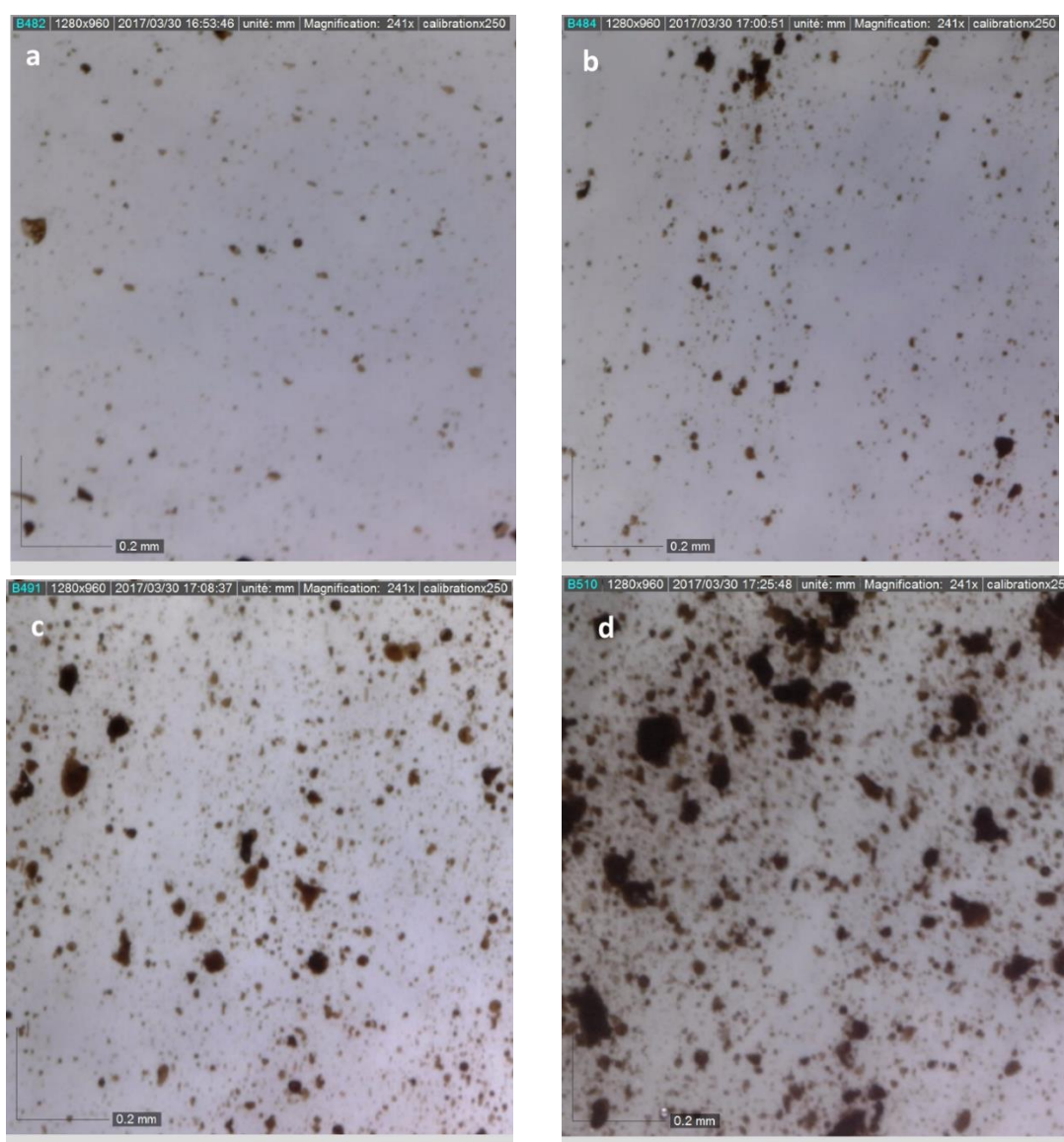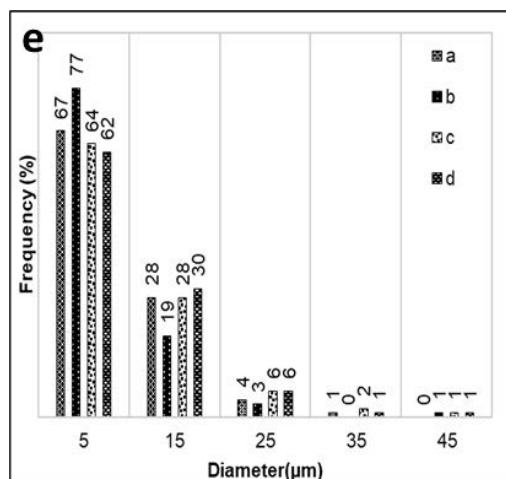
Figure 2-2. Micrographs of PP/TH composites: (a) 5TH, (b) 10TH, (c)15TH, (d) 30TH, (e) particles size distributions

2.3.1. Tensile Properties

The results of tensile tests of PP/TH composites as a function of cross-linked tannin content is shown in Figure 2-3. As can be seen, Young's modulus increases with increasing TH content. Similar results were described for organic filler-reinforced PP composites [270,271]. It is generally believed that the capability of a composite interface to transfer elastic deformation depends on the interfacial stiffness and static adhesion strength [272] . During a dynamic extrusion process, extensive cross-linking between tannin and hexamine at high temperature formed stiff tannin thermoset particles. These stiff particles contribute to the improvement of Young's modulus at increasing TH content. Besides, the crosslinking process appeared to reduce the hydroxyl groups content of the tannin developing a better interaction with hydrophobic PP matrix. Moreover, the rigid TH restricts the chain mobility of the PP matrix yielding a better static adhesion. This phenomenon can be confirmed by the supplementary experimental results (Supplementary Materials, Table S 1), Young's moduli of PP combined with uncross-linked tannin (1.41 ± 0.08 GPa) being slightly lower compared with PP alone (1.53 ± 0.08 GPa), while it is 21.5% lower compared to the combination with cross-linked tannin (TH, 1.80 ± 0.05 GPa). Furthermore, the PP/TH composite without MAPP exhibits a lower modulus (Supplementary Materials, Table S 2, 1.60 ± 0.05 GPa), indicating its positive effect on tensile properties. Without the MAPP compatibilizer, the absence of covalent bonds across the TH-PP matrix interface results in a worse static adhesion strength.

Figure 2-3 gives the tensile strengths and elongations of the composites versus TR

content, respectively. A decreasing trend can be observed with increasing TH content. Unlike Young's modulus, tensile strengths measured at larger deformations are much more sensitive to interactions than the modulus, which means it strongly depends on the interfacial adhesion between the filler and the matrix [273]. The tensile strength of composites containing less than 10% TH are slightly lower than PP and quickly decrease in the composite containing more than 15%TH. Similar trends can be found for the elongations results. The TH agglomeration observed under optical microscopy can be an explanation. Conversely, the higher loading of TH would weaken the interfacial adhesion because of the increasing TH-PP matrix interfacial areas. However, a slightly positive effect of MAPP on the tensile strength of a PP/TH composite can be found when comparing it with the PP/TH composite without compatibilizer. The tensile strength and elongation of PP/10TH are respectively 31 ± 1 MPa and $15 \pm 2\%$ with MAPP and; 30 ± 1 and $32 \pm 10\%$ without MAPP (Supplementary Materials, Table S 2). This implies that covalent bonds between MAPP and TH may contribute to such an improvement [274,275].
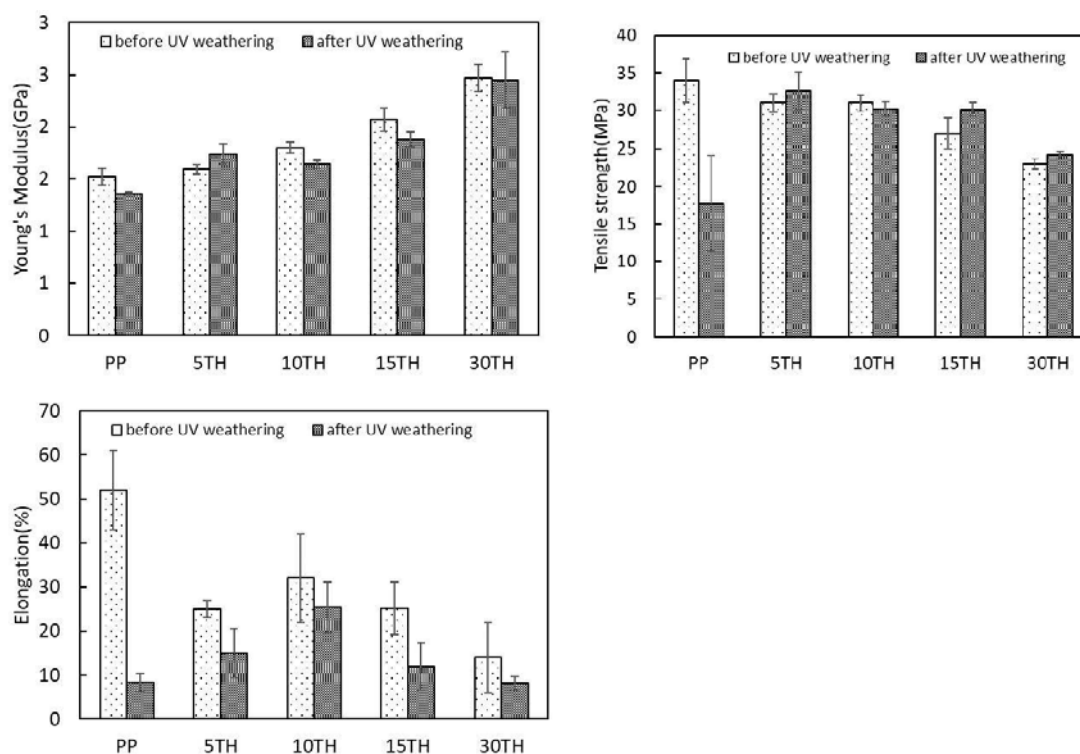
Figure 2-3. The tensile property of PP and PP/TH composite before and after UV weathering.

2.3.2. Rheological Behavior

The influence of the TH content on the melting rheology behavior of PP was studied by rheometer under the linear viscoelastic region. The complex viscosity (η^*), storage

modulus (G′) and loss modulus (G″) as a function of frequency (ω) were plotted in Figure 2-4. In Figure 2-4 (a), all curves of η* are observed to decrease with increasing ω, indicating that PP and PP/TH composites exhibit a typical shear-thinning behavior. TH has a positive effect on complex viscosity at low frequency, especially PP containing 5%–15% TH. At high ω, η* of PP/TH composites coincide with PP and an increase is observed for PP/TH composites at low η*, replying TH enable a greater resistance to flow. However, 30TH has a lower ω, which suggests that an easier flow tendency caused by weaker interfacial adhesion due to the increase of interfacial areas between TH and PP matrix. A similar trend is also observed in storage modulus (Figure 4b). At low ω, PP/TH composites show a significant increase of G′, which is common in filled polymer system [276–278]. This suggests that the presence of cross-linked tannin in the matrix reinforces the internal network structure, enhancing the storage modulus and reduce the deformation degree under a low ω. All studied samples are dominated by the viscous behavior according to loss modulus G″ which is generally higher than the storage modulus G′. However, PP/TH composites present a more solid-like response than PP at low frequency because of the reinforcement of TH in the PP matrix. Unlike tannin-based epoxy resin that behaves like a plasticizer in a PVC matrix [54], cross-linked TH in a PP matrix behaves more like an organic filled PP, for instance, silica reinforced PP [276] and plate-like carbonaceous particles reinforced PP [277].

(a)   (b)
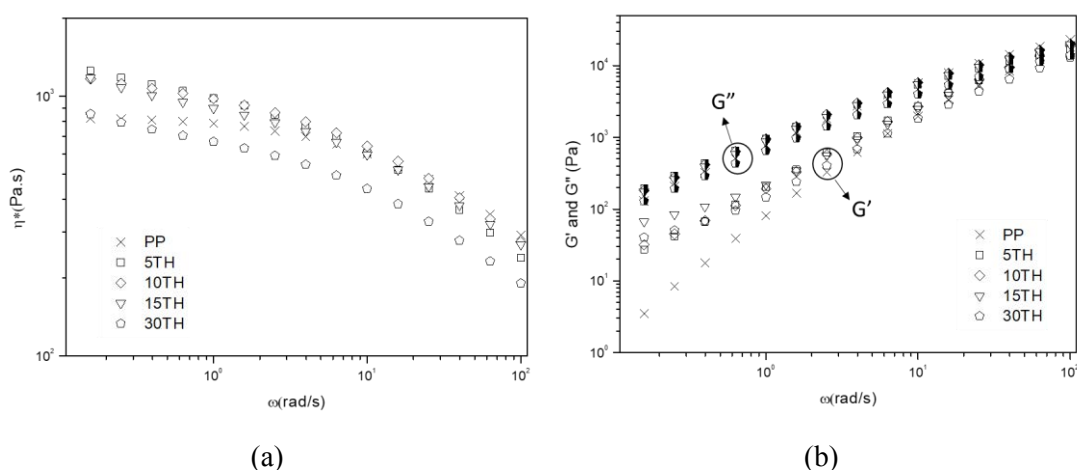
*Figure 2-4. Rheology behavior of PP and PP/TH composites: **(a)** Complex viscosity η*; **(b)** Storage modulus G′ and Loss modulus G″.*

2.3.3.   Crystallinity

Since PP is a semi-crystalline material, crystallinity has a significant influence on

the mechanical properties of PP. In this study, the effect of cross-linked tannin on the crystallinity of PP was characterized by differential scanning calorimetry (DSC). The melting temperature (T_m), melting enthalpy (H_m), and degree of crystallinity (X_c) are presented in Table 2-1. According to the summarized data, the melting temperature (T_m) of PP was slightly affected by the loading of cross-linked tannin. Like PP-based composites combined with lignin [279], inorganic filler [280], cellulose fiber [259] et al., the crystallinity degree of PP increases with the addition of cross-linked tannin. Thus, it can be concluded that cross-linked tannin can be a nucleating agent for the PP matrix. This nucleation effect might also contribute to the improvement of Young's modulus.

Table 2-1. Crystallinity of PP and PP/TH composites before and after UV accelerated weathering

Sample	Before			After		
	H_m	X_c	T_m	H_m	X_c	T_m
	(J/g)	%	℃	(J/g)	%	℃
PP	−71.6	34.6	165.0	−53.3	25.7	163.3
5TH	−74.9	38.1	166.5	−72.0	36.6	166.8
10TH	−75.6	40.6	164.1	−62.0	33.3	167.6
15TH	−71.3	40.5	164.0	−57.7	32.8	164.7
30TH	−59.1	40.8	164.2	−49.6	34.2	165.1

2.3.4. Thermogravimetric Analyses

To better understand the thermal behavior in our environment, the thermal characteristics were determined by thermogravimetric analyses in an air atmosphere. The weight loss of PP/TH composites as a function of temperature (a) as well as their DTG data (b) are plotted in Figure 2-5. The weight losses show that degradation of PP and PP/TH composites occurs almost as a one-step process as can be concluded by the presence of only one peak in the DTG curves. A slight weight loss in all the PP/TH composites before the thermal degradation temperature (about 250 °C) is due to either the degradation of small oligomers in TH or the emission of water caused by the crosslinking of the unbound tannin-hexamine component. A general lower degradation speed can be observed in all PP/TH composites, implying a better thermal resistance due to the stabilization of the cross-linked tannin and the restriction of the polymer

chains slippage in the presence of cross-linked tannin [281]. It is worth noting that 5TH has the best stabilization performance, followed by 10TH, 15TH and 30TH. This trend might be due to the MAPP compatibilizer, resulting in better compatibility of the 5% cross-linked tannin and PP. Conversely, PP/TH composites present an improvement in char yield when increasing TH content, suggesting a potential flame-retardant property of the cross-linked tannin. Indeed, the char can effectively hamper the oxygen to reach the combustion zone, reducing the combustion rate of polymeric materials.

(a) (b)
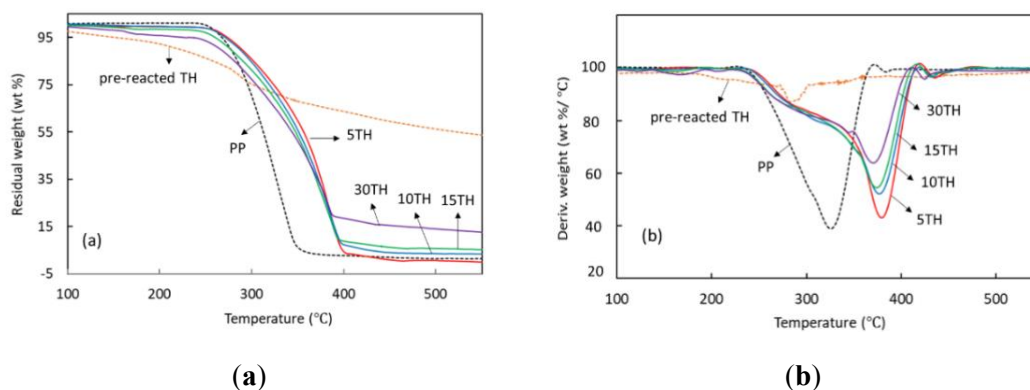
Figure 2-5. Thermal behaviors of PP and PP/TH composites: (a) TGA curves; (b) DTG curves.

2.4. Anti-UV Performance of Cross-Linked TH

The degradation of PP caused by sunlight or UV radiation in the air can cause color changes, while also causing surface cracking, and ultimately lower mechanical properties [116]. Figure 2-6 shows the comparison of microphotographs of unexposed and exposed PP and PP/TH composites characterized by SEM. Both show similarly smooth surfaces without any crack before weathering. However, after one-week UV weathering, surface cracks had appeared in all samples. In the exposed surfaces of PP, large and long cracks mixed with various tiny cracks can be easily observed. Whereas the cracks clearly appeared to be smaller and less severe with an increase of TH content. The cracks were generally found in PP-based composite products in UV exposed surface [281,282], which is caused by the chain scission of the polymer promoted by UV irradiation. The appearance of the cross-linked tannin would indicate that it could prevent photodegradation of the PP matrix.
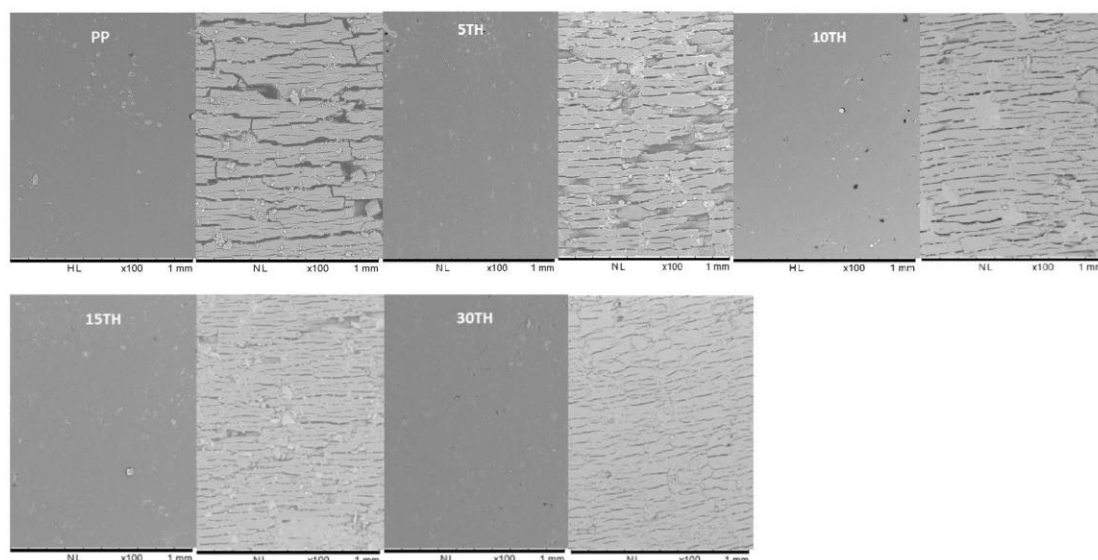
Figure 2-6. SEM microscopy of PP and PP/TH composites before (left) and after (right) UV weathering.

The Young's modulus, tensile strength, elongation of PP and PP/TH composites are presented in Figure 2-3, and their changes are plotted in Figure 2-7. According to the report of Badji et al. [281], the frequency and size of cracks have a positive correlation with the mechanical properties. As seen in Figure 2-3, PP has the worst mechanical performance to resist to large deformations, a significant loss in both tensile strength and elongation being observed after UV weathering. The photodegradation caused by UV irradiation is generally concentrated near the surface. The presence of cracks enhances the permeability to oxygen, resulting in further interior degradation. As a result, PP presents a strong decrease in tensile strength and elongation compared to the sample including cross-linked tannin.
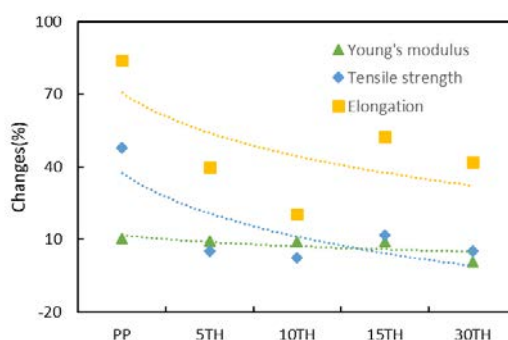
Figure 2-7. The changes of tensile property on PP and PP/TH composite before and after UV weathering.

A significant crystallinity decrease of PP after 1-week exposure can be observed, from 34.6% to 25.7% (Table 2-1) while in presence of TH the crystallinity decrease is clearly lower. The drop of crystallinity is mainly observed for the samples with surface cracks and drop of tensile properties. According to some studies of PP-based composites, an increase in crystallinity can be observed after weathering because the chains scission results in smaller molecules which can undergo recrystallization [261,283]. However, as the chain scission continues, the molecular weight of PP decreases and causes irregular and chemical imperfect recrystallization. Therefore, the less significant changes of crystallinity of PP/TH composites confirm that TH has the ability to hinder chains scission. According to the curing mechanism of tannin-hexamine [33,266,284], the crosslink reaction of TH is mainly dominated by benzylamine bridges between the reactive carbon sites on the flavonoid molecules of tannin and hexamine. As a result, radical capacity is promoted due to unsaturated hydroxyl groups.

The chemical changes of PP and PP/TH composites were characterized by FTIR. Before UV weathering, main chemical bands of PP in the range of 2760–3020 cm^{-1}, at 1449 cm^{-1} and 1375 cm^{-1} are visible from Figure 2-8 (a). A carbonyl absorption band (1700–1800 cm^{-1}) from PP/TH composites attribute to the structure of tannin. In comparison with initial stage, an intensity increases or appearance (PP) of the carbonyl group after UV weathering can be observed in Figure 2-8 (b). While a decreasing trend in the intensity of the carbonyl group region with increased addition of cross-linked tannin can be observed, this decrease is confirmed by the changes of carbonyl index from Figure 2-8 (c), implying a serious degradation of the PP polymer chains. TH-containing PP instead shows a clear slowdown in degradation due to the formation of hydroperoxides in a lesser extent. Tannins are well known radical scavengers [285] and could be capable to deactivate free radicals by donating a hydrogen atom, preventing the initiation of new radicals in the polymer. In our case, although tannins undergo a dynamic extrusion process of a high temperature in an extruder, its crosslink with hexamine did not consume whole hydroxyl groups. Moreover, the limited residence time in the extruder (approximately 2 min 30 s), compared with more than 5 min for wood bonding [286], and the steric hindrance of tannin might also contribute to an incomplete cross-linked.
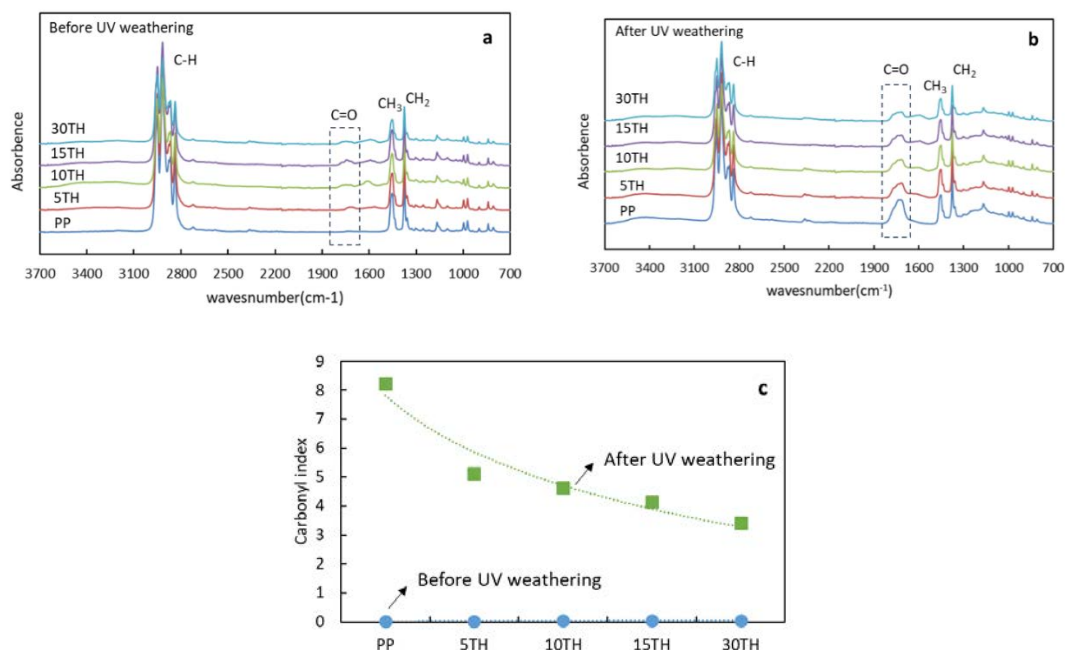
Figure 2-8. (a) FTIR spectra of PP and PP/TH composite before UV weathering (a); after UV weathering (b) and their carbonyl index (c).

In order to better understand how the cross-linked tannin affects PP polymer chains after UV weathering, PP and PP containing 10TH and 30TH were investigated by dynamic rheology, which is a sensitive technique to investigate the structural changes on the weathering degradation process [287]. A comparison of complex viscosity η^* and loss modulus G' between initial and weathered samples is given in Figure 2-9. The significant drop of η^* and G' for PP suggests a severe chain scission and molecular mass decrease. In agreement with our previous discussion, PP without cross-linked tannin presents severe surface cracks, low crystallinity, and high carbonyl index; therefore, it is much more sensitive to degradation. Whereas, the presence of cross-linked tannin has a lower influence on the melt rheology in both η^* and G', implying a lower chain scission degree. Besides, in those weathered samples, cross-linked tannin might also contribute to the entanglement of degraded PP chain, thus limiting the movement of polymer chains according to G'-ω data. In 10TH and more obviously in 30TH at low frequency, G' of a weathered sample is slightly higher than the initial one. The more significant increase of η^* in 30TH can support this explanation.

(a)   (b)
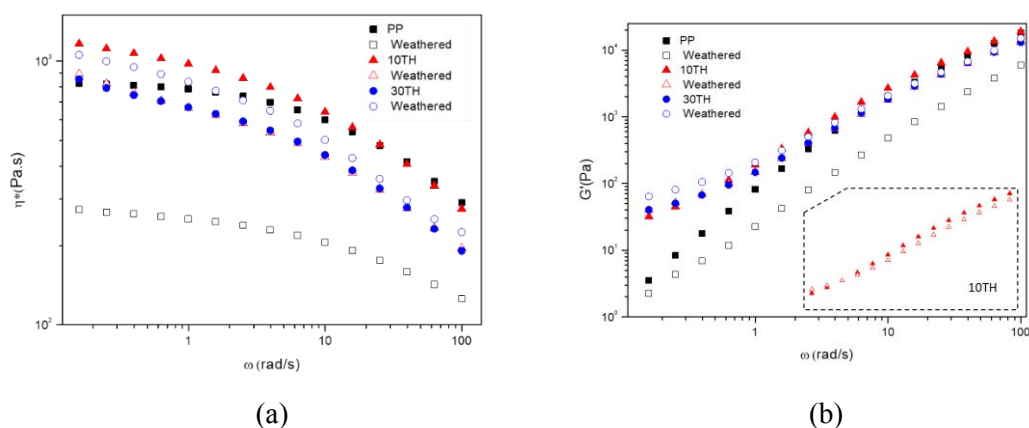
Figure 2-9. *A comparation of (**a**) complex viscosity η* and (**b**) loss modulus G' of initial and weathered PP, 5TH and 30TH.*

3. Conclusions

PP-based composite combined with tannin has been successfully processed through dynamic extrusion. In this process, tannin was cross-linked with hexamine in different proportion. The morphology study showed small particles of cross-linked tannin well dispersed in the PP matrix. From Young's modulus and rheological behaviors of tested samples, cross-linked tannin performed as a stiffness filler and reinforced the PP matrix. In addition, cross-linked tannin had a positive performance towards PP crystallinity and thermal stability. Moreover, when composites were subjected to UV accelerated weathering, PP/TH composites presented a much better performance on photodegradation resistance characterized by fewer surface cracks, lower carbonyl index and less crystallinity decrease, thus slowed down the chain scissions of PP. Furthermore, TH addition to PP can prevent the loss of mechanical properties in physically limiting the mobility of polymer chains.

Article 2: Polypropylene blend with polyphenols through dynamic vulcanization: mechanical, rheological, crystalline, thermal and UV protective property

Abstract: Tannin and lignin were blended with PP through dynamic vulcanization technique. Their influences of mechanical property, crystallinity, thermal stability, as well as UV protection property on PP matrix were investigated and compared with native tannin and lignin. According to our experimental results, tannin and lignin undergo dynamic vulcanization, were more compatible with the PP matrix. Besides, tannin and vulcanized tannin can perform as nucleating agents of PP because of their relatively small particle size. Moreover, vulcanized tannin/lignin have a better performance on the thermal stability of PP compared with native tannin/lignin, especially PP/vulcanized lignin blend. Furthermore, vulcanized tannin/lignin present better UV protective performance concluded from fewer changes on surface morphology, carbonyl index, crystallinity, viscosity, and tensile property.

Keywords: tannin, lignin, dynamic vulcanization, polypropylene, UV weathering

1. Introduction

Polypropylene (PP) is a typical semi-crystalline thermoplastic derived from the olefin monomer propylene. Since discovered in 1954, PP quickly becomes one of the most popular commodity plastics due to its low density and low cost with good mechanical property [255]. Today, PP is widely used as a composite matrix to process composite materials because of its excellent chemical resistance hence it can be easily processed by many efficient converting methods, like injection molding and extrusion [125]. The combination of PP with polymers from sustainable resources has been extensively studied over the past decades in order to reduce the dependence on petrochemical-based plastics [124]. Generally, composite materials based on PP and biopolymers have a lower lightweight and less environment impact [124]. Apart from these major advantages, biopolymers bearing individual structural features, associating with specific properties, hence they are potential functional elements for PP. For example, cellulose is generally used as a reinforcement of PP [167]; starch and polylactic acid can improve the degradability of PP [154]; carbohydrates, proteins, lipids, and phenolic compounds can be flame retardants of PP [288]. Among these biopolymers, phenolic compounds (e.g. lignin and tannin) incorporated to PP have attracted interest for both academia and industry, because PP is highly sensitive to UV light and oxygen compared with other polyolefins, while phenolic compounds can prevent its thermo- and photo-degradation owing to their chemical structure. As shown in Figure 2-10, flavonoid structure of tannin (Figure 2-10, a) [11] and the phenylpropanoid (C9) units of lignin (Figure 2-10, b)[262] are inherent hindered phenolic structures, which can stabilize themselves into stable phenoxy radicals, preventing initiation of new radicals[116].
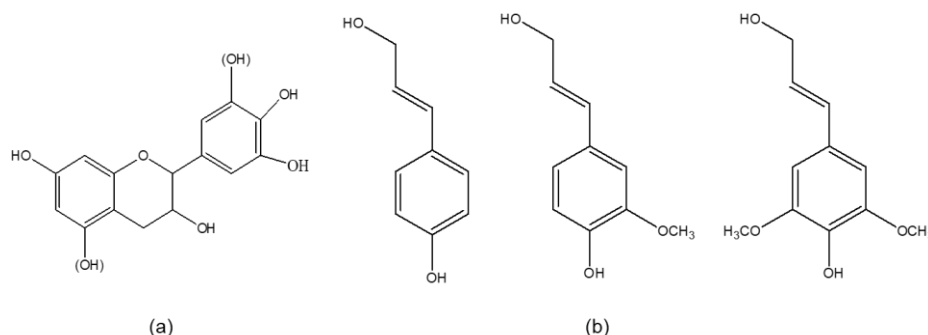
Figure 2-10. Structure of flavonoid unit of condensed tannins(a) and phenylpropanoid units of lignin(b)

Lignin is the most abundant phenolic compound on the earth and is a widely distributed biopolymer. Lignin is usually viewed as a waste in the pulp and paper industry [121]. According to the published reports, lignin can be a potential precursor for synthesized thermoset resin, like polyurethanes [289], epoxy resins [290], wood adhesives [32]. Moreover, lignin has been considered as potential functional element for polymer composites in the past decades and has been included as compatibilizer [291], antioxidant [212,264], stabilizer [265,213], and reinforcement [263]. However, the large molecular weight and hydrophilic characteristic of lignin lead to low reactivity and poor compatibility with the hydrophobic polymer matrix and would result in the deterioration of the polymer's mechanical properties [205,292]. To solve this problem, chemically modified lignin (e.g. esterification, etherification, polymer grafting) has been examined to enhance the compatibility with polymers [205]. However, esterification significantly decreased the phenolic content of lignin and consequently decreased the anti-oxidant effect [292].

Tannins are widely present in soft tissues of woody plants like leaves, needles, and bark. They are easily extracted using water or organic solvent, include methanol, ethanol, and acetone [266]. Tannins have been extensively described for the production of green wood adhesives, which displayed properties comparable to those of conventional phenolic adhesives [266]. Unlike lignin, the researches about tannins-based thermoplastic composites are rare. Published studies focus on the preparation of thermoset tannin resins, namely polyurethane foam material [293], thermoset plastic [70,72,77]. Tannins used as an additive at low content have been reported as a good stabilizer with antioxidant and UV-protective properties on polypropylene [96,97], polyethylene [294], poly (vinyl chloride)(PVC) [295], and polyvinyl alcohol [104].

The chemical modifications of tannin have been investigated to improve its compatibility with the polymer matrix. For example, esterified tannin exhibited improved miscibility with hydrophobic plastic matrix (e.g., poly(butylene succinate) [105], PP [106], aliphatic polyester [106], poly(lactic acid) [101,296]). In addition, it has been shown that low esterified tannin displayed UV stability, and tannin with long ester chain length exhibited plasticity function. According to the report of Bridson [297] and co-workers, PLA had the possibility to incorporate high content of hydroxypropylated tannin through trans-esterification reactions, this totally bio-composite material had revealed potential as a precursor for carbon material. Besides, another research reported PVC incorporated with epoxied tannin, that can enhance dynamic thermal and process stability, and improve the rheological properties on PVC [298]. Dynamic vulcanization is an efficient and common pathway to prepare thermoplastic - rubber composites by extrusion [299]. Generally, high shear rate conditions above the melting temperature of the thermoplastic are required to provoke the rubber crosslinked under dynamic conditions. Few researches reported the successful utilization of dynamic vulcanization of PP/thermoset resin system [232,270,300,301] like epoxy and novolac. These experimental results exhibited higher modulus, stiffness as well as thermal stability compared to neat PP.

In our recent work, we reported for the first time the production of PP/tannin resin composites through dynamic vulcanization [112]. According to our experimental results, tannin was crosslinked by hexamine, forming thermoset particles, well dispersed in PP matrix. The final product displayed higher Young's modulus and good UV protection capacity. However, even if tannin is well known for its antioxidant property, the effect of the crosslinking process on its UV protection capacity is still unclear. Besides, it should be interesting to use dynamic vulcanization with PP/lignin blends since lignin is widely studied and a low-cost polyphenol. For this purpose, in our current work, native tannin/lignin and crosslinked tannin/lignin were blended with PP, respectively. The influence of phenolics on the mechanical property, crystallinity, thermal stability, as well as UV protection property of PP matrix was investigated.

2. Materials and Methods

2.1. Materials

The PP was supplied by TOTAL with a melt flow index of 25 g/min according to

the standard test method ISO 3146 and a melting temperature of 165 °C. Mimosa tannin was purchased from Silva Chimica, in Mondovi, Italy. Lignin was a desulfurized softwood kraft lignin, namely Biochoice kraft lignin supplied by Domtar Inc. (Montreal, QC, Canada) from their Plymouth, North Carolina mill (Plymouth, NC, USA). The paraformaldehyde and sodium hydroxide were purchased at Acros Organics (Illkirch-Graffenstaden, France) and VWR company (Radnor, PA, USA). The hexamethylenetetramine 99% (hexamine) and glyoxal (40 wt% solution in H_2O) were purchased at Acros organics (Illkirch-Graffenstaden, France). All the chemicals were used without further purification.

2.2. Pre-reacted tannin and lignin with glyoxal

In our last work, the preparation of tannin-hexamine pre-reactor has been described in detail. The same pathway was applied to prepare tannin-glyoxal pre-reactors.

The lignin-glyoxal pre-reactor was prepared as follow: the 100 parts of Kraft lignin was dissolved to 100 parts of water. Sodium hydroxide solution(30wt%) was used to keeping the pH of the solution between 12 and 12.5 for better dissolution of lignin. One hundred parts of glyoxal were added and the lignin solution was then continuously stirred with a magnetic stirrer/hot plate for 30 min. All the compounds were added based on the weight of the dry lignin.

2.3. Spray dried the pre-reacted tannin and lignin

The pre-reacted samples were dissolved with 500 parts of water for spray drying. The parameters of the spray dryer (BUCHI mini spray dryer B-290, Flawil, Switzerland) were described elsewhere, tabulated in Table 2-2:

Table 2-2 The parameters of spray-drying

Inlet temperature	Aspirator	Pump rate	Nozzle cleaner	Feed switch valve	Flow meter (mm)
150°C	100%	10%	6	1	40

2.4. Composites preparation

The PP powder was respectively well blended with tannin (T), lignin (L), pre-reacted tannin-glyoxal (TG), and lignin-glyoxal (LG) in 90/10 weight proportion in a baker. All blended mixtures were separately carried out in a twin-screw extruder

(Thermo Scientific^{TM} Process 11, Villebon-sur-Yvette, France) with a screw rotation speed of 200 rpm at 190°C. The extruder had a screw diameter 11mm and a length-to-diameter ratio L/D=40. The screw profile is composed of three mixing zones with different configurations of kneading blocks for promoting dispersive and distributive mixing. The residence time was approximate 2 minutes 30 seconds. The pre-reacted tannin and lignin were expected to be cured under the pressure and temperature of the extruder. Unreacted species and reaction by-products were removed by a highly efficient vacuum. Those extruded composites were noted as PPT, PPL, PPTG, PPLG, respectively. PP along was extruded in the same condition as a reference.

2.5. Characterization

UV accelerated weathering test was carried out by a QUV accelerated weathering tester (SOLAR EYE, Q-Panel Lab Products, Saarbrucken, Germany). The specimens in dimension 80×10×4 mm was exposed under continuous irradiation with an irradiance intensity of approximately 0.68 W/m^2/nm at λ= 340 nm for 168 h, 336h at 60°C. The anti-UV properties of tannin, crosslinked tannin, lignin, and crosslinked lignin were evaluated by the changes in the mechanical property (specimens under 168h UV exposure, 3 repetitions), surface morphology, surface chemical property, rheological behavior, and crystallinity.

The tensile test was molded by a micro-injection molder (Xplore, Sittard, the Netherlands) and performed at room temperature with standard dog-bone shaped (ISO 527, type 1A) tensile test specimens. The Instron tensile testing machine (model 5569) was equipped with a 50 kN load cell, operated according to EN ISO 527:1996 with a 10 mm/min cross-head speed. Four repetitions of non-weathering samples and three repetitions of weathering samples were calculated in the average value.

The rheological property was performed by using a rheometer (TA instrument, G2 ARES, New Castle, DE, USA) with parallel-plate geometry (25 mm diameter, 1 mm gap) with the protection of nitrogen under 180°C. Frequency sweeps between 0.1 to 100 rad/s were carried out at 10% strain in the linear viscoelastic region (LVE).

The differential scanning calorimetry (DSC, METTLER TOLEDO, Columbus, Ohio, United States) was employed to measure the melting temperature (T_m) and crystallinity temperature (T_c) of samples in the second heat-cool-heat circle with a scan rate of 10°C/min within the temperature range of -50°C to 220°C. The measurements

were using aluminum crucibles with a total sample weight 3-4 mg under a nitrogen atmosphere (50 mL/min). Values for melting temperatures (T_m) and enthalpy of melting (H_m) were analyzed by STARe evaluation software (version 10.0). The percentage of crystallinity Xc was estimated by the following equation:

$$X_c(\%) = \frac{100 \times H_m}{\Delta H_m^0 \times w} \tag{1}$$

where Xc is the crystallinity (%), ΔH_m^0 is the enthalpy of melting 100% crystallized PP, which is equal to 207 J/g [269], H_m is the enthalpy required for melting each sample, and w is the weight fraction of PP in blends.

Thermogravimetric analysis (TGA) was carried out in a METTLER TOLEDO (Columbus, Ohio, United States). All samples (6–8 mg) were scanned in the range of 30-600°C with a heating rate 10°C /min in an air atmosphere (50 mL/min). The obtained data were analyzed by STARe evaluation software (version 10.0).

The morphology of fracture surface and UV exposed surface were characterized by a scanning electron microscopy (SEM, JEOL JSM-6490LV, Peabody, USA; Hitachi S4800, Los Angeles, CA, USA) with an acceleration voltage of 5kV. All the samples were sputter coated with a thin layer of carbon.

The Fourier transform infrared (FT-IR) spectra of the non-weathered and weathered surface of specimens measured by a NICOLET 6700 FT-IR (MA, USA) spectrometer attenuated total reflection (ATR) mode for 16 scans in the range 4000-650 cm^{-1} with a resolution of 4 cm^{-1}. The curves were normalized, and peaks were analyzed without smoothing the data. The degradation of composites was characterized by carbonyl index(CI) [269]. The calculation equation as follows:

$$CI = \frac{A_c}{A_r} \tag{2}$$

where Ac is the area of the carbonyl absorption band (1670-1820cm^{-1}, C=O). A_r is the area of C-H stretch from CH$_3$ (2760-3020cm^{-1}). The latter one was used as a reference band because it was minimally affected by UV irradiation. For a more precise evaluation, the calculated carbonyl area Ac of each sample has been minus the area before aging, considering that tannin and lignin have carbonyl groups in their structure.

3. Results and discussion

3.1. The effects of native tannin/lignin and vulcanized tannin/lignin on PP matrix

3.1.1. Mechanical, crystalline and thermal properties

The tensile test results of PP/tannin blend (PPT), PP/tannin-glyoxal blend (PPTG), PP/lignin blend (L), and PP/lignin-glyoxal blend (PPLG) are shown in Figure 2-11. As can be seen from the bar chart, a clear decrease of Young's moduli can be found for PPT and especially for PPL. However, PPTG and PPLG display a general increasing trend compared with PPT and PPL. Young's modulus is the stiffness of material at the elastic stage of a tensile test. For thermoplastic composite materials, this property can be readily improved by adding rigid fillers because the rigidity of fillers is generally much higher than that of PP matrix [302]. Therefore, a further crosslinked process happens to both pre-reacted tannin and lignin during extrusion process producing rigid fillers. This can explain the improvement of Young's moduli.

A lower Young's modulus was observed for PPL when compared to PPT. This result can be explained by worse lignin particles dispersion in the PP matrix (Figure 2-12, f). According to the study of Bozsódi [273], particle size is a very important factor that can significantly affect the mechanical properties of PP/lignin blends. At the same mixing condition, the utilization of coupling agent can prevent lignin from agglomeration, thus, reduce particle size and improve the miscibility. In our case, glyoxal can reduce the coalescence of lignin oligomer, thus, smaller lignin particle sizes resulting in a better dispersion (Figure 2-12, f). Therefore, the dispersion degree of polyphenols in the polymer matrix can be improved through the dynamic vulcanization process; this can be a potential pathway to process thermoplastic/polyphenols composites, especially for polypropylene/lignin blends.
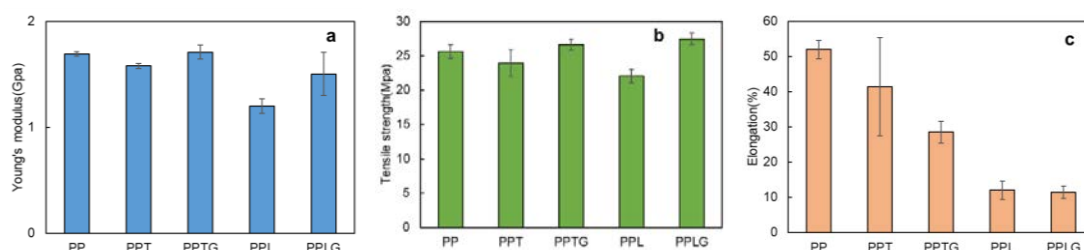
Figure 2-11. The tensile property of pure PP, PP/polyphenol blends and PP/crosslinked polyphenol blends

Similarly, the tensile strength of PP blended with crosslinked tannins (PPTG) and crosslinked lignin (PPLG) display higher tensile strength compared with that blended with PPT, PPL, even with PP. Tensile strength is the maximum stress of material can sustain under uniaxial tensile loading. For composite material, tensile strength depends

on the stress transfer capacity between fillers and polymer matrix, which is significantly affected by particle size, particle distribution, and particle/matrix interfacial strength [273]. Considering the structure of PP is a very polar polymer that contains only carbon and hydrogen atoms and capable of forming very weak dispersion interactions, the blends of PP and hydrophilic tannin and lignin is expected to form poor interface adhesion, resulting in a poor tensile strength. However, the increase of tensile strength of those blends with crosslinked tannins and lignin confirms better compatibility with PP matrix. Because the dynamically vulcanized process reduces the hydrophilic characteristic of both tannin and lignin, those crosslinked tannin and lignin are easier to disperse in PP matrix during the extrusion process, thus, a good particle distribution attribute to a better stress transfer capacity between polyphenols and PP matrix. In Figure 2-11c, it can be observed a general decrease of elongation in all PP/polyphenols blends. The crosslinked tannin and lignin displaying high moduli, those rigid fillers would lend stiffness to the composite material [215].

A separation of filler and PP matrix can be observed from their SEM micrographs in Figure 2-12. Unlike the relatively smooth surface of native PP, plastic matrix pulls are generally observed. As commonly observed in filled PP composites, PP matrix deformed independently due to the weak filler-matrix adhesion between polyphenols and PP matrix until the polyphenol particles restrict the deformation. In PP/tannin blends, the identification of tannin particles in tensile fracture surface is difficult because of their low particle size. However, the crosslinked tannin particles in different sizes and irregular shapes particles are clearly found in Figure 2-12, c (marked in yellow narrow), which confirmed the formation of tannin thermoset particles. Similarly, results can be found in PP blends with crosslinked lignin (Figure 2-12, e). Unlike PP/tannin blends, obvious agglomeration of lignin can be found in both SEM micrographs (Figure 2-12, d). and image of tested specimen (Figure 2-12, f), this result confirmed that lignin agglomeration easily occurs in the melt blending process without modification. Therefore, it can be concluded that the dispersion degree can be the main reason for the improvement of the tensile property.
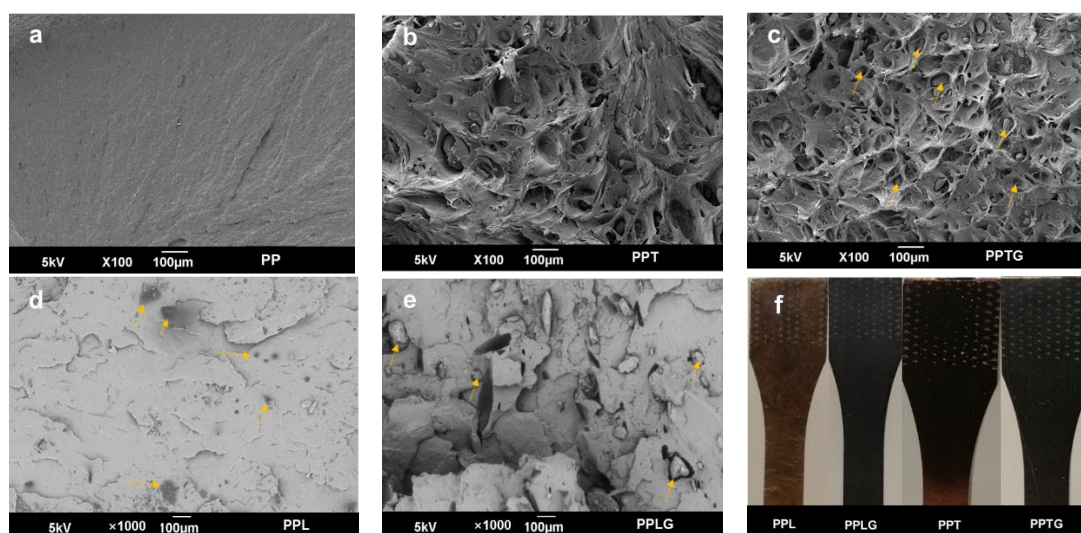
Figure 2-12. SEM images of fractured surfaces of pure PP(a), PP/polyphenol blends(b,d), PP/crosslinked polyphenol blends(c,e) tested by tensile measurements; images of tested dog-bond specimens(f).

The addition of filler is commonly affecting the crystallinity of the polymer matrix, especially in PP a semi-crystalline polymer. Figure 2-13 presents the crystallinity of PP/polyphenol blends (PPT, PPL), and PP/crosslinked polyphenol blends (PPTG, PPLG). Various fillers [163,280,303] including thermoset resin [233] have been reported to provide positive effects on the crystallinity of PP. Similar results can be found in our recent publication regarding tannin-hexamine thermoset particle filled PP [112]. In this study, both PPT and PPTG present higher crystallinity compared with PP. This result is in accordance with the improvement of tensile properties previously observed (Figure 2-11). The higher crystallinity of PPT compared to PPTG can be rationalized by the smaller particle sizes of the non-cross-linked tannins observed in SEM images (Figure 2-12). In contrast with previous reports [269], the addition of lignin reduced the crystallinity of PP matrix. This can be explained by the agglomeration of lignin particles previously observed. With reducing the hydrophilic property of lignin through the dynamic crosslinked process, the better particles dispersion resulted in an increase in the number of nucleating agents and a further increase the crystallization rate of PP in the blends.
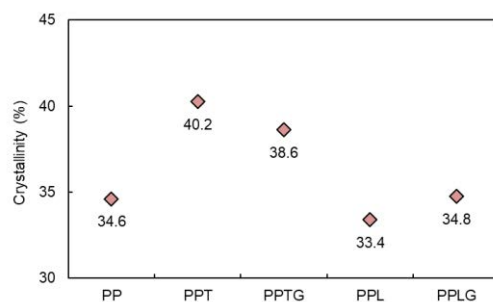
Figure 2-13. Crystallinity index of PP, PP/polyphenol blends and PP/crosslinked polyphenol blends

The effects of native and crosslinked tannin/lignin on the thermal behavior of the PP matrix were determined by thermogravimetric analyses in an air atmosphere. Their weight loss as a function of temperature and DTG data are plotted in Figure 2-14. All samples degraded in a one-step process, from 220°C to 410°C, as can be concluded by the presence of only one peak in the DTG curves. Pure PP degraded completely without any char while the PP/polyphenol blends exhibited some char at 420 °C. The behavior leads to the formation of a protective surface shield and their interactions between PP contributing to the considerable heat resistance [304]. However, PP/polyphenol blends represent noticeable differences in the thermo-gravimetric curves. The PP/lignin blends have a better heat resistance compared with PP/tannin blends. The different char forming capacity can be an explanation. According to the report of Sonnier[288], the char yield of lignin was 57 wt% while that of tannin was generally 30wt%. Another possible reason could be related to molecular weight differences. According to the published articles [305–307], the average molecular weight of mimosa tannin (600-2300 Da [306]) was generally much lower than that of Kraft lignin (approximately 10000 g/mol [292]). On this basis, the large molecular weight of lignin under thermo-degradation process results in the breakdown of linkages producing reactive and unstable lignin-derived fragments. These fragments may further react through rearrangement, electron abstraction or radical–radical interactions, to effectively delay PP from degradation [308]. However, a similar thermo-degradation and interaction may occur in PPTG and PPLG blends, considering that uncrosslinked tannin/lignin was existed because of their stereo-chemical structure and the limited resident time in the extruder (approximately 2 min 30 seconds). Besides, the pre-reactions of tannin and lignin were performed in alkaline condition (see Material and Methods section) [32,266] which resulted in linkage breakdown of polymers, increasing the phenolic

content and promoting the antioxidant property [292]. The phenolics basic depolymerization could improve the radical capturing capacity of crosslinked tannin and lignin, resulting in better heat resistant of PPTG and PPLG.
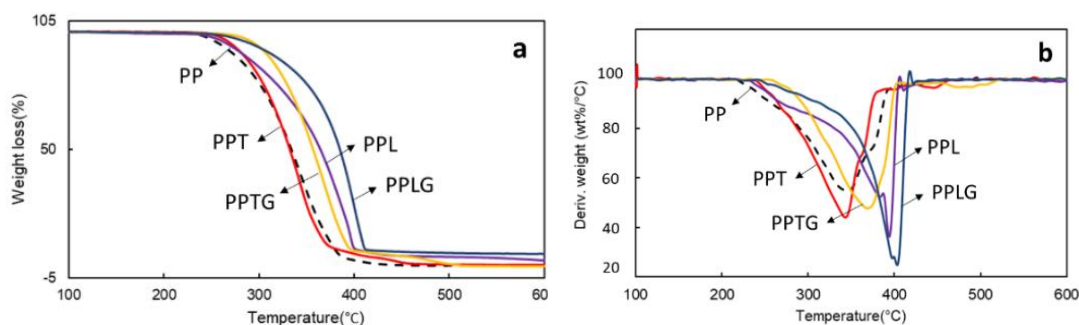
Figure 2-14. Thermal behaviors of PP, PP/polyphenol blends and PP/crosslinked polyphenol blends: (a) TGA curves; (b) DTG curves.

3.1.2. Rheological behavior

Figure 2-15 a-d presents the rheological behaviors including complex viscosity(η^*), storage modulus(G'), loss modulus(G'') and tan(delta) of PP, PP/polyphenol blends (PPT and PPL), and PP/crosslinked polyphenol blends (PPTG and PPLG). In particulate-filled polymers, melt rheological property provide an efficient and reliable way to investigate filler properties and dispersion quality [276,309,310]. Particulate dispersion, which is related to particulate characteristics (surface property, shape, and size), particle content, and particle-matrix interaction, can significantly influence the viscoelastic response of filled polymers. As presented in Figure 6a, complex viscosity in all curves decrease as a function of angular frequency, exhibiting a typical shear-thinning behavior. As is reported by Hornsby [311], surface treatment organic fillers normally reduce the complex viscosity since the decrease of particle agglomeration. Similarly, a decrease of complex viscosity is generally found in all curves (except PPL) compared with PP, indicating a better dispersion of fillers because the crosslinking process reduces the hydrophilicity of tannin and lignin. For those uncrosslinked tannin and lignin, PPL displayed an increase of complex viscosity in low-frequency region mainly caused by the agglomeration of lignin which can be clearly observed in the image of specimen (Figure 2-12, f). While it is hardly found the agglomeration of tannin in the PP matrix may due to the lower molecular weight of tannin compared with lignin. Besides, as observed from SEM microscopy (Figure 2-12), the bigger particle size of lignin tends to effectively restrict the PP chain movements.

Figure 2-15 (b, c) present the storage moduli and loss moduli as a function of the frequency of all tested samples. From those figures, a generally higher value of loss moduli than that of storage moduli can be observed. For loss moduli, there is no significant difference in all samples, however, an increase of storage moduli can be found in all filled PP samples at low frequency, suggesting that the presence of both native and crosslinked tannin/lignin limits the mobility of polymer chain, reinforces the internal network structure. However, both PPTG and PPLG have higher storage moduli compared with PPT and PPL; this confirms the formation of thermoset particles in the PP matrix. In Figure 2-15d, tan(delta), which is defined as the ratio of loss moduli and storage moduli, is plotted as a function of angular frequency. The tan(delta) values of all tested samples are above 1, this implies that they are viscous like material. With the addition of tannin or lignin, tan(delta) is clearly observed lower than PP in the low frequency region. This suggests that the mobility of the polymer chains is limited by polyphenols, thus, those filled samples show more elastic behaviors. Particularly, it is worth noting that PPTG and PPLG present a lower tan(delta) compared with PPT and PPL, referring that crosslinked tannin or lignin more significantly restrict the movement of PP polymer chain. This can be explained by the formation and better dispersion of rigid thermoset particle through the dynamic extrusion.
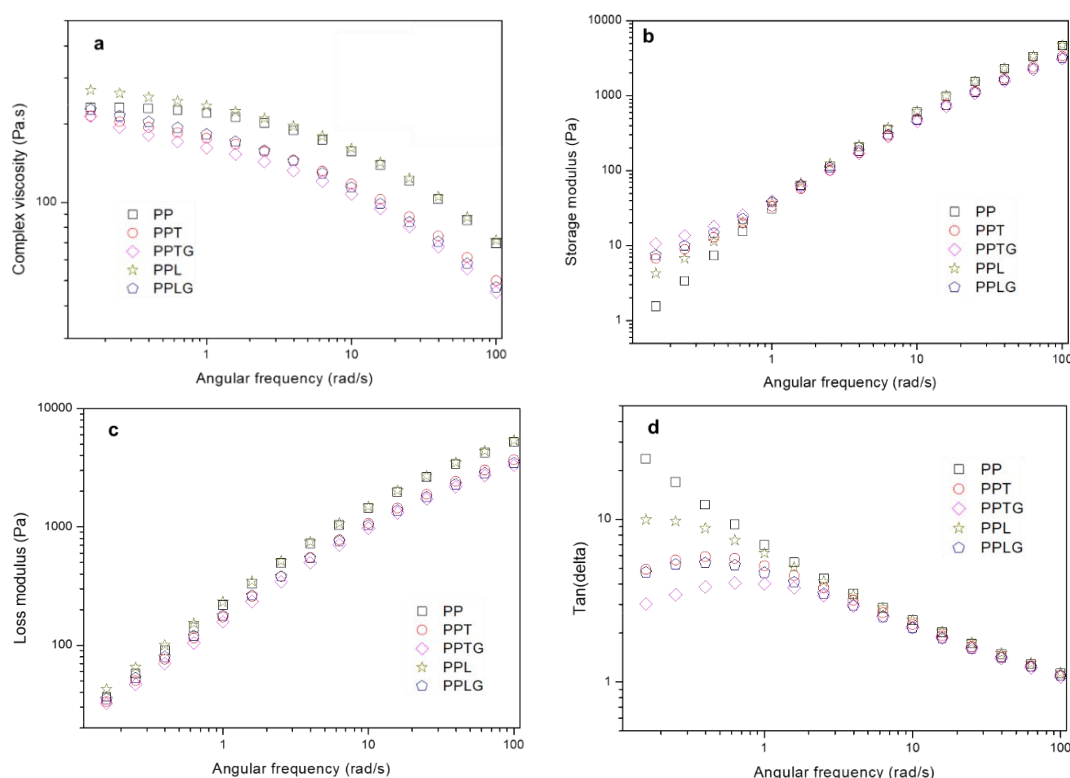
Figure 2-15. Rheological behaviors of PP, PP/polyphenol blends and PP/crosslinked polyphenol blends

3.2. Characterization of UV protection property of native tannin/lignin and vulcanized tannin/lignin on PP matrix

The photo-degradation of PP commonly starts from the surface, results in surface cracking, and ultimately lower mechanical properties. Thus, surface morphology is an efficient pathway to evaluate the degree of degradation. The surface exposed at 0h, 168h and 336h UV irradiate of PP, PP/polyphenol blends and PP/crosslinked polyphenol blends were characterized by SEM and are presented in Figure 2-16. The micrographs before UV weathering with no visual cracks can be observed at the surface. However, after UV weathering, all exposed materials present strong visual surface variations. In the micrographs with 168h exposition, PPTG and PPLG with similarity surface morphology exhibit micro-cracks at the surface, whereas large and long cracks were observed in PP, PPT, PPL. More obvious differences can be found in the micrographs with 336h exposition. At the surface of PP, PPT, and PPL, large and deep cracks are clearly observed whereas only some large cracks mixed with tiny cracks occurred at the surface of PPTG and PPLG. Besides, the morphology of PPL was similar to PP and severer cracks can be found compare with PPT, that might be caused

108

by the worse dispersion of lignin in the PP matrix. All the mentioned phenomena were similar to their thermal behaviors because either photo-degradation or thermo-degradation mechanisms of PP is due to the appearance of free-radical species or peroxides in the polymer initiated by UV irradiation or temperature. In conclusion, both native or crosslinked tannin/lignin can prevent or interrupt the degradation processes. But crosslinked tannin or lignin appears to more significantly inhibit oxidation or inhibit reactions promoted by oxygen or peroxides.
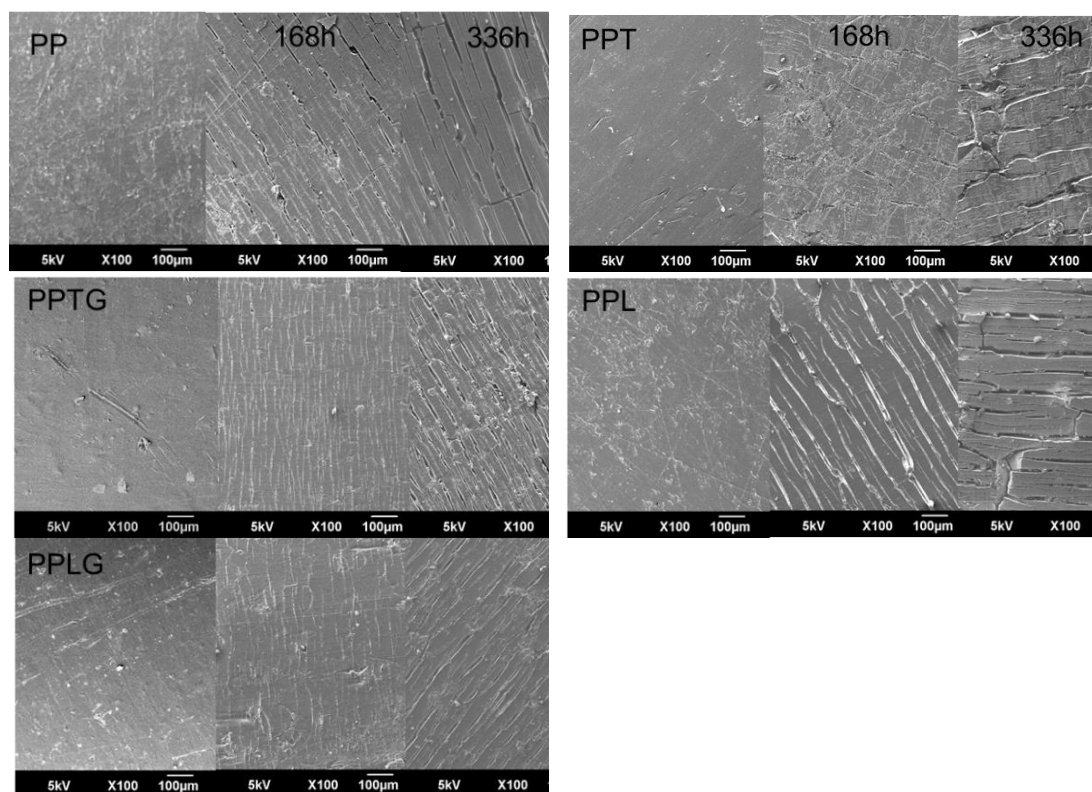
Figure 2-16. SEM microscopy of PP and PP/polyphenol blends over exposure time

Figure 2-17 presents the calculated carbonyl index of PP and PP/polyphenol blends at 168h and 336h exposure. The carbonyl indexes were established from FTIR spectra (see Mat & Met section). As previously proposed, the carbonyl groups concentration exhibits a close correlation with the degradation degree since carboxylic acids are produced during the oxidation process [281,312]. As expect, all the samples show on the exposed surface an increasing carbonyl index with UV exposure time. However, compared to neat PP, the increase of carbonyl index for PP/polyphenol blends was lower attesting the fact that polyphenols can capture free radicals and inhibited the oxidative reaction. Moreover, in accordance with the result from SEM micrographs (Figure 2-16), PPT and PPL present lower carbonyl index compared with PPTG and

PPLG, respectively. This confirms that dynamic curing tannin/ lignin improved their antioxidant capacity.
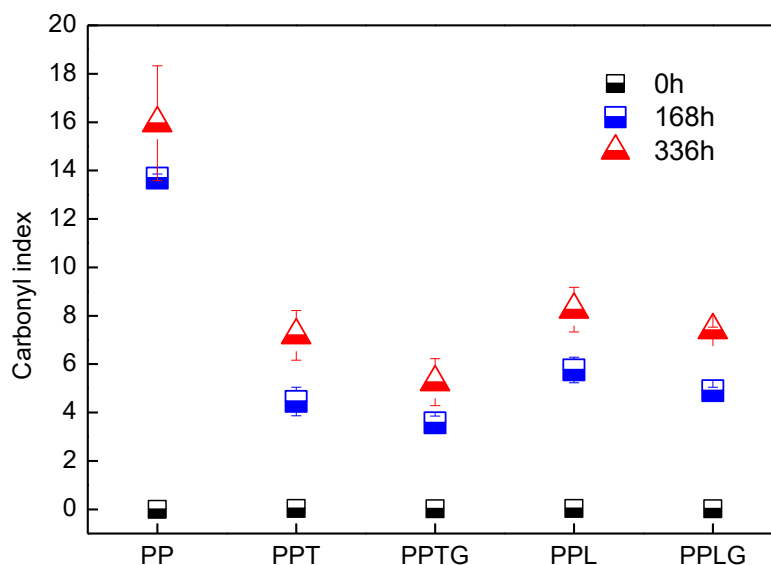
Figure 2-17. Carbonyl index of PP and PP/polyphenol blends over exposure time

Figure 2-18 display the crystallinity of PP and PP/polyphenols blends over UV exposure. Their crystallinities reduction ratio from 168h to 336h are plotted as well. A drop of crystallinity can be observed after UV exposure in all samples because of the chain scission. Between 168h and 336h of UV weathering, a decrease of crystallinity clearly more important was observed for neat PP (20.5%) compared to phenolic-based composites (<10%). Upon exposure to air and UV, photo-oxidant occurs by the appearance of free radicals. This oxidation is a circular, self-propagating process that, unless intruded by an antioxidant, progressively leads to increasing the breaking and shortening of the polymer chain [116]. Therefore, the presence of tannin/lignin with the radical scavenge capacity inhibit chain scission of the polymer chain, reducing the decrease of crystallinity.
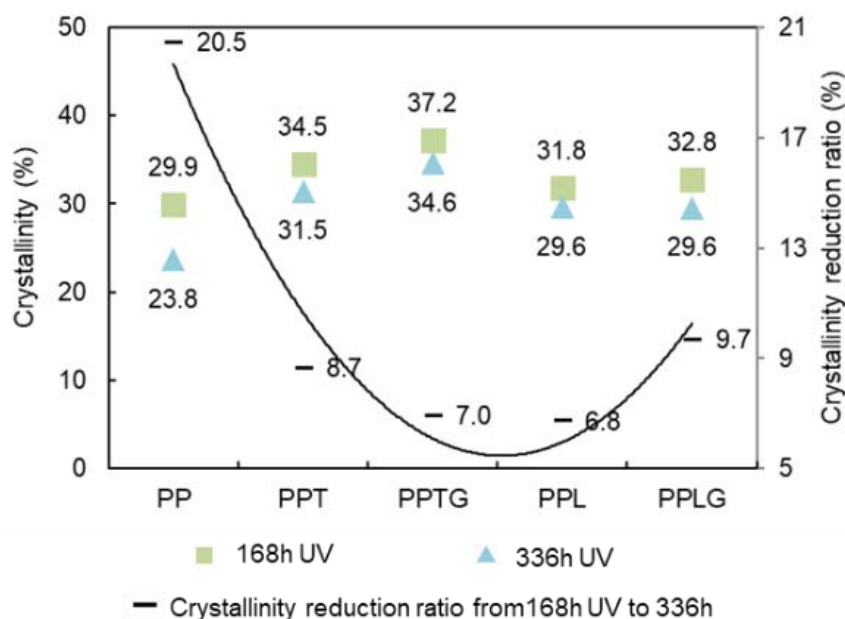
Figure 2-18. The crystallinity of PP and PP/polyphenol blends over exposure time

Figure 2-18 displays complex viscosity, storage modulus and tan (delta) as a function of the angular frequency of PP and all PP/polyphenol blends at 168h UV exposure. Compared to PP/polyphenol blends, a sharp drop of viscosity can be observed for neat PP after weathering explained by the oxidative reduction of molecular weight. In addition to the inhibition of degradation, tannin and lignin might also contribute to the entanglement of degraded PP chain, thus limiting the melting flow of polymer chains [112]. As a result, for PPTG and PPLG an increase of viscosity can be observed at high frequency because of the good dispersion of crosslinked tannin or lignin. In Figure 2-18c and Figure 2-18e, we observed comparable results to those described for non-weathering samples (Figure 2-15). This confirms their reinforcing role in PP matrix even after UV weathering. However, some decreases can be observed in storage modulus and tan (delta), suggesting that weathering samples appeared to have more viscous behaviors, the polymer degradation increasing the melting flow.
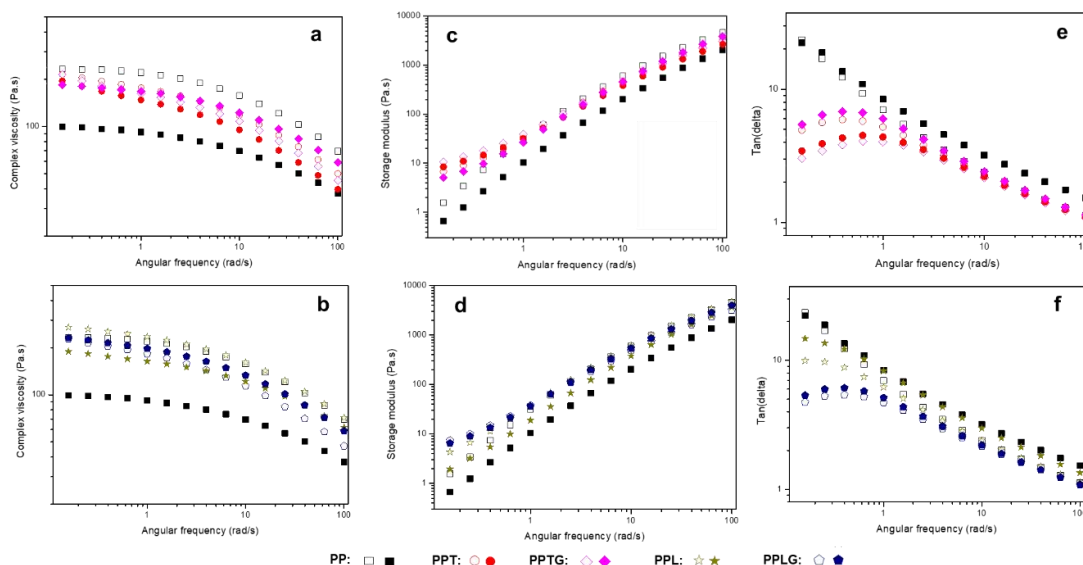
Figure 2-19. A comparison of rheological behavior of PP, PP/tannin blends(up) and PP/lignin blends(down) at 168h UV weathering

In Figure 2-20, a rise of Young's moduli can be found in all samples after 168 hours of UV exposure at 60 °C, which is generally found in PP/polyphenol blends [260,313]. This can be explained by chain scission and the crosslinked phenomenon of molecules chain during accelerated weathering and chain movement obstacle caused by polyphenols. UV weathering did not significantly deteriorate the tensile strength of PP composite containing polyphenols. According to the work of Stark [261], serious mechanical loss of polyolefin occurs in sufficient photodegradation, accompanying with serious severe surface cracks and crystallinity decrease. PP/polyphenol blends have been proved to undergo less photodegradation with PP (see Figure 2-16, Figure 2-17, Figure 2-18, Figure 2-19 and related discussion). Therefore, PP/polyphenols blends display comparable or increasing tensile strength after UV exposition with consideration of entanglement of polyphenols and PP polymer. A decrease of elongation can be found in all samples. The elongation of polyolefin has been found to be a more sensitive measurement of the extent of degradation than the tensile strength because the elongation at break of PP is dependent on its crystallinity[314]. In our case and in accordance with Lv et coworkers [312], the changes of crystallinity (Figure 4 and Figure 9) are in agreement with the elongation decrease. In addition, the entanglement of polyphenols and PP polymer chain can be another reason for less drop on elongation. This confirms the UV protection capacity of both native and crosslinked tannin/lignin.
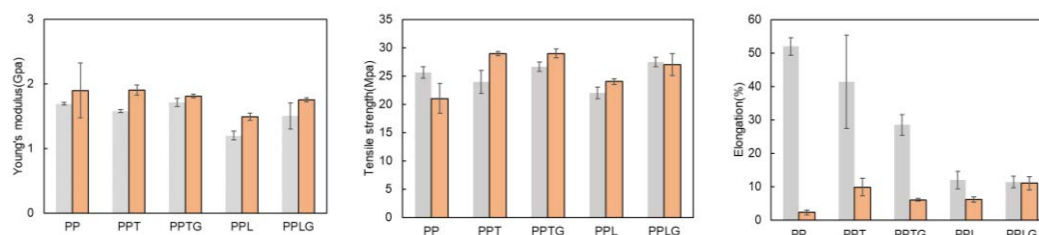
Figure 2-20. Young's modulus, tensile strength, and elongation of PP and PP/polyphenol blends after weathering: green-before weathering; orange: 168h UV weathering

4. Conclusions

In this study, dynamic vulcanization has been successfully applied to PP/tannin and PP/lignin blends. The influence of vulcanized tannin/lignin on mechanical property, crystallinity, thermal stability, rheology behavior as well as UV protection property of PP matrix was investigated. This extrusion process leads to tannin and lignin crosslinking into rigid thermoset particles, contributing to the improvement of Young's modulus of the composite. After vulcanized extrusion, the hydrophilicity of tannin and lignin were reduced, thus increasing the compatibility in the PP matrix. Besides, tannin and vulcanized tannin can act as nucleating agents of PP because of their particle size. Vulcanized tannin/lignin have a better performance on the thermal stability of PP compared with native tannin/lignin, especially for PP-vulcanized lignin. From the rheological data, vulcanized tannin/lignin displayed a reinforce function and confirmed their better dispersion capacity in the PP matrix compared with native tannin/lignin. Furthermore, vulcanized tannin/lignin present better UV protective performance, demonstrated by fewer changes on surface morphology, carbonyl index, crystallinity, viscosity, and tensile property.

Chapter 3.   Tannin modified via acetylation as a feedstock material for poly (lactic acid) 3D printing filament

Introduction

This chapter we reported an approach to utilize tannin, a sustainable phenolic biopolymer, to partially replace PLA as feedstock material in 3D printing. Tannin was acetylated with acetic anhydride to enhance the miscibility with hydrophobic PLA polymer matrix. A solvent-free melt blending process was developed to ensure good dispersion of tannin. The blends of tannin and PLA with a varied ratio up to 30 wt% were extruded into filaments via an extrusion process.

Article 3: 3D printing filament based on poly (lactic acid) and acetylated tannin

Abstract: The main object of this study is to develop a new approach to utilize tannin to partially replace PLA in 3D printing material and investigate the fused deposition modeling (FDM) feasibility. Tannin was modified with an acid anhydride to enhance the compatibility of tannin and PLA polymer matrix. The composite filament was carried out in a twin-screw extruder. The effects of loading content of acetylated tannin (AT) on the final properties of the composite material were characterized by tensile property and UV weathering resistant. Besides, the AT-filled PLA composite filaments have investigated the changes of crystalline property, thermal degradation behavior, color, and hydrolysis degradation. PLA incorporated with up to 20 wt% AT did not deteriorate the mechanical property and surface morphology. The AT-filled PLA filaments are highly amorphous structures material and are in brown. AT improve water absorption of filaments and enhance hydrolysis degradation of PLA, especially in an alkaline environment. Various AT loading content filament are printable via FDM with a 250°C lower printing temperature will not be causing material decomposition. Imperfect printing appearance is observed by using AT-filled filament because of the phase separation and AT aggregation, especially high AT loading content filament.

Keywords: tannin, poly (lactic acid), filament, melt blending process, fused deposition modeling

1. Introduction

Additive manufacturing, commonly known as 3D printing, is an innovating process for manufacturing 3D physical objects from digital models through the successive layer-by-layer deposition of materials, including plastic, metal, ceramics, living cells [235,237]. This technology has made a significant impact on various fields (e.g. construction, aerospace, healthcare, automotive, food industry, etc.) since the complex, high-resolution, and reproducible parts can be rapidly manufactured through a computer-aided design model and computer-controlled software [315]. Additive manufacturing processes can be divided into seven categories, including material extrusion, vat photopolymerization, material jetting, binder jetting, powder bed fusion, direct energy deposition, and sheet lamination [237]. Among all the methods, material extrusion, well-known as fused deposition modeling (FDM) or fused filament fabrication (FFF), has shown the greatest versatility to process thermoplastic prototype parts [316]. Many materials can be used for FDM process (e.g. acrylonitrile butadiene styrene (ABS), nylon, polylactic acid (PLA)); however, PLA is one of the most popular materials since its printability, favorable mechanical properties, and user-friendly characteristic.

Polylactic acid (PLA) is a sustainable aliphatic polyester, which can be synthesized from direct polycondensation of renewable lactic acid or ring-opening polymerization of lactide (a cyclic diester of lactic acid) [128]. PLA is one of the most consumption bio-based and biodegradable polymers owing to its sustainability, processability, and biocompatibility. These excellent properties combined with FDM process technology have made PLA a promising 3D printing material in various applications ranging from plastic cups to medical implants. In past decades, PLA composites with superior characteristic compared with pure PLA have been widely reported allowing diversification of their application fields [115,127]. However, the researches regarding PLA-based biocomposites applied to 3D printing are still limited.

Sustainable materials or biopolymers as 3D printing feedstocks are promising substitutes for fossil-based fillers due to their sustainability, biodegradability, and cost-efficient characteristics. Wood powder is a commercially available feedstock for 3D printing PLA-based filament. This type of filaments is typically consisting of around 30% wood particles, including wood dust, cork, and other powdered wood derivatives,

but the exact composition varies depending on the commercial brand. The presence of wood filler displays slightly higher stiffness, but less abrasive properties compared to other composite filaments such as carbon-fiber filled PLA filament, and metal filled PLA filament. To process such quality wood powder filled filaments, toughening agents and lubricant/plasticizers were generally used to address the filler agglomeration and incompatibility of filler and PLA matrix [245]. In addition, fibers such as wood fiber, bamboo fiber, and cellulose fiber were also investigated as feedstocks for PLA-based filaments since their positive effects of the mechanical properties and heat resistance on PLA matrix [246,247]. The fiber-filled PLA filament can lead to printed parts with oriented characteristic by controlling the printing parameter [248]. Recently, hemicellulose up to 25% loading content has been investigated to partially replace PLA as feedstock material in 3D printing [201]. The scaffold was successfully printed from the composite filaments by the FDM process. This approach uses favorable characteristics of hemicelluloses such as biocompatibility, biodegradability feature, and the presence of versatile active sites which makes it possible to consider this new composite material in various biomedical applications such as tissue engineering and drug-eluting scaffolds. Besides, lignin has been developed as a potential functional filler for PLA-based composites since its attracting characteristics such as antioxidant, antifungal and antimicrobial capacities, UV-radiation, and fire-retardant properties. However, reports of lignin-filled PLA filament for 3D printing are rare. One example of PLA/lignin filament for the FDM process was reported by Gkartzou [254]. The lignin aggregation and its low compatibility with PLA matrix caused imperfect printed objects and surface roughness, even at low loading content (5 wt%.). Thus, according to these published literature it appears that the dispersion and distribution of fillers are key factors for processing 3D printing material.
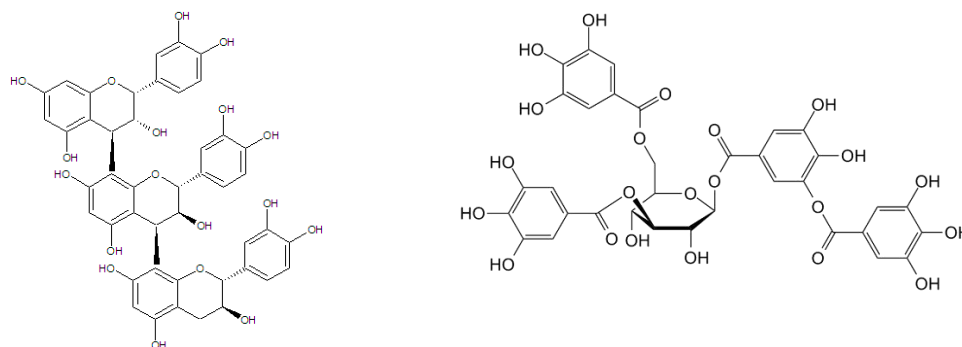
Figure 3-1. Structure of condensed tannins (left); Structure of hydrolyzable tannins(right).

Tannins are one of the most abundant and sustainable biopolymers in plant and they can be structurally divided into hydrolyzable tannins and condensed tannins (Figure 3-1). Condensed tannins, mainly composed of flavonoid units, are widely distributed in nature and constitute more than 90% of the total world production of commercial tannins. In this basis, condensed tannin is more interesting for composite preparation. It has been shown that tannins display great potential as a component of PLA biocomposites due to their characteristics like antioxidant, antimicrobial and stabilizing properties. However, there is no related research about their application in the field of 3D printing. In recent five years, tannins have been investigated as functional additives or one component of polymeric composites. For instance, tannins as an additive have been reported as a good stabilizer with antioxidant and UV-protective properties on polypropylene [96,97], polyethylene [294], poly (vinyl chloride)(PVC) [295], and polyvinyl alcohol [104]. Anwer et al. reported a native tannin as a filling component of PLA composite material [100]. In this study, poor adhesion between tannin and PLA matrix resulting in poor dispersion and distribution of tannin in PLA matrix, thus, poor tensile strength can be found at higher filler content (15%). It has been shown that esterification and hydroxypropylation of tannins resulted in an improved compatibility and dispersion capacity with various plastic [19,101,105,106,267,296]. According to the study of Grigsby [105], esterified tannin can significantly reduce their incompatibility with PLA polymer matrix and tannin ester-bearing long ester chain lower melting temperature, leading better processability. However, the substitution of higher chain length on tannin flavonoid units becomes increasingly difficult due to the increasing steric hindrance. Another work of Grigsby reported that a high tannin ester loading content (50%) reinforced PLA fine fiber processed via melt spinning with the

presence of transesterification catalyst [101].

According to this literature, biomaterials or biopolymers are promising feedstocks for 3D printing material because of their biodegradability, sustainability, harmlessness, and cost-efficient. The reported regarding the incorporation of tannins with PLA indicated the possibility to process tannin-filled filament for 3D printing. The main challenges of tannin filled composites for the FDM process are the dispersion and distribution of tannin in the PLA matrix, which might cause the clogging at the printing nozzle and discontinuous layer deposition. The most efficient way to address this problem is to reduce the hydrophilic characteristic of tannin.

The main object of this study is to develop a new approach to utilize tannin for partially replacing PLA in 3D printing constructs and to investigate the FDM feasibility. For this purpose, tannin was acetylated to enhance the hydrophobic property, this method has been proved to improve the compatibility of tannin thermoplastic polymeric matrix without severe agglomeration [267,296]. The composite filament was performed in a twin-screw extruder. The effects of loading content of acetylated tannin (AT) on the final properties of the composite material were characterized by tensile property. While the AT-filled PLA composite filaments were evaluated the changes of crystalline property, thermal degradation behavior, color, and hydrolysis degradation. The printability of AT-containing filament was also investigated.

2. Materials and Methods

2.1. Materials

PLA trademarked under the name of IngeoTM Biopolymer (Grade 3D850) with a melt flow index of 7-9 g/10min. was obtained from Natureworks LLC (Minnesota, USA). Mimosa tannins were purchased from Silva Chimica, in Mondovi, Italy. Pyridine was obtained from Acros-Organics and used as received. Acetic anhydride, buffer solution pH=4.0 (consist of citric acid/ sodium hydroxide, sodium chloride solution) and pH=10.0 (consist of boric acid/ potassium chloride, sodium hydroxide) were obtained from Sigma-Aldrich. Dulbecco's Phosphate Buffered Saline (PBS), pH=7.4, purchased from Sigma-Aldrich, which is a liquid solution without calcium chloride and magnesium chloride and is suitable for cell culture.

2.2. Preparation of PP/TH Composites

2.2.1. Tannin acetylation

Acetylated tannin(AT) was prepared by mimosa tannin and acetic anhydride in a weight proportion of tannin: anhydride=1:5, and pyridine as catalyst (1 wt% on tannin) in a round bottom flask fitted with a condenser and continuously stirring with a magnetic stirrer [39]. The mixture was heated at 60°C for 6 hours. After acetylation, the suspension was precipitated in iced water and centrifuged to separate the solution. The acetylated tannin powder was washed 5 times with distilled water and air-dried for several days at room temperature.

2.2.2. Filament preparation via melt blending extrusion

PLA was ground into powder by a grinder for better mixing with tannin. PLA and tannin acetylated powder were oven dried at 80℃ for more than 12 hours to eliminate possible absorbed water on the surface. The blending of PLA and AT were carried out in a twin-screw extruder (Thermo Scientific™ Process 11, Villebon-sur-Yvette, France). Two mixing zones of screw profile offer an enhancement of dispersion of tannin in the PLA polymer matrix. The temperature of the die and the heating zones across the extruder barrel ranged were shown in Figure 3-2. The filaments were extruded via hot melt extrusion via a nozzle diameter of 4 mm at 180℃. The filament in diameter 1.75 ± 0.1mm was controlled by the speed of spool rotation and conveyer belt and the obtained filament for 3D printing was collected by a spool.

Temperature of screw profile

Zone	die	8	7	6	5	4	3	2	1
T (°C)	185	155	180	190	190	190	200	200	200

Blending proportion

Sample notations	9PLAT	8PLAT	7PLAT
PLA	10	20	30
AT	90	80	70
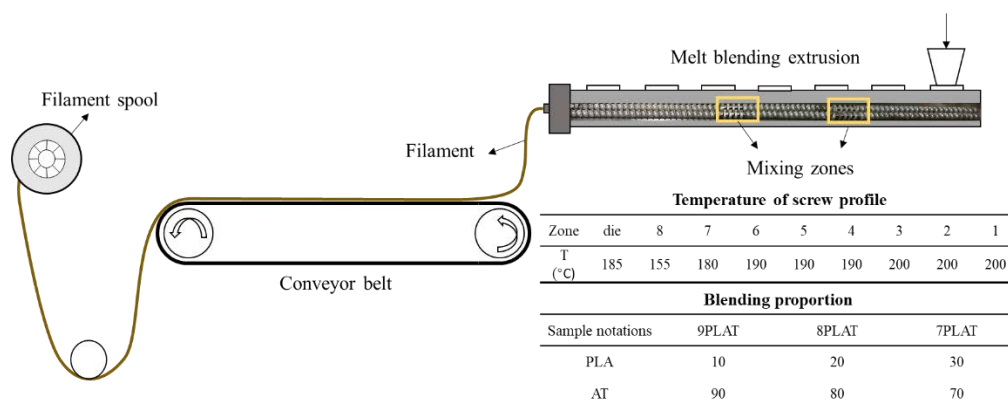
Figure 3-2. Filament preparation via melt blending extrusion. The parameters of screw profile and blending components proportion.

2.2.3. 3D printing process

PLA filaments (ø = 1.75 ± 0.1 mm) reinforced with AT were used to print 3D model scaffold (20.1× 20.1× 3 mm) and dog bones (length = 80 mm, width = height = 3 mm)

on an open source 3D printer (Mondrian 3.0) at 190℃ . Only one dog bone of PLA, 9PLAT, and 7PLAT was tested because of limited filament amounts, and these series appeared to be the most interesting to evaluate AT-filled filaments in this study. The scaffolds were printed with PLA and AT-filled PLA filament in three printing temperature (180℃ , 200℃ , 220℃). The 3D printer was equipped with a nozzle having a diameter of 0.4 mm. The used printing parameters were shown in Table 3-1. The design of a model figure and dog bones were modeled using a slic3r program. The software used for 3D printing was Pronterface.

Table 3-1. 3D printing parameters

Printing temperature	180 -220 °C
Layer height	0.2 mm
Infill density	100%
Infill pattern	linear
Layer angle	45°
Printing speed	12 mm/s
Nozzle diameter	0.4 mm

2.3. Characterization

The NICOLET 6700 FT-IR spectrometer attenuated total reflection (ATR) mode was used to detect the chemical changes of tannin and acetylated tannin, and UV exposure surface of PLA and AT filled PLA composites. The scanning parameters are 16 scans in the range 4000-400 cm^{-1} with a resolution of 4 cm^{-1}. The curves were normalized, and peaks were analyzed without smoothing the data. Tannin and acetylated tannin were dried in an oven at 40 °C for 24 hours before testing.

The tensile test was performed at room temperature with standard dog-bone shaped (ISO 527, type 1A) tensile test specimens, which was molded by a micro-injection molder (Xplore), on an Instron tensile testing machine (model 5569) equipped with a 50 kN load cell, operated according to EN ISO 527:1996. The cross-head speed used was of 1 mm/min. All the samples were measured four times and the average value was calculated.

The morphology of 3D printed scaffold was characterized by a scanning electron microscopy (SEM, JSM-6490LV) with an acceleration voltage of 5kV. All the samples

were sputter coated with a thin layer of carbon.

The differential scanning calorimetry (DSC) was carried out using a METTLER TOLEDO DSC. The melting temperature (T_m) and crystallinity temperature (T_c) of samples with a scan rate of 10°C/min within the temperature range of 30°C to 220 °C and 220°C to -10°C in the second scanning cycle. The measurements were using aluminum crucibles with a total sample weight 5.00±1 mg under a nitrogen atmosphere (50 mL/min). Values for melting temperatures (T_m) and enthalpy of melting (H_m) and cold crystallization (H_c) were analyzed by STARe evaluation software. ΔH_m^0 is the enthalpy of melting 100% crystallized PLA, which is equal to 93.7 J/g, and w is the weight fraction of PLA. The percentage crystallinity X_c (%) was estimated by the following equation:

$$X_c(\%) = \frac{H_m - H_c}{\Delta H_m^0 \times w} \times 100\%$$

Thermogravimetric analysis (TGA) was carried out in a METTLER TOLEDO. The samples with a total weight in the 5–10 mg range were scanned in the range of 30-600°C with a heating rate 10°C /min in air atmosphere (50 mL/min). The obtained data were analyzed by STARe evaluation software.

Color measurement. Color is an important factor for 3D printing filament. The color of AT filled PLA filament was measured by a spectrophotometer (X·rite, model 5P60). According to the CIE L*a*b* color system. L* represents the lightness, whereas a* and b* are the chromaticity coordinates. A higher L* value refers to an increase in lightness. The a* coordinate represents red-green hue, while b* coordinate means yellow-blue hue.

Water absorption. The hydrophobicity of the filaments was investigated by measuring their water absorption[252]. Each filament was cut into length=70±1 mm and submerged in 50 mL of distilled water in a plastic tube for 30 days under room temperature. The tested filaments were vacuum-dried for 6 h at 80 ℃ before submerged into water, and the dried weight (W_0) was measured. After 30 days, the specimens were sorted from water and wiped by filter paper. The weight recorded as W_1. The water uptake of the filaments was calculated according to the following equation:

$$\text{Water absorption (\%)} = \frac{|W_1 - W_0|}{W_0} \times 100 \tag{1}$$

Solvent degradation. In order to understand the degradation of AT filled PLA

composites, printed specimens in dimension 2.5×30×2 mm were carried out in buffer pH solution (pH=4, pH=10) and PBS solution (pH 7.4) at 40 °C for 50 days in an oven. Initial weight (W_0) of each specimen was measured before soaked into solvent in glass tube containing 50ml buffer solution. After 50 days, the samples were removed from the tubes and washed with stilled water in 3 times and then oven dried at 40 °C for 12 hours. The weight of each specimen after degradation recorded as W_1. The weight loss was calculated based on the equation (1).

3. Results and discussion

3.1. Characterization of acetylated tannin

The hydrophilic characteristics of tannin being incompatible with hydrophobic polymers, tannin acetylation can improve the miscibility with the PLA matrix. Figure 3-3 presents the FTIR spectra of tannin (T) and acetylated tannin (AT). For T, the broad band from 3700 to 2500 cm^{-1} is assigned to -OH stretching vibrations of tannin. The peak at 1614 cm^{-1} refers to aromatic ring stretching vibration. The sharply decrease of -OH band and the emergence of typical ester functional group (C=O stretching) at 1750 cm^{-1} prove the substitution of acetyl functional group [18]. Besides, the increased absorption at 1178 cm^{-1} and 1044 cm^{-1} attributed to the C-O stretching is also in accordance with the structure of acetylated tannin [317,318].
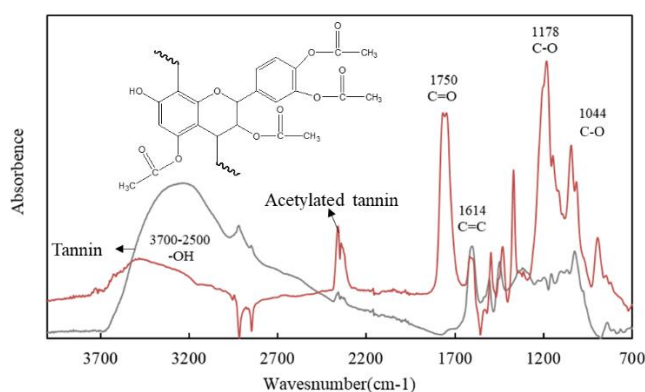
Figure 3-3. FTIR spectra of tannin (T) and acetylated tannin (AT)

3.2. Mechanical properties of AT filled PLA composites

The tensile properties of PLA and AT filled PLA composites are given in Figure

3-4. Young's moduli increased as the function of AT loading content since the filled component restrict the chain mobility of the polymer chain yielding a better static adhesion [272]. A similar result can be found in lignin filled PLA [317,319]. For composite material, tensile strength depends on the stress transfer capacity between fillers and polymer matrix, which is significantly affected by particle size, particle distribution, and particle/matrix interfacial strength [302]. The dispersion of AT into a thermoplastic polymer matrix without severe agglomeration has been previously reported [267,296] by an enhancement of hydrophobic characteristic. Unlike native tannin-filled PLA[100], the incorporation of 10% and 20% of AT in PLA did not have a significant effect on tensile strength of AT filled PLA composites (Figure 3-4). As generally observed for biopolymer filled polymeric materials [112], regarding higher AT content (7PLAT), filler agglomeration during melt blending process could result in a poorer particle distribution and stress transfer capacity between AT and PLA matrix. Besides, the higher loading of AT increases AT-PLA matrix interfacial areas, weakening the interfacial adhesion especially without any chemical bond between AT and PLA. Without exception, a lower elongation can be found in all AT-filled PLA composites compared with neat PLA since lack of plasticizers to release the stress concentration between the interface of AT and PLA or compatibilizer to limit the slide of molecular chains [320].
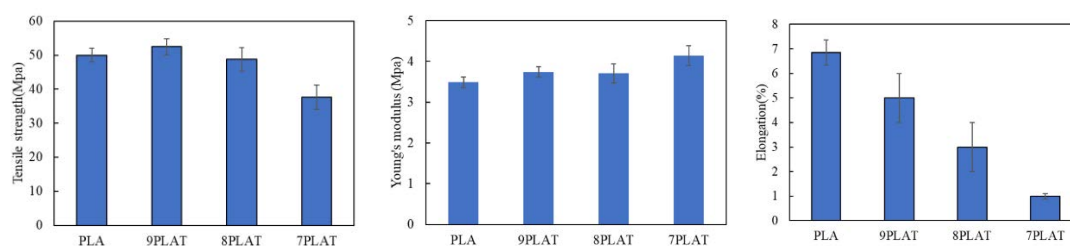
Figure 3-4. Tensile property of AT filled PLA composites

3.3. Crystallinity

DSC analysis is performed in order to estimate glass transition temperature, crystallization and melting behaviors of PLA and AT-filled PLA filaments. The tested results from second heat-cool circle were tabulated in Table 3-2. The incorporation of AT showed no significant effect on the melting and glass transition temperature (T_g). This observation suggested a non-significative impact on the PLA molecular weight [321]. which has been confirmed by the SEC results given in the supplementary

material (Figure S 3). The increase of T_c means that composite filaments are more difficult to undergo cold crystallization process at high temperature than pure PLA filaments [249]. As can be found in Table 3-2, the crystallinity of AT-filled PLA filaments is gradually decreased. Therefore, the AT-filled filaments are highly amorphous structure material and they are expected to have a higher degradation rate. This property probably benefits to the short-term application like implantable devices in biomedical applications [322] since the degradation of PLA occurs during a generally long period [323,324].

Table 3-2. DSC results of PLA and AT filled PLA biocomposites

Sample	T_g (°C)	ΔH_c (J/g)	T_c(°C)	ΔH_m (J/g)	T_m(°C)	X_c(%)
PLA	56.7	14.2	120.2	20.4	152.5	6.6
9PLAT	56.3	4.23	127.5	10.9	152.6	7.9
8PLAT	56.8	0.78	129.4	3.01	151.9	3.0
7PLAT	58.6	0.26	129.7	0.06	151.1	----

3.4. Thermal property

The thermal behavior of PLA and AT-filled PLA filament was determined by thermogravimetric analyses in an air atmosphere. Their weight loss as a function of temperature and DTG data are plotted in Figure 3-5. All tested materials degraded in a one-step process, from 250°C to 370°C, as deduced from the single peak in the DTG curves. The recorded results showed that the incorporation of AT to PLA matrix results in a decrease of thermal stability due to the decrease of crystallinity of AT-filled filaments (see, Table 3-2). This phenomenon is generally found in PLA biocomposites [106,320,325]. The onset decomposition temperature of all AT-filled filaments is similar to PLA at 250℃ while the major decomposition happened at 350 ℃ . On this regard, the printing temperature lower than 250℃ is suitable for AT-filled filament and will not cause material decomposition.

125

<div align="center">(a)   (b)</div>
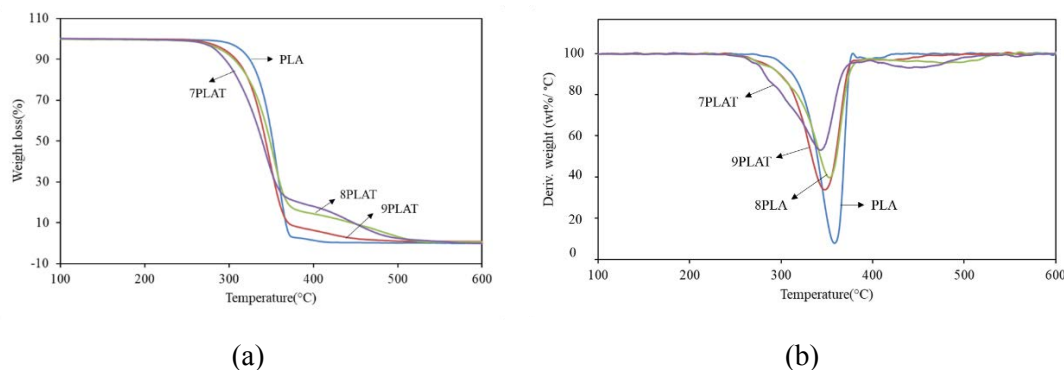
Figure 3-5. Thermal decomposition curves of PLA and AT filled PLA filaments: (a) TGA curves; (b) DTG curves.

3.5. Water absorption and hydrolysis degradation properties

PLA is a well-known degradable polymer, however, the total degradation of PLA into carbon dioxide, water, and methane in the environment needs over a period of several months to 2 years [324]. PLA is easily hydrolyzed by moisture, therefore, higher water absorption capacity has been considered as an important factor to accelerated the degradability of PLA [326] when exposed to moisture environment. Hydrolysis degradation property of PLA is important for the application in medical applications and devices designed to hydrolyze in the body fluids. As a potential 3D printing composite material, hydrolysis degradation property of AT-filled PLA filament is also interested to consider. The water absorption and hydrolysis degradation of PLA and AT-filled PLA filament was presented in Figure 3-6.

With the addition of AT, the composite filaments have a higher water absorption property (Figure 3-6, a) maybe because of the free hydroxyl groups in AT and the free volume of polymer chain caused by AT. The absorption of water is related to its rate of diffusion into the composites and to faster degradation of AT-filled PLA filament in various solvent condition (Figure 3-6, b). The devices are firstly hydrolyzed in vivo by body fluids by absorbing water causing cleavage of ester bonds [326]. The Phosphate-buffered saline (PBS) solution represent body fluids and neutral condition (pH=7.4). Acidic and basic condition was also investigated. All tested samples in three solvent environment exhibit boosting degradation rate with increasing the AT loading content. The fast degradation appears in strong basic condition since the degradation under basic condition via random ester cleavage, while the degradation under acidic condition based on chain-end cleavage [327].

(a)   (b)
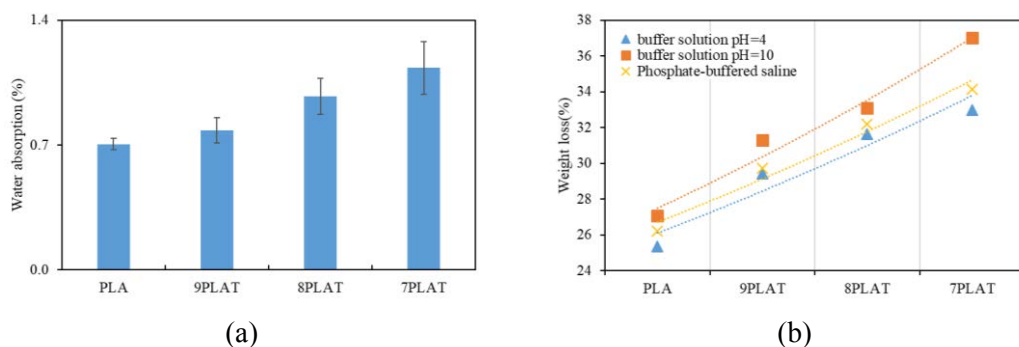
Figure 3-6 Water absorption of 3D printing filament with various AT content in 30 days.

Hydrolysis degradation of PLA with various AT content in a different solvent in 50 days.

3.6.   AT-filled PLA filament for 3D printing

Color is an important appearance factor for 3D printing product. As can be seen from Table 3-3, PLA is a colorless and transmitting polymer. The combination of PLA with dyes for producing vibrant colors are necessary for commercial applications[328]. AT filled PLA filaments displayed a brown color with a decrease of lightness. The L*, a*, and b* value of AT-filled filament increased with increasing of AT content. That means the filaments showed a more lightness, red, and yellow color. Therefore, AT-filled filaments could be a promising colored filament for 3D printing parts.

Table 3-3. Color measurement of PLA and AT filled PLA composite filaments
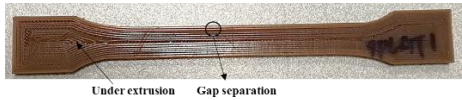
sample	Image of filament	L*	a*	b*
PLA		70.93	+0.91	+5.43
9PLAT		28.07	+7.91	+7.80
8PLAT		29.77	+9.09	+10.05
7PLAT		31.42	+10.22	+8.41

The dog bone tensile test specimens were printed to evaluate the tensile property of AT-filled filament. The image and tested value of printed specimens were tabulated in Table 3-4. From the images, AT-filled PLA samples exhibited some printed defects,

127

including under-extrusions, infill and outline separations. These printed issues are not only because of printing parameter setting but also caused by the dispersion and agglomeration of the fillers [252]. Imperfect printed is commonly found in composite material since fillers in polymer matrix change the materials characteristics and their printability [244]. Therefore, correlating the printing-process features to AT-filled composite filament is the key principle to obtain qualified printed objects. This will be considered in our future work.

The tensile specimens obtained from FDM process exhibited lower tensile properties compared with specimens processed by traditional manufacturing methods. The relatively high porosity of the dog bones caused by 3D printing setup is probably an explanation[252]. Another possible reason could be related to the interlayer adhesion that determines the mechanical properties of printed specimen[243]. However, the tensile properties of printed tensile specimen exhibited a similar trend compared with that of traditional manufacturing methods (see Figure 3-4).

Table 3-4. Printed dog bone specimens for tensile test
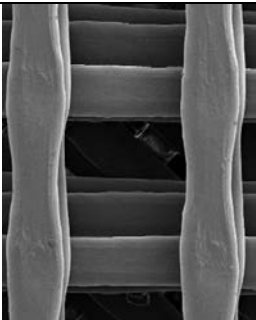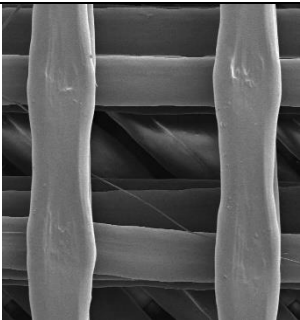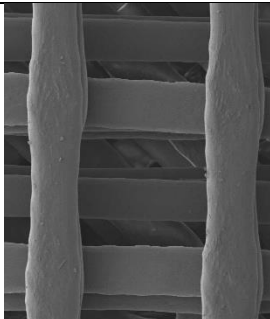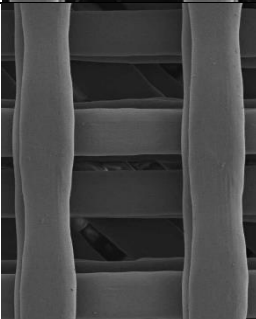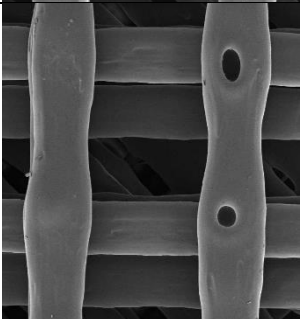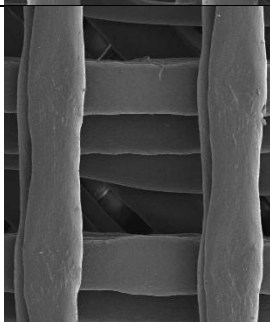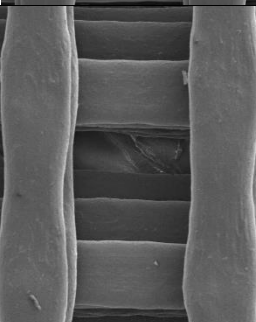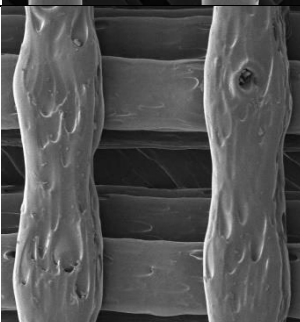
specimen	Image	Young's modulus Gpa	Tensile strength Mpa
PLA		2.6	27
9PLAT		2.1	26
7PLAT		2.9	31

For a specific material, the temperature is one of the most important parameters to control the shear viscosity and flow rate for offering successive layer deposition. The dimensional stability of each printed layer depends on the rapid solidification capacity. Thus, the temperature should be carefully chosen for achieving the balance between flowability and solidification. On this regard, scaffold prototypes were used to investigate the printability and printed morphology at different temperatures. For better understanding the effect of temperature on AT-filled PLA filament, the printing parameters were fixed during the printing process.

Table 3-5 displays SEM images of the printed scaffolds obtained from different

FDM printing temperature. All AT-filled PLA filaments are printable via FDM at a temperature range from 180 to 220 °C. However, the surface morphology was strongly affected by temperature. As can be seen from the images, both lower and higher printing temperature results in unsatisfied printing surface, performing in a rough surface and phase separation, respectively. The printing flaws occur in all temperatures in 7PLAT, which means that the high AT loading content filament is more sensitive to temperature due to the phase separation and AT aggregation. Similar results can be found in hemicellulose-filled filament[201]. The failure of printing PLA scaffold at 180°C since the first layer failed to stick to the build platform. This might due to the fast extruded PLA cooling before bonding to the building platform and to the poor flowability of PLA at 180℃ (high extruded viscosity). In other word, the addition of AT reduced the melting viscosity of PLA polymer, thus improving the printability at a lower temperature.

Table 3-5. SEM image of printed scaffolds via different FDM printing temperature

Temperature	180°C	200°C	220°C
PLA	Failed to print the scaffold.		
9PLAT			
8PLAT			

7PLAT
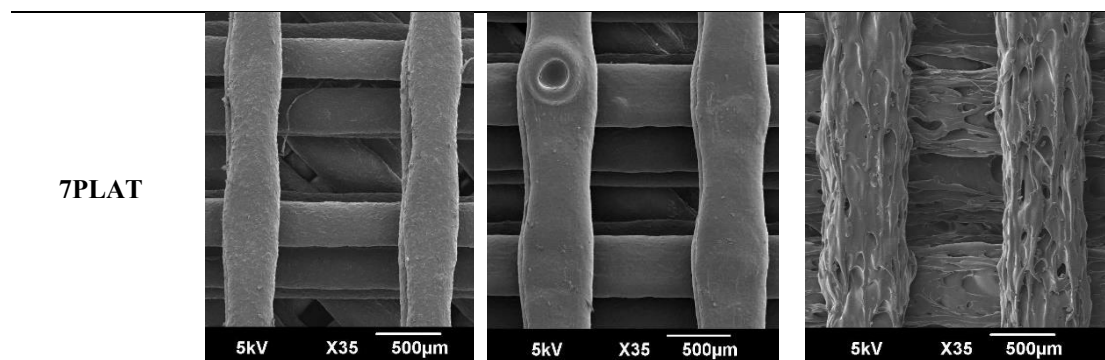
4. Conclusions

In this study, we developed a new approach to utilize tannin for partially replacing PLA as 3D printing material. The fused deposition modeling (FDM) feasibility of tannin-filled PLA was also investigated. Tannin modified with acetic anhydride improve the compatibility with PLA, guaranteeing the successful fabrication of PLA/tannin filament via a twin-screw extruder. PLA replacing by 20 wt% AT did not significantly deteriorate the mechanical property of final products. The AT-filled PLA composites displayed higher hydrolysis degradation compared with PLA, especially in an alkaline environment. These properties could probably be of benefit to short-term applications like implantable devices in biomedical applications. The incorporation of AT showed no significant effect on the melting and glass transition temperature. According to thermogravimetric analysis, a printing temperature lower than 250°C is suitable for such filaments without causing material decomposition. PLA incorporated with various AT content was printable. However, unlike pure PLA filament, the printing temperature is more important for biopolymer filled composites, high printing temperature (220°C) easily resulted in printing defects because of the phase separation and AT aggregation, especially high AT loading content filament.

Chapter 4. **Poly (lactic acid)/tannin composites prepared and modified via reactive blending process**

In this chapter, we propose to improve the interfacial adhesion between PLA and tannin via reactive compatibilization pathway by using silane coupling agent (3-aminopropytriethoxysilane), compatibilizers (methylene diphenyl diisocyanate, p-MDI), and dicumyl peroxide (DCP). For slow down the kinetics of complex reactions, tannin was partially acetylated when use DCP as adhesion promoter.

Organization of chapter 4:

Article 1. Compatibility improvement of poly (lactic acid) and tannin via one-step compatibilization

Article 2. Interfacial improvement in poly (lactic acid) and tannin via in Situ reactive extrusion

Article 4: Compatibility improvement of poly (lactic acid) and tannin via one-step compatibilization

Abstract: This work described the improvement of PLA-tannin compatibility via one-step compatibilization process with the addition of methylene diphenyl diisocyanate (p-MDI) and 3-aminopropytriethoxysilane (APS). The compatible capacity of p-MDI and APS were characterized by the resulting composites by tensile, morphological, rheological, and thermal properties. The tensile results showed that the PLA/tannin blends compatibilized by p-MDI and APS displayed higher Young's moduli and tensile strength. The formation of crosslinking microstructure between tannin and PLA polymer chains was confirmed by the rheological behavior because of the plateau-like behavior and the enhance of complex viscosity with the addition of APS and p-MDI. In addition, the thermal behavior displayed an increase of T_m and a reduced of crystallinity, suggesting the improvement of interfacial interaction between tannin and PLA matrix. The thermogravimetric analysis results revealed that the addition of tannin reduced the onset decomposition temperature, while the crosslinked network between PLA and tannin led to an increase of residues at high temperature. This efficient compatibility improving approach has the potential to be adapted to other PLA/biopolymers composites system.

Keywords: Poly (lactic acid), condensed tannin, compatibility, one-step compatibilization

1. Introduction

Biocomposite materials have been widely studied in past years driven by the gradually diminishing of global petroleum resources and the awareness of global environmental problems. Such biocomposites can be broadly described as composite materials consisting of a natural filler and a fossil-based polymer (e.g. polypropylene, polyethylene) or bio-based polymer (e.g. poly(lactic acid)) [329]. However, fully biocomposites are more attracting because both polymer matrix and natural fillers are degradable, this can minimize the environmental concerns. Polylactic acid (PLA) is obtained from agricultural products such as corn, sugar cane, and sugar beet via polycondensation or ring-opening polymerization process [131]. Some favorable attributes, such as sustainability, biocompatibility, biodegradability, favorable mechanical properties, have rendered PLA one of the most promising candidates to replace fossil-based polymers [131]. Besides, PLA has good thermal processability, which makes it suitable to produce composites with various fibers, fillers and/or polymers [115] through an efficient process such as injection molding, compression molding, extrusion, etc. [218,330,331]. However, the wide range of applications is limited by its high cost compared with petroleum-based polymers [115]. The incorporation of PLA and biopolymers has been proved to be an efficient and useful approach to produce relatively inexpensive full biocomposites with superior characteristics [43,127,178,179,332]. These biocomposites have been developed in the applications of packaging, textile sectors, or medical devices [333]. These successful applications are generally owing to the improved compatibility between hydrophilic biopolymers and hydrophobic PLA polymer matrix because poor interfacial adhesion generally results in severe deterioration of mechanical properties [115]. The chemical modification of biopolymers or the use of adhesion promoters is generally used to address this problem [115,329]. The former approach generally aims to reduce the hydroxyl groups content in biopolymers, while the latter is based on the formation of chemical bonds between composite components (either covalent bonding or physicochemical interactions) [115].

The utilization of adhesion promoters (e.g. coupling agents, compatibilizers) has been described to be a suitable approach to improve the interfacial adhesion since the bonding between component can promote good phase stress transmission and positively

contributes to mechanical property[115]. The interfacial adhesion of composites can be improved with the presence of adhesion promoter during the melt extrusion process because the melt temperature, mix and dispersion capacity of the extrusion process. This constitutes a promising methodology, named reactive compatibilization, for a short time and efficient development of novel composite materials with improved interfacial adhesion. González-Lópe [229] proposed three possible strategies for reactive compatibilization, including coupling agent incorporation, pretreatment of filled component (fiber surface treatment), and one-step compatibilization. With the latter one, polymer (PLA), filler (cellulosic fibers), and adhesion promoters (maleic anhydride, free radical initiator) were introduced together into the extruder. Bonding between polymer matrix-filler might be created at high temperature and filler was dispersed into polymer matrix synchronously. According to the experimental results, the properties of the biocomposites process via one-step compatibilization were comparable with the others.

Condensed tannins, composed of flavonoid units (Figure 4-1), are one of the most abundant and sustainable biopolymers in the plant. Their characteristics like antioxidant, antimicrobial and stabilizing properties are attracting for polymer materials. It has been shown that tannins displayed antioxidant and UV-protective properties on polypropylene [96,97], polyethylene [294], poly (vinyl chloride) (PVC) [295], and polyvinyl alcohol [104]. The incorporation of tannins to PLA has been also studied to develop composite materials [100]. However, the presence of highly polarized hydroxyl groups in tannin molecules makes it difficult to achieve good interfacial bonding with low polarity PLA matrix, resulting in poor dispersion and distribution of tannin in the PLA matrix. Esterification and hydroxypropylation of tannin have performed in order to increase the compatibility and the dispersion capacity with various plastic matrix [19,101,105,105,106,267,296]. However, a series of pretreated processes, including long-term chemical reaction, precipitation, filtration, and purification, should be performed before compounding with PLA. Inspired by one-step compatibilization approach, it is possible to improve the interfacial adhesion of PLA-tannin with adhesion promoters since tannins can react with various functional groups due to their high chemical reactivity [8,9].
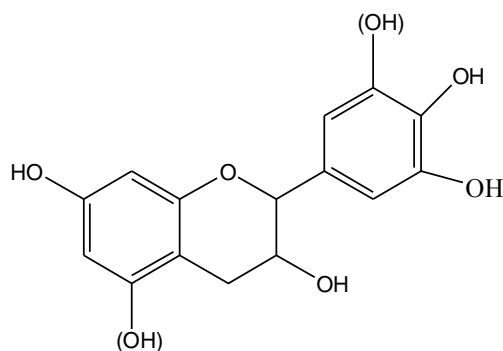
Figure 4-1. Structure of flavonoid unit of condensed tannins

Isocyanate derivatives are widely used as adhesion promoters to improve the interface between PLA and biofillers because isocyanate group is highly reactive towards hydroxyl moieties, yielding a urethane linkage between the polymer and natural fillers [334,335,335–337]. As a result, composites based on a high content of lignin (up to 65%) and polybutylene succinate (PBS) using polymeric methylene diphenyl diisocyanate as a compatibilizer were prepared via melt mixing process and displayed an improved interfacial adhesion [338]. Tannins containing various hydroxyl groups and PLA chains bearing functional end-extremities (e.g. hydroxyl and carboxylic acid), can both react with diisocyanate [8,9]. Garcia [107] reported the utilization of polymeric methyl diisocyanate to improve the compatibility between hydroxypropyl tannin and PLA matrix through a polymerization during the melt-blending in a rheometer chamber. The urethanization during the melt-blending was evidenced by the carbamate moiety (R1–O–CO–NH–R2) identified by the FTIR analysis and the atypical fluorescence pattern detected by confocal microscopy. Thus, isocyanates can be utilized to enhance the compatibility of hydrophilic tannin with hydrophobic PLA.

The phenolic hydroxyl groups of tannins can easily react with amine even at room temperature [71,339–341]. On this basis, silane bearing amine functional groups could be a suitable adhesion promoter for processing polymeric composites containing tannin. The work of Zhu reported that the mechanical properties of flax/tannin composites were boosted by aminopropytriethoxysilane (APS) [342]. Amino-silanes are commonly found to improve the interfacial bonding of biofillers containing numerous hydroxyl groups (e.g. fiber, flax, wood flour) and PLA matrix [343–346]. According to the work of Lu, the primary amine group of APS can react with PLA via ammonolysis to form

covalent bonding between cellulose and PLA under mild conditions [343]. The hydrolysis and condensation reaction of alkoxysilanes were shown in Figure 4-2. Under suitable conditions, silanes undergo hydrolysis, alcohol condensation, and/or water condensation to create Si-O-Si bonds. Based on this mechanism, Meng created a super tough PLA-silane nanohybrids via in situ crosslinking PLA-silanes [347]. Amino-silane was also reported to improve the interfacial interaction of PLA-nanocellulose based on the successful silane grafting of PLA via melt blending [345]. Therefore, amino-silanes were supposed to improve the interfacial adhesion of PLA-tannin via reactive extrusion.

$$\equiv\text{Si}-\text{OR} + \text{H}_2\text{O} \xrightleftharpoons[\text{Esterification}]{\text{Hydrolysis}} \equiv\text{Si}-\text{OH} + \text{R}-\text{OH}$$

$$\equiv\text{Si}-\text{OR} + \text{HO}-\text{Si}\equiv \xrightleftharpoons[\text{Alcoholysis}]{\substack{\text{Alcohol} \\ \text{condensation}}} \equiv\text{Si}-\text{O}-\text{Si}\equiv + \text{R}-\text{OH}$$

$$\equiv\text{Si}-\text{OH} + \text{HO}-\text{Si}\equiv \xrightleftharpoons[\text{Hydrolysis}]{\substack{\text{Water} \\ \text{condensation}}} \equiv\text{Si}-\text{O}-\text{Si}\equiv + \text{H}_2\text{O}$$
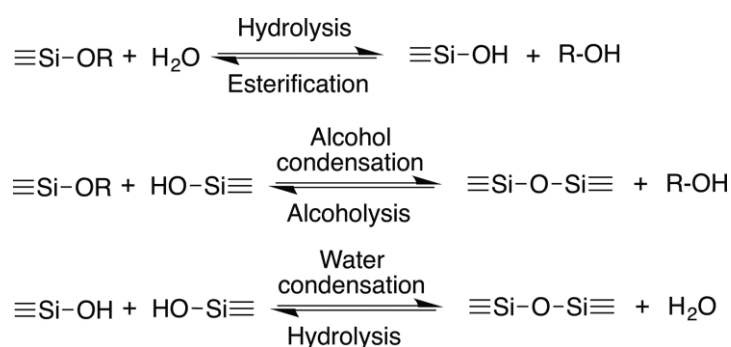
Figure 4-2. Hydrolysis and Condensation Reactions of Alkoxysilanes[347]

Inspired by those previous studies, we herein report a novel and easy method to improve the compatibility of PLA/tannin blends via reactive blending. Methylene diphenyl diisocyanate (p-MDI) and 3-aminopropytriethoxysilane (APS) were chosen as adhesion promoters. The PLA/tannin composites produced via one-step compatibilization process with APS and p-MDI was discussed. The final composites were characterized by tensile, morphological, rheological, and thermal property.

2. Materials and Methods

2.1. Materials

PLA trademarked under the name of IngeoTM Biopolymer (Grade 3D850), was obtained from Natureworks LLC (Minnesota, USA). Mimosa tannins were purchased from Silva Chimica, in Mondovi, Italy. methylene diphenyl diisocyanate (p-MDI) was used as a compatibilizer, which is a commercial resin with 57% polyisocyanates content fabricated by Bayer. Silane coupling agent (3-aminopropytriethoxysilane, APS) was obtained from Alfa Aesar. The chemical structures of the used chemicals and PLA were shown in Figure 4-3.

<div align="center">PLA   p-MDI   APS</div>
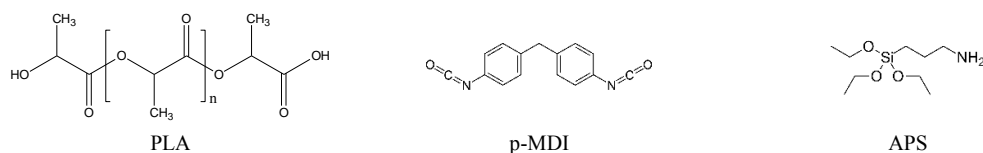
Figure 4-3. Chemical structures of PLA and chemicals used in this study

2.2. Preparation of PP/TH Composites

PLA was ground into powder by a grinder for better mixing with tannin. PLA and tannin (T) powder were oven-dried at 80℃ for more than 12 hours to eliminate possible absorbed water on the surface. The blending ratio of PLA and T was 90/10 (w/w). The Silane was fed directly via syringe, while p-MDI was diluted with acetone (p-MDI: acetone=75:25 v/v) to reduce the viscosity before injection.

The blending of PLA and T were carried out in a twin-screw extruder (Thermo Scientific^{TM} Process 11, Villebon-sur-Yvette, France), the temperature of the die and the heating zones across the extruder barrel ranged were shown in *Table 4-1*. The screw speed was 100 RPM. In the current experiment, the screw profile was designed two mixing zones for obtaining effective mixing perform: zone 1 designed before the addition of compatibilizer for premixing PLA and tannin, while zone 2 aimed to guarantee well blend with compatibilizer. The compatibilizers (liquid) were fed by using a syringe, the injecting speed was controlled by a syringe pump (WPI, SP120PZ). The flow rate of PLA/T powder was 6.6 g/min while the flow rate speed of the silane and p-MDI was 0.8 g/min and 1g/min, respectively. The PLA/tannin blend without compatibilizer noted as PLT, while with silane and p-MDI were named as PLTSi and PLTM, respectively.

The extruded composite materials were ground into small particles by a grinder for further use. The tensile test specimens (dog-bone-shaped, ISO 527, type 1A) were carried out by a micro-compounder (Micro 15, DSM Xplore, Netherlands) and a micro-injection molder (Xplore).
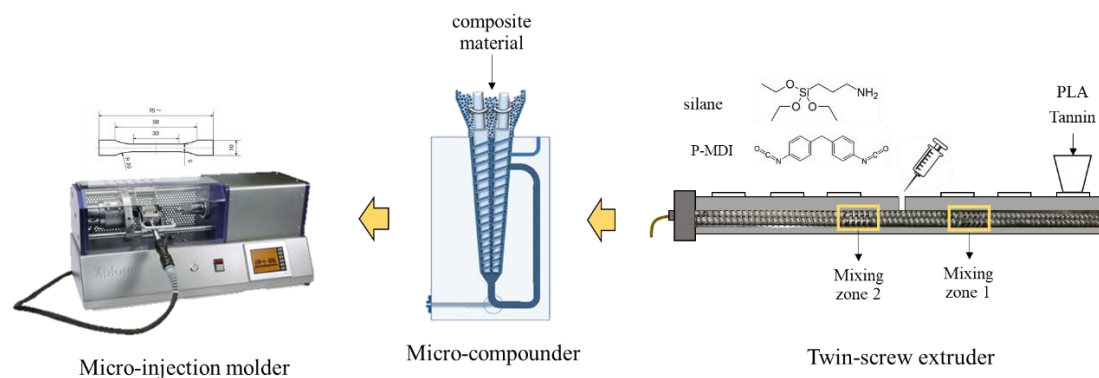
Figure 4-4. Reactive blending process by a twin-screw extruder; The specimens molding process by micro-compounder and micro-injection molder.

Table 4-1. Temperature of screw profile

Zone	die	8	7	6	5	4	3	2	1
T (°C)	185	155	180	190	190	190	200	200	200

2.3. Characterization

The tensile test was performed at room temperature on an Instron tensile testing machine (model 5569) equipped with a 50 kN load cell, operated according to EN ISO 527:1996. The cross-head speed used was of 1 mm/min. Four replicates were tested for each sample to obtain an average value.

The morphology of fracture surface after the tensile test was characterized by a scanning electron microscopy (SEM, JSM-6490LV) with an acceleration voltage of 5kV. All the samples were sputter coated with a thin layer of gold.

Rheological properties of PLA/tannin composites were analyzed on a rheometer (TA instrument, G2 ARES) using a parallel-plate geometry (25 mm diameter, 1 mm gap). Dynamic strain sweep tests to determine the linear viscoelastic region (LVR) was realized at 1 rad/s, in a range of 0.1-1000%, resulting in a strain applied of 10% chosen for frequency tests. Dynamic frequency sweep tests were performed over an angular frequency range of 0.1-623.3 rad/s at 190°C. All the experiments were performed under a nitrogen atmosphere, in order to prevent thermo-oxidative degradation. The viscoelastic behavior of samples was characterized by complex viscosity (η^*), storage modulus (G'), loss modulus (G") and tan (delta).

The Differential scanning calorimetry (DSC) was carried out using a METTLER TOLEDO DSC. The melting temperature (T_m) and crystallinity temperature (T_c) of

samples with a scan rate of 10°C/min within the temperature range of 30°C to 220 °C and 220°C to -10°C in the second scanning cycle. The measurements were using aluminum crucibles with a total sample weight 3-4 mg under a nitrogen atmosphere (50 mL/min). Values for melting temperatures (T_m) and enthalpy of melting (ΔH_m) and cold crystallization (ΔH_c) were analyzed by STARe evaluation software (version 10.00). ΔH_m^0 is the enthalpy of melting 100% crystallized PLA, which is equal to 93.7 J/g[348], and w is the weight fraction of PLA. The percentage crystallinity X_c (%) was estimated by the following equation:

$$X_c(\%) = \frac{H_m - H_c}{\Delta H_m^0 \times w} \times 100\%$$

Thermogravimetric analysis (TGA) was carried out in a METTLER TOLEDO. The samples with a total weight in the 6–7 mg range were scanned in the range of 30-600°C with a heating rate 10°C /min in an air atmosphere (50 mL/min). The obtained data were analyzed by STARe evaluation software (version 10.00).

3. Results and discussion

3.1. Tensile property

Figure 4-5 presents the tensile test results of PLA-tannin blends with or without compatibilizer. Compared with PLA, PLA/tannin blend without compatibilizer (PLT) presented a comparable Young's modulus but a lower tensile strength due to the low PLA-tannin compatibility. With the addition of a compatibilizer (PLTM or PLTSi), an increase of both Young's moduli and tensile strength were observed. For thermoplastic composite materials, Young's moduli are generally improved by adding a filler because the filled components restrict the chain mobility of the polymer chain [272]. The tensile strength of PLTM and PLTSi are 19.1% and 12.8% higher than that of PLT, respectively, referring to better interfacial adhesion between tannin and PLA matrix. While the elongation of PLA/tannin blends was observed a decrease without exception compared with neat PLA since lack of plasticizers to release the stress concentration between the interface of tannin and PLA [320]. These results are in agreement with the work of García [107].

(a)　　　　　　　　　　　(b)　　　　　　　　　　　(c)
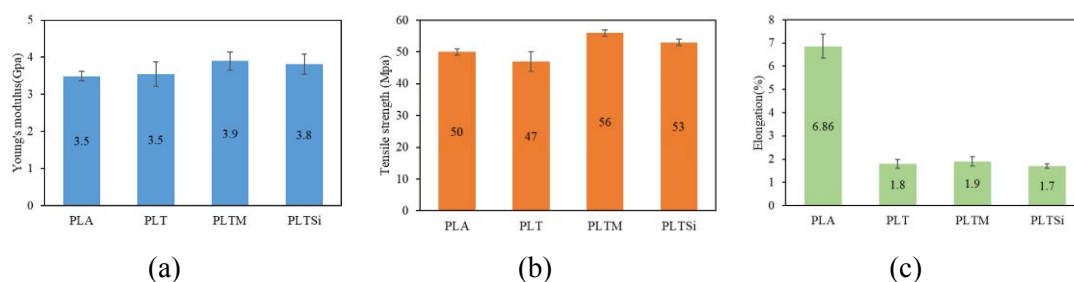
Figure 4-5. Tensile property of PLA/tannin composites

The changes of tensile property can be explained by the interaction of PLA, tannin, and p-MDI/Silane, forming crosslinked tannin particles and/or local crosslinking and interpenetrating network structure of tannin-PLA during the melt blending process (Scheme 4-1). According to previous studies, the reaction under mild conditions of PLA by both hydroxyl and carboxylic acid groups with isocyanates have been reported by Borda [349]. The urethanization of PLA, tannin, and p-MDI during the melt-blending reported by García [107] have been identified by the FTIR analysis and confocal microscopy. For silane coupling agent, amine group on APS have been proved to react with esters to form amide through ester-amide exchange reaction [343,347]. The proposed representative microstructure of PLA/tannin blends compatibilized by p-MDI/APS was represented in Scheme 4-1 (a). In the blending system, tannin was proposed to crosslink with p-MDI/APS leading to the formation of stiff thermoset particles and dispersed in the PLA matrix. Besides, the crosslinking-grafting reactions between PLA, tannin and p-MDI/APS created a macromolecular network, enhancing interfacial adhesion and stress transfer between the two phases. This contributes to the improvement of tensile strength compared with PLT. The illustration of the proposed crosslinking-grafting reactions between PLA, tannin and p-MDI/APS can be seen in Scheme 4-1 (b) and (c).

Scheme 4-1. The proposed representative microstructure of PLA/tannin blends and illustration of the proposed crosslinking-grafting reactions between PLA, tannin and p-MDI/APS

(b)

(c)
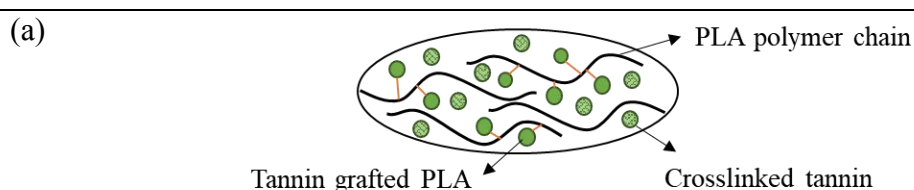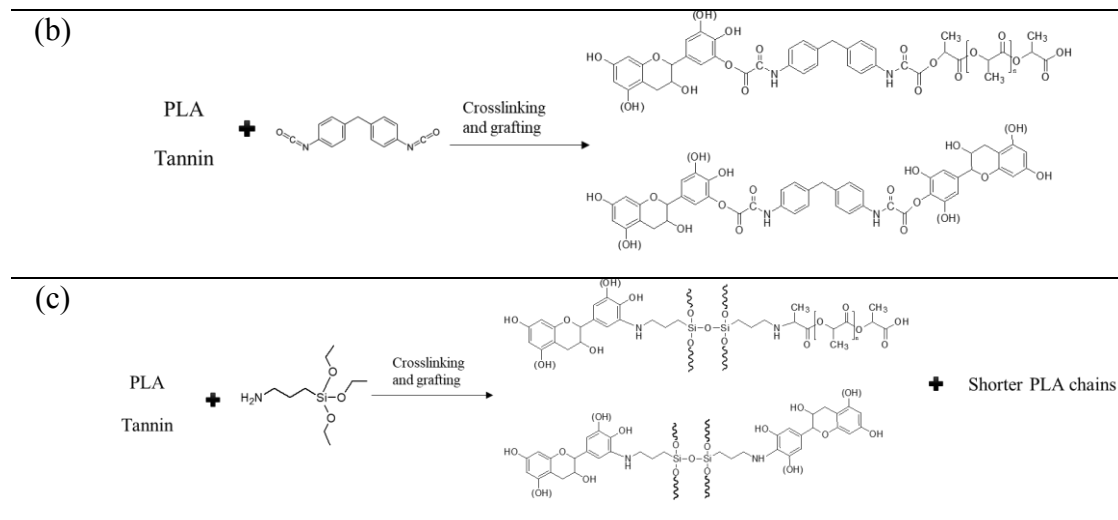
The improvement of interfacial adhesion can be confirmed by SEM microscopy. As can be seen from Figure 4-6, the morphology of PLA reveals a smooth and uniform fractured surface. There are no visible tannin particles in the images, tannin being well wetted in PLA matrix[100]. PPT was observed a distinct coarse fracture surface morphology while this rough surface tends to be less obvious with the addition of compatibilizer, a similar phenomenon can be found in the PLA/starch blend compatilized by isocyanate[335].
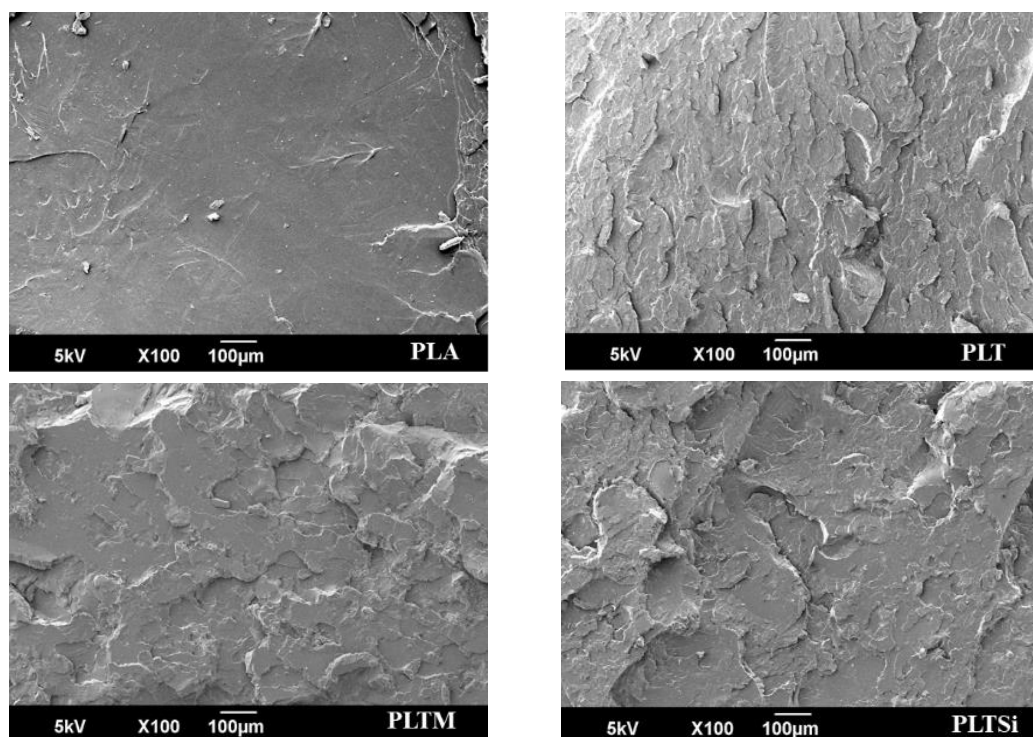
Figure 4-6. SEM micrographs of the fracture surface of PLA and PLA/tannin blends.

3.2. Rheology property

The measurement of rheological properties of polymeric materials under the molten state is useful to detect changes in the molecular structure via a one-step compatibilization process. The complex viscosity and storage modulus was used to characterize the interaction strength of PLA-tannin. As presented in Figure 4-7, complex viscosity in all curves decreased as a function of angular frequency, exhibiting a typical shear-thinning behavior. The complex viscosity of PLT sharply decreased compared with PLA due to poor surface interfacial. On the other hand, complex viscosities increased with the addition of APS and p-MDI, suggesting the formation of bonding between tannin and PLA polymer chain and/or crosslink of tannin (see Scheme 4-1). This increase in complex viscosity is particularly marked for PLTM and is associated with a tensile strength improvement of and smoother fracture surface, indicating a stronger interfacial adhesion between two components. As previously described for filled polymer systems, a plateau-like behavior of storage moduli was observed in all PLA/tannin blends at low frequency(<5 rad/s), suggesting that the presence of tannin limited the mobility of polymer chains and reinforced the internal network structure [276,277]. For PPTM and PPTSi, the network structure created by the crosslinking-grafting reaction of PLA could also contribute to such plateau-like behavior. PLTSi exhibited lower complex viscosity and storage modulus compared with PLTM since the reaction between APS and PLA generated shorter chain since the amine group on APS reacted with PLA through ester-amide exchange reactions, resulting in chain scission [347], see Scheme 4-1 (c). These results are in accordance with the work of Meng [347].
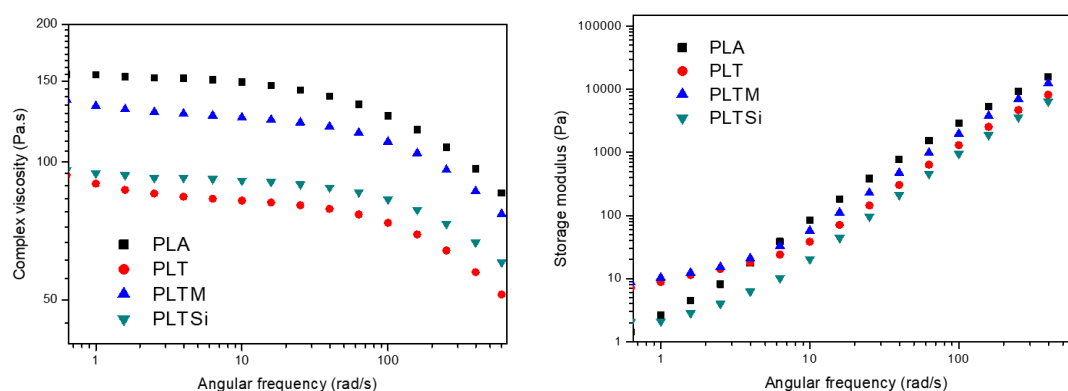
Figure 4-7. Rheological behavior of PLA and PLA/tannin blends

3.3. Crystallization and melting behaviors

The effect of tannin and compatibilizers on the glass transition temperature, crystallization and melting behaviors of PLA and PLA/tannin blends were characterized by differential scanning calorimetry (DSC), and are shown in Figure 4-8. The related results from the second heat-cool circle are given in Table 4-2. All samples displayed clear glass transition, cooling crystallization and melting peak. Compared with PLA, a slight shift to a higher temperature for T_g and T_c of PLA/tannin blends was observed indicating a decrease in the mobility of polymer molecules in the vicinity of the interface [350]. This is generally found in the blends of PLA and biofillers even without compatibilizers, such as starch [351], cellulose [345], coconut shell powder [346], etc. PLA exhibited two obvious melting peaks revealing two kinds of lamellae structure. The low-melting peak is attributed to an imperfect crystal structure, while the high-melting peak refers to a more orderly crystal structure [352]. The addition of tannin inhibited the crystallization of PLA, thus PLT has a broad melting enthalpy and the crystallinity of PLA disappeared. However, T_m of PLA/tannin blends shifts to a higher temperature by adding p-MDI and APS, referring to an improvement of the interfacial interaction between tannin and PLA matrix. Similar results can be found in PLA biocomposites compatilized by either isocyanates [107,335,353,354] or silanes [345,355]. The crosslinking structure in PLA polymer may also inhibit chain segments motion for crystallization [348], thus, a decrease of X_c can be found in PLTM and PLTSi.
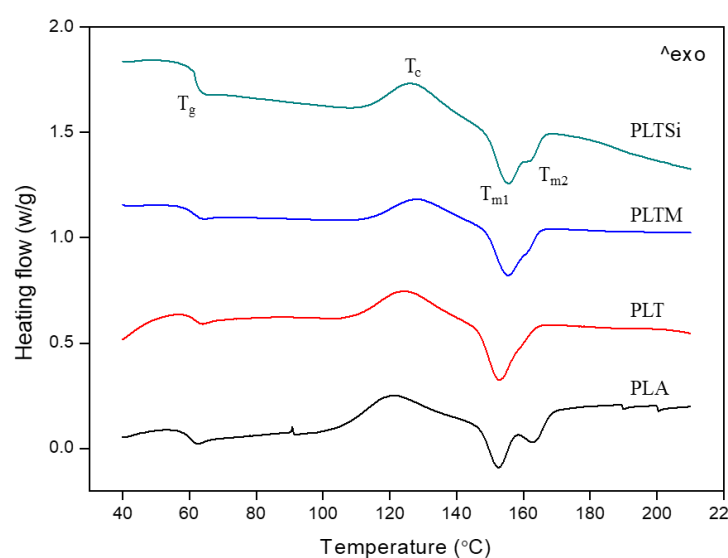
Figure 4-8. DSC thermograms of PLA and PLA/tannin blends

Table 4-2. DSC data of PLA and PLA/tannin blends

Sample	T_g (°C)	ΔH_c (J/g)	T_c (°C)	ΔH_m (J/g)	T_{m1}; T_{m1} (°C)	X_c(%)
PLA	55.9	14.0	120.4	20.7	152.5;162.9	8.0
PLT	58.6	17.8	125.2	14.7	152.8	--
PLTM	57.2	9.6	128.0	15.7	155.3;161.4	7.3
PLTSi	60.0	15.9	126.8	17.0	155.4;161.9	1.2

3.4. Thermal property

The thermal degradation behavior of PLA and PLA/tannin blends was determined by thermogravimetric analyses in an air atmosphere. Their weight loss as a function of temperature and DTG data are presented in Figure 4-9. All blends showed a one-step degradation process, which was represented by a single peak as shown in the DTG curves, while char formation can be observed with the addition of tannin at high temperature (~350°C) during the pyrolysis process. The char acts as a protective barrier that can suppress the thermal decomposition of the PLA matrix [346]. Tannin results in a lower onset decomposition temperature which can be explained by the reduction of crystallinity of PLA/tannin blends. Besides, the decomposition process of composites also relies on the thermal stability of each component, interfacial adhesion between the two components and molecular weight of the polymer matrix [107,335]. The higher decomposition temperature of PLTM can be further confirmed the improvement of interfacial adhesion, which can be found PLA/biopolymer blends compatibilized with isocyanate [335,353]. In accordance with Meng [347], the decomposition temperature of PLTSi is close to that of PLT, probably due to ester-amide exchange reactions of PLA and APS, causing chain scissions. The higher residues of PLTSi and PLTM at a high temperature can be rationalized by the crosslinked network between PLA and tannin.

| (a) | (b) |
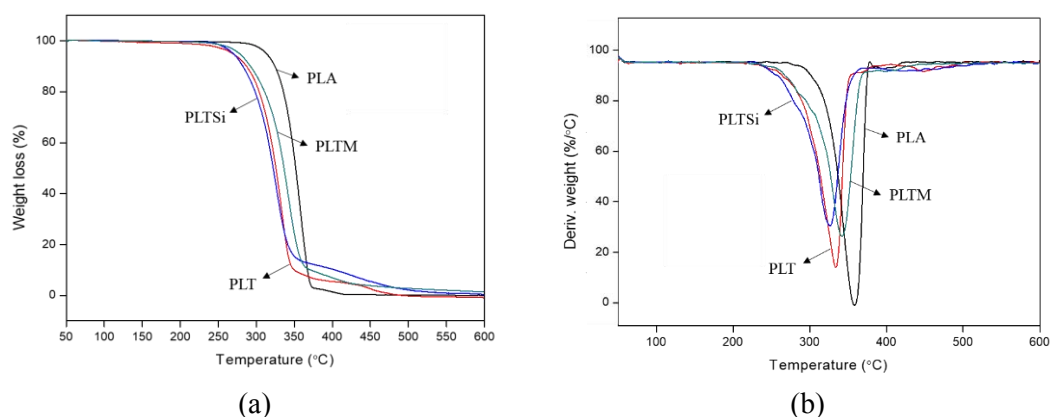
*Figure 4-9. Thermal stability of PLA and PLA/tannins blends: (**a**) TGA curves; (**b**) DTG curves.*

4. Conclusions

In this work, the compatibility of PLA and tannin have been improved by using p-MDI and APS as compatibilizers via a one-step process. The PLA/tannin blends displayed higher Young's moduli and tensile strengths with compatibilizers. The rheological behavior confirmed the formation of crosslinking microstructure between tannin and PLA polymer chains due to the plateau-like behavior and the enhance of complex viscosity with the addition of APS and p-MDI compared with PLT. The increase of T_m can be found in both PLTM and PLTSi, exhibiting the improvement of interfacial interaction between tannin and PLA matrix. The addition of tannin reduced crystallinity of PLA/tannin blends, resulting in a lower onset decomposition temperature. However, higher residues of PLTSi and PLTM at high temperature revealed a crosslinked network between PLA and tannin. This approach can be potentially adapted to other PLA/biopolymers composite systems.

Article 5: Interfacial improvements in poly (lactic acid) and tannin via in Situ reactive extrusion

Prepared for *ASC sustainable chemistry & engineering*

Abstract: Green composites based on poly (lactic acid) (PLA) and acetylated tannin (AT) were successfully prepared via free radical grafting during melt extrusion to improve interfacial adhesion. The effects of AT acetylation rate on interfacial improvement were investigated. The high molecular weight of PLA/AT blends characterized by size-exclusion chromatography confirmed the chain grafting and branching reactions of PLA and ATs. The rheological behavior revealed a crosslinked structure in PLA/AT blends due to higher complex viscosity, storage moduli and loss moduli compared with the PLA blend with peroxide. The modified PLA/AT blends exhibited good tensile strength and Young's moduli due to strong filler/matrix interfacial strength. The thermal behavior of PLA/AT blends displayed an increase of T_g since their crosslinked structure resulted in lower macromolecular mobility of polymer chains. The incorporation of AT onto PLA had no negative impact on the thermal stability of the resulting composite; this further demonstrated a strong interfacial adhesion. This study provides an efficiency pathway to utilize tannin as a component in a biodegradable polymer with good performance.

Keywords: poly(lactic acid); tannin; peroxide; interfacial adhesion; biocomposite; reactive extrusion;

1. Introduction

Polylactic acid (PLA) is a polyester produced from agricultural products such as corn, sugar cane, and sugar beet via polycondensation or ring-opening polymerization process[131]. The characteristics, including sustainability, biocompatibility, biodegradability, processability, and favorable mechanical properties have rendered PLA one of the most promising candidates to replace fossil-based polymers[131]. PLA incorporated with biopolymers to develop fully biocomposites are gaining interesting due to the low environmental impact.

Tannins are one of the most abundant and sustainable biopolymers and widely present in soft tissues of woody plants like leaves, needles, and bark. They are easily extracted using water or organic solvent, include methanol, ethanol, and acetone[266]. Tannins can be structurally divided into hydrolyzable tannins and condensed tannins. Condensed tannins (CTs, Figure 4-10), mainly composed of flavonoid units, are widely distributed in nature and constitute more than 90% of the total world production of commercial tannins. CTs have been extensively reported for the production of green wood adhesives, which displayed properties comparable to those of conventional phenolic adhesives [356]. CTs have been proved great potential as a component of poly(lactic acid) (PLA) biocomposites due to their low-cost [8] and characteristics like antioxidant, antimicrobial and stabilizing properties [11]. However, the interface adhesion of CTs and PLA still faces major challenges.
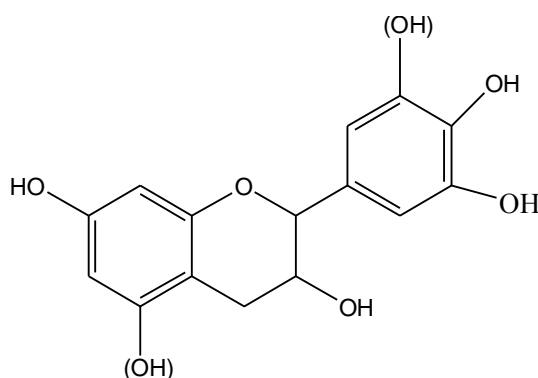
Figure 4-10. Structure of flavonoid unit of condensed tannins.

Various approaches can be used to improve the compatibility between hydrophilic biopolymers and hydrophobic polymer matrix, including chemical modified biopolymers, the use of compatibilizer/coupling agent and/or free radical grafting. For example, esterified tannin improved miscibility with hydrophobic plastic matrix,

including poly(butylene succinate), polypropylene, aliphatic polyester, and PLA [101,105,106,296]. Among these modifications, the tannin in low esterification rate displayed UV stability, and tannin with long ester chain length exhibited plasticity function. Hydroxypropylated tannins showed higher compatibility with PLA compared with native tannins because such modified tannins have higher hydrophobic characteristic [357]. The high content of hydroxypropylated tannins incorporation with PLA through trans-esterification reactions were reported as a potential precursor for carbon material [297]. Epoxidized tannin also reported to present good compatibility with hydrophobic polymers and to act as a stabilizer for PVC [53,54]. Tannins can also be copolymerized via grafting onto polyvinyl chloride or poly(ε-caprolactone) [110] to increase the compatibility[109]. They have been applied to high-density polyethylene and poly (lactic acid), respectively. Compatibilizers including ethylene vinyl alcohol, maleic anhydride modified polyethylene and ethylene acrylic ester maleic anhydride have been used to promote the compatibility of tannin and linear low-density polyethylene [108]. Recently, free radical grafting has been exploited as a simple and powerful technique to improve the interfacial adhesion of multiphase composites since the bond between the components ensures a good phase stress transmission resulting in good mechanical properties [358–361]. Peroxides initiator can generate free radicals during melting blending, inducing chain scission, branching, and crosslinking [348]. Luo has successfully prepared bacterial polyester poly(3-hydroxybutyrate-co-3-hydroxyvalerate) and softwood Kraft lignin composite using dicumyl peroxide (DCP) as a free radical initiator during the melt extrusion to improve interfacial adhesion [219]. The improvement of the mechanical, rheological, and thermal property has been justified by better molecular interactions by grafting.

According to our preliminary experiment, the incorporation of native tannin into PLA in the presence of peroxide results in extremely fragile materials. Given the high chemical reactivity of these components, the poor mechanical properties of the resulting composite could be due to the strong cross-linking reactions between tannin-tannin and tannin-PLA. Therefore, in this study, the reactivity of tannin was tuned by esterification using acetic anhydride. The goal is to modulate the kinetics of complex reactions involving DCP as a free radicals generator, acetylated tannin (AT) and PLA matrix during the extrusion process. Small amounts of DCP are expected to act as an interfacial promoter to improve the interfacial adhesion of AT and PLA matrix via reactive

blending. The effects of the degree of substitution of AT on the properties of the final composite were investigated by the tensile property, rheological behavior, molecular weight distribution, and thermal behavior.

2. Materials and Methods

2.1. Materials

PLA trademarked under the name of IngeoTM Biopolymer (Grade 3D850) with a melt flow index of 7-9 g/10min. was obtained from Natureworks LLC (Minnesota, USA). Mimosa tannins were purchased from Silva Chimica, in Mondovi, Italy. and pyridine was obtained from Acros-Organics and used as received. Acetic anhydride and dicumyl peroxide (DCP), purchased from Sigma-Aldrich, DCP was used as an adhesion promoter (radical initiator).

2.2. Sample preparation

2.2.1. Tannin acetylation

AT was prepared by mimosa tannin and in a weight proportion of tannin: anhydride=1:5 in a round bottom flask fitted with a condenser and continuously stirring with a magnetic stirrer at 60°C for 6 hours[39]. In order to obtain tannin substituted with acetyl functional groups in different degree, different concentration of pyridine (0%, 1%, 5% on weight of tannin) was used. After acetylation, the suspension was precipitated in iced water and centrifuged to separate the solution. The AT powder was washed 5 times with distilled water and air-dried for several days at room temperature. According to the catalyst concentration, the obtained acetylated tannins were noted as AT0, AT1, AT5.

2.2.2. Melt blending extrusion

PLA was ground into powder by a grinder for better mixing with tannin. PLA and tannin (T) powder were oven-dried at 80℃ for more than 12 hours to eliminate possible absorbed water on the surface. The blending ratio of PLA and ATs was 90/10 (w/w). Each blending formula was coated with a previously prepared acetone: water solution (80:20 v/v) of DCP in 0.3 wt% of each blending. PLA also coated with DCP used as a control, noted as PLD.

The blending of PLA and AT were carried out in a twin-screw extruder (Figure

4-11, Thermo Scientific^{TM} Process 11, Villebon-sur-Yvette, France). Two mixing zones of screw profile offer effective mixing perform and reaction between AT and PLA interface. The temperature of the die and the heating zones across the extruder barrel ranged were shown in *Table 4-1*. The obtained composites containing AT0, AT1, and AT5 were named as PLAT0, PLAT1, PLAT5, respectively.
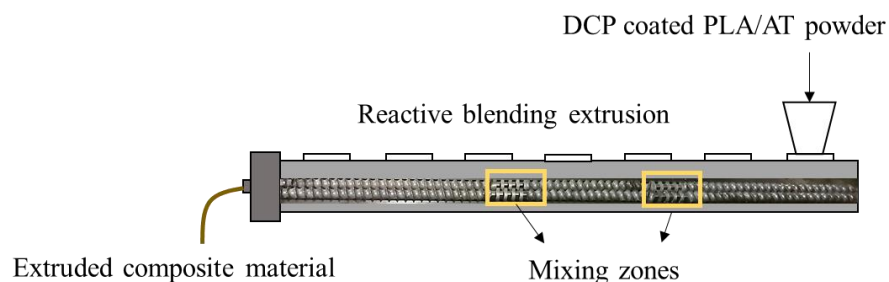
Figure 4-11. Interfacial adhesion promoted via reactive blending extrusion.

Table 4-3. Temperature of screw profile

Zone	die	8	7	6	5	4	3	2	1
T (°C)	185	155	180	190	190	190	200	200	200

The extruded composite materials were grinded into small particles by a grinder for further use. The tensile test specimens (dog-bone shaped, ISO 527, type 1A) were carried out by a micro-compounder (Micro 15, DSM Xplore, Netherlands) and a micro-injection molder (Xplore).

2.3.   Charaterization

The FT-IR spectrometer (NICOLET 6700) attenuated total reflection (ATR) mode to evaluate the acetylated tannins. The scanning parameters of FTIR are 16 scans in the range 4000-400 cm^{-1} with a resolution of 4 cm^{-1}. Tannin and acetylated tannin were dried in an oven at 40 °C for 24 hours before testing. The absorbance spectra were baseline corrected and averaged using ThermoScientific Omnic v9.0 software.

Proton nuclear magnetic resonance (Bruker, 300 MHz) wass used to analyse the chemical structure of ATs and PLA/ATs blends. Before ^{1}H NMR analysis, tannin and acetylated tannins were dissolved in DMSO, while PLA and PLA/ATs blends were dissolved in CDCl$_3$. All chemical shifts are reported in ppm.

Molecular weight distributions were measured by size-exclusion chromatography (SEC) using a Styragel column (HR-4) from Waters, with tetrahydrofuran (THF) as

solvent at a flow rate of 1.0 mL/min. Number- and weight-average molecular weights were calculated using a universal calibration method using PS standards.

Rheological properties of PLA/tannin composites were analyzed on a rheometer (TA instrument, G2 ARES) using a parallel-plate geometry (25 mm diameter, 1 mm gap). Dynamic strain sweep tests to determine the linear viscoelastic region (LVR) was realized at 1 rad/s, in a range of 0.1-1000%, resulting in a strain applied of 10% chosen for frequency tests. Dynamic frequency sweep tests were performed over an angular frequency range of 0.1-623.3 rad/s at 190°C. All the experiments were performed under a nitrogen atmosphere, in order to prevent thermo-oxidative degradation. The viscoelastic behavior of samples was characterized by complex viscosity (η^*), storage modulus (G'), loss modulus (G") and tan (delta).

The tensile test was performed at room temperature with standard dog-bone shaped (ISO 527, type 1A) tensile test specimens on an Instron tensile testing machine (model 5569) equipped with a 50 kN load cell. The cross-head speed used was of 1 mm/min. All the samples were measured four times and the average value was calculated.

The differential scanning calorimetry (DSC) was carried out using a METTLER TOLEDO DSC. The melting temperature (T_m) and crystallinity temperature (T_c) of samples with a scan rate of 10°C/min within the temperature range of 30°C to 220 °C and 220°C to -10°C in the second scanning cycle. The measurements were using aluminum crucibles with a total sample weight 3-4 mg under a nitrogen atmosphere (50 mL/min). Values for melting temperatures (T_m) and enthalpy of melting (ΔH_m) and cold crystallization (ΔH_c) were analyzed by STARe evaluation software (version 10.00). ΔH_m^0 is the enthalpy of melting 100% crystallized PLA, which is equal to 93.7 J/g [348], and w is the weight fraction of PLA. The percentage crystallinity X_c (%) was estimated by the following equation:

$$X_c(\%) = \frac{H_m - H_c}{\Delta H_m^0 \times w} \times 100\%$$

Thermogravimetric analysis (TGA) was carried out in a METTLER TOLEDO. The samples with a total weight in the 6–7 mg range were scanned in the range of 30-600°C with a heating rate 10°C /min in an air atmosphere (50 mL/min). The obtained data were analyzed by STARe evaluation software (version 10.00).

3. Results and discussion

3.1. Characterization of acetylated tannins

Tannin was modified by acid anhydride (tannin/Ac$_2$O 1/5 w/w) is the presence of 0%, 1% and 5% of pyridine as catalyst (TA0, TA1, and TA5 respectively). The substitution degree of tannin was determined by FTIR and the results are presented in Figure 4-12. For tannin, a broad band from 3700 to 2500 cm^{-1} is assigned to -OH stretching vibrations and the peak at 1614 cm^{-1} refers to aromatic ring stretching vibration. The acetylation reaction was confirmed by a strong decrease of -OH band of ATs and the emergence of a typical ester functional group (C=O stretching) at 1750 cm^{-1} [18]. Besides, the increased absorption at 1178 cm^{-1} and 1044 cm^{-1} was attributed to the C-O stretching in accordance with the structure of acetylated tannin [317,318]. The increasing intensity of C=O and C-O peaks with an increase of the catalyst concentration is clearly observed.
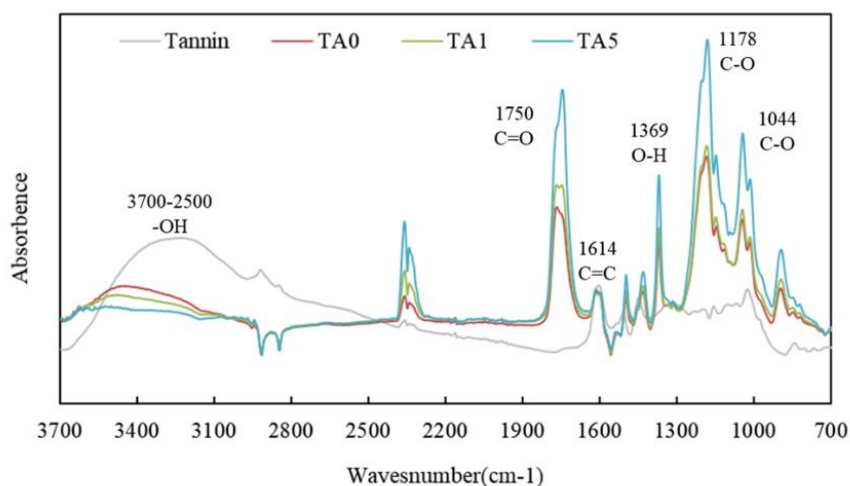
Figure 4-12. FTIR spectra of tannin and acetylated tannins

The acetylation of tannin can be confirmed by ^{1}H NMR results (Figure 4-13) by the disappearance of the strong peak at 6-7 ppm in the tannin spectrum, assigned to hydroxyl groups, and by the emerge a new signal at 2.2 ppm assigned to acetyl groups. It is known that the reactivity of tannins towards acetic anhydride is a function of the pyridine content [39]. As observed from Fig.3, an increasing amount of pyridine in the reaction media resulted in an increasing acetylation degree [101]. According to Nicollin [39], total acetylation was observed from FTIR and NMR spectra with 5% of pyridine catalyst after 6 h of reaction [39].
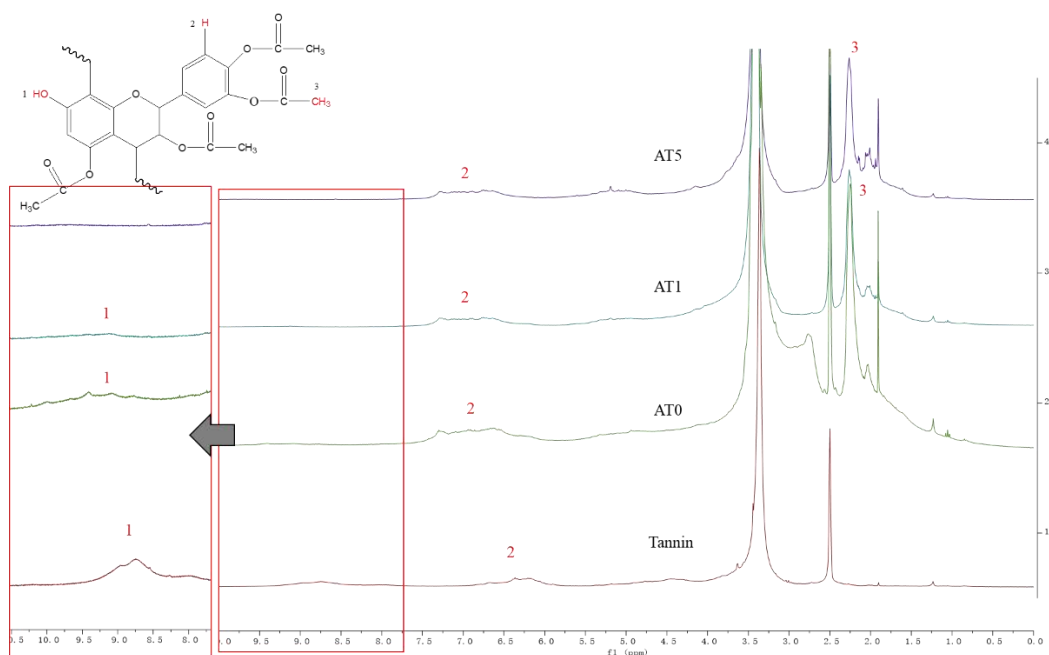
Figure 4-13. ^{1}H NMR spectra of tannin and acetylated tannins

3.2.   Grafting mechanism and structure

Reactions potentially involved during the melt-blending process are given in Scheme 1. In the reaction medium, DCP initially decomposed by β-scission into acetophenone and methyl radicals (Scheme 4-2, (a)) [362] which can further react with PLA and ATs, resulting in PLA· and AT· radicals. Radicals preferentially attack free phenolic OH groups of TA (or either proton on phenyl ring according to the acetylation level of ATs), providing different reacting sites. For PLA, preferential removal of the tertiary proton has been reported, resulting to chain scission (Scheme 4-2, (b)), branching, and crosslinking reactions during melt blending [348,362]. According to the study of Wei [360] using ESR and ^{13}C NMR spectroscopy analysis, cellulose can produce alkoxy radicals and carbon radicals hence produce C-OC bonds and C-C bonds with polyhydroxybutyrate. These free radicals formed on PLA and ATs readily undergo secondary /binary terminations leading to the formation of C-OC (Scheme 4-2, (c)) and C-C bonds (Scheme 4-2, (d)). On this basis, the possible reactions and structures of PLA/AT blends are summarized in Scheme 4-2.
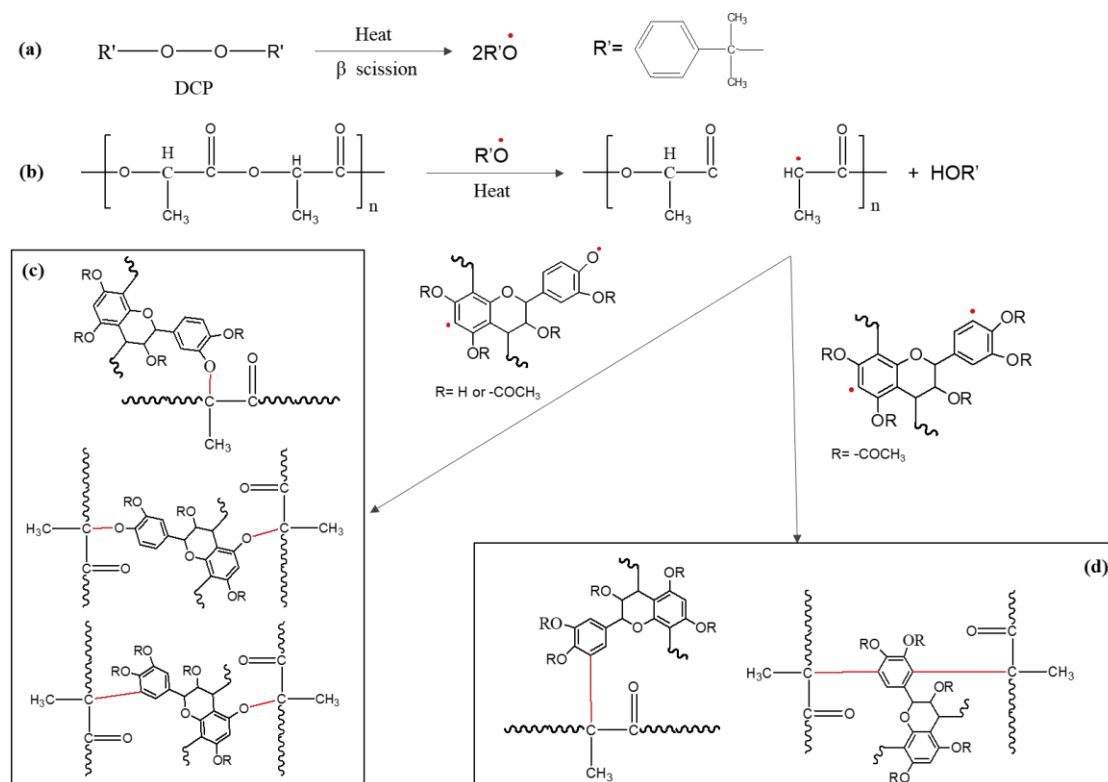
Scheme 4-2. Schematic illustration of the reactive grafting of AT onto PLA

Taking into account the complexity of the phenomena involved during in situ peroxide radicals-initiated copolymerization of composite components, the accurate determination of the reactions involved, and the structures produced is very challenging. However, physicochemical analysis of the resulting composites given in Figure 15-17 allowed us to draw some observations and conclusions.

Figure 4-14 presents ^{1}H NMR spectra of PLA and PLA/AT blends. Signals observed at 1.6 ppm and 5.2 ppm are assigned to methyl (=C-H) and methyne (-CH$_3$) protons in PLA, respectively [363]. For PLA/AT blends, the strong peak at 2.2-2.3 ppm is assigned to acetyl groups in AT (see Figure 4-13) and its intensity is a function of the acetylation rate (PLAT0<PLAT1<PLAT5).

From Figure 4-15 and Figure 4-16 (a), PLAT0 has lower M$_w$ and complex viscosity compared with PLAT1 and PLAT5. These observations can be rationalized by the presence of residual phenolic OH groups in PLA0 previously mentioned which can act as radical scavengers [4] limiting the potential of free radical polymerization. On the other hand, the covalent bonds between PLA and ATs have been confirmed by the improvement of molecular weight, complex viscosity, glass transition temperature, as well as the mechanical property (see the following discussion).
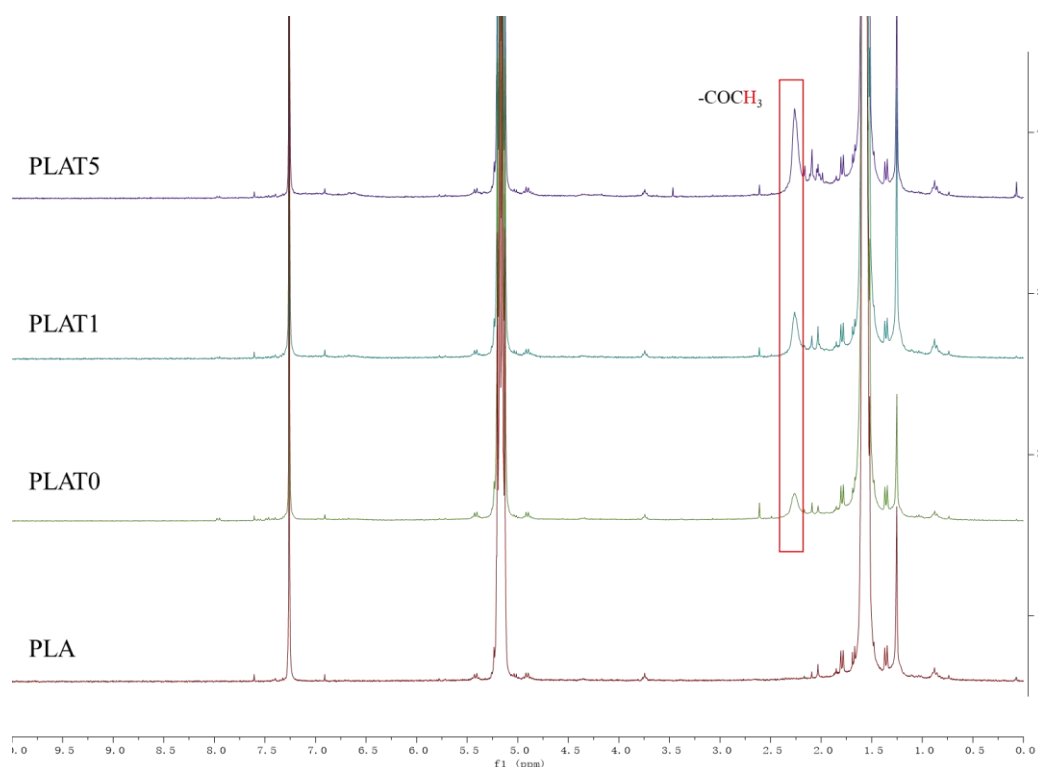
Figure 4-14. ^1H NMR spectra of PLA and PLA/AT blends

The molecular weight distributions of PLA, PLD (PLA + DCP without AT) and PLA/AT (PLA + DCP + AT) have been determined by SEC and the results are given in Figure 4-15. In Fig. 5b are given Mw corresponding to main SEC signals ($\approx$ 16 min) assigned to PLA and grafted PLA polymer chains. Higher Mw was observed for neat PLA, attesting the chain scission effect of DCP used as radical initiator [364] in PLD and PLA/AT. The small signals $\approx$ 23 min. found in all PLA/AT blends are probably due to unreacted ATs or low molecular weight PLA segments. From Figure 4-15 (b), it appeared that, compared to the control, higher M_w were obtained for PLA/AT attesting the formation of covalent bonds between PLA and ATs during the melt-blending. Moreover, an increase of M_w is observed with increasing the acetylation level, indicating the formation of a higher degree of crosslinking via different chain grafting or branching reaction between PLA and ATs.

(a)   (b)
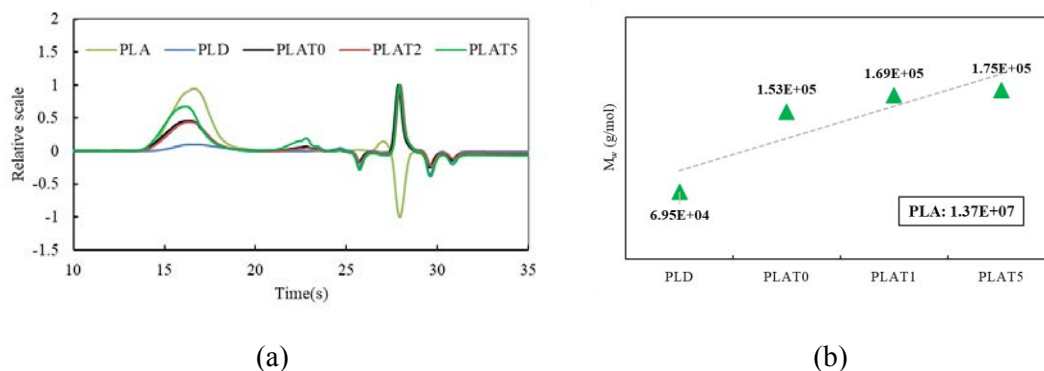
Figure 4-15. SEC molecular weight results of PLA, PLD and PLA/AT blends run with THF solvent

3.3.   Rheological property

The rheological measurements provide key insights into the molecular structure after in situ reactive extrusion. The formation of a crosslinked structure between the PLA polymer chain will inhibit the flow of molten material compared with a linear polymer. As can be seen from Figure 4-16 (a), the complex viscosity of PLA, PLD, and PLA/AT blends as a function of angular frequency at 190 °C, exhibited a typical shear-thinning behavior. A significant drop of complex viscosity can be observed in PLD compared with pure PLA since the generation of radical results in chain scission of the PLA ester bonds [348]. However, the incorporation of ATs led to an increase of the complex viscosity compared with PLD, which is an indication of intensive long chain branching or partial crosslinking [365]. The viscosity of PLAT1 and PLAT5 are close to that of PLA, confirming the higher branch or crosslink level between PLA polymer chain and AT1 and AT5. This phenomenon also is attributed to the improvement of the interfacial adhesion, which is generally found in polymer blends via peroxide radicals-initiated copolymerization [361,366].

Figure 4-16 (b, c) present the storage moduli and loss moduli as function of frequency of all tested samples. The former corresponds to the elastic character of the blends or the energy stored during the deformation, while the latter represents the amount of energy dissipated in the flow [360]. The utilization of DCP produced radicals leading to chain scission of PLA, shorter polymer chain and less chains entanglement. As a result, a drop of storage modulus and loss modulus can be observed. For PLA/AT blending system, peroxide initiated PLA· and AT· radicals leading to covalent bonds between PLA and ATs. The crosslinking between PLA and AT can increase the

entanglement density of the composite system, resulting in an improvement of storage modulus and loss modulus due to higher intermolecular resistance. Besides, the high storage moduli of PLA/AT blends display a similar trend in all angular frequency region, suggesting that ATs have been grafted onto and/or crosslinked PLA polymer chains. The AT grafted/ crosslinked long PLA polymer chain dominates the storage modulus. This phenomenon is different from filled polymer systems [276,277]. In our previous works concerning tannin filled polymer systems, (crosslinked tannin filled polypropylene [112] and PLA/tannin blends, to be published), the blending composites displayed higher storage moduli at low angular frequency. In fact, PLA polymer dominated the flow-deformation behavior at high angular frequency. In the present study, the relatively lower storage modulus and loss modulus of PLAT1 suggested a less cross-linked structure in PLA/AT1 blending system. This can be explained by the presence of free phenolic –OH moieties groups in PLA/AT1 which are in competition to react with the DCP radicals. As a result, less branching and crosslinking reactions occurred between PLA and AT1.

(a)

(b)

(c)
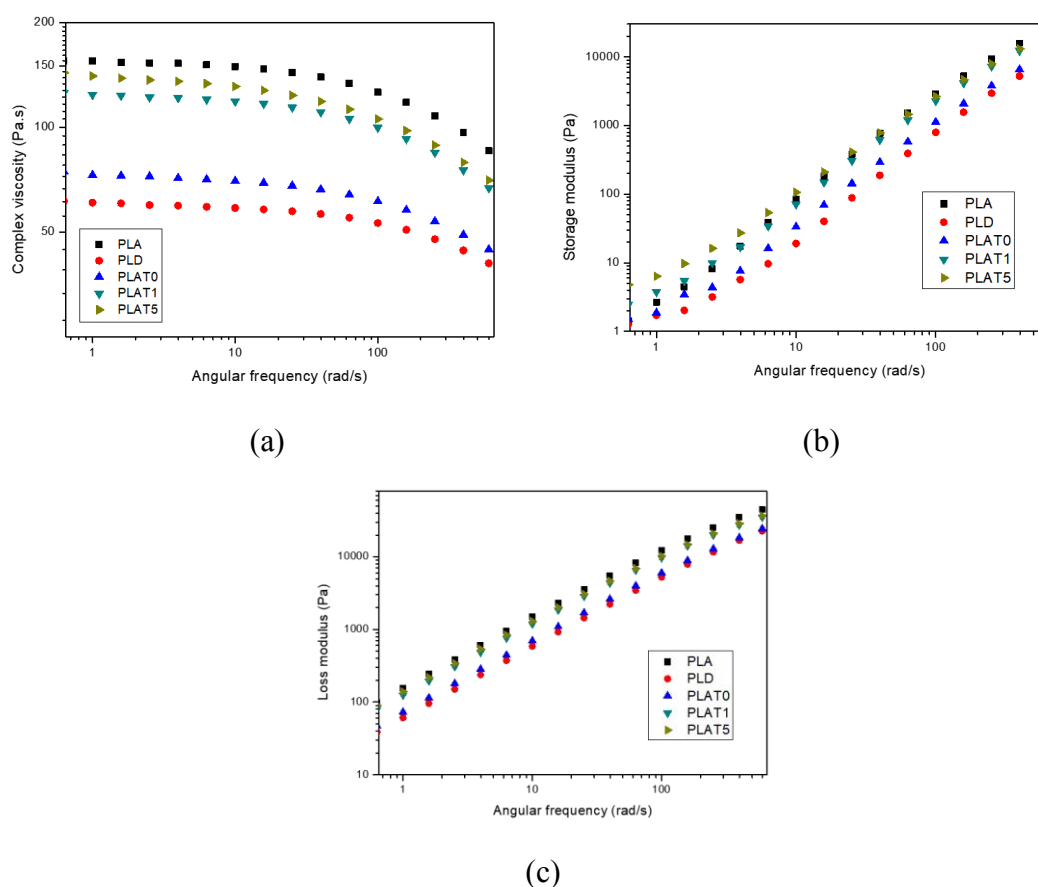
Figure 4-16. Rheological behavior of PLA, PLD, and PLA/AT blends.

157

3.4. Tensile property

The tensile property of PLA, PLD, and PLA/AT blends are presented in Figure 4-17. Compared with neat PLA, the control sample PLD displayed a higher Young's modulus and tensile strength probably due to the branching and crosslinking reactions caused by DCP radicals (Figure 4-17, (a,b)). Besides, shorter polymer chain could facilitate the polymer chains rearrangement leading to relatively higher crystallinity (Table 4-4) compared with PLA/AT blends and also contributes higher Young's modulus and tensile strength. For polymer blends, weak filler/matrix interfacial strength generally displays poor tensile strength due to poor stress transfer capacity between fillers and polymer matrix [302]. In the presence of radicals, in addition to PLA chain scissions, the initiated PLA· radicals provided reacting sites for grafting or crosslinking with ATs. Consequently, a general higher Young's moduli and tensile strength can be found in PLA/AT blends implying strong intermolecular interactions between two components. A generally decrease of elongation can be found in PLD and PLA/AT blends (Figure 4-17 (c)), crosslinked structure improving the stiffness of the material. The PLAT0 has relatively low performance compared with PLAT1/PLAT5 probably because of the inefficient grafting onto PLA chain.

(a)

(b)

(c)
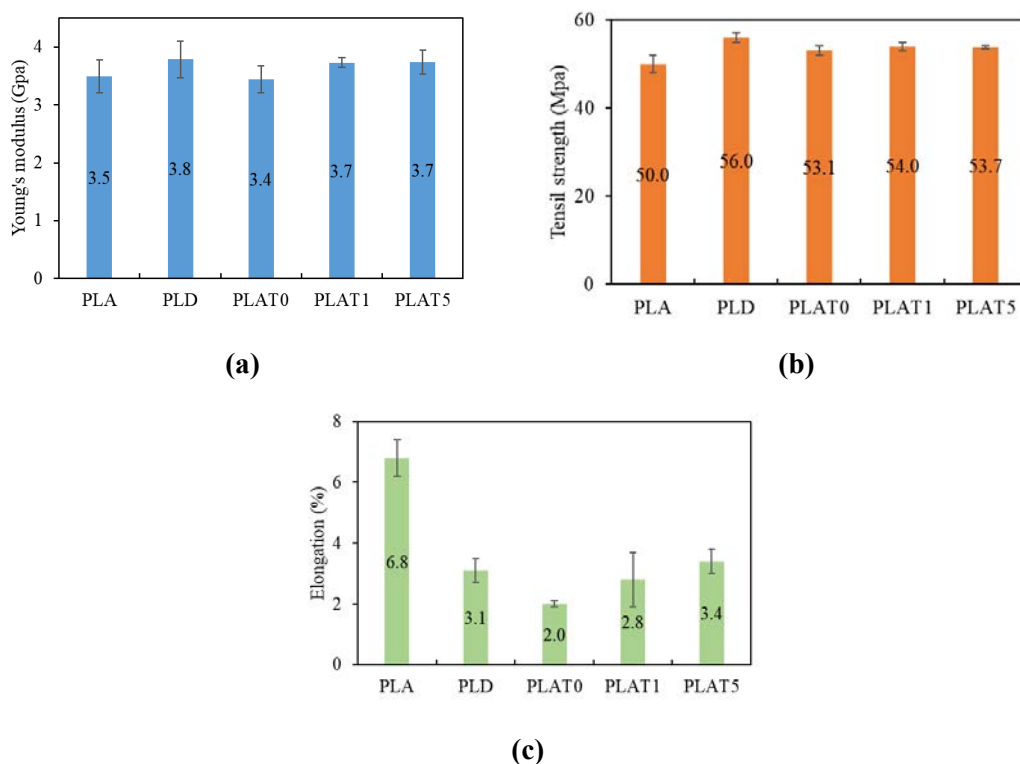
Figure 4-17. Tensile properties of PLA/AT blends

3.5. Crystallization and melting behavior

The microstructural changes will affect the crystallization and melting behavior. To better understand the effect of DCP on the copolymerization of PLA/AT blends, thermal behavior was characterized by differential scanning calorimetry (DSC). The DSC thermographs are presented in Figure 4-18, and the related results from second heating are given in Table 4-4. All DSC curves have three peaks corresponding to the glass transition temperature (T_g), cold crystallization temperature (T_c) and melting temperature (T_{m1}, T_{m1}). Two typical melting peaks can be the result of different types of a crystalline structure or a melt/re-crystallization process upon heating [367,368]. The introduction of DCP into PLA (PLD) caused chain scission leading to a decrease of the T_g, T_c, and T_m. Besides, the DCP peroxides generated branching and crosslinking during melt blending leading to a decrease of crystallinity (X_c). Since higher T_g refers to low macromolecular mobility of polymer chains [369], the formation of crosslinking structures in PLA/AT blends copolymerize by DCP required higher energy for the polymer chains mobility in the amorphous phase. Compared with PLD, the T_c of PLA/AT blends shifted to a higher temperature and exhibited higher cold crystallization (ΔH_c), suggesting an inhomogeneity of the polymer chain segment[370]. These observations can explain the lower X_c of PLA/AT blends. The higher enthalpy of melting (ΔH_m) and the relatively higher T_m of PLA/AT blends confirmed that the crosslinked structures formed in presence of DCP suppressed the molecular motion, therefore increased the T_m and ΔH_m.
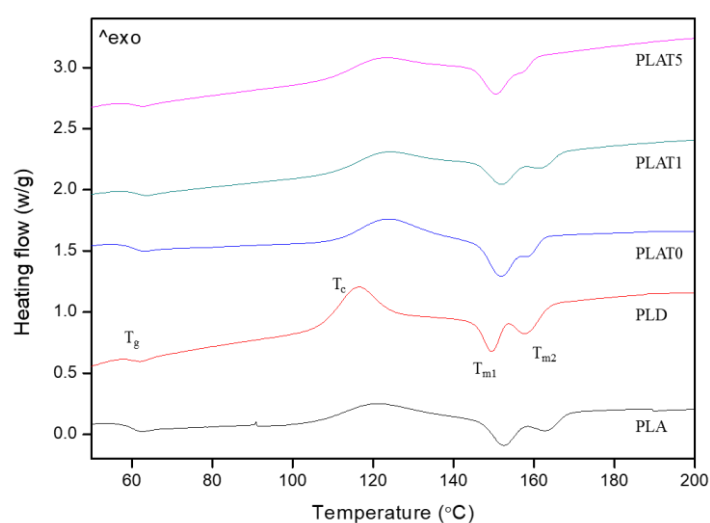
Figure 4-18. DSC thermograms of PLA, PLD, and PLA/AT blends (2nd heating)

159

Table 4-4. DSC results of PLA, PLD and PLA/AT blends

Sample	T_g (°C)	ΔH_c (J/g)	T_c (°C)	ΔH_m (J/g)	T_{m1}; T_{m1} (°C)	X_c(%)
PLA	61.6	14.2	120.2	20.4	152.5;163.0	6.6
PLD3	60.7	8.8	117.1	13.2	149.2;158.3	5.2
AT0	63.0	17.2	123.4	18.8	151.8;158.8	2.0
AT1	64.8	14.6	122.8	16.3	152.3;162.0	2.1
AT5	62.5	12.5	121.5	16.4	150.8;157.1	4.6

3.6.   Thermal degradation behavior

The thermal degradation behavior of PLA/AT blends was determined by thermogravimetric analyses in an air atmosphere. The PLA and PLD have been measured as references. Their weight loss as a function of temperature and DTG data are presented in Figure 4-19. All blends showed a one-step degradation process, which was represented by a single peak as shown in the DTG curves, while char formation can be observed with the addition of ATs at high temperature (~350°C) during the pyrolysis process. This phenomenon is generally found in the polymer/natural phenolic compounds blends (e.g. tannin, lignin) [18,112]. The char acts as a protective barrier that can suppress the thermal decomposition of the PLA matrix [346]. The decomposition process of composites relies on the thermal stability of each component, interfacial adhesion between the two components and molecular weight of the polymer matrix [107,335]. Despite PLD and PLA/AT blends had lower molecular weight, the considerable similarity of degradation behavior suggests strong interfacial adhesion because of the peroxide radicals-initiated copolymerization of PLA and AT. In our previous work, PLA blend with AT1 without any compatibilizer displayed a decrease of thermal stability (see chapter 3, Figure 3-5) due to weak interfacial adhesion between the filler and the polymer matrix. This phenomenon is generally found in PLA biocomposites [106,320,325]. Therefore, the covalent bonds between PLA and ATs have been further demonstrated by TGA results.

(a)   (b)
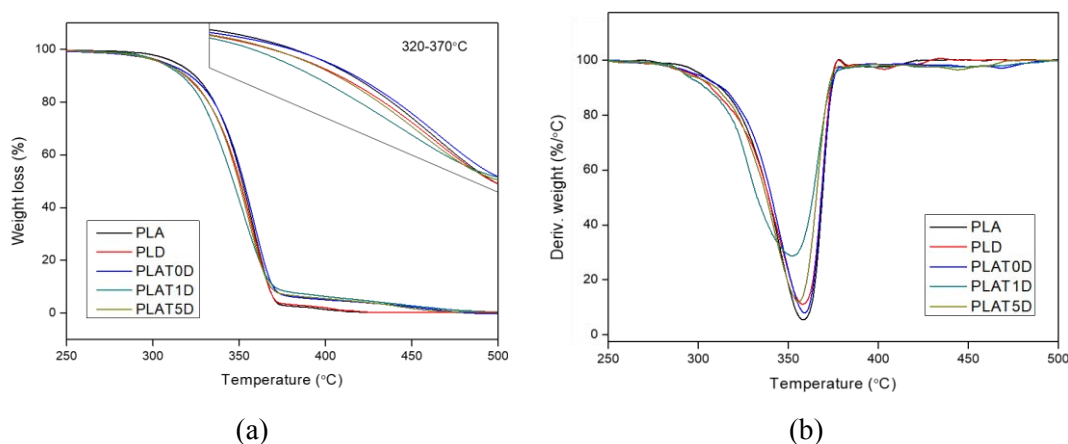
Figure 4-19. Thermal decomposition curves of PLA, PLD and PLA/AT blends: (a) TGA curves; (b) DTG curves

4. Conclusions

The improvement interfacial adhesion of PLA and acetylated tannin (AT) composite was achieved via in situ free radical grafting initiated by DCP. The peroxide radicals-initiated copolymerizing reactions are complex, which could include chain scission, grafting and branching reactions of PLA/AT blends. The successful grafting of AT onto PLA via in situ reactive extrusions was verified by ^{1}H NMR spectra. The improvement of molecular weight on PLA/AT blends confirmed the formation of the crosslinked structure via chain grafting or branching reactions of PLA and ATs. This crosslinked structure in PLA/AT blends results in higher complex viscosity, storage moduli and loss moduli compared with PLD. The DCP modified PLA/AT blends exhibited good tensile strength and Young's moduli, implying strong filler/matrix interfacial strength. The higher T_g also confirmed the crosslinked structure of PLA/AT blends since such structure leads to difficult macromolecular mobility of polymer chains. The considerable similarity of thermal stability of PLA/AT blends further suggested strong interfacial adhesion. According to the experimental results, high acetylation level of tannin led to a higher grafted efficiency. This one-step in situ reactive extrusion method provides a practical and simple strategy to develop thermoplastic/biopolymer blends with improved performance. This grafting modification can be applied to incorporate tannin as a component of value-added polymers to give special properties and reduce the cost of these materials.

Chapter 5.   Conclusions and perspectives

1. Conclusions

Polyphenols are highly abundant in nature. In the past several decades, great efforts have been made to investigate the synthesis and applications of polyphenols-based thermosetting adhesives and materials, including phenolic resins, polyurethane, epoxy resins because of their chemical reactivity. However, inherent properties of polyphenols, such as UV resistance, antioxidant, antimicrobial activity, and char forming capacity, have attracted increasing interest for developing thermoplastic composites. In order to transform polyphenols from traditional application to a broaden application in thermoplastic materials, enhance the compatibility of tannin in a polymer matrix is the critical factor to consider. This thesis focus on the combination of polyphenols and functional versatility with thermoplastic via reactive extrusion, meanwhile, to improve the interfacial adhesion during the extrusion process. The main conclusions of the thesis are summarized as follows:

Chapter 2 describes the preparation of PP/polyphenols composites via dynamic vulcanization. Two reactive reagents, including hexamethylenetetramine (hexamine) and glyoxal, were used as crosslinkers to crosslink tannin during the extrusion process. The antioxidant capacity of crosslinked polyphenols was investigated.

The **first article of chapter 2** presents the success process of PP/tannin composite through dynamic vulcanization tannin in different proportion. The cross-linked tannin (TH) can be well dispersed in the PP matrix as small stiffness particles. These stiffness particles reinforced the PP matrix, resulting in an improvement of Young's modulus and rheological behaviors. In addition, cross-linked tannin had a positive performance of PP crystallinity and thermal stability. The formation of char at high temperature, suggesting a potential flame-retardant property of the cross-linked tannin. When composites were subjected to UV accelerated weathering, PP/TH composites presented a much better performance on photodegradation resistance characterized by fewer surface cracks, lower carbonyl index, and less crystallinity decrease thus slowed down the chain scissions of PP. Besides, the cross-linked tannin addition to PP can prevent the loss of mechanical properties in physically limiting the mobility of polymer chains.

In **the second article of chapter 2,** the compatibility of tannin and lignin with PP have been improved modified via dynamic vulcanization technique with glyoxal. The

162

effect of the dynamic vulcanization process on the UV protection capacity of polyphenols was evaluated and compared with native polyphenols. From the experimental results, the extrusion process leads to polyphenols crosslinking into rigid thermoset particles, contributing to the improvement of Young's moduli of the composites. After vulcanized extrusion, the hydrophilicity of polyphenols was reduced, thus increasing the compatibility in the PP matrix, resulting in an increase of tensile strength. Besides, tannin and vulcanized tannin can act as nucleating agents of PP because of their smaller particle sizes and less agglomeration compared with lignin. Vulcanized polyphenols have a better performance on the thermal stability of PP compared with native polyphenols, especially for PP-vulcanized lignin. From the rheological data, vulcanized polyphenols displayed a reinforce function and confirmed their better dispersion capacity in the PP matrix compared with native polyphenols. Furthermore, vulcanized polyphenols present better UV protective performance, demonstrated by fewer changes on surface morphology, carbonyl index, crystallinity, viscosity, and tensile property.

In **chapter 3**, we developed a new approach to utilize tannin for partially replacing PLA as 3D printing material. The fused deposition modeling (FDM) feasibility of tannin-filled PLA was also investigated. Tannin modified with acetic anhydride improve the compatibility with PLA, guaranteeing the successful fabrication of PLA/tannin filament via a twin-screw extruder. PLA replacing by 20 wt% AT did not significantly deteriorate the mechanical property of final products. The AT-filled PLA composites displayed higher hydrolysis degradation compared with PLA, especially in an alkaline environment. These properties could probably be of benefit to short-term applications like implantable devices in biomedical applications. The incorporation of AT showed no significant effect on the melting and glass transition temperature. According to thermogravimetric analysis, a printing temperature lower than 250°C is suitable for such filaments without causing material decomposition. PLA incorporated with various AT content was printable. However, unlike pure PLA filament, the printing temperature is more important for biopolymer filled composites, high printing temperature (220°C) easily resulted in printing defects because of the phase separation and AT aggregation, especially high AT loading content filament.

Chapter 4 propose to improve the interfacial adhesion between PLA and tannin via reactive compatibilization pathway by using silane coupling agent (3-

aminopropytriethoxysilane), compatibilizers (methylene diphenyl diisocyanate, p-MDI) (Article 1), and dicumyl peroxide (DCP) (Article 2). For slow down the kinetics of complex reactions, tannin was partially acetylated when useing DCP as an adhesion promoter.

The **first article of chapter 4** described the improvement of PLA-tannin compatibility via one-step compatibilization process with the addition of methylene diphenyl diisocyanate (p-MDI) and 3-aminopropytriethoxysilane (APS). The tensile results showed that the PLA/tannin blends compatibilized by p-MDI and APS displayed higher Young's moduli and tensile strength, referring to better interfacial adhesion between tannin and PLA matrix. The changes of tensile property can be explained by the interaction of PLA, tannin, and p-MDI/APS, forming crosslinked tannin particles and/or local crosslinking and interpenetrating network structure of tannin-PLA during the melt blending process, the proposed crosslinking-grafting reactions between PLA, tannin and p-MDI/APS are shown in Scheme 4-1. The formation of crosslinking microstructure between tannin and PLA polymer chains was confirmed by the rheological behavior because of the plateau-like behavior and the enhance of complex viscosity with the addition of APS and p-MDI. In addition, the thermal behavior displayed an increase of T_m and a reduced crystallinity, suggesting the improvement of interfacial interaction between tannin and PLA matrix. The thermogravimetric analysis results revealed that the addition of tannin reduced the onset decomposition temperature, while the crosslinked network between PLA and tannin led to an increase of residues at high temperature. This efficient compatibility improving approach has the potential to be adapted to other PLA/biopolymers composites system.

The **second article of chapter 4** is the preparation of PLA/AT green composites via free radical grafting during melt extrusion to improve interfacial adhesion. The effects of AT acetylation rate on interfacial improvement were investigated. In the reaction medium, DCP initially decomposed by β-scission into acetophenone and methyl radicals which can further react with PLA and AT, resulting in PLA· and AT· radicals. Radicals preferentially attack free phenolic OH groups of TA (or either proton on phenyl ring according to the acetylation level of ATs), providing different reacting sites. For PLA, preferential removal of the tertiary proton has been reported, resulting in chain scission, branching, and crosslinking reactions during melt blending.

Taking into account the complexity of the phenomena involved during in situ

164

peroxide radicals-initiated copolymerization of composite components, the accurate determination of the reactions involved, and the structures produced is very challenging. However, physicochemical analysis of the resulting composites allowed us to draw some observations and conclusions. The improvement of molecular weight on PLA/AT blends confirmed the formation of the crosslinked structure via chain grafting or branching reactions of PLA and ATs. This crosslinked structure in PLA/AT blends results in higher complex viscosity, storage moduli and loss moduli compared with PLD. The DCP modified PLA/AT blends exhibited good tensile strength and Young's moduli, implying strong filler/matrix interfacial strength. The higher T_g also confirmed the crosslinked structure of PLA/AT blends since such structure lead to difficult macromolecular mobility of polymer chains. The considerable similarity of thermal stability of PLA/AT blends further suggested strong interfacial adhesion. According to the experimental results, high acetylation level of tannin led to a higher grafted efficiency. This one-step in situ reactive extrusion method provides a practical and simple strategy to develop thermoplastic/biopolymer blends with improved performance. This grafting modification can be applied to incorporate tannin as a component of value-added polymers to give special properties and reduce the cost of these materials.

2. Perspectives

The incorporation of polyphenols, especially tannins, in thermoplastics just occurred in the past 10 years. Despite some progress of compatibility between polyphenols and thermoplastic (PP and PLA), which is a critical factor for thermoplastic/biopolymer composites, have been made in this thesis, issues remain to perfectly transform polyphenols from traditional application to a broaden application in polymeric materials. According to the literature reviews and our work, several perspectives can be considered:

➢ The extrusion process is the most widely used for developing thermoplastic materials. The twin extruder offers various experimental conditions by changing the screw profile, temperature profile, screw speed and residence time. The degradation onset temperature of tannin is generally ranged from 200-250 °C, thus, tannins are suitable to blend with polymer matrix via melt blending process. The stable capacity of tannins might prevent polymers from thermal

165

degradation. Besides, chemical reactions can be also performed in an extruder. This is a fast, solvent-free, and low-cost method for effective compatibilization of polymer blends and dynamic vulcanization elastomer or dynamic curing thermoset. However, limited reports regarding polymeric matrix modified/functionalized/copolymerized with tannins via reactive blending process. The copolymerization of tannin can be performed during the melt extrusion process since its high chemical reactivity, especially those reactions with high reactive. Furthermore, thermoplastics blend with tannin-based thermoset resin (e.g. polyurethane, epoxy resin) and tannin-based polyesters (2.1.5) could be promising to develop novel green materials with stiffness and toughness, respectively.

➢ Polypropylene/polyphenols composites prepared and modified via dynamic vulcanization to improve the compatibility of tannin and polymer matrix. This method aimed to copolymer polyphenols with monomers (e.g. aldehydes, hexamine, isocyanates, epoxy, fatty acids) through the aromatic structure or hydroxyl groups to form a cross-linked three-dimensional network. This polymerization of tannins mainly occurred in the nucleophilic site of the aromatic ring, and the polymerization degree is generally limited by the complicated stereo structure and large steric hindrance of tannin; thus, unsaturated phenolic hydroxyl groups contribute to anti-UV and antioxidant function. However, this method is unsuitable for polymers that are sensitive to water (e.g. PLA), because this copolymerization reaction generates water, which results in polymer degradation during dynamic extrusion.

➢ The acetylation of tannins is a useful approach to increase their compatibility with non-polar polymer matrices. While, these reactions are usually minimized the functional properties (e.g. antioxidant, anti-UV, antimicrobial, etc.). In the case of tannins as functional additives, choose a suitable pathway to improve the interfacial adhesion without significate effect their functional characteristics is the critical to the functional diversity of polymeric material. According to various chemical reaction and modification of tannins, we propose some possible solutions:

1) Partially modified the hydroxyl groups rather than consume all hydroxyl groups. For example, partly esterified tannins via transesterification (Figure

166

1-12). This modification pathway provides different site selectivity compared to conventional acylation approaches.

2)   Synthesize tannin-based copolymers is also a potential pathway to improve the interfacial adhesion of tannin-polymer matrix (see Chapter 1.Part I1.5.6, Chapter 1.Part I2.2.2.4). For instance, tannin grafted polyvinyl chloride copolymer[109] and tannin-grafted poly(e-caprolactone) [110] have been dominated by good compatibility with PE and PLA, respectively.

3)   Transform raw tannin into nanoparticles. The recent innovation of nanoscale lignin has been proved not only greater antioxidant and UV-protection properties, but also better miscibility with hydrophobic plastics than the bulk lignin [371]. Besides, such nanoscale lignin can be exploited as reinforcing agents in polymer matrix and nanocomposites, better biocompatibility, mechanical and thermal properties than the original polymers. Inspired by lignin nanoparticles, transform raw tannins into nanoscale might be a promising route for high-value application, such as nanocomposites, biomedical materials. Another promising approach is to assemble tannin with nanoparticles. For example, titanium dioxide nanoparticles assembled with tannin acid as a UV filter [372].

➢ PP represented UV sensitive polymer in this thesis, tannins are potential natural antioxidants for PP to replace synthetic counterparts. Even though the price of tannins seems not cost-efficient compared with PP (Table 5-1), the safe and efficient antioxidants may be of interest in the food packaging industry. Besides, the antimicrobial capacity of tannins might open up new applications in the field of food preservation [373]. From Table 5-1, the price of tannins is range from 700 to 1500 euro/tons according to the extraction, purification and dying process and depending on the botanical resource and the product purity [8].

Table 5-1. The price of tannins, PP and PLA

Polymer	Tannins	PP	PLA
Price (€/tons)	700-1500	1197	1816-2437

Note: *The price of tannins were described in Reference* [8]. *The price of PP reported in the journal (plastiques & caoutchoucs, n° 951) in July 2018. The price of PLA from website Plastics Insight. Trading price in Germany in 2017.*

➤ The price of PLA is about 1860-2437 euro/tons. For economic consideration, tannin is an attracting biopolymer filler for biodegradable and/or biocompatible polymeric materials to reduce the cost of final products. The biocompatibility, biodegradable, physicochemical, biological properties might versatile characteristics of PLA as well as other biocompatible or biodegradable polymers.

➤ The application of composite material containing biopolymers for 3D printing is still facing a big challenge since the addition of functional fillers and additives in the polymer matrix changes the characteristics and rheological properties of the material. Therefore, suitable printing parameters should be set based on the characteristics and rheological properties of composites to guarantee the quality printed products. On the other hand, the composite material can be designed to improve the printing feasibility. The stiffness, the shear rate, temperature-dependent rheological parameters, and the thermal conductivity are critical factors to consider for processing an ideal filament for the FDM process[244]. The stiffness of filament ensures the entre into the heated zone. Shear-thinning of the polymer melt at a high shear rate offers better flow through the nozzle. Higher zero-shear viscosity of the material and rapid solidification via improved heat dissipation are highly desired to eliminate the dimensional instability of the printed layer. With this in mind, 3D printing composites filament based on PLA and tannin could be improved by (1) improve the interfacial adhesion between two polymer components, solving the phase separation for obtaining constant deposition throughput; (1) By using some plasticizers to improve the flow through the nozzle; (3) tannin could be copolymerized with long chain polymers to improve the flexibility.

Supplementary materials
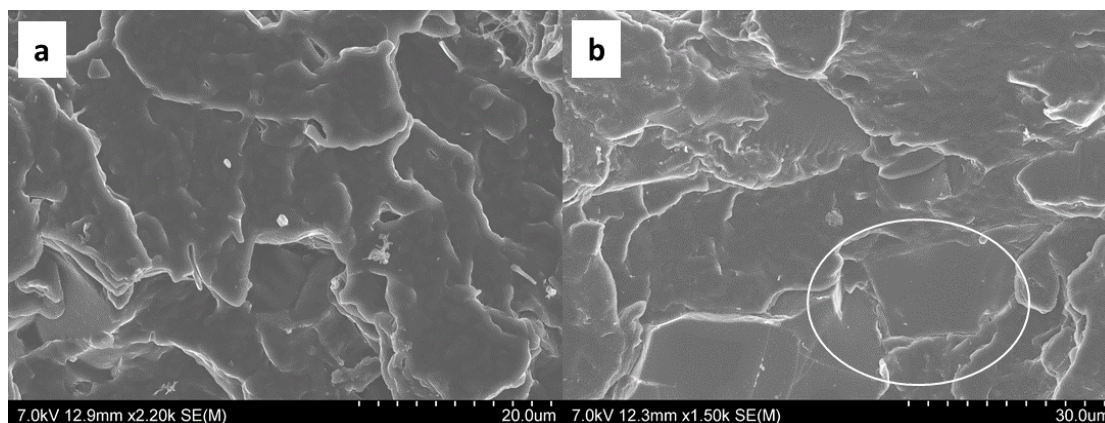
Figure S 1. SEM micrographs of (a) PP+10% crosslinked tannin; (b) PP+ 30% crosslinked tannin

Table S 1. The comparasion of the tensile property of tannin(T), dynamic crosslinked tannin(TH)

Sample	Young's modulus (GPa)	Tensile strength (MPa)	Elongation (%)
PP	1.53±0.08	34±3	52±28
PP+10T+PPMA	1.41±0.08	33±1	21±8
PP+10TH+PPMA	1.80±0.05	31±1	32±10

.

Table S 2. The comparasion of the tensile property with or without compatibilizer (MAPP)

Sample	Young's modulus (GPa)	Tensile strength (MPa)	Elongation (%)
PP	1.53±0.08	34±3	52±28
PP+10TH	1.60±0.05	30±1	15±2
PP+10TH+MAPP	1.84±0.05	31±1	32±10
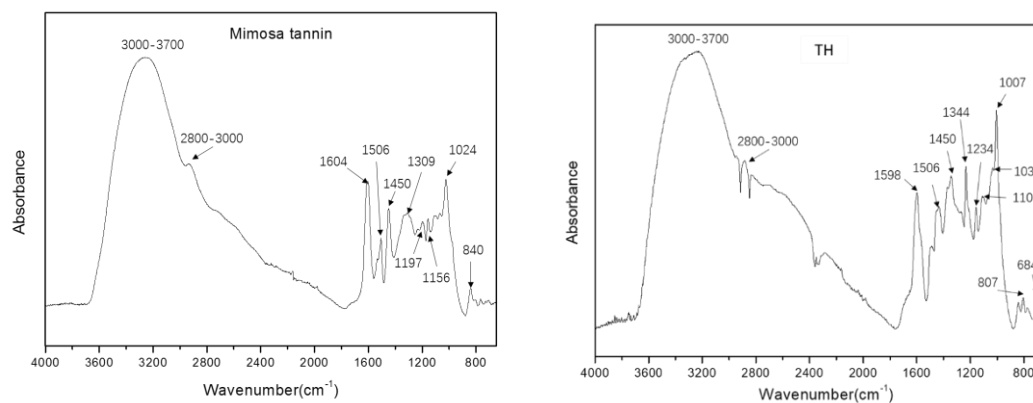
Figure S 2. FTIR spectra of pre-reacted tannin-hexamine (TH)

Table S 3. Assignment of FT-IR spectra of mimosa tannin and pre-reacted TH

Peak(cm^{-1})	Assignment
3000-3700	O-H stretching of benzene nucleus, methylol groups of tannins
2700-2800	C-H stretching, -CH2- and -CH2OCH2- bridges
1604,1598	C=C aromatic rings stretching
1506	C=C aromatic rings stretching
1450	C=C aromatic rings stretching
1309	C-C frame stretching
1197	C-OH bending
1156	C-O groups of the A-ring resorcinol-like structure
1024	C–H aromatic rings in-plane bending
840	C–H deformation in plane
1344	the C-O stretching of the B-ring of pyrogallic moieties.
1234	antisymmetric deformation of C-O-C in ether groups
1007	C-N groups
807	Deformation vibrations CH bonds

(a)   (b)
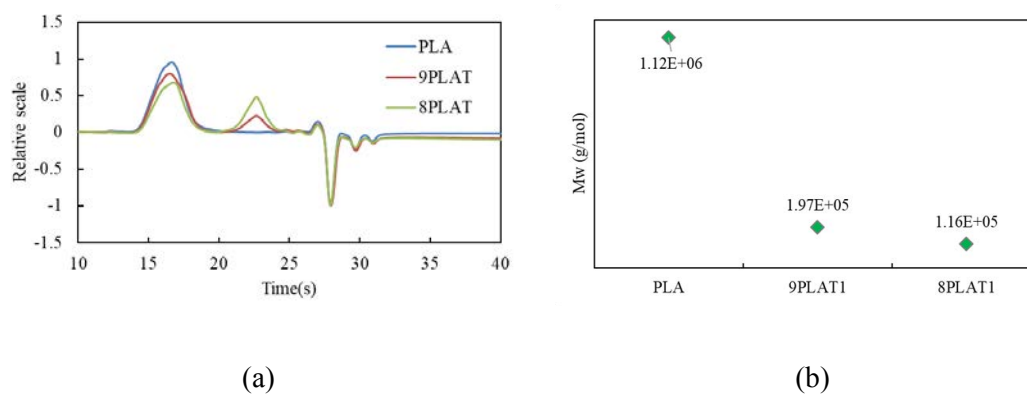
Figure S 3. Molecular weight distribution (a) and average molecular weight (b) of PLA and AT-filled PLA filaments measured by size-exclusion chromatography (SEC). Failed to measure 7PLAT due to its insolvability in THF solvent.

Abbreviations

CTs	condensed tannins
PP	polypropylene
PLA	poly (lactic acid)
TH	tannin-hexamine
MAPP	maleic anhydride grafted polypropylene
T	tannin
L	lignin
TG	tannin-glyoxal
LG	lignin-glyoxal
PPT	PP/tannin blend
PPTG	PP/tannin-glyoxal blend
PPL	PP/lignin blend
PPLG	PP/lignin-glyoxal blend
AT	acetylated tannin
FDM	fused deposition modeling
PLAT	poly (lactic acid)/ acetylated tannin blend
PBS	Phosphate Buffered Saline
p-MDI	methylene diphenyl diisocyanate
APS	3-aminopropytriethoxysilane
PLT	poly (lactic acid)/tannin blend
PLTM	poly (lactic acid)/tannin blend compatibilized with p-MDI
PLTSi	poly (lactic acid)/tannin blend compatibilized with APS
DCP	dicumyl peroxide
AT0	Tannin modified with acid anhydride with 0% catalyst
AT1	Tannin modified with acid anhydride with 1% catalyst
AT5	Tannin modified with acid anhydride with 5% catalyst
THF	Tetrahydrofuran
DSC	differential scanning calorimetry
TGA	thermogravimetric analysis

DTG	differential thermogravimetry
SEM	scanning electron microscopy
FT-IR	Fourier transform infrared
CI	carbonyl index
SEC	size-exclusion chromatography
^{1}H NMR	Proton nuclear magnetic resonance
η^*	complex viscosity
G'	storage modulus
G''	loss modulus
T_m	melting temperature
T_c	crystallinity temperature
ΔH_m	enthalpy of melting
ΔH_c	cold crystallization
X_c	percentage crystallinity

List of publications

1.   **Jingjing Liao,** Nicolas Brosse, Antonio Pizzi, and Sandrine Hoppe. "Dynamically Cross-Linked Tannin as a Reinforcement of Polypropylene and UV Protection Properties." Polymers 11, no. 1 (2019): 102.

2.   **Jingjing Liao,** Nicolas Brosse, Antonio Pizzi, Sandrine Hoppe, and Xuedong XI 2019. Polypropylene blend with polyphenols through dynamic vulcanization: mechanical, rheological, crystalline, thermal and UV protective property. Polymers, received.

3.   **Jingjing Liao,** Nicolas Brosse, Antonio Pizzi, and Sandrine Hoppe. Tannin modified via acetylation as a feedstock material for poly (lactic acid) 3D printing filament. (in preparation)

4.   **Jingjing Liao,** Nicolas Brosse, Antonio Pizzi, and Sandrine Hoppe. Compatibility improvement of poly (lactic acid) and tannin via one-step compatibilization. (in preparation)

5.   **Jingjing Liao,** Nicolas Brosse, Antonio Pizzi, and Sandrine Hoppe. Interfacial improvements in poly (lactic acid) and tannin via in Situ reactive extrusion. (in preparation)

6.   Xi, Xuedong, **Jingjing Liao**, Antonio Pizzi, Christine Gerardin, Siham Amirou, and Luc Delmotte. "5-Hydroxymethyl furfural modified melamine glyoxal resin." The Journal of Adhesion (2019): 1-19.

References

1.   Balasundram, N.; Sundram, K.; Samman, S. Phenolic compounds in plants and agri-industrial by-products: Antioxidant activity, occurrence, and potential uses. *Food Chem.* **2006**, *99*, 191–203.

2.   Goldstein, J.; Swain, T. Changes in tannins in ripening fruits. *Phytochemistry* **1963**.

3.   Hagerman, A.E.; Butler, L.G. Protein precipitation method for the quantitative determination of tannins. *J. Agric. Food Chem.* **1978**, *26*, 809–812.

4.   Quideau, S.; Deffieux, D.; Douat-Casassus, C.; Pouysegu, L. Plant polyphenols: chemical properties, biological activities, and synthesis. *Angew. Chem. Int. Ed.* **2011**, *50*, 586–621.

5.   Koleckar, V.; Kubikova, K.; Rehakova, Z.; Kuca, K.; Jun, D.; Jahodar, L.; Opletal, L. Condensed and hydrolysable tannins as antioxidants influencing the health. *Mini Rev. Med. Chem.* **2008**, *8*, 436–447.

6.   Bele, A.A.; Jadhav, V.M.; Kadam, V.J. Potential of tannnins: A review. *Asian J. Plant Sci.* **2010**, *9*, 209.

7.   Brosse, N.; Pizzi, A. Tannins for wood adhesives, foams and composites. **2017**.

8.   Arbenz, A.; Avérous, L. Chemical modification of tannins to elaborate aromatic biobased macromolecular architectures. **2015**, *17*, 2626–2646.

9.   Pizzi, A. Tannin-Based Adhesives. *J. Macromol. Sci. Part C* **1980**, *18*, 247–315.

10.   *Monomers, Polymers and Composites from Renewable Resources*; Elsevier, 2008; ISBN 978-0-08-045316-3.

11.   García, D.; Glasser, W.; Pizzi, A.; Paczkowski, S.; Laborie, M.-P. Modification of condensed tannins: from polyphenol chemistry to materials engineering. *New J Chem* **2015**, *40*, 36–49.

12.   E. García, D.; G. Glasser, W.; Pizzi, A.; P. Paczkowski, S.; Laborie, M.-P. Modification of condensed tannins: from polyphenol chemistry to materials engineering. *New J. Chem.* **2016**, *40*, 36–49.

13.   Hernes, P.J.; Hedges, J.I. Tannin signatures of barks, needles, leaves, cones, and wood at the molecular level 1 1Associate editor: C. Arnosti. *Geochim. Cosmochim. Acta* **2004**, *68*, 1293–1307.

14.   Bakkalbaşi, E.; Menteş, Ö.; Artik, N. Food Ellagitannins–Occurrence, Effects of Processing and Storage. *Crit. Rev. Food Sci. Nutr.* **2008**, *49*, 283–298.

15.   Lochab, B.; Shukla, S.; Varma, I.K. Naturally occurring phenolic sources: monomers and polymers. *Rsc Adv* **2014**, *4*, 21712–21752.

16.   Ping, L.; Pizzi, A.; Guo, Z.; Brosse, N. Condensed tannins from grape pomace: Characterization by FTIR and MALDI TOF and production of environment friendly wood adhesive. *Ind Crop Prod* **2012**, *40*, 13–20.

17.   Gaugler, M.; Grigsby, W.J. Thermal Degradation of Condensed Tannins from Radiata Pine Bark. **2009**, *29*, 305–321.

18.   Luo, C.; Grigsby, W.; Edmonds, N.; Easteal, A.; Al-Hakkak, J. Synthesis, characterization, and thermal behaviors of tannin stearates prepared from quebracho and pine bark extracts. *J. Appl. Polym. Sci.* **2010**, *17*, 352–360.

19.   García, D.E.; Glasser, W.G.; Pizzi, A.; Paczkowski, S.; Laborie, M.-P. Hydroxypropyl tannin from Pinus pinaster bark as polyol source in urethane chemistry. **2015**, *67*, 152–165.

20.   Duval, A.; Avérous, L. Characterization and Physicochemical Properties of Condensed Tannins fromAcacia catechu. **2016**, *64*, 1751–1760.

21.   Cui, C.; Sadeghifar, H.; Sen, S.; Argyropoulos, D.S. Toward Thermoplastic Lignin Polymers; Part II: Thermal & Polymer Characteristics of Kraft Lignin & Derivatives. *Bioresources* **2012**, *8*, 864–886.

22.   Arbenz, A.; Avérous, L. Oxyalkylation of gambier tannin—Synthesis and characterization of ensuing biobased polyols. **2015**, *67*, 295–304.

23.   Zhang, A.; Li, J.; Zhang, S.; Mu, Y.; Zhang, W.; Li, J. Characterization and acid-catalysed depolymerization of condensed tannins derived from larch bark. **2017**, *7*, 35135–35146.

24.   Ben Mahmoud, S.; Saad, H.; Charrier, B.; Pizzi, A.; Rode, K.; Ayed, N.; Charrier-El Bouhtoury, F. Characterization of sumac (Rhus tripartitum) root barks tannin for a potential use in wood adhesives formulation. *Wood Sci. Technol.* **2015**, *49*, 205–221.

25.   Bruyne, T.D.; Pieters, L.; Deelstra, H.; Vlietinck, A. Condensed vegetable tannins: Biodiversity in structure and biological activities. *Biochem. Syst. Ecol.* **1999**, *27*, 445–459.

26.   Pizzi, A. Wood products and green chemistry. *Ann. For. Sci.* **2016**, *73*, 185–203.

27.   Pizzi, A.; Cameron, F.A. Decrease of pressing temperature and adhesive content by metallic ion catalysis in tannin-bonded particleboard. *Holz Als Roh- Werkst.* **1981**, *39*, 463–467.

28.   Mittal, K.L. *Adhesive Joints, Formation, Characteristics, and Testing*; 1984; ISBN 978-1-4612-9702-4.

29.   Pizzi, A. Wattle-base adhesives for exterior grade particleboards. *For. Prod. J.* **1978**, *28*, 42–47.

30.   D.E. García; W.G. Glasser; A. Pizzi; C. Lacoste; M.-P. Laborie Polyphenolic resins prepared with maritime pine bark tannin and bulky-aldehydes. *Polyphenolic Resins Prep. Marit. Pine Bark Tann. Bulky-Aldehydes* **2014**, *62*, 84–93.

31.   Tondi, G. Tannin-based copolymer resins: Synthesis and characterization by solid state 13C NMR and FT-IR spectroscopy. *Polymers* **2017**, *9*, 223.

32.   A. Pizzi Recent developments in eco-efficient bio-based adhesives for wood bonding: opportunities and issues. *Recent Dev. Eco-Effic. Bio-Based Adhes. Wood Bond. Oppor. Issues* **2006**, *20*, 829–846.

33.   Pichelin, F.; Kamoun, C.; Pizzi, A. Hexamine hardener behaviour: effects on wood glueing, tannin and other wood adhesives. *Holz Als Roh- Werkst.* **1999**, *57*, 305–317.

34.   Abdullah, U.H.B.; Pizzi, A. Tannin-furfuryl alcohol wood panel adhesives without formaldehyde. *Eur. J. Wood Wood Prod.* **2013**, *71*, 131–132.

35.   Beltrán Heredia, J.; Sánchez Martín, J. Removing heavy metals from polluted surface water with a tannin-based flocculant agent. *J. Hazard. Mater.* **2009**, *165*, 1215–1218.

36.   Doszlop, S.; Vargha, V.; Horkay, F. Reactions of Epoxy with Other Functional Groups and the Arising Sec-Hydroxyl Groups. *Period. Polytech. Chem. Eng.* **1978**, *22*, 253–275.

37.   Jin-jie, G.; ゲジンジェ Synthesis of Biodegradable Polyurethane Foams from Condensed Tannin and Bark of Acacia mearnsi. **1998**, 21–85.

38.   Kaspar, H.R.E.; Pizzi, A. Industrial plasticizing/dispersion aids for cement based on polyflavonoid tannins. *J. Appl. Polym. Sci.* **1996**, *59*, 1181–1190.

39.   Nicollin, A.; Zhou, X.; Pizzi, A.; Grigsby, W.; Rode, K.; Delmotte, L. MALDI-TOF and 13C NMR analysis of a renewable resource additive—Thermoplastic acetylated tannins. *Ind. Crops Prod.* **2013**, *49*, 851–857.

40.   Grigsby, W.J.; Bridson, J.H.; Lomas, C.; Elliot, J.-A. Esterification of Condensed Tannins and Their Impact on the Properties of Poly(Lactic Acid). **2013**, *5*, 344–360.

41.   Danny E. García; Johannes Gavino; Danilo Escobar; Rodrigo A. Cancino Maleinated polyflavonoids and lignin as functional additives for three kinds of thermoplastics. *Iran. Polym. J.* **2017**, *26*, 295–304.

42.   Bridson, J.H.; Grigsby, W.J.; Main, L. Synthesis and characterization of flavonoid laurate esters by transesterification. *J Appl Polym Sci* **2013**, *129*, 181–186.

43.   Wang, C.; Kelley, S.S.; Venditti, R.A. Lignin-Based Thermoplastic Materials. *ChemSusChem* **2016**, *9*, 770–783.

44.   Marrero, D.E.; Glasser, W.G.; Pizzi, A.; Paczkowski, S.; Laborie, M.G. Substitution pattern elucidation of hydroxypropyl Pinus pinaster (Ait.) bark polyflavonoid derivatives by ESI(−)-MS/MS. *J. Mass Spectrom.* **2014**, *49*, 1050–1058.

45.   García, D.E.; Glasser, W.G.; Pizzi, A.; Anayancy, O.-M.; Laborie, M.-P. Hydroxypropyl tannin derivatives from Pinus pinaster (Ait.) bark. *Ind Crop Prod* **2013**, *49*, 730–739.

46.   García, D.E.; Glasser, W.G.; Pizzi, T.A.; Anayancy, O.-M.; Laborie, M.-P.G. Synthesis and physicochemical properties of hydroxypropyl tannins from maritime pine bark (Pinus pinaster Ait.). *Holzforschung* **2014**, *68*, 411–418.

47.   Garcia, D. Bark polyflavonoids from Pinus radiata as functional building-blocks for polylactic acid (PLA)-based green composites. *Express Polym Lett* **2016**, *10*, 835–848.

48.   García, D.E.; Fuentealba, C.A.; Salazar, J.P.; Pérez, M.A.; Escobar, D.; Pizzi, A. Mild hydroxypropylation of polyflavonoids obtained under pilot-plant scale. *Ind. Crops Prod.* **2016**, *87*, 350–362.

49.   Bridson, J.H.; Grigsby, W.J.; Main, L. One-pot solvent-free synthesis and characterisation of hydroxypropylated polyflavonoid compounds. **2018**, *111*, 529–535.

50.   Roux, D.; Ferreira, D.; Hundt, H.; Symp, M.E. Structure, stereochemistry, and reactivity of natural condensed tannins as basis for their extended industrial application. **1975**.

51.   Mohanty, A.K.; Misra, M.; Drzal, L.T. Sustainable Bio-Composites from Renewable Resources: Opportunities and Challenges in the Green Materials World. *J. Polym. Environ.* **2002**, *10*, 19–26.

52.   Hélène Nouailhas; Chahinez Aouf; Christine Guerneve; Sylvain Caillol; Bernard Boutevin; Hélène Fulcrand Synthesis and properties of biobased epoxy resins. part 1. Glycidylation of flavonoids by epichlorohydrin. *Synth. Prop. Biobased Epoxy Resins Part 1 Glycidylation Flavonoids Epichlorohydrin* **2011**, *49*, 2261–2270.

53.   Shnawa, H.A.; Khalaf, M.N.; Jahani, Y. Thermal degradation, dynamic mechanical and morphological properties of PVC stabilized with natural polyphenol-based epoxy resin. *Polym. Bull.* **2018**, *75*, 3473–3498.

54.   Shnawa, H.A.; Jahani, Y.; Khalaf, M.N. Rheological properties of PVC stabilized with tannin based epoxy resin as non metallic thermal stabilizer. *Polym. Bull.* **2017**, *74*, 1077–1090.

55.   Jahanshahi, S.; Pizzi, A.; Abdulkhani, A.; Shakeri, A. Analysis and Testing of Bisphenol A—Free Bio-Based Tannin Epoxy-Acrylic Adhesives. *Polymers* **2016**, *8*, 143.

56.   Benyahya, S.; Aouf, C.; Caillol, S.; Boutevin, B.; Pascault, J.P.; Fulcrand, H. Functionalized green tea tannins as phenolic prepolymers for bio-based epoxy resins. *Ind. Crops Prod.* **2014**, *53*, 296–307.

57.   Song, P.; Jiang, S.; Ren, Y.; Zhang, X.; Qiao, T.; Song, X.; Liu, Q.; Chen, X. Synthesis and characterization of tannin grafted polycaprolactone. *J. Colloid Interface Sci.* **2016**, *479*, 160–164.

58.   Maris, J.P.; Joutang, I. Anti-Adhesive Coatings Based on Condensed Tannins 2018.

59.	Lindert, A.; Wolpert, S.M. Tannin mannich adducts for improving corrosion resistance of metals 1990.

60.	Matamala, G.; Smeltzer, W.; Droguett, G. Use of Tannin Anticorrosive Reaction Primer to Improve Traditional Coating Systems. *CORROSION* **1994**, *50*, 270–275.

61.	Mohammad, A.; M.m, S.; Esmaeil, G. Selective separation of PVC from PET/PVC mixture using floatation by tannic acid depressant. **2010**, *19*, 483–489.

62.	Sarquís, P.E.; Menéndez-Aguado, J.M.; Mahamud, M.M.; Dzioba, R. Tannins: the organic depressants alternative in selective flotation of sulfides. *J. Clean. Prod.* **2014**, *84*, 723–726.

63.	Markham, A.E.; Adolphson, C. Drilling composition and method 1972.

64.	Mosiewicki, M.; Aranguren, M.I.; Borrajo, J. Thermal and mechanical properties of woodflour/tannin adhesive composites. *J. Appl. Polym. Sci.* **2004**, *91*, 3074–3082.

65.	Mosiewicki, M.A.; Aranguren, M.I.; Curvelo, A. a. S.; Borrajo, J. Effect of natural rubber on wood-reinforced tannin composites. *J. Appl. Polym. Sci.* **2007**, *105*, 1825–1832.

66.	Nicollin, A.; Kueny, R.; Toniazzo, L.; Pizzi, A. High Density Biocomposite from Natural Fibers and Tannin Resin. *J. Adhes. Sci. Technol.* **2012**, *26*, 1537–1545.

67.	Pizzi, A.; Kueny, R.; Lecoanet, F.; Massetau, B.; Carpentier, D.; Krebs, A.; Loiseau, F.; Molina, S.; Ragoubi, M. High resin content natural matrix–natural fibre biocomposites. *Ind. Crops Prod.* **2009**, *30*, 235–240.

68.	Zhu, J.; Zhu, H.; Njuguna, J.; Abhyankar, H. Recent Development of Flax Fibres and Their Reinforced Composites Based on Different Polymeric Matrices. *Materials* **2013**, *6*, 5171–5198.

69.	Sauget, A.; Nicollin, A.; Pizzi, A. Fabrication and mechanical analysis of mimosa tannin and commercial flax fibers biocomposites. *J. Adhes. Sci. Technol.* **2013**, *27*, 2204–2218.

70.	Li, X.; Nicollin, A.; Pizzi, A.; Zhou, X.; Sauget, A.; Delmotte, L. Natural tannin–furanic thermosetting moulding plastics. *RSC Adv.* **2013**, *3*, 17732–17740.

71.	Basso, M.C.; Lacoste, C.; Pizzi, A.; Fredon, E.; Delmotte, L. MALDI-TOF and 13C NMR analysis of flexible films and lacquers derived from tannin. *Ind. Crops Prod.* **2014**, *61*, 352–360.

72.	Lagel, M.C.; Zhang, J.; Pizzi, A. Cutting and grinding wheels for angle grinders with a bioresin matrix. *Ind. Crops Prod.* **2015**, *67*, 264–269.

73.	Lagel, M.C.; Hai, L.; Pizzi, A.; Basso, M.C.; Delmotte, L.; Abdalla, S.; Zahed, A.; Al-Marzouki, F.M. Automotive brake pads made with a bioresin matrix. *Ind. Crops Prod.* **2016**, *85*, 372–381.

74. Abdullah, U.; Zhou, X.; Pizzi, A.; Merlin, A. Note on surface quality of plywood overlaid with mimosa (Acacia mearnsii) tannin and melamine urea formaldehyde impregnated paper: effects of moisture content of resin impregnated papers before pressing on physical properties of overlaid panels. *Int Wood Prod J* **2013**, *4*, 253–256.

75. Abdullah, U.H.; Pizzi, A.; Zhou, X. High pressure paper laminates from mimosa tannin resin. *Int. Wood Prod. J.* **2014**, *5*, 224–227.

76. Meikleham, N.E.; Pizzi, A. Acid- and alkali-catalyzed tannin-based rigid foams. *J. Appl. Polym. Sci.* **1994**, *53*, 1547–1556.

77. Li, X.; Pizzi, A.; Lacoste, C.; Fierro, V.; Celzard, A. Physical Properties of Tannin/Furanic Resin Foamed With Different Blowing Agents. *Bioresources* **2012**, *8*, 743–752.

78. Rao, W.-H.; Zhu, Z.-M.; Wang, S.-X.; Wang, T.; Tan, Y.; Liao, W.; Zhao, H.-B.; Wang, Y.-Z. A reactive phosphorus-containing polyol incorporated into flexible polyurethane foam: Self-extinguishing behavior and mechanism. *Polym. Degrad. Stab.* **2018**, *153*, 192–200.

79. Čop, M.; Gospodarič, B.; Kemppainen, K.; Giovando, S.; Laborie, M.-P.; Pizzi, A.; Sernek, M. Characterization of the curing process of mixed pine and spruce tannin-based foams by different methods. *Eur. Polym. J.* **2015**, *69*, 29–37.

80. Li, X.; Pizzi, A.; Zhou, X.; Fierro, V.; Celzard, A. Formaldehyde-Free Prorobitenidin/Profi setinidin Tannin/Furanic Foams Based on Alternative Aldehydes: Glyoxal and Glutaraldehyde. *J. Renew. Mater.* **2015**, *3*, 142–150.

81. Zhao, W.; Fierro, V.; Pizzi, A.; Celzard, A. Bimodal cellular activated carbons derived from tannins. *J. Mater. Sci.* **2010**, *45*, 5778–5785.

82. Zhao, W.; Pizzi, A.; Fierro, V.; Du, G.; Celzard, A. Effect of composition and processing parameters on the characteristics of tannin-based rigid foams. Part I: Cell structure. *Mater. Chem. Phys.* **2010**, *122*, 175–182.

83. Zhao, W.; Fierro, V.; Pizzi, A.; Du, G.; Celzard, A. Effect of composition and processing parameters on the characteristics of tannin-based rigid foams. Part II: Physical properties. *Mater. Chem. Phys.* **2010**, *123*, 210–217.

84. Sánchez-Martín, J.; Beltrán-Heredia, J.; Delgado-Regaña, A.; Rodríguez-González, M.A.; Rubio-Alonso, F. Optimization of tannin rigid foam as adsorbents for wastewater treatment. *Ind. Crops Prod.* **2013**, *49*, 507–514.

85. Kaylo, A.J.; Castellucci, N.T. Tannin-epoxy reaction products and compositions thereof 1984.

86. Shang, L.; Zhang, X.; Zhang, M.; Jin, L.; Liu, L.; Xiao, L.; Li, M.; Ao, Y. A highly active bio-based epoxy resin with multi-functional group: synthesis, characterization, curing and properties. *J. Mater. Sci.* **2018**, *53*, 5402–5417.

87.   Narita Khundamri; Chahinez Aouf; Hélène Fulcrand; Eric Dubreucq; Varaporn Tanrattanakul Bio-based flexible epoxy foam synthesized from epoxidized soybean oil and epoxidized mangosteen tannin. *Bio-Based Flex. Epoxy Foam Synth. Epoxidized Soybean Oil Epoxidized Mangosteen Tann.* **2019**, *128*, 556–565.

88.   Ge, J.; Wu, R.; Shi, X.; Liu, Y.; Min, W. Application of tannin and starch as crosslinker in modification of polyurethane. *Acta Polym. Sin.* **2003**, *6*, 809–815.

89.   Luo, C.; Grigsby, W.J.; Edmonds, N.R.; Jafar, A.-H. Vegetable oil thermosets reinforced by tannin–lipid formulations. **2013**, *9*, 5226–5233.

90.   Basso, M.C.; Giovando, S.; Pizzi, A.; Pasch, H.; Pretorius, N.; Delmotte, L.; Celzard, A. Flexible-elastic copolymerized polyurethane-tannin foams. *J. Appl. Polym. Sci.* **2014**, *131*.

91.   Sunija, A.J.; Ilango, S.S.; Kumar, K.P.V. Synthesis and Characterization of Bio-Based Polyurethane from Benzoylated Cashewnut Husk Tannins. *Bull. Mater. Sci.* **2014**, *37*, 735–741.

92.   Ge, J.; Shi, X.; Cai, M.; Wu, R.; Wang, M. A novel biodegradable antimicrobial PU foam from wattle tannin. *J. Appl. Polym. Sci.* **2003**, *90*, 2756–2763.

93.   Peng, Y.; Zheng, Z.; Sun, P.; Wang, X.; Zhang, T. Synthesis and characterization of polyphenol-based polyurethane. *New J. Chem.* **2013**, *37*, 729.

94.   Kirschweng, B.; Tátraaljai, D.; Földes, E.; Pukánszky, B. Natural antioxidants as stabilizers for polymers. *Polym Degrad Stabil* **2017**, *145*, 25–40.

95.   Nanni, A.; Messori, M. A comparative study of different winemaking by-products derived additives on oxidation stability, mechanical and thermal proprieties of polypropylene. *Polym. Degrad. Stab.* **2018**, *149*, 9–18.

96.   Ambrogi, V.; Cerruti, P.; Carfagna, C.; Malinconico, M.; Marturano, V.; Perrotti, M.; Persico, P. Natural antioxidants for polypropylene stabilization. *Polym. Degrad. Stab.* **2011**, *96*, 2152–2158.

97.   Samper, M.D.; Fages, E.; Fenollar, O.; Boronat, T.; Balart, R. The potential of flavonoids as natural antioxidants and UV light stabilizers for polypropylene. *J. Appl. Polym. Sci.* **2013**, *129*, 1707–1716.

98.   Olejar, K.J.; Ray, S.; Kilmartin, P.A. Enhanced antioxidant activity of polyolefin films integrated with grape tannins: Enhanced antioxidant activity of polyolefin films integrated with grape tannins. *J. Sci. Food Agric.* **2016**, *96*, 2825–2831.

99.   Shnawa, H.A.; Jahani, Y.; Khalaf, M.N.; Taobi, A.H. The potential of tannins as thermal co-stabilizer additive for polyvinyl chloride. *J. Therm. Anal. Calorim.* **2016**, *123*, 1253–1261.

100.   Anwer, M.; Naguib, H.E.; Celzard, A.; Fierro, V. Comparison of the thermal, dynamic mechanical and morphological properties of PLA-Lignin & PLA-Tannin particulate green composites. *Compos Part B Eng* **2015**, *82*, 92–99.

101. Grigsby, W.; Kadla, J. Evaluating Poly(lactic acid) Fiber Reinforcement with Modified Tannins. *Macromol Mater Eng* **2014**, *299*, 368–378.

102. Sunthornvarabhas, J.; Liengprayoon, S.; Aouf, C.; Rungjang, W.; Sangseethong, K.; Lecomte, J.; Suwonsichon, T.; Boonreungrod, C.; Dubreucq, E.; Fulcrand, H. Tara tannin as active ingredient in electrospun fibrous delivery system. *J. Appl. Polym. Sci.* **2016**, *133*.

103. Garro, G.J.M.; Riedl, B.; Conner, A.H. Analytical Studies on Tara Tannins. *Holzforsch. - Int. J. Biol. Chem. Phys. Technol. Wood* **2009**, *51*, 235–243.

104. Zhai, Y.; Wang, J.; Wang, H.; Song, T.; Hu, W.; Li, S. Preparation and Characterization of Antioxidative and UV-Protective Larch Bark Tannin/PVA Composite Membranes. *Molecules* **2018**, *23*, 2073.

105. Grigsby, W.J.; Bridson, J.H.; Schrade, C. Modifying biodegradable plastics with additives based on condensed tannin esters. *J Appl Polym Sci* **2015**, *132*, 41626.

106. Grigsby, W.; Bridson, J.; Lomas, C.; Frey, H. Evaluating Modified Tannin Esters as Functional Additives in Polypropylene and Biodegradable Aliphatic Polyester. *Macromol Mater Eng* **2014**, *299*, 1251–1258.

107. García, D.E.; Salazar, J.P.; Riquelme, S.; Delgado, N.; Paczkowski, S. Condensed Tannin-Based Polyurethane as Functional Modifier of PLA-Composites. *Polym.-Plast. Technol. Eng.* **2018**, *57*, 709–726.

108. Bridson, J.H.; Kaur, J.; Zhang, Z.; Donaldson, L.; Fernyhough, A. Polymeric flavonoids processed with co-polymers as UV and thermal stabilisers for polyethylene films. *Polym Degrad Stabil* **2015**, *122*, 18–24.

109. Shnawa, H.A.; Khaleel, M.I.; Muhamed, F.J. Oxidation of HDPE in the Presence of PVC Grafted with Natural Polyphenols (Tannins) as Antioxidant. **2015**, *05*, 9–16.

110. Jiang, S.; Song, P.; Guo, H.; Zhang, X.; Ren, Y.; Liu, H.; Song, X.; Kong, M. Blending PLLA/tannin-grafted PCL fiber membrane for skin tissue engineering. *J. Mater. Sci.* **2017**, *52*, 1617–1624.

111. Shnawa, H.A. Thermal stabilization of polyvinyl chloride with traditional and naturally derived antioxidant and thermal stabilizer synthesized from tannins. *J. Therm. Anal. Calorim.* **2017**, *129*, 789–799.

112. Liao, J.; Brosse, N.; Pizzi, A.; Hoppe, S. Dynamically Cross-Linked Tannin as a Reinforcement of Polypropylene and UV Protection Properties. *Polymers* **2019**, *11*, 102.

113. Composite Materials. In *Materials Handbook: A Concise Desktop Reference*; Cardarelli, F., Ed.; Springer London: London, 2008; pp. 1019–1035 ISBN 978-1-84628-669-8.

114. Landel, R.F.; Nielsen, L.E.; Nielsen, L.E. *Mechanical Properties of Polymers and Composites*; CRC Press, 1993; ISBN 978-1-4822-7743-2.

115.   *Biocomposites for high-performance applications: current barriers and future needs towards industrial development*; Ray, D., Ed.; Woodhead Publishing series in composites science and engineering; Woodhead Publishing, an imprint of Elsevier: Duxford, United Kingdom, 2017; ISBN 978-0-08-100793-8.

116.   Tolinski, M. *Additives for polyolefins: getting the most out of polypropylene, polyethylene and TPO*; PDL handbook series; Second edition.; Elsevier, William Andrew is an imprint of Elsevier: Kidlington, Oxford, UK, 2015; ISBN 978-0-323-35884-2.

117.   Thakur, V.K. *Green Composites from Natural Resources*; CRC Press, 2013; ISBN 978-1-4665-7070-2.

118.   Baillie, C. *Green Composites: Polymer Composites and the Environment*; CRC Press, 2005; ISBN 978-0-8493-2576-2.

119.   Mohanty, A.K.; Misra, M.; Drzal, L.T.; Misra, M.; Drzal, L.T. *Natural Fibers, Biopolymers, and Biocomposites*; CRC Press, 2005; ISBN 978-0-203-50820-6.

120.   Wool, R.; Sun, X.S. *Bio-based polymers and composites*; Elsevier, 2011;

121.   Sorieul, M.; Dickson, A.; Hill, S.; Pearson, H. Plant Fibre: Molecular Structure and Biomechanical Properties, of a Complex Living Material, Influencing Its Deconstruction towards a Biobased Composite. *Materials* **2016**, *9*, 618.

122.   Xiaodong, W.; Xuan, G.; Rakshit, S.K. Direct fermentative production of lactic acid on cassava and other starch substrates. *Biotechnol. Lett.* **1997**, *19*, 841–843.

123.   Narine, S.S.; Kong, X. Vegetable Oils in Production of Polymers and Plastics. In *Bailey's Industrial Oil and Fat Products*; Shahidi, F., Ed.; John Wiley & Sons, Inc.: Hoboken, NJ, USA, 2005 ISBN 978-0-471-67849-6.

124.   *Polypropylene-based biocomposites and bionanocomposites*; P. M., V., Poletto, M., Eds.; Scrivener Publishing, Wiley: Hoboken, NJ, 2018; ISBN 978-1-119-28356-0.

125.   *Handbook of polypropylene and polypropylene composites*; Karian, H.G., Ed.; Plastics engineering; 2. ed., rev. and expanded.; Marcel Dekker: New York, NY, 2003; ISBN 978-0-8247-4064-1.

126.   Karger-Kocsis, J. *Polypropylene structure, blends and composites: Volume 3 composites*; Polypropylene structure, blends and composites: Volume 3 composites; Springer Science & Business Media, 2012;

127.   Basu, A.; Nazarkovsky, M.; Ghadi, R.; Khan, W.; Domb, A.J. Poly(lactic acid)-based nanocomposites. **2017**, *28*, 919–930.

128.   Ren, J. *Biodegradable poly (lactic acid) synthesis, modification, processing and applications*; Tsinghua University Press : Springer: Beijing; Heidelberg, 2011; ISBN 978-3-642-17595-4.

129.   Flynt, J. All About Polypropylene Plastic: Advantages and Disadvantages. *3D Insid.* 2018.

130. *Poly(lactic acid) science and technology: processing, properties, additives and applications*; Jiménez, A., Peltzer, M., Ruseckaite, R., Eds.; RSC polymer chemistry series; Royal Society of Chemistry: Cambridge, 2015; ISBN 978-1-84973-879-8.

131. *Synthesis, structure and properties of poly(lactic acid)*; Di Lorenzo, M.L., Androsch, R., Abdel-Rahman, M.A., Eds.; Advances in polymer science; Springer: Cham, Switzerland, 2018; ISBN 978-3-319-64230-7.

132. EUBIO_Admin Market. *Eur. Bioplastics EV*.

133. Pan, H.; Kong, J.; Chen, Y.; Zhang, H.; Dong, L. Improved heat resistance properties of poly(l-lactide)/basalt fiber biocomposites with high crystallinity under forming hybrid-crystalline morphology. *Int. J. Biol. Macromol.* **2019**, *122*, 848–856.

134. Rasal, R.M.; Janorkar, A.V.; Hirt, D.E. Poly(lactic acid) modifications. *Prog. Polym. Sci.* **2010**, *35*, 338–356.

135. Djafari Petroudy, S.R. Physical and mechanical properties of natural fibers. In *Advanced High Strength Natural Fibre Composites in Construction*; Fan, M., Fu, F., Eds.; Woodhead Publishing, 2017; pp. 59–83 ISBN 978-0-08-100411-1.

136. Cellulose. *Wikipedia* 2019.

137. Cellulose fiber. *Wikipedia* 2019.

138. Fortea-Verdejo, M.; Bumbaris, E.; Burgstaller, C.; Bismarck, A.; Lee, K.-Y. Plant fibre-reinforced polymers: where do we stand in terms of tensile properties? *Int. Mater. Rev.* **2017**, *62*, 441–464.

139. Ragoubi, M.; George, B.; Molina, S.; Bienaimé, D.; Merlin, A.; Hiver, J.-M.; Dahoun, A. Effect of corona discharge treatment on mechanical and thermal properties of composites based on miscanthus fibres and polylactic acid or polypropylene matrix. *Compos. Part Appl. Sci. Manuf.* **2012**, *43*, 675–685.

140. Ragoubi, M.; Bienaimé, D.; Molina, S.; George, B.; Merlin, A. Impact of corona treated hemp fibres onto mechanical properties of polypropylene composites made thereof. *Ind. Crops Prod.* **2010**, *31*, 344–349.

141. Cavalcante Cordeiro, R.; Villela Pacheco, L.; Schierl, S.; Víana, H.; Antoun Simão, R. Effects of different plasma treatments of short fibers on the mechanical properties of polypropylene-wood composites. *Polym. Compos.* **2018**, *39*, 1468–1479.

142. Hoque, M.B.; Solaiman; Alam, A.B.M.H.; Mahmud, H.; Nobi, A. Mechanical, Degradation and Water Uptake Properties of Fabric Reinforced Polypropylene Based Composites: Effect of Alkali on Composites. *Fibers* **2018**, *6*, 94.

143. George, M.; Mussone, P.G.; Bressler, D.C. Surface and thermal characterization of natural fibres treated with enzymes. *Ind. Crops Prod.* **2014**, *53*, 365–373.

144. Asumani, O.M.L.; Reid, R.G.; Paskaramoorthy, R. The effects of alkali–silane treatment on the tensile and flexural properties of short fibre non-woven kenaf reinforced polypropylene composites. *Compos. Part Appl. Sci. Manuf.* **2012**, *43*, 1431–1440.

145. Sullins, T.; Pillay, S.; Komus, A.; Ning, H. Hemp fiber reinforced polypropylene composites: The effects of material treatments. *Compos. Part B Eng.* **2017**, *114*, 15–22.

146. Yu, T.; Jiang, N.; Li, Y. Study on short ramie fiber/poly(lactic acid) composites compatibilized by maleic anhydride. *Compos. Part Appl. Sci. Manuf.* **2014**, *64*, 139–146.

147. Guo, C.; Li, L.; Li, H. Evaluation of interfacial compatibility in wood flour/polypropylene composites by grafting isocyanate silane coupling agent on polypropylene. *J. Adhes. Sci. Technol.* **2018**, 1–11.

148. Karmarkar, A.; Chauhan, S.S.; Modak, J.M.; Chanda, M. Mechanical properties of wood–fiber reinforced polypropylene composites: Effect of a novel compatibilizer with isocyanate functional group. *Compos. Part Appl. Sci. Manuf.* **2007**, *38*, 227–233.

149. Yu, T.; Hu, C.; Chen, X.; Li, Y. Effect of diisocyanates as compatibilizer on the properties of ramie/poly(lactic acid) (PLA) composites. *Compos. Part Appl. Sci. Manuf.* **2015**, *76*, 20–27.

150. Dong, Y.; Ghataura, A.; Takagi, H.; Haroosh, H.J.; Nakagaito, A.N.; Lau, K.-T. Polylactic acid (PLA) biocomposites reinforced with coir fibres: Evaluation of mechanical performance and multifunctional properties. *Compos. Part Appl. Sci. Manuf.* **2014**, *63*, 76–84.

151. El-Sabbagh, A. Effect of coupling agent on natural fibre in natural fibre/polypropylene composites on mechanical and thermal behaviour. *Compos. Part B Eng.* **2014**, *57*, 126–135.

152. Yussuf, A.A.; Massoumi, I.; Hassan, A. Comparison of Polylactic Acid/Kenaf and Polylactic Acid/Rise Husk Composites: The Influence of the Natural Fibers on the Mechanical, Thermal and Biodegradability Properties. *J. Polym. Environ.* **2010**, *18*, 422–429.

153. Nourbakhsh, A.; Ashori, A.; Kazemi Tabrizi, A. Characterization and biodegradability of polypropylene composites using agricultural residues and waste fish. *Compos. Part B Eng.* **2014**, *56*, 279–283.

154. Serra, T.; Ortiz-Hernandez, M.; Engel, E.; Planell, J.A.; Navarro, M. Relevance of PEG in PLA-based blends for tissue engineering 3D-printed scaffolds. *Mater. Sci. Eng. C* **2014**, *38*, 55–62.

155. Khalil, H.P.S.; Bhat, A.H.; Yusra, A.F. Green composites from sustainable cellulose nanofibrils: A review. *Carbohyd Polym* **2012**, *87*, 963–979.

156. Wilson, K.; White, D.J.B. *The anatomy of wood: its diversity and variability.*; Stobart & Son Ltd., 1986;

157. Siqueira, G.; Bras, J.; Dufresne, A. Cellulosic Bionanocomposites: A Review of Preparation, Properties and Applications. *Polymers* **2010**, *2*, 728–765.

158.   Mhd Haniffa, M.A.C.; Ching, Y.C.; Abdullah, L.C.; Poh, S.C.; Chuah, C.H. Review of Bionanocomposite Coating Films and Their Applications. *Polymers* **2016**, *8*, 246.

159.   Kamal, M.R.; Khoshkava, V. Effect of cellulose nanocrystals (CNC) on rheological and mechanical properties and crystallization behavior of PLA/CNC nanocomposites. *Carbohydr. Polym.* **2015**, *123*, 105–114.

160.   Missoum, K.; Belgacem, M.N.; Bras, J. Nanofibrillated Cellulose Surface Modification: A Review. *Materials* **2013**, *6*, 1745–1766.

161.   Abdulkhani, A.; Hosseinzadeh, J.; Ashori, A.; Dadashi, S.; Takzare, Z. Preparation and characterization of modified cellulose nanofibers reinforced polylactic acid nanocomposite. *Polym. Test.* **2014**, *35*, 73–79.

162.   Zhang, Y.; Li, X.; Yang, Y.; Lan, A.; He, X.; Yu, M. In situ graft copolymerization of l -lactide onto cellulose and the direct melt spinning. *Rsc Adv* **2014**, *4*, 34584–34590.

163.   Qiu, W.; Endo, T.; Hirotsu, T. Interfacial interaction, morphology, and tensile properties of a composite of highly crystalline cellulose and maleated polypropylene. *J. Appl. Polym. Sci.* **2006**, *102*, 3830–3841.

164.   Bondeson, D.; Oksman, K. Dispersion and characteristics of surfactant modified cellulose whiskers nanocomposites. *Compos. Interfaces* **2007**, *14*, 617–630.

165.   Zhou, L.; He, H.; Li, M.; Huang, S.; Mei, C.; Wu, Q. Enhancing mechanical properties of poly(lactic acid) through its in-situ crosslinking with maleic anhydride-modified cellulose nanocrystals from cottonseed hulls. *Ind. Crops Prod.* **2018**, *112*, 449–459.

166.   Yang, H.-S.; Kiziltas, A.; Gardner, D.J. Thermal analysis and crystallinity study of cellulose nanofibril-filled polypropylene composites. *J. Therm. Anal. Calorim.* **2013**, *113*, 673–682.

167.   Hassan, M.L.; Mathew, A.P.; Hassan, E.A.; Fadel, S.M.; Oksman, K. Improving cellulose/polypropylene nanocomposites properties with chemical modified bagasse nanofibers and maleated polypropylene. *J. Reinf. Plast. Compos.* **2014**, *33*, 26–36.

168.   Li, H.; Cao, Z.; Wu, D.; Tao, G.; Zhong, W.; Zhu, H.; Qiu, P.; Liu, C. Crystallisation, mechanical properties and rheological behaviour of PLA composites reinforced by surface modified microcrystalline cellulose. *Plast. Rubber Compos.* **2016**, *45*, 181–187.

169.   Sullivan, E.; Moon, R.; Kalaitzidou, K. Processing and Characterization of Cellulose Nanocrystals/Polylactic Acid Nanocomposite Films. *Materials* **2015**, *8*, 8106–8116.

170.   Karkhanis, S.S.; Stark, N.M.; Sabo, R.C.; Matuana, L.M. Water vapor and oxygen barrier properties of extrusion-blown poly(lactic acid)/cellulose nanocrystals nanocomposite films. *Compos. Part Appl. Sci. Manuf.* **2018**, *114*, 204–211.

171. Martin, C.; Smith, A.M. Starch Biosynthesis. *Plant Cell* **1995**, *7*, 971.

172. Whistler, R.L.; BeMiller, J.N.; Paschall, E.F. *Starch: Chemistry and Technology*; Academic Press, 2012; ISBN 978-0-323-13950-2.

173. Belgacem, M.N.; Gandini, A. *Monomers, Polymers and Composites from Renewable Resources*; Elsevier, 2011; ISBN 978-0-08-056051-9.

174. Johnson, K.E.; Pometto, A.L.; Nikolov, Z.L. Degradation of Degradable Starch-Polyethylene Plastics in a Compost Environment. *Appl. Environ. Microbiol.* **1993**, *59*, 1155–1161.

175. Bastioli, C. Starch-polymer composites. In *Degradable Polymers: Principles and applications*; Scott, G., Gilead, D., Eds.; Springer Netherlands: Dordrecht, 1995; pp. 112–137 ISBN 978-94-011-0571-2.

176. Huneault, M.A.; Li, H. Morphology and properties of compatibilized polylactide/thermoplastic starch blends. *Polymer* **2007**, *48*, 270–280.

177. Nie, S.; Song, L.; Guo, Y.; Wu, K.; Xing, W.; Lu, H.; Hu, Y. Intumescent Flame Retardation of Starch Containing Polypropylene Semibiocomposites: Flame Retardancy and Thermal Degradation. *Ind. Eng. Chem. Res.* **2009**, *48*, 10751–10758.

178. Wang, X.; Hu, Y.; Song, L.; Xuan, S.; Xing, W.; Bai, Z.; Lu, H. Flame Retardancy and Thermal Degradation of Intumescent Flame Retardant Poly(lactic acid)/Starch Biocomposites. *Ind. Eng. Chem. Res.* **2011**, *50*, 713–720.

179. Réti, C.; Casetta, M.; Duquesne, S.; Bourbigot, S.; Delobel, R. Flammability properties of intumescent PLA including starch and lignin. *Polym. Adv. Technol.* **2008**, *19*, 628–635.

180. Xia, Y.; Larock, R.C. Vegetable oil-based polymeric materials: synthesis, properties, and applications. *Green Chem.* **2010**, *12*, 1893.

181. Finkenstadt, V.L.; Liu, C.-K.; Evangelista, R.; Liu, L.; Cermak, S.C.; Hojilla-Evangelista, M.; Willett, J.L. Poly(lactic acid) green composites using oilseed coproducts as fillers. *Ind. Crops Prod.* **2007**, *26*, 36–43.

182. Chieng, B.W.; Ibrahim, N.A.; Then, Y.Y.; Loo, Y.Y. Epoxidized Vegetable Oils Plasticized Poly(lactic acid) Biocomposites: Mechanical, Thermal and Morphology Properties. *Molecules* **2014**, *19*, 16024–16038.

183. Karmalm, P.; Hjertberg, T.; Jansson, A.; Dahl, R. Thermal stability of poly(vinyl chloride) with epoxidised soybean oil as primary plasticizer. *Polym. Degrad. Stab.* **2009**, *94*, 2275–2281.

184. Fore, S.P.; Magne, F.C.; Bickford, W.G. Epoxidized jojoba oil as a stabilizer for vinyl chloride containing plastics. *J. Am. Oil Chem. Soc.* **1958**, *35*, 469–472.

185. Miao, S.; Wang, P.; Su, Z.; Zhang, S. Vegetable-oil-based polymers as future polymeric biomaterials. *Acta Biomater.* **2014**, *10*, 1692–1704.

186. Guo, B.; Chen, Y.; Lei, Y.; Zhang, L.; Zhou, W.Y.; Rabie, A.B.M.; Zhao, J. Biobased Poly(propylene sebacate) as Shape Memory Polymer with Tunable Switching

Temperature for Potential Biomedical Applications. *Biomacromolecules* **2011**, *12*, 1312–1321.

187.   Miao, S.; Sun, L.; Wang, P.; Liu, R.; Su, Z.; Zhang, S. Soybean oil-based polyurethane networks as candidate biomaterials: Synthesis and biocompatibility. *Eur. J. Lipid Sci. Technol.* **2012**, *114*, 1165–1174.

188.   Carbonell-Verdu, A.; Garcia-Garcia, D.; Dominici, F.; Torre, L.; Sanchez-Nacher, L.; Balart, R. PLA films with improved flexibility properties by using maleinized cottonseed oil. *Eur. Polym. J.* **2017**, *91*, 248–259.

189.   Ferri, J.M.; Garcia-Garcia, D.; Sánchez-Nacher, L.; Fenollar, O.; Balart, R. The effect of maleinized linseed oil (MLO) on mechanical performance of poly(lactic acid)-thermoplastic starch (PLA-TPS) blends. *Carbohydr. Polym.* **2016**, *147*, 60–68.

190.   Rowell, R.M. *Handbook of Wood Chemistry and Wood Composites*; CRC Press, 2012; ISBN 978-1-4398-5381-8.

191.   *Polysaccharides I: Structure, Characterisation and Use*; Heinze, T., Ed.; Advances in Polymer Science; Springer-Verlag: Berlin Heidelberg, 2005; ISBN 978-3-540-26112-4.

192.   Fang, J.M.; Sun, R.C.; Tomkinson, J.; Fowler, P. Acetylation of wheat straw hemicellulose B in a new non-aqueous swelling system. *Carbohydr. Polym.* **2000**, *41*, 379–387.

193.   SCHOULTZ, S.V. Method for extracting biomass 2014.

194.   Persson, T.; Jönsson, A.-S. Isolation of hemicelluloses by ultrafiltration of thermomechanical pulp mill process water—Influence of operating conditions. *Chem. Eng. Res. Des.* **2010**, *88*, 1548–1554.

195.   Huang, B.; Tang, Y.; Pei, Q.; Zhang, K.; Liu, D.; Zhang, X. Hemicellulose-Based Films Reinforced with Unmodified and Cationically Modified Nanocrystalline Cellulose. *J. Polym. Environ.* **2018**, *26*, 1625–1634.

196.   Dong, F.; Li, S.; Yan, M.; Li, C. Preparation and Properties of Chitosan/Nanocrystalline Cellulose Composite Films for Food Packaging. *Asian J. Chem.* **2014**, *26*, 5895–5898.

197.   Liu, R.; Du, J.; Zhang, Z.; Li, H.; Lu, J.; Cheng, Y.; Lv, Y.; Wang, H. Preparation of polyacrylic acid-grafted-acryloyl/hemicellulose (PAA-g-AH) hybrid films with high oxygen barrier performance. *Carbohydr. Polym.* **2019**, *205*, 83–88.

198.   Lian, Y.; Zhang, J.; Li, N.; Ping, Q. Preparation of Hemicellulose-based Hydrogel and its Application as an Adsorbent Towards Heavy Metal Ions. *BioResources* **2018**, *13*.

199.   Hosseinaei, O.; Wang, S.; Enayati, A.A.; Rials, T.G. Effects of hemicellulose extraction on properties of wood flour and wood-plastic composites. *Compos. Part - Appl. Sci. Manuf.* **2012**, *43*, 686–694.

200.   Marais, A.; Kochumalayil, J.J.; Nilsson, C.; Fogelström, L.; Gamstedt, E.K. Toward an alternative compatibilizer for PLA/cellulose composites: Grafting of xyloglucan with PLA. *Carbohydr. Polym.* **2012**, *89*, 1038–1043.

201.   Xu, W.; Pranovich, A.; Uppstu, P.; Wang, X.; Kronlund, D.; Hemming, J.; Öblom, H.; Moritz, N.; Preis, M.; Sandler, N.; et al. Novel biorenewable composite of wood polysaccharide and polylactic acid for three dimensional printing. *Carbohydr. Polym.* **2018**, *187*, 51–58.

202.   Chirkova, J.; Andersone, I.; Irbe, I.; Spince, B.; Andersons, B. Lignins as agents for bio-protection of wood. *Holzforschung* **2011**, *65*, 497–502.

203.   Zhao, W.; Simmons, B.; Singh, S.; Ragauskas, A.; Cheng, G. From lignin association to nano-/micro-particle preparation: extracting higher value of lignin. *Green Chem.* **2016**, *18*, 5693–5700.

204.   Figueiredo, P.; Lintinen, K.; Hirvonen, J.T.; Kostiainen, M.A.; Santos, H.A. Properties and chemical modifications of lignin: Towards lignin-based nanomaterials for biomedical applications. *Prog. Mater. Sci.* **2018**, *93*, 233–269.

205.   Wang, C.; Kelley, S.; RA, C., Venditti- Lignin-Based Thermoplastic Materials. *ChemSusChem* **2016**.

206.   Nadji, H.; Bruzzèse, C.; Belgacem, M.; Benaboura, A.; Gandini, A. Oxypropylation of Lignins and Preparation of Rigid Polyurethane Foams from the Ensuing Polyols. *Macromol Mater Eng* **2005**, *290*, 1009–1016.

207.   El Mansouri, N.-E.; Yuan, Q.; Huang, F. Synthesis and characterization of kraft lignin-based epoxy resins. *BioResources* **2011**, *6*, 2492–2503.

208.   Yeo, J.-S.; Seong, D.-W.; Hwang, S.-H. Chemical surface modification of lignin particle and its application as filler in the polypropylene composites. *J. Ind. Eng. Chem.* **2015**, *31*, 80–85.

209.   Laurichesse, S.; Avérous, L. Chemical modification of lignins: Towards biobased polymers. *Prog. Polym. Sci.* **2014**, *39*, 1266–1290.

210.   Thunga, M.; Chen, K.; Grewell, D.; Kessler, M.R. Bio-renewable precursor fibers from lignin/polylactide blends for conversion to carbon fibers. *Carbon* **2014**, *68*, 159–166.

211.   Maharana, T.; Pattanaik, S.; Routaray, A.; Nath, N.; Sutar, A.K. Synthesis and characterization of poly(lactic acid) based graft copolymers. *React. Funct. Polym.* **2015**, *93*, 47–67.

212.   Renan Gadioli; Walter Ruggeri Waldman; Marco Aurelio De Paoli Lignin as a green primary antioxidant for polypropylene. *Lignin Green Prim. Antioxid. Polypropyl.* **2016**, *133*.

213.   Blanco, I.; Cicala, G.; Latteri, A.; Saccullo, G.; El-Sabbagh, A.M.M.; Ziegmann, G. Thermal characterization of a series of lignin-based polypropylene blends. *J. Therm. Anal. Calorim.* **2017**, *127*, 147–153.

214. Morandim-Giannetti, A.A.; Agnelli, J.A.M.; Lanças, B.Z.; Magnabosco, R.; Casarin, S.A.; Bettini, S.H.P. Lignin as additive in polypropylene/coir composites: Thermal, mechanical and morphological properties. *Carbohydr. Polym.* **2012**, *87*, 2563–2568.

215. Toriz, G.; Denes, F.; Young, R.A. Lignin-polypropylene composites. Part 1: Composites from unmodified lignin and polypropylene. *Polym. Compos.* **2002**, *23*, 806–813.

216. Toriz, G.; Ramos, J.; Young, R.A. Lignin–polypropylene composites. II. Plasma modification of kraft lignin and particulate polypropylene. *J. Appl. Polym. Sci.* **2004**, *91*, 1920–1926.

217. Domenek, S.; Louaifi, A.; Guinault, A.; Baumberger, S. Potential of Lignins as Antioxidant Additive in Active Biodegradable Packaging Materials. *J. Polym. Environ.* **2013**, *21*, 692–701.

218. Formela, K.; Zedler, Ł.; Hejna, A.; Letters, T.A. Reactive extrusion of bio-based polymer blends and composites-Current trends and future developments. *Express Polym. Lett.* **2018**, *12*.

219. Luo, S.; Cao, J.; McDonald, A.G. Interfacial Improvements in a Green Biopolymer Alloy of Poly(3-hydroxybutyrate-co-3-hydroxyvalerate) and Lignin via in Situ Reactive Extrusion. *ACS Sustain. Chem. Eng.* **2016**, *4*, 3465–3476.

220. Chung, C.I. *Extrusion of polymers: theory and practice*; 2. ed.; Hanser: Munich, 2010; ISBN 978-1-56990-459-6.

221. An Introduction to Single Screw Extrusion Available online: https://www.azom.com/article.aspx?ArticleID=13566 (accessed on Mar 30, 2019).

222. da Silva, A.S.; Teixeira, R.S.S.; Endo, T.; Bon, E.P.S.; Lee, S.-H. Continuous pretreatment of sugarcane bagasse at high loading in an ionic liquid using a twin-screw extruder. *Green Chem.* **2013**, *15*, 1991.

223. Yang, H.-S.; Wolcott, M.P.; Kim, H.-S.; Kim, S.; Kim, H.-J. Properties of lignocellulosic material filled polypropylene bio-composites made with different manufacturing processes. *Polym. Test.* **2006**, *25*, 668–676.

224. Gallos, A.; Paës, G.; Allais, F.; Beaugrand, J. Lignocellulosic fibers: a critical review of the extrusion process for enhancement of the properties of natural fiber composites. *RSC Adv.* **2017**, *7*, 34638–34654.

225. Berzin, F.; Vergnes, B.; Beaugrand, J. Evolution of lignocellulosic fibre lengths along the screw profile during twin screw compounding with polycaprolactone. *Compos. Part Appl. Sci. Manuf.* **2014**, *59*, 30–36.

226. Mano, B.; Araújo, J.R.; Spinacé, M.A.S.; De Paoli, M.-A. Polyolefin composites with curaua fibres: Effect of the processing conditions on mechanical properties, morphology and fibres dimensions. *Compos. Sci. Technol.* **2010**, *70*, 29–35.

227.	Alvarez, V.; Iannoni, A.; Kenny, J.M.; Vazquez, A. Influence of Twin-Screw Processing Conditions on the Mechanical Properties of Biocomposites. *J. Compos. Mater.* **2005**, *39*, 2023–2038.

228.	Feldmann, M.; Heim, H.-P.; Zarges, J.-C. Influence of the process parameters on the mechanical properties of engineering biocomposites using a twin-screw extruder. *Compos. Part Appl. Sci. Manuf.* **2016**, *83*, 113–119.

229.	González-López, M.E.; Robledo-Ortíz, J.R.; Manríquez-González, R.; Silva-Guzmán, J.A.; Pérez-Fonseca, A.A. Polylactic acid functionalization with maleic anhydride and its use as coupling agent in natural fiber biocomposites: a review. *Compos. Interfaces* **2018**, *25*, 515–538.

230.	Nanthananon, P.; Seadan, M.; Pivsa-Art, S.; Hamada, H.; Suttiruengwong, S. Reactive Compatibilization of Short-Fiber Reinforced Poly(lactic acid) Biocomposites. *J. Renew. Mater.* **2018**, *6*, 573–583.

231.	Kang, H.; Hu, X.; Li, M.; Zhang, L.; Wu, Y.; Ning, N.; Tian, M. Novel biobased thermoplastic elastomer consisting of synthetic polyester elastomer and polylactide by in situ dynamical crosslinking method. *RSC Adv.* **2015**, *5*, 23498–23507.

232.	Cui, L.; Wang, S.; Zhang, Y.; Zhang, Y. Dynamically cured polypropylene/Novolac blends compatibilized with maleic anhydride-g-polypropylene. *J Appl Polym Sci* **2007**, *104*, 3337–3346.

233.	Jiang, X.; Zhang, Y.; Zhang, Y. Crystallization behavior of dynamically cured polypropylene/epoxy blends. *J. Polym. Sci. Part B Polym. Phys.* **2004**, *42*, 1181–1191.

234.	Coogan, T.J.; Kazmer, D.O. In-line rheological monitoring of fused deposition modeling. *J. Rheol.* **2018**, *63*, 141–155.

235.	Tappa, K.; Jammalamadaka, U. Novel Biomaterials Used in Medical 3D Printing Techniques. *J. Funct. Biomater.* **2018**, *9*.

236.	Bakrani Balani, S.; Chabert, F.; Nassiet, V.; Cantarel, A. Influence of printing parameters on the stability of deposited beads in fused filament fabrication of poly(lactic) acid. *Addit. Manuf.* **2019**, *25*, 112–121.

237.	Lee, J.-Y.; An, J.; Chua, C.K. Fundamentals and applications of 3D printing for novel materials. *Appl. Mater. Today* **2017**, *7*, 120–133.

238.	Chacón, J.M.; Caminero, M.A.; García-Plaza, E.; Núñez, P.J. Additive manufacturing of PLA structures using fused deposition modelling: Effect of process parameters on mechanical properties and their optimal selection. *Mater. Des.* **2017**, *124*, 143–157.

239.	Afrose, M.F.; Masood, S.H.; Iovenitti, P.; Nikzad, M.; Sbarski, I. Effects of part build orientations on fatigue behaviour of FDM-processed PLA material. *Prog. Addit. Manuf.* **2016**, *1*, 21–28.

240.	Fatimatuzahraa, A.W.; Farahaina, B.; Yusoff, W.A.Y. The effect of employing different raster orientations on the mechanical properties and microstructure of Fused

Deposition Modeling parts. In Proceedings of the 2011 IEEE Symposium on Business, Engineering and Industrial Applications (ISBEIA); IEEE: Langkawi, Malaysia, 2011; pp. 22–27.

241. de Ciurana, J.; Serenóa, L.; Vallès, È. Selecting Process Parameters in RepRap Additive Manufacturing System for PLA Scaffolds Manufacture. *Procedia CIRP* **2013**, *5*, 152–157.

242. Bellehumeur, C.; Li, L.; Sun, Q.; Gu, P. Modeling of Bond Formation Between Polymer Filaments in the Fused Deposition Modeling Process. *J. Manuf. Process.* **2004**, *6*, 170–178.

243. Bakrani Balani, S.; Chabert, F.; Nassiet, V.; Cantarel, A. Influence of printing parameters on the stability of deposited beads in fused filament fabrication of poly(lactic) acid. *Addit. Manuf.* **2019**, *25*, 112–121.

244. Nguyen, N.A.; Barnes, S.H.; Bowland, C.C.; Meek, K.M.; Littrell, K.C.; Keum, J.K.; Naskar, A.K. A path for lignin valorization via additive manufacturing of high-performance sustainable composites with enhanced 3D printability. *Sci. Adv.* **2018**, *4*, eaat4967.

245. Guo, R.; Ren, Z.; Bi, H.; Song, Y.; Xu, M. Effect of toughening agents on the properties of poplar wood flour/poly (lactic acid) composites fabricated with Fused Deposition Modeling. *Eur. Polym. J.* **2018**, *107*, 34–45.

246. Long, H.; Wu, Z.; Dong, Q.; Shen, Y.; Zhou, W.; Luo, Y.; Zhang, C.; Dong, X. Mechanical and thermal properties of bamboo fiber reinforced polypropylene/polylactic acid composites for 3D printing. *Polym. Eng. Sci.* **2019**, *59*, E247–E260.

247. Li, T.; Aspler, J.; Kingsland, A.; Cormier, L.M.; Zou, X. 3D PRINTING – A REVIEW OF TECHNOLOGIES, MARKETS, AND OPPORTUNITIES FOR THE FOREST INDUSTRY. *J Sci Technol Prod Process 5*, 30.

248. Liu, H.; He, H.; Peng, X.; Huang, B.; Li, J. Three-dimensional printing of poly(lactic acid) bio-based composites with sugarcane bagasse fiber: Effect of printing orientation on tensile performance. *Polym. Adv. Technol.* **2019**, *30*, 910–922.

249. Dong, J.; Li, M.; Zhou, L.; Lee, S.; Mei, C.; Xu, X.; Wu, Q. The influence of grafted cellulose nanofibers and postextrusion annealing treatment on selected properties of poly(lactic acid) filaments for 3D printing. *J. Polym. Sci. Part B Polym. Phys.* **2017**, *55*, 847–855.

250. Murphy, C.A.; Collins, M.N. Microcrystalline cellulose reinforced polylactic acid biocomposite filaments for 3D printing. *Polym. Compos.* **2018**, *39*, 1311–1320.

251. Winter, A.; Mundigler, N.; Holzweber, J.; Veigel, S.; Müller, U.; Kovalcik, A.; Gindl-Altmutter, W. Residual wood polymers facilitate compounding of microfibrillated cellulose with poly(lactic acid) for 3D printer filaments. *Philos. Trans. R. Soc. Math. Phys. Eng. Sci.* **2018**, *376*, 20170046.

252. Filgueira, D.; Holmen, S.; Melbø, J.K.; Moldes, D.; Echtermeyer, A.T.; Chinga-Carrasco, G. Enzymatic-Assisted Modification of Thermomechanical Pulp Fibers To Improve the Interfacial Adhesion with Poly(lactic acid) for 3D Printing. *ACS Sustain. Chem. Eng.* **2017**, *5*, 9338–9346.

253. Wang, Q.; Sun, J.; Yao, Q.; Ji, C.; Liu, J.; Zhu, Q. 3D printing with cellulose materials. *Cellulose* **2018**, *25*, 4275–4301.

254. Gkartzou, E.; Koumoulos, E.P.; Charitidis, C.A. Production and 3D printing processing of bio-based thermoplastic filament. *Manuf. Rev.* **2017**, *4*, 1.

255. Hisham, M.H. Polypropylene as a promising plastic: A review. *Am. J. Polym. Sci.* **2016**, *6*, 1–11.

256. Yang, J.; Lu, S.; Luo, Q.; Song, L.; Li, Y.; Yu, J. Enhanced mechanical and thermal properties of polypropylene/cellulose fibers composites with modified tannic as a compatibilizer. *Polym. Compos.* **2018**, *39*, 2036–2045.

257. Jang, S.Y.; Kim, D.S. Preparation and Physical Properties of Polypropylene/Cellulose Composites. *Polym. Korea* **2015**, *39*, 130–135.

258. de la Orden, M.U.; González Sánchez, C.; González Quesada, M.; Martínez Urreaga, J. Novel polypropylene–cellulose composites using polyethylenimine as coupling agent. *Compos. Part Appl. Sci. Manuf.* **2007**, *38*, 2005–2012.

259. Qiu, W.; Zhang, F.; Endo, T.; Hirotsu, T. Effect of maleated polypropylene on the performance of polypropylene/cellulose composite. *Polym. Compos.* **2005**, *26*, 448–453.

260. Beg, M.D.H.; Pickering, K.L. Accelerated weathering of unbleached and bleached Kraft wood fibre reinforced polypropylene composites. *Polym. Degrad. Stab.* **2008**, *93*, 1939–1946.

261. Stark, N.M.; Matuana, L.M. Surface chemistry and mechanical property changes of wood-flour/high-density-polyethylene composites after accelerated weathering. *J. Appl. Polym. Sci.* **2004**, *94*, 2263–2273.

262. Stewart, D. Lignin as a base material for materials applications: Chemistry, application and economics. *Ind Crop Prod* **2008**, *27*, 202–207.

263. Alexy, P.; Košíková, B.; Podstránska, G. The effect of blending lignin with polyethylene and polypropylene on physical properties. *Polymer* **2000**, *41*, 4901–4908.

264. Pouteau, C.; Dole, P.; Cathala, B.; Averous, L.; Boquillon, N. Antioxidant properties of lignin in polypropylene. *Polym. Degrad. Stab.* **2003**, *81*, 9–18.

265. Gregorová, A.; Cibulková, Z.; Košíková, B.; Šimon, P. Stabilization effect of lignin in polypropylene and recycled polypropylene. *Polym Degrad Stabil* **2005**, *89*, 553–558.

266. Pizzi, A. Tannin-based adhesives, in Wood Adhesives: Chemistry and Technology,. *Tann.-Based Adhes. Wood Adhes. Chem. Technol.* **1983**.

267.   Gaugler, M.; Grigsby, W.; Harper, D.; Rials, T. Chemical imaging of the spatial distribution and interactions of tannin dispersal in bioplastic systems. **2007**, *29*.

268.   Kim, S.-J.; Moon, J.-B.; Kim, G.-H.; Ha, C.-S. Mechanical properties of polypropylene/natural fiber composites: Comparison of wood fiber and cotton fiber. *Polym. Test.* **2008**, *27*, 801–806.

269.   Chen, F.; Dai, H.; Dong, X.; Yang, J.; Zhong, M. Physical properties of lignin-based polypropylene blends. *Polym Compos.* **2011**, *32*, 1019–1025.

270.   Chiang, W.-Y.; Wu, W.-C.; Pukánszky, B. Modification of polypropylene, blending with resole type phenol-formaldehyde resins. *Eur. Polym. J.* **1994**, *30*, 573–580.

271.   Wu, C.L.; Zhang, M.Q.; Rong, M.Z.; Friedrich, K. Tensile performance improvement of low nanoparticles filled-polypropylene composites. *Compos. Sci. Technol.* **2002**, *62*, 1327–1340.

272.   Wacker, G.; Bledzki, A.K.; Chate, A. Effect of interphase on the transverse Young's modulus of glass/epoxy composites. *Compos. Part Appl. Sci. Manuf.* **1998**, *29*, 619–626.

273.   Bozsódi, B.; Romhányi, V.; Pataki, P.; Kun, D.; Renner, K.; Pukánszky, B. Modification of interactions in polypropylene/lignosulfonate blends. *Mater Des.* **2016**, *103*, 32–39.

274.   Tajvidi, M.; Falk, R.H.; Hermanson, J.C. Effect of natural fibers on thermal and mechanical properties of natural fiber polypropylene composites studied by dynamic mechanical analysis. *J. Appl. Polym. Sci.* **2006**, *101*, 4341–4349.

275.   Nayak, S.K.; Mohanty, S.; Samal, S.K. Influence of short bamboo/glass fiber on the thermal, dynamic mechanical and rheological properties of polypropylene hybrid composites. *Mater. Sci. Eng. A* **2009**, *523*, 32–38.

276.   Zoukrami, F.; Haddaoui, N.; Sclavons, M.; Devaux, J.; Vanzeveren, C. Rheological properties and thermal stability of compatibilized polypropylene/untreated silica composites prepared by water injection extrusion process. *Polym Bull* **2018**, *75*, 5551–5566.

277.   Lin, X.; Zhang, K.; Li, K.; Ren, D. Dependence of rheological behaviors of polymeric composites on the morphological structure of carbonaceous nanoparticles. *J. Appl. Polym. Sci.* **2018**, *135*, 46416.

278.   Azizi, H.; Ghasemi, I. Investigation on the dynamic melt rheological properties of polypropylene/wood flour composites. *Polym. Compos.* **2009**, *30*, 429–435.

279.   Peng, Y.; Liu, R.; Cao, J. Characterization of surface chemistry and crystallization behavior of polypropylene composites reinforced with wood flour, cellulose, and lignin during accelerated weathering. *Appl. Surf. Sci.* **2015**, *332*, 253–259.

280. Liang, J.-Z.; Du, Q.; Tsui, G.; Tang, C.-Y. Tensile properties of graphene nano-platelets reinforced polypropylene composites. *Compos Part B Eng* **2016**, *95*, 166–171.

281. Badji, C.; Soccalingame, L.; Garay, H.; Bergeret, A.; Bénézet, J.-C. Influence of weathering on visual and surface aspect of wood plastic composites: Correlation approach with mechanical properties and microstructure. *Polym Degrad Stabil* **2017**, *137*, 162–172.

282. Fabiyi, J.S.; McDonald, A.G.; Wolcott, M.P.; Griffiths, P.R. Wood plastic composites weathering: Visual appearance and chemical changes. *Polym. Degrad. Stab.* **2008**, *93*, 1405–1414.

283. Matuana, L.M.; Jin, S.; Stark, N.M. Ultraviolet weathering of HDPE/wood-flour composites coextruded with a clear HDPE cap layer. *Polym. Degrad. Stab.* **2011**, *96*, 97–106.

284. Pizzi, A.; Tekely, P. Mechanism of polyphenolic tannin resin hardening by hexamethylenetetramine: CP–MAS 13C-NMR. *J. Appl. Polym. Sci.* **1995**, *56*, 1645–1650.

285. Noferi, M.; Masson, E.; Merlin, A.; Pizzi, A.; Deglise, X. Antioxidant characteristics of hydrolysable and polyflavonoid tannins: An ESR kinetics study. *J. Appl. Polym. Sci.* **1997**, *63*, 475–482.

286. Theis, M.; Grohe, B. Biodegradable lightweight construction boards based on tannin/hexamine bonded hemp shaves. *Holz Als Roh- Werkst.* **2002**, *60*, 291–296.

287. Hussein, I.A. Rheological investigation of the influence of molecular structure on natural and accelerated UV degradation of linear low density polyethylene. *Polym. Degrad. Stab.* **2007**, *92*, 2026–2032.

288. Sonnier, R.; Taguet, A.; Ferry, L.; Lopez-Cuesta, J.-M. *Towards Bio-based Flame Retardant Polymers*; Biobased Polymers; Springer International Publishing, 2018; ISBN 978-3-319-67082-9.

289. Cinelli, P.; Anguillesi, I.; Lazzeri, A. Green synthesis of flexible polyurethane foams from liquefied lignin. *Eur. Polym. J.* **2013**, *49*, 1174–1184.

290. Asada, C.; Basnet, S.; Otsuka, M.; Sasaki, C.; Nakamura, Y. Epoxy resin synthesis using low molecular weight lignin separated from various lignocellulosic materials. *Int. J. Biol. Macromol.* **2015**, *74*, 413–419.

291. Sakai, H.; Kuroda, K.; Tsukegi, T.; Ogoshi, T.; Ninomiya, K.; Takahashi, K. Butylated lignin as a compatibilizing agent for polypropylene-based carbon fiber-reinforced plastics. *Polym. J.* **2018**, *50*, 997–1002.

292. Kabir, A.; Yuan, Z.; Kuboki, T.; Xu, C. De-polymerization of industrial lignins to improve the thermo-oxidative stability of polyolefins. *Ind Crop Prod* **2018**, *120*, 238–249.

293.   Becker, D.; Roeder, J.; Oliveira, R.V.B.; Soldi, V.; Pires, A.T.N. Blend of thermosetting polyurethane waste with polypropylene: influence of compatibilizing agent on interface domains and mechanical properties. *Polym Test* **2003**, *22*, 225–230.

294.   Bridson, J.; Kaur, J.; Zhang, Z.; Donaldson, L.; Fernyhough, A. Polymeric flavonoids processed with co-polymers as UV and thermal stabilisers for polyethylene films. *Polym Degrad Stabil* **2015**, *122*, 18–24.

295.   Shnawa, H.; Khaleel, M.; Muhamed, F. Oxidation of HDPE in the Presence of PVC Grafted with Natural Polyphenols (Tannins) as Antioxidant. *J. Polym. Chem.* **2015**, *05*, 9–16.

296.   Grigsby, W.J.; Bridson, J.H.; Lomas, C.; Elliot, J.-A. Esterification of Condensed Tannins and Their Impact on the Properties of Poly(Lactic Acid). *Polymers* **2013**, *5*, 344–360.

297.   Bridson, J.H.; Grigsby, W.J.; Main, L. One-pot solvent-free synthesis and characterisation of hydroxypropylated polyflavonoid compounds. *Ind Crop Prod* **2018**, *111*, 529–535.

298.   Shnawa, H.A.; Jahani, Y.; Khalaf, M.N. Rheological properties of PVC stabilized with tannin based epoxy resin as non metallic thermal stabilizer. *Polym. Bull.* **2017**, *74*, 1077–1090.

299.   George, S.; Ramamurthy, K.; Anand, J.S.; Groeninckx, G.; Varughese, K.T.; Thomas, S. Rheological behaviour of thermoplastic elastomers from polypropylene/acrylonitrile–butadiene rubber blends: effect of blend ratio, reactive compatibilization and dynamic vulcanization. *Polymer* **1999**, *40*, 4325–4344.

300.   Nakason, C.; Worlee, A.; Salaeh, S. Effect of vulcanization systems on properties and recyclability of dynamically cured epoxidized natural rubber/polypropylene blends. *Polym. Test.* **2008**, *27*, 858–869.

301.   Børve, K.; Kotlar, H. Preparation of high viscosity thermoplastic phenol formaldehyde polymers for application in reactive extrusion. **1998**.

302.   Fu, S.-Y.; Feng, X.-Q.; Lauke, B.; Mai, Y.-W. Effects of particle size, particle/matrix interface adhesion and particle loading on mechanical properties of particulate–polymer composites. *Compos. Part B Eng.* **2008**, *39*, 933–961.

303.   Srivabut, C.; Ratanawilai, T.; Hiziroglu, S. Effect of nanoclay, talcum, and calcium carbonate as filler on properties of composites manufactured from recycled polypropylene and rubberwood fiber. *Constr Build Mater* **2018**, *162*, 450–458.

304.   Canetti, M.; Bertini, F.; Chirico, A.; Audisio, G. Thermal degradation behaviour of isotactic polypropylene blended with lignin. *Polym Degrad Stabil* **2006**, *91*, 494–498.

305.   Tolbert, A.; Akinosho, H.; Khunsupat, R.; Naskar, A.K.; Ragauskas, A.J. Characterization and analysis of the molecular weight of lignin for biorefining studies. *Biofuels Bioprod. Biorefining* **2014**, *8*, 836–856.

306.   Pasch, H.; Pizzi, A.; Rode, K. MALDI–TOF mass spectrometry of polyflavonoid tannins. *Polymer* **2001**, *42*, 7531–7539.

307.   Kardel, M.; Taube, F.; Schulz, H.; Schuetze, W.; Gierus, M. Different approaches to evaluate tannin content and structure of selected plant extracts-review and new aspects. *J. Appl. Bot. Food Qual.* **2013**, *86*, 154–66.

308.   Brebu, M.; Vasile, C. Thermal degradation of lignin-a review. *Cellul. Chem. Technol.* **2010**, *44*, 353–363.

309.   Jahani, Y. Comparison of the effect of mica and talc and chemical coupling on the rheology, morphology, and mechanical properties of polypropylene composites. *Polym Advan Technol* **2011**, *22*, 942–950.

310.   Bailly, M.; Kontopoulou, M. Preparation and characterization of thermoplastic olefin/nanosilica composites using a silane-grafted polypropylene matrix. *Polymer* **2009**, *50*, 2472–2480.

311.   Hornsby, P.; Mthupha, A. Rheological characterization of polypropylene filled with magnesium hydroxide. *J Mater Sci* **1994**, *29*, 5293–5301.

312.   Lv, Y.; Huang, Y.; Yang, J.; Kong, M.; Yang, H.; Zhao, J.; Li, G. Outdoor and accelerated laboratory weathering of polypropylene: A comparison and correlation study. *Polym Degrad Stabil* **2015**, *112*, 145–159.

313.   Soccalingame, L.; Perrin, D.; Bénézet, J.-C.; Mani, S.; Coiffier, F.; Richaud, E.; Bergeret, A. Reprocessing of artificial UV-weathered wood flour reinforced polypropylene composites. *Polym. Degrad. Stab.* **2015**, *120*, 313–327.

314.   Zaaba, N.; Ismail, H.; Jaafar, M. A study of the degradation of compatibilized and uncompatibilized peanut shell powder/recycled polypropylene composites due to natural weathering. *J Vinyl Addit Technol.* **2017**, *23*, 290–297.

315.   Liu, J.; Sun, L.; Xu, W.; Wang, Q.; Yu, S.; Sun, J. Current advances and future perspectives of 3D printing natural-derived biopolymers. *Carbohydr. Polym.* **2019**, *207*, 297–316.

316.   Boparai, K.S.; Singh, R. Advances in Fused Deposition Modeling. In *Reference Module in Materials Science and Materials Engineering*; Elsevier, 2017; p. B9780128035818041000 ISBN 978-0-12-803581-8.

317.   Vila, C.; Santos, V.; Saake, B.; Parajó, J.C. Manufacture, Characterization, and Properties of Poly-(lactic acid) and its Blends with Esterified Pine Lignin. *BioResources* **2016**, *11*, 5322–5332.

318.   Smith, B.C. The C=O Bond, Part IV: Acid Anhydrides Available online: http://www.spectroscopyonline.com/co-bond-part-iv-acid-anhydrides (accessed on Apr 16, 2019).

319.   Spiridon, I.; Leluk, K.; Resmerita, A.M.; Darie, R.N. Evaluation of PLA–lignin bioplastics properties before and after accelerated weathering. *Compos. Part B Eng.* **2015**, *69*, 342–349.

320. Zhang, L.; Lv, S.; Sun, C.; Wan, L.; Tan, H.; Zhang, Y. Effect of MAH-g-PLA on the Properties of Wood Fiber/Polylactic Acid Composites. *Polymers* **2017**, *9*, 591.

321. Müller, A.J.; Ávila, M.; Saenz, G.; Salazar, J. CHAPTER 3. Crystallization of PLA-based Materials. In *Polymer Chemistry Series*; Jiménez, A., Peltzer, M., Ruseckaite, R., Eds.; Royal Society of Chemistry: Cambridge, 2014; pp. 66–98 ISBN 978-1-84973-879-8.

322. Lyu, S.; Untereker, D. Degradability of Polymers for Implantable Biomedical Devices. *Int. J. Mol. Sci.* **2009**, *10*, 4033–4065.

323. Tokiwa, Y.; Calabia, B.P. Biodegradability and biodegradation of poly(lactide). *Appl. Microbiol. Biotechnol.* **2006**, *72*, 244–251.

324. Karamanlioglu, M.; Preziosi, R.; Robson, G.D. Abiotic and biotic environmental degradation of the bioplastic polymer poly(lactic acid): A review. *Polym. Degrad. Stab.* **2017**, *137*, 122–130.

325. Boruvka, M.; Behalek, L.; Lenfeld, P.; Ngaowthong, C.; Pechociakova, M. Structure-related properties of bionanocomposites based on poly(lactic acid), cellulose nanocrystals and organic impact modifier. *Mater. Technol.* **2019**, *34*, 143–156.

326. Yew, G.H.; Mohd Yusof, A.M.; Mohd Ishak, Z.A.; Ishiaku, U.S. Water absorption and enzymatic degradation of poly(lactic acid)/rice starch composites. *Polym. Degrad. Stab.* **2005**, *90*, 488–500.

327. Elsawy, M.A.; Kim, K.-H.; Park, J.-W.; Deep, A. Hydrolytic degradation of polylactic acid (PLA) and its composites. *Renew. Sustain. Energy Rev.* **2017**, *79*, 1346–1352.

328. Scheyer, L.E.; Chiweshe, A. Application and Performance of Disperse Dyes on Polylactic Acid (PLA) Fabric. *AATCC Rev.* **2001**, 5.

329. La Mantia, F.P.; Morreale, M. Green composites: A brief review. *Compos. Part Appl. Sci. Manuf.* **2011**, *42*, 579–588.

330. Lim, L.-T.; Auras, R.; Rubino, M. Processing technologies for poly(lactic acid). *Prog. Polym. Sci.* **2008**, *33*, 820–852.

331. Huda, M.S.; Drzal, L.T.; Mohanty, A.K.; Misra, M. Chopped glass and recycled newspaper as reinforcement fibers in injection molded poly(lactic acid) (PLA) composites: A comparative study. *Compos. Sci. Technol.* **2006**, *66*, 1813–1824.

332. Jha, K.; Kataria, R.; Verma, J.; Pradhan, S. Potential biodegradable matrices and fiber treatment for green composites: A review. *Mater. 2019 Vol 6 Pages 119-138* **2019**.

333. Murariu, M.; Dubois, P. PLA composites: From production to properties. *Adv. Drug Deliv. Rev.* **2016**, *107*, 17–46.

334. Wang, H.; Sun, X.; Seib, P. Mechanical properties of poly(lactic acid) and wheat starch blends with methylenediphenyl diisocyanate. *J. Appl. Polym. Sci.* **2002**, *84*, 1257–1262.

335.   Yu, L.; Petinakis, E.; Dean, K.; Liu, H.; Yuan, Q. Enhancing compatibilizer function by controlled distribution in hydrophobic polylactic acid/hydrophilic starch blends. *J. Appl. Polym. Sci.* **2011**, *119*, 2189–2195.

336.   Krishnan, S.; Smita, M.; Sanjay, K.N. Renewable Resource based blends of Polylactic acid (PLA) and Thermoplastic starch (TPS) using Novel Reactive Compatibilization - ProQuest. *J. Polym. Mater.* **2017**, *34*, 525–538.

337.   Baek, B.-S.; Park, J.-W.; Lee, B.-H.; Kim, H.-J. Development and Application of Green Composites: Using Coffee Ground and Bamboo Flour. *J. Polym. Environ.* **2013**, *21*, 702–709.

338.   Sahoo, S.; Misra, M.; Mohanty, A.K. Enhanced properties of lignin-based biodegradable polymer composites using injection moulding process. *Compos. Part Appl. Sci. Manuf.* **2011**, *42*, 1710–1718.

339.   Braghiroli, F.; Fierro, V.; Pizzi, A.; Rode, K.; Radke, W.; Delmotte, L.; Parmentier, J.; Celzard, A. Reaction of condensed tannins with ammonia. *Ind. Crops Prod.* **2013**, *44*, 330–335.

340.   Kida, K.; Suzuki, M.; Takagaki, A.; Nanjo, F. Deodorizing Effects of Tea Catechins on Amines and Ammonia. *Biosci. Biotechnol. Biochem.* **2002**, *66*, 373–377.

341.   Hashida, K.; Makino, R.; Ohara, S. Amination of pyrogallol nucleus of condensed tannins and related polyphenols by ammonia water treatment. *Holzforschung* **2008**, *63*, 319–326.

342.   Zhu, J.; Zhu, H.; Immonen, K.; Brighton, J.; Abhyankar, H. Improving mechanical properties of novel flax/tannin composites through different chemical treatments. *Ind. Crops Prod.* **2015**, *67*, 346–354.

343.   Lu, Y.; Cueva, M.C.; Lara-Curzio, E.; Ozcan, S. Improved mechanical properties of polylactide nanocomposites-reinforced with cellulose nanofibrils through interfacial engineering via amine-functionalization. *Carbohydr. Polym.* **2015**, *131*, 208–217.

344.   Georgiopoulos, P.; Kontou, E.; Georgousis, G. Effect of silane treatment loading on the flexural properties of PLA/flax unidirectional composites. *Compos. Commun.* **2018**, *10*, 6–10.

345.   Rahmat, M.; Karrabi, M.; Ghasemi, I.; Zandi, M.; Azizi, H. Silane crosslinking of electrospun poly (lactic acid)/nanocrystalline cellulose bionanocomposite. *Mater. Sci. Eng. C* **2016**, *68*, 397–405.

346.   Chun, K.S.; Husseinsyah, S.; Osman, H. Mechanical and thermal properties of coconut shell powder filled polylactic acid biocomposites: effects of the filler content and silane coupling agent. *J. Polym. Res.* **2012**, *19*, 9859.

347.   Meng, X.; Nguyen, N.A.; Tekinalp, H.; Lara-Curzio, E.; Ozcan, S. Supertough PLA-Silane Nanohybrids by in Situ Condensation and Grafting. *ACS Sustain. Chem. Eng.* **2018**, *6*, 1289–1298.

348.   Yamoum, C.; Maia, J.; Magaraphan, R. Rheological and thermal behavior of PLA modified by chemical crosslinking in the presence of ethoxylated bisphenol A dimethacrylates. **2017**, *28*, 102–112.

349.   Borda, J.; Bodnár, I.; Kéki, S.; Sipos, L.; Zsuga, M. Optimum conditions for the synthesis of linear polylactic acid-based urethanes. *J. Polym. Sci. Part Polym. Chem.* **2000**, *38*, 2925–2933.

350.   Droste, D.H.; Dibenedetto, A.T. The glass transition temperature of filled polymers and its effect on their physical properties. *J. Appl. Polym. Sci.* **1969**, *13*, 2149–2168.

351.   Zuo, Y. feng; Gu, J.; Qiao, Z.; Tan, H.; Cao, J.; Zhang, Y. Effects of dry method esterification of starch on the degradation characteristics of starch/polylactic acid composites. *Int. J. Biol. Macromol.* **2015**, *72*, 391–402.

352.   Frone, A.N.; Berlioz, S.; Chailan, J.-F.; Panaitescu, D.M. Morphology and thermal properties of PLA–cellulose nanofibers composites. *Carbohydr. Polym.* **2013**, *91*, 377–384.

353.   Wang, H.; Sun, X.; Seib, P. Strengthening blends of poly(lactic acid) and starch with methylenediphenyl diisocyanate. *J. Appl. Polym. Sci.* **2001**, *82*, 1761–1767.

354.   Ke, T.; Sun, X. Physical Properties of Poly(Lactic Acid) and Starch Composites with Various Blending Ratios. *Cereal Chem.* **2000**, *77*, 761–768.

355.   Lee, S.-Y.; Kang, I.-A.; Doh, G.-H.; Yoon, H.-G.; Park, B.-D.; Wu, Q. Thermal and Mechanical Properties of Wood Flour/Talc-filled Polylactic Acid Composites: Effect of Filler Content and Coupling Treatment. *J. Thermoplast. Compos. Mater.* **2008**, *21*, 209–223.

356.   Brosse, N.; Pizzi, A. Tannins for wood adhesives, foams and composites. In *Bio-based Wood Adhesives Preparation, characterization, and Testing*; CRC Press, 2017; pp. 197–220.

357.   Garcia, D.E.; Carrasco, J.C.; Salazar, J.P.; Perez, M.A.; Cancino, R.A.; Riquelme, S. Bark polyflavonoids from Pinus radiata as functional building-blocks for polylactic acid (PLA)-based green composites. *Express Polym. Lett.* **2016**, *10*, 835–848.

358.   Wang, Y.; Weng, Y.; Wang, L. Characterization of interfacial compatibility of polylactic acid and bamboo flour (PLA/BF) in biocomposites. *Polym. Test.* **2014**, *36*, 119–125.

359.   Semba, T.; Kitagawa, K.; Ishiaku, U.S.; Hamada, H. The effect of crosslinking on the mechanical properties of polylactic acid/polycaprolactone blends. *J. Appl. Polym. Sci.* **2006**, *101*, 1816–1825.

360.   Wei, L.; McDonald, A.G. Peroxide induced cross-linking by reactive melt processing of two biopolyesters: Poly(3-hydroxybutyrate) and poly(l-lactic acid) to improve their melting processability. *J. Appl. Polym. Sci.* **2015**, *132*.

361. Ma, P.; Cai, X.; Zhang, Y.; Wang, S.; Dong, W.; Chen, M.; Lemstra, P.J. In-situ compatibilization of poly(lactic acid) and poly(butylene adipate-co-terephthalate) blends by using dicumyl peroxide as a free-radical initiator. *Polym Degrad Stabil* **2014**, *102*, 145–151.

362. Takamura, M.; Nakamura, T.; Takahashi, T.; Koyama, K. Effect of type of peroxide on cross-linking of poly(l-lactide). *Polym. Degrad. Stab.* **2008**, *93*, 1909–1916.

363. Choi, K.; Choi, M.-C.; Han, D.-H.; Park, T.-S.; Ha, C.-S. Plasticization of poly(lactic acid) (PLA) through chemical grafting of poly(ethylene glycol) (PEG) via in situ reactive blending. *Eur Polym J* **2013**, *49*, 2356–2364.

364. Quero, F.; Eichhorn, S.J.; Nogi, M.; Yano, H.; Lee, K.-Y.; Bismarck, A. Interfaces in Cross-Linked and Grafted Bacterial Cellulose/Poly(Lactic Acid) Resin Composites. *J. Polym. Environ.* **2012**, *20*, 916–925.

365. Dorgan, J.R.; Williams, J.S.; Lewis, D.N. Melt rheology of poly(lactic acid): Entanglement and chain architecture effects. *J. Rheol.* **1999**, *43*, 1141–1155.

366. Du, J.; Wang, Y.; Xie, X.; Xu, M.; Song, Y. Styrene-Assisted Maleic Anhydride Grafted Poly(lactic acid) as an Effective Compatibilizer for Wood Flour/Poly(lactic acid) Bio-Composites. *Polymers* **2017**, *9*, 623.

367. Kaczmarek, H.; Nowicki, M.; Vuković-Kwiatkowska, I.; Nowakowska, S. Crosslinked blends of poly(lactic acid) and polyacrylates: AFM, DSC and XRD studies. *J. Polym. Res.* **2013**, *20*, 91.

368. Żenkiewicz, M.; Malinowski, R.; Rytlewski, P.; Richert, A.; Sikorska, W.; Krasowska, K. Some composting and biodegradation effects of physically or chemically crosslinked poly(lactic acid). *Polym. Test.* **2012**, *31*, 83–92.

369. Dong, W.; Ma, P.; Wang, S.; Chen, M.; Cai, X.; Zhang, Y. Effect of partial crosslinking on morphology and properties of the poly(β-hydroxybutyrate)/poly(d,l-lactic acid) blends. *Polym. Degrad. Stab.* **2013**, *98*, 1549–1555.

370. Quynh, T.M.; Mitomo, H.; Nagasawa, N.; Wada, Y.; Yoshii, F.; Tamada, M. Properties of crosslinked polylactides (PLLA & PDLA) by radiation and its biodegradability. *Eur. Polym. J.* **2007**, *43*, 1779–1785.

371. Graupner, N. Application of lignin as natural adhesion promoter in cotton fibre-reinforced poly(lactic acid) (PLA) composites. *J. Mater. Sci.* **2008**, *43*, 5222–5229.

372. Son, H.Y.; Jun, H.; Kim, K.R.; Hong, C.A.; Nam, Y.S. Tannin-mediated assembly of gold–titanium oxide hybrid nanoparticles for plasmonic photochemical applications. *J. Ind. Eng. Chem.* **2018**, *63*, 420–425.

373. Panzella, L.; Napolitano, A. Natural Phenol Polymers: Recent Advances in Food and Health Applications. *Antioxidants* **2017**, *6*, 30.

Préparation et modification de composites thermoplastiques/tanins par extrusion réactive

Résumé: Les tanins condensés sont largement répandus et très abondants dans la nature. Au cours des dernières décennies, ces tanins ont été abondamment utilisés pour la production de formulations thermodurcissables (par exemple, les adhésifs pour le collage du bois, les matériaux en mousse) en raison de leur réactivité chimique. Cependant, ils présentent également un grand potentiel en tant que composants pour la conception de matériaux polymères innovants en raison de leurs propriétés physico-chimiques (p. ex. antioxydantes, antimicrobiennes et stabilisantes). Afin d'étendre les domaines d'utilisation des tanins aux matériaux polymères, le principal verrou scientifique et technique réside dans leur incompatibilité avec les polymères hydrophobes. À cette fin, trois voies de modification ont été mises au point pour améliorer la compatibilité des tanins avec les matrices PP ou PLA. Dans la première partie, les PP/ tanins ont été modifiés avec du glyoxal par vulcanisation dynamique. Après extrusion réactive, les tanins vulcanisés présentent une meilleure compatibilité avec la matrice PP et des propriétés anti-UV. La deuxième approche consiste en une modification par estérification à l'aide d'anhydride acétique. Avec cette méthode, des teneurs élevées en AT ont pu être incorporées au PLA, jusqu'à 30 % en poids et jusqu'à 20 % sans diminution notable des propriétés mécaniques ni impact sur la morphologie de surface. Ces composites PLA/AT sont imprimabdwles en impression 3D par dépôt de matière fondue. Dans la troisième partie, une compatibilisation réactive a été réalisée avec succès pour améliorer l'adhésion interfaciale entre PLA et les tanins condensés en utilisant du 3-aminopropytriéthoxysilane, du diisocyanate de méthylène diphényle et du peroxyde de dicumyle (DCP).

Mots clés: polypropylène, poly(acide lactique), tannin condensé, extrusion, modélisation du dépôt fondu, compatibilité réactive.

Preparation and modification of thermoplastic/tannins composites via reactive extrusion

Abstract: Condensed tannins are widely distributed and highly abundant in nature. In the past decades, such tannins have played an important role in thermosetting systems (e.g. adhesives for wood bonding, foam material) because of their chemical reactivity. However, they also exhibit great potential as a component of polymeric materials because of their physicochemical properties (e.g. antioxidant, antimicrobial and stabilizing properties), which are promising for material preparation. In order to transform tannins from traditional application to a broaden application in polymeric materials, the main challenge facing tannins are their incompatibility with hydrophobic polymer. For this purpose, three modification pathways were developed to improve the compatibility of tannins with PP or PLA matrix. In the first part, PP/ tannins were modified with hexamine or glyoxal via dynamic vulcanization technique. After vulcanized extrusion, vulcanized tannins present better compatibility and UV protective performance in PP matrix. The second approach is CTs modified with acetic anhydride. With this method, up to 30 wt% acetylated tannin (AT) can be well incorporated with PLA while PLA containing up to 20 wt% AT did not deteriorate the mechanical property and surface morphology. This PLA/AT composites are printable via fused deposition modeling process. In the third part, the efficient reactive compatibilization have been successful used to improve the interfacial adhesion between PLA and CTs by using 3-aminopropytriethoxysilane, methylene diphenyl diisocyanate, and dicumyl peroxide (DCP).

Key words: polypropylene, poly (lactic acid), condensed tannin, extrusion, fused deposition modeling, reactive compatibilization